CLIMATE CHANGE WATER RESOURCES IMPACTS AND UNCERTAINTIES

Najmur Rizwan Nawaz

B.Eng., M.Sc.

Thesis Submitted for the Degree of

Doctor of Philosophy

Heriot-Watt University

Department of Civil and Offshore Engineering

Riccarton, Edinburgh, EH14 4AS

United Kingdom

August 2001

DECLARATION

Except where reference is made to the work of others,

This thesis is believed to be original and has not been

submitted for any other degree

Najmur Rizwan Nawaz (candidate)

Dr Adebayo J. Adeloye (supervisor)

4 JANUARY, 2002

Date

"To see the future is good, to prepare for it is better"

Anonymous

ACKNOWLEDGEMENTS

The work reported in this thesis has benefited from the advice and assistance of a number of individuals and organisations. The key figure devoting much of his time and effort in guiding me through the research was my supervisor, Dr Adebayo Johnson Adeloye. It was a pleasure to work under the supervision of such a lively and enthusiastic individual. Only through his encouragement, sound advice, constructive criticisms and patience, has it been possible for me to complete this work.

The financial support, in the form of a scholarship from Heriot-Watt University is also acknowledged.

I am also grateful to Dr Majid Montaseri, formerly a PhD student at Heriot-Watt University, for his advice and friendship. My thanks also to Mr Ian Stevens and Dr Jason Ball of Yorkshire Water Services Ltd. for providing relevant data. The assistance of Dr Chong-Yu Xu of Uppsala University, Sweden is acknowledged. I should also not forget to mention several organisations for supplying me with climate data. These are the British Atmospheric Data Centre (BADC), UK Climate Impacts Programme (UKCIP), Climate Research Unit (CRU) at the University of East Anglia, UK, Canadian Climate Centre and the Australian Commonwealth Scientific & Industrial Research Organisation (CSIRO). Moreover, I wish to extend my sincerest thanks to all my friends and colleagues, too numerous to mention.

Finally, I wish to express my sincere gratitude to my parents and siblings for their kind support and encouragement throughout the duration of this research.

ABSTRACT

As a result of the evidence provided by the IPCC on the accelerated change of climate caused by human activities, numerous studies have been carried out to assess the impact of climate change on water resource systems such as reservoirs. Although these studies employed different schemes for baseline climate perturbation, and different models for simulating the resulting catchment rainfall-runoff response, the impacts assessment is based on the single realisation of the perturbed and baseline climate. As a consequence, it has been difficult to estimate the sampling variability of the assessed impacts or to attach confidence limits to them. In this work, Monte Carlo simulation experiments were performed to assess the sampling uncertainties in impacts on water resources of projected climate changes. The investigation employed data from five catchments in Yorkshire, England and three basins in Iran, both of which incorporate water supply reservoirs. The approach enabled the "population of impacts" to be obtained, which allowed risks of having different levels of impacts to be quantified. Confidence limits for the impacts were also developed.

Three important outcomes have resulted from this research. First, the impacts of climate change on reservoir storage-yield-performance functions are highly variable and could be very different from the mean impact assessed using single realisations of baseline and future climate data. Secondly, climate change scenarios from different GCM experiments result in different, and sometimes opposite impacts on the same reservoir system. Thirdly, the assessed impacts on annual runoff and reservoir characteristics are not particularly sensitive to either the baseline climate perturbation scheme or the catchment runoff response model used.

TABLE OF CONTENTS

LIST OF TABLES

LIST OF FIGURES

LIST OF SYMBOLS

A: coefficient matrix of disaggregation model

A_s: reservoir water surface area

a: percentage of short-wave radiation received at the top of the atmosphere reaching the Earth's surface on a completely cloud-covered day

a_1: soil permeability parameter

a_2: storage constant

a_3: fast runoff parameter (without snow module)

a_4: evapotranspiration parameter

a_5: slow runoff parameter

a_6: fast runoff parameter (with snow module)

a_{ads}: fraction of total catchment area with depressions

a_{co}: routing coefficient

a_{coeff}: infiltration loss parameter

a_{crack}: constant of proportionality in groundwater recharge calculation

a_{dlev}: deep seepage parameter

a_{dsc}: depression storage capacity

a_{em}: maximum vegetation controlled rate of evapotranspiration

a_{locate}: parameter fixing origin in cycle of seasonal fluctuation of a_{coeff}, a_{crak} and a_{sub}

a_{power}: routing exponent

a_{rinsc}: interception storage capacity

a_{rk_1}: constant of proportionality in linear component of stream-aquifer flow equation

a_{rk_2}: constant of proportionality in exponential component of stream-aquifer flow equation

a_{rk_3}: exponent in exponential component of stream-aquifer flow equation

a_{rmd}: exponent in depression flow equation

a_{seas}: parameter fixing amplitude in seasonal fluctuation of a_{coeff}, a_{crak} and a_{sub}

a_{smsc}: soil moisture store capacity

a_{sq}: exponent in infiltration capacity equation

a_{sub}: constant of proportionality in interflow calculation

a_{vcond}: constant of proportionality in deep seepage equation

$\tilde{\alpha}$: likely value of α

α: true (unknown) lag-one autoregressive model parameter

$\hat{\alpha}$: sample estimate of α

B: coefficient matrix of disaggregation model

b: percentage of short-wave radiation received at the top of the atmosphere absorbed by clouds on a completely cloud-covered day

b_r: Bowen ratio

β: true (unknown) lag-one autoregressive model parameter

$\hat{\beta}$: sample estimate of β

$\tilde{\beta}$: likely value of β

c_e: factor changes in the actual evapotranspiration as a result of climate change

c_f: climatic factor (excluding carbon dioxide)

c_p: factor changes in the annual precipitation as a result of climate change

c_s: specific heat of moist air

χ^2_{y-2}: Chi-squared distribution with (y – 2) degrees of freedom

D: demand as ratio of mean annual flow

D_{em_d}: exponential distribution of 'medium' precipitation

D_i^s: distance from site to GCM grid point i

D_t: volumetric demand during t

D_{us_m}: uniform distribution of 'small' precipitation

D_w: window width duration in moving window (non-parametric) sampling

$\Delta\Omega_{2x}$: climate sensitivity

$\Delta\Omega_{year}$: global annual temperature change (based on simple climate model)

δ: time-based reliability

ET_0: potential evapotranspiration

E': actual evapotranspiration

E_t: evapotranspiration at time t

E'_t: actual evapotranspiration at time t

E_1: evapotranspiration under current carbon dioxide concentration

E_2: changed evapotranspiration caused by a doubling of CO_2 concentrations

E_b: baseline evapotranspiration

E_c: coefficient of efficiency

e_d: saturation vapour pressure at dew point temperature

E_f: future evapotranspiration

E_m: long-term average potential evapotranspiration

ε_p: precipitation elasticity of runoff

E_o: open water evaporation

E_s: evapotranspiration due to CO_2-induced change in plant stomatal resistance alone

e_s: saturation vapour pressure at air temperature

$\hat{E}_t$: volumetric reservoir surface net evaporation during t

f: fractional area of catchment covered by vegetation

f_p: total number of failure periods

f_s: number of continuous sequences of failure periods

Φ_{r,l_g}: fitted parameter of short dry series

Φ_{r,s_l}: fitted parameter of long dry series

Geom[ ]: geometric distribution for a short series

$G_f(0,1)$: Gauss function with parameters 0 and 1

g_p: increased plant foliage factor

γ_b: runoff ratio

Γ_{le}: average 'large' precipitation

h: Hurst coefficient

η: vulnerability

I_{fi}: infiltration

φ: sustainability index

ϑ: latent heat of vapourisation of water

K_t: volumetric sequential deficits at the beginning of period t

K_{t+1}: volumetric sequential deficits at the end of period t

κ: wet and dry series

k: standard normal variate for a given level of significance

L: sum total of (water balance) losses due to infiltration, seepage and deep percolation.

l: length of series or position within the series

M: soil moisture store

M_{dep}: depression store

M_{gw}: groundwater store

M_t: available storage at time t

M_t^s: available storage (including snow) at time t

μ_{ln}: mean of the three-parameter log normal distribution

μ_q: mean of annual flows

$\mu_{q,i}$: likely value of μ_q for period i

μ_x: sample of data sample x

μ: standard deviation

N: theoretical maximum sunshine hours at a specified location

n: observed number of sunshine hours

n_u: number of observations in the series data

n_w: length of series

OBJ: objective function

OBS_t: recorded flow at time t

p_1: model parameter in 2-parameter exponential curve relating reservoir storage and yield

p_2: model parameter in 2-parameter exponential curve relating reservoir storage and yield

P: precipitation

P_t^a: active rainfall at time t

P_b: baseline precipitation

$P_d(d)$: probability distribution of dry series lengths on day d

P_f: future precipitation

$P_n(d)$: probability distribution of sunshine hours on day d

$P_p(d)$: probability distribution of precipitation on day d

$P_t(d)$: probability distribution of temperature on day d

P_t^r: rainfall at time t

$P_w(d)$: probability distribution of wet series lengths on day d

$\Pi_{\kappa,n}$ parameter of normal probability distribution for modelling sunshine hours

$\Pi_{\kappa,t}$: parameter of normal probability distribution for modelling temperature

q: time series of annual flow data

q_i: annual flow during year i

q_i: annual flows for the i-th year

Q_t: volumetric inflow during t

q_{max}: largest observation of annual flows

q_{med}: sample median of annual flows

q_{min}: smallest observation of annual flows

$\hat{Q}_{i,j}$: generated flow for month j and year i

$\overline{q}^n$: mean annual flow for reservoir group n (Yorkshire system)

$\overline{Q}_j$: mean flow estimate for month j

$\overline{q}$: mean of the observed annual flow, q

θ: matrix of the true (unknown) parameters (α, β) of lag-one autoregressive model

$\tilde{\theta}$: matrix of likely values of θ

$\hat{\theta}$: matrix of sample estimate of θ

$\Theta_{\kappa,n}$ parameter of normal probability distribution for modelling sunshine

$\Theta_{\kappa,t}$: parameter of normal probability distribution for modelling temperature hours

R: runoff

r: dry series

R_a: total short-wave solar radiation received at the top of the Earth's atmosphere

r_a: aerodynamic resistance

R_b: baseline runoff

R_{bf}: baseflow

R_{dep}: depression flow

R_f: future runoff

R_{gw}: groundwater recharge

R_{int} interflow

R_m: soil moisture flow

R_n: total daily incident net solar radiation

R_{over}: overland flow

R_r: river recharge

r_s: stomatal resistance

R_{seep}: deep seepage

R_{sur}: surface runoff

R_t^D: drought release of reservoir system during the t-th failure periods

R_t^f: fast runoff at time t

R_t^s: slow runoff at time t

R_t^*: target demand during the t-th period

R^2: coefficient of determination

$r(X_j^n X_l^k)$: lag-zero cross correlation between the flows of seasons j (site n) and season l (site k)

$r(X_j^n Z^k)$: lag-zero cross-correlation between the annual flows at site k and the flows of season j at site n

$\Re$: resilience

ρ_a: density of moist air

ρ: probability

ρ_{l_e}: probability of occurrence of large precipitation

ρ_{m_d}: probability of occurrence of medium precipitation

ρ_{s_m}: probability of occurrence of small precipitation

ρ_w: water density

S: reservoir storage

SE: standard error of sample skewness estimates

S_f: factor used for scaling GCM output

SIM_t: simulated flow at time t

S_K: reservoir active storage capacity

s_q: standard deviation of the observed annual flows

S_T: catchment storage

S_{XX}: lag-zero covariance matrix between different seasons

S_{XZ}: lag-zero covariance matrix between the annual and seasonal flows

S_{ZX}: transposed matrix of S_{XZ}

S_{ZZ}: lag-zero covariance matrix between the annual flow (multiple-site)

s_q^2: variance of observed annual flows

S_j^2: variance of flow estimate for month j

S_t^f : snowfall at time t

S_t^m : snowmelt at time t

S_t^p : snowpack at time t

σ_{ln}: variance of the three-parameter log normal distribution

σ_v^2 : true (unknown) variance of independent random variable, v_i

$\tilde{\sigma}_v^2$: likely values of σ_v^2

σ_q^2 : variance of annual flows

$\sigma_{q,i}^2$: likely value of σ_q^2 for period i

σ_x : standard deviation of sample x

T_p: total number of periods

$\tilde{\tau}$: lower bound of the three-parameter log normal distribution

V: vector of independent normal random variables with zero mean

V_i : vector of independent standard normal random variables during peroid i

V′ : vector of independent standard normal variables with zero mean and unit variance

v_i: independent zero mean normal random variable with

VAR_{CGCM1}: downscaled climate variable based on CGCM1 GCM

VAR_{CSIRO1}: downscaled climate variable based on CSIRO1 GCM

VAR_D: downscaled GCM simulated climate variable

VAR_{HadCM3}: downscaled climate variable based on HadCM3 GCM

VAR_i: GCM simulated climate variable at grid point i

υ: volumetric reliability

ς: range of cumulative departures from the mean value in a time series

ϖ : psychometric constant

w: wet series

W_t: available water at time t

Ω: temperature

Ω_m: long-term average air temperature

X_{Mi}^N : transformed zero mean seasonal flow for season M, year i, and site N

X_i : vector of transformed zero mean seasonal flows at sites for year i

y: sample size

Ψ_t: correlation coefficient between two continuous days

$z_{i,j}$: standardised monthly flow, i.e. zero mean and unit variance, for month j, year i

Z_i, Z_{i-1} vector (N x 1) of annual flows at the different sites for the i-th and (i-1)-th years, respectively

Z_i: vector of transformed zero mean annual flows at the different sites during year i

CHAPTER ONE

INTRODUCTION

1.1 Statement of the Problem

It is now widely accepted that the Earth is warming (IPCC, 2001a). Historical records indicate that although the Earth has experienced periods of cooling and warming in the past, the present rise in temperature is far greater than for any previously recorded period (IPCC, 2001a). Globally, ten of the warmest years since records began in 1860 have all occurred since 1983, and eight of these occurred since 1990. Moreover, studies of a large number of proxy records (from trees, ice cores, fossils, sediment and lakes in closed catchments) show that the 1990s was the warmest decade of the last millennium in the Northern Hemisphere with the 20th century being the warmest century (IPCC, 2001a). 1998 was an unusually warm year, and according to the proxy records, the warmest year of the last millennium in the Northern Hemisphere (IPCC, 2001a; Mann and Bradley, 1999).

To investigate the effects of global warming, possible causes have to be first identified. In 1896 the Swedish chemist Svante Arrhenius first calculated the effects of carbon dioxide concentration on temperature. He estimated that a doubling of carbon dioxide would increase the global mean temperature by up to 5°C to 6°C - a value not far from current estimates (Houghton, 1997). Later, ReVelle and Suess (1957) linked the rise in levels of so called 'greenhouse gases' such as carbon dioxide and methane, to global warming.

Over recent years, the global warming debate has heightened with a focus on the human influences on global temperature. However, some climate analysts have even dismissed rising global temperatures altogether (see e.g. Michaels and Knappenberger, 1996; Win-Nielsen, 1999). They have argued that a closer inspection of temperature measurements made using satellites and microwave sounders reveals no statistically significant temperature change to have taken place over recent decades. Others accepting the warming to be occurring have argued that the warming has nothing to do with human influences and have attributed it to the large range of climate variability. Climate variability occurs as a result of natural processes that are both external and internal to the Earth's oceans and atmosphere such as variations in solar and volcanic activity, respectively (Woodward and Gray, 1993, 1995). It has also been suggested that the warming may be buffered, to some extent, by the cooling effects of sulphate aerosols (Mitchell and Johns, 1997).

While the above controversy about the precise cause of the warming rages on, the average global temperature is continuing to rise. This led numerous investigators to attempt to establish the underlying cause of the rising temperature (see e.g. Hegerl et al., 1996; Santer et al., 1996; Tett et al., 1997). In particular, their investigations have sought to determine whether this rise is within the expected range of natural variability or whether anthropogenic influences are also involved and to what extent. After carefully examining the conclusions from these and countless other relevant studies, a body of experts forming the Intergovernmental Panel on Climate Change (IPCC) recently issued a clear statement supporting the hypothesis of human induced global warming. In a report published only recently (IPCC, 2001a), the IPCC state that '*.....most of the warming observed over the last 50 years is attributable to human activities.*' Furthermore, another finding of the IPCC which does not bode well is that

'*..human influences will continue to change atmospheric composition throughout the 21st century.*'

It is inevitable that global warming will lead to long-term shifts in regional climatic patterns. This will undoubtedly put increasing pressure on water resources, particularly in arid and semi-arid regions across the world. To this end, numerous studies have been carried out over the last decade or so to assess the impact of climate change on water resource systems (see Chalecki and Gleick, 1999 for a review).

However, despite the admittedly voluminous literature on the subject of climate change water resources impacts, it is argued by some (Gleick, 2000) that impacts of regional climate change on water resources are still only poorly understood. It is therefore crucial that more research is conducted in this area. The relatively little understanding of the way in which anthropogenic climate change may influence water resources is largely due in part to the various uncertainties introduced at successive stages of the assessment. Impact assessment often involves three distinct stages: The first stage is to construct catchment-scale GCM-based climate change scenarios and use these to perturb baseline (current) climate to obtain future climate. This is then followed by forcing a catchment response model with both the current and future climate to obtain the corresponding runoff records. Finally, the hydrological data series are then input into a water resource simulation model to obtain possible impacts.

A primary source of uncertainty therefore stems from the inability to accurately forecast levels of greenhouse gases and hence the degree of global warming. Additionally, there are other uncertainties due to errors in global climate modelling and in 'downscaling' climate to the catchment scale, the imprecision in hydrological and water resource

systems modelling, and the limitation caused by using only single records for the impacts assessment (sampling uncertainty). It is therefore important that any assessed impacts are viewed with caution (Hulme et al., 1999a).

It is possible, however, that if the problem is posed in a sensitivity analysis context which is commonplace (Arnell, 1996; Wood et al., 1997), rather than prediction, then climate modelling errors and possibly downscaling errors are largely removed (Wood et al., 1997). Similarly, where both the baseline and future hydrology are based on the hypothesised rainfall-runoff scheme, the uncertainty due to this should also cancel out, leaving only the sampling uncertainty of the hydroclimate. By employing Monte Carlo simulation experiments, it is possible to assess the sampling uncertainties in impacts on water resources of projected climate changes. Such an approach enables the 'population of impacts' to be obtained as opposed to the single realisation of impact possible with traditional methods of assessment. These impacts can then be subject to standard statistical analysis to determine mean, variance and several quantiles as well as to construct confidence limits for the impacts.

This PhD research has in the main therefore implemented a series of Monte Carlo simulation experiments to characterise the sampling uncertainties of impacts of climate change on case study water resources systems. Analyses were also carried out using the much simpler traditional single records approach to allow for comparisons with results obtained using the two different methods of assessment. Furthermore, various techniques for perturbing baseline climate, and different rainfall-runoff models of catchment response were tested in the work. All of this provided a rigorous and sound basis for examining the extent to which the assessed impacts are affected by various assumptions and models.

1.2 Aim and Objectives

The aim of this research is to investigate the effects of climate change on water resources systems and to characterise the uncertainties of such effects.

This aim was achieved using the following specific objectives:

(i) to carry out a literature review on the origin of rapid global warming observed in recent years;

(ii) to extensively review the literature on climate change water resources impacts assessments, thereby identifying any voids in current knowledge;

(iii) to construct climate change scenarios based on outputs of several recommended GCMs;

(iv) to select suitable case study catchments for the application of the methodology;

(v) to apply climate change scenarios to baseline climate data of the selected catchments (to obtain future climate) using both a simple mean monthly factored approach and a statistically more robust stochastic weather generation model;

(vi) to calibrate catchment rainfall-runoff response models of varying complexity for the selected catchments for use in the climate change water resource impacts assessment;

(vii) to calibrate stochastic models of streamflow for replicating streamflow data;

(viii) to investigate the effects of climate change on water resources using both the traditional and a Monte Carlo simulation approach;

(ix) to compare the obtained climate change water resource impacts based on the simple and more detailed methodologies and make appropriate recommendations.

1.3 Thesis Outline

This thesis comprises six chapters. In Chapter 2, past changes in climate are discussed and the current climate change is placed within a historical context. Changes in temperature, precipitation and runoff occurring in the past are summarised in section 2.2. The greenhouse effect and how it may lead to global warming is described in section 2.3. In section 2.4, efforts by numerous analysts to detect human influence on global climate are briefly summarised. Also in section 2.4, the main findings of the UN Intergovernmental Panel on Climate Change (IPCC) on the human influences on global climate are noted. Section 2.5 explains the likely effects of rising temperatures on water resources

Chapter 3 reviews approaches to climate change water resources impacts assessment with a particular emphasis on the uncertainties at successive stages of the assessment. Section 3.2 summarises the three main approaches to climate impacts assessment. Section 3.3 provides a discussion on climate change scenarios which are central to impacts assessments. A discussion on downscaling GCM output and their application to baseline hydroclimatological data using various approaches are also discussed in section 3.3. Sections 3.4 and 3.5 provide a discussion on the methodologies used to assess the hydrological and water resources impacts of climate change, respectively. Limitations of the traditional 'single records' approach to impacts assessment are also highlighted in this section 3.4 and the advantages of using a Monte Carlo simulation technique are discussed.

Case studies from Yorkshire in northeast England and Urmia in northwest Iran, are presented in Chapter 4. These studies use selected techniques from Chapter 3 to

investigate the effects of climate change on water resources. In sections 4.2 and 4.3, the catchment and data information from these two case study systems are discussed and this is followed in section 4.4 by a discussion of the application of two climate change water resources impacts studies (i.e. preliminary and intermediate studies). The preliminary study uses the traditional approach to impacts assessment whilst the intermediate study also adopts a Monte Carlo simulation approach in addition to the traditional approach. Both studies use a simple baseline climate perturbation scheme. Climate change scenarios for Yorkshire and Urmia are introduced in section 4.4, and a monthly water balance model and a stochastic streamflow generation model are calibrated. Details are also presented on the water resources systems' response modelling. Section 4.5 describes the detailed investigation of the Yorkshire system. In particular, further climate scenarios are presented, a stochastic weather generator is used for perturbing baseline climate and a daily water balance model is calibrated. In addition to assessing the effects of climate change on reservoir storage-yield-performance, the effects of climate change on a number of aspects related to water resources are also briefly investigated.

In Chapter 5, the numerous results obtained in this work are presented and discussed. Results of the preliminary study are presented and discussed in section 5.2. The results concern the possible effects of climate change on runoff and reservoir storage-yield. In section 5.3, results of the intermediate study are discussed. Results on the impacts of climate change on runoff and reservoir storage-yield-performance constitute this section 5.3. Moreover, the major part of this section presents findings on the effects of data sampling uncertainty on reservoir yield impacts. Results of the final detailed study are presented and discussed in section 5.4. In addition to presenting results on the climate change impacts on runoff and reservoir storage-yield-performance, further results are

also contained in section 5.4. These are: (i) the effects of vegetation feedback on runoff and reservoir characteristics, (ii) climate change impacts on flow frequency curves, (iii) effects of climate change on groundwater recharge, (iv) climate change-induced increase in water demand on reservoir storage and (v) climate change impacts on reservoir control curves. In section 5.5, possible adaptation strategies designed to cope with the potential climate change impacts, discussed in previous sections, are summarised.

Both the preliminary and intermediate studies have been published in the open literature, and for completeness, copies of the papers have been included as appendices to the thesis (see Appendices A and B).

Finally, Chapter 6 contains the main conclusions of the study and also makes suggestions for further research.

CHAPTER TWO

CLIMATE CHANGE, HYDROLOGY AND WATER RESOURCES

2.1 Introduction

The Earth's climate is driven by solar radiation. Most of this radiation is absorbed by the oceans and land surfaces whilst a small proportion is absorbed by the atmosphere. The radiation is then distributed by the atmospheric and oceanic circulation and radiated back to space. Factors that change the amount of radiation received from the Sun or re-radiated back to space or which change the redistribution of energy within the atmosphere, and between the atmosphere, land and ocean can change the climate. Such factors fall into two categories: those that are external to the Earth and those that are internal. External processes contributing to climate variability include variations in solar output as a result of phenomena such as sunspot activity (Kelly and Wigley, 1992; Crowley and Kim, 1993; Lean et al., 1992), and variations in solar radiation reaching the Earth caused by periodic variations in the Earth's orbit known as the Milankovitch cycle. Internal processes that affect the climate range from volcanic activity to the periodic warming of the Pacific waters off the coast of South America known as El Niño. Because both the external and internal natural processes have always taken place, it is reasonable to assume that the Earth's climate has always changed. Consequently, the option available to humans has usually been one of learning to cope with natural climate variability.

However, there are now concerns that in addition to natural climate variability, anthropogenic influences may be responsible for rapid climate change. The cause of

climate change has been attributed to global warming as a result of human activities such as atmospheric pollution and deforestation both of which increase the concentrations of the so-called greenhouse gases in the atmosphere. Many argue that climate change is already evident (e.g. see IPCC, 2001a; Mann and Bradley, 1999; Santer et al., 1996) with an increase in record breaking climatic events during the 1990s. For example, globally, eight of the warmest years since records began in 1860 have all occurred since 1990 (IPCC, 2001a).

If indeed this is the case then the impacts of global warming will be far-reaching. Global warming will lead to changes in precipitation and evaporation which will have profound effects on hydrological processes and consequently, water resource systems. Moreover, combined with a rise in the demand for water due to climate change and a rising global population, serious threats would be posed to the security of future water resources throughout the world.

In this chapter, the role of humans in warming the Earth is reviewed. This is followed by a review of the possible effects of global warming on the hydroclimate and water resources. The review begins in section 2.2 with a summary of past and recent climatic changes. Changes in temperature, precipitation and runoff are presented. The role of the Earth's atmosphere in regulating the global temperature is discussed in section 2.3. The natural greenhouse effect is described and the implications of an enhanced greenhouse effect are also discussed. In section 2.4, efforts to detect the underlying cause of recent climate change are reviewed. Whether there is enough evidence linking global warming to anthropogenic influences is also discussed in this section. In section 2.5, inferences are made from climatic changes on the likely influences on hydrological processes and water resources. The chapter is then summarised in the last section 2.6.

2.2 Global Warming and a Brief History of Climate

As previously mentioned, the climate has always been changing due to natural processes that are both external and internal to the Earth. A study of past climates can reveal whether or not the climate change observed in the latter half of the 20th century is unprecedented in human history. To ascertain the extent of past climatic changes, it is useful to examine hydroclimatological records obtained using different techniques.

2.2.1 Temperature Changes

Proxy records constructed from tree rings, ice cores and sediment cores show that the Earth's climate has undergone periods of cooling and warming throughout its history (Nicholls et al., 1996). Data from ice cores suggest that rapid climatic changes did occur during the last ice age which came to an end about 20,000 years ago, and during the period leading up to the present Holocene period which began about 10,000 years ago (Nicholls et al., 1996). From data, especially in the North Atlantic, it is estimated that the changes took place over the time-scale of a human life (Nicholls et al., 1996). The changes affected atmospheric temperature and circulation, precipitation patterns and the hydrological cycle, and temperature and circulation of the ocean. Central Greenland ice cores and a number of deep-sea sediment core records from the North Atlantic show that the climatic changes were often large in magnitude. For example, there is evidence that about 11,500 years ago, Central Greenland temperatures increased by 7°C in a matter of just a few decades (Dansgaard et al., 1989; Grootes et al., 1993). This particular rapid change in climate was associated with the melting of a large ice sheet in North America that resulted in dense cold freshwater being poured into the North Atlantic. This would have led to a change in the North Atlantic oceanic

circulation and even perhaps the global oceanic circulation thus impacting the climate (Arnell, 1996; Nicholls et al., 1996). Over a more recent period, dating back 10,000 years (Holocene period), Wigley and Kelly (1990) have shown that it is unlikely that global mean temperatures have varied by 1°C or more in a century at any time during that time. Although relatively few investigations have been able to reconstruct such long records as Wigley and Kelly (1990), a plethora of reconstructed temperature records for the more recent period of the last 1,000 years is available.

The climate of the last 1,000 years is relevant as the physical world was much similar to today. An examination of the medieval warm period taken as the period between 9th and 14th centuries, shows warm conditions during this period, especially in the 11th and 12th centuries (Lamb, 1965, 1988). Lamb (1988) derived temperature records for Central England dating back 1000 years. He concluded that there had been a warm period during the 11th and 12th centuries followed by the little Ice Age in the 13th century lasting until 1850. In another study, Mann et al. (1998) extended Northern Hemispherical surface temperature data records back to 1400 AD as shown in Figure 2.1. The basis for temperature record extension was the calibration of high-resolution proxy annual climate indicators with instrumental annual temperature data over the period 1902-1995. The annual-resolution proxy indicators comprised dendroclimatic, ice core, ice melt and coral records. The record extension showed that average annual surface temperatures in the Northern Hemisphere towards the end of the 20th century were at their highest since at least the 15th century (see Figure 2.1).

Despite the advent of recording instrumentation, proxy data continue to be used in reconstructing climatic records over the last two centuries where recorded data are unavailable. In a recent study Magnuson et al. (2000) examined freeze and break-up

dates of ice on lakes and rivers from information from sites in Russia, Finland and Japan. The data went back to 1846 for a large number of sites and back before 1800 for three sites in each of the three countries. The data indicate later freezing and earlier ice break-up from 1846-1995, which corresponds to increasing air temperatures of about 1.2°C per 100 years. The longer records show a reduced ice cover due to a warming trend commencing as far back as the 16th century with increasing rates of change around 1850.

The development of measuring instruments led to the recording of temperature, precipitation and streamflow for the first time. For example, a long temperature record starting in 1659 exists for central England (Manley, 1974; Parker et al., 1992). The record, shown in Figure 2.2, has been used by Hulme and Jenkins (1998) to obtain the variability in the central England temperature of around +/- 0.5°C of the long-term average. Hulme and Jenkins (1998) also note that four of the five warmest years in central England over the last 340 years occurred after 1988. It can be seen in Figure 2.2 that the annual average temperature change from the 1961-1990 period is gradually increasing towards the latter part of the 20th century.

The global mean temperature record has also been constructed from instrumental data. This record, constructed by the Climate Research Unit (CRU) in East Anglia in the UK, spans 1860-2000 and is provided in Figure 2.3. The temperature record is based on temperature at the sea surface and close to land surface. Land records were obtained from weather stations where consistent recordings of temperature have been made in the same location over a large proportion of the period since 1860. Changes in sea surface temperature have been estimated by processing over sixty million observations largely from merchant ships over the same period (Houghton, 1997). Once temperature data

from land stations and ships are collected, they are located within a grid square (e.g. 1° latitude by 1° longitude). The temperature data in each grid square are then averaged and the global average is determined by averaging (after weighting them by area) over the averages for each of the squares (Houghton, 1997). This laborious task has been made easier during the last 30 years or so as a result of observations from space satellites that provide data with global coverage (Houghton, 1997).

The temperature record presented in Figure 2.3 is the global mean annual temperature relative to the baseline (1961-1990) period. The baseline period has been defined as 1961-1990 by the World Meteorological Organisation since complete climate data are generally available over this period and it also provides a basis for comparison with other studies. In agreement with Figure 2.2, Figure 2.3 shows a tendency for warming during the 1990s although the warming is the global average. Figure 2.3 has been used by the United Nations Intergovernmental Panel on Climate Change (IPCC) to obtain the extent of global warming over the last decade (IPCC 2001a). The IPCC recently concluded that the ten warmest years since records began all occurred since 1983, and eight of these occurred since 1990. Globally, it is very likely that the 1990s was the warmest decade and 1998 the warmest year in the mean observed global temperature record dating back to 1860 (IPCC, 2001a).

2.2.2 Precipitation and Runoff Changes

In the UK, Wigley et al. (1984) derived a rainfall record beginning 1766 for England and Wales (see Figure 2.4). Arnell (1996) used this precipitation record to show that when averaged over a few years, the multi-year precipitation can vary by up to 10% of the long-term average.

Like long temperature records, it is possible to derive long hydrological data records based on proxy data (e.g. tree-rings and lake levels). For instance, sedimentalogical, morphological and palynological evidence can be used to construct lake levels back through time (Street-Perrot and Roberts, 1994) which form the basis for streamflow time-series. However, Knox (1995) emphasises that the reconstructed data obtained from proxy records tend to identify periods of high flows rather than low flows.

Most of the early recorded streamflow records date back to about the 19th century. In the UK, for instance, the first continually measured streamflow record available is for the river Lea in Essex, which dates back to 1879 (Marsh, 1996). Recorded streamflow data are also available for the River Thames at Teddington Weir - first measured in 1882 and this is shown in Figure 2.5. Because land use changes may have altered the volume and timing of streamflow, the consistency of records becomes questionable. Arnell (1996) points out that, in general, only relatively recent streamflow records (since the last 50 years) may be assumed to be consistent. However, it should be noted that Arnell's (1996) assumption is not based on any quantitative analysis.

2.3 The Greenhouse Effect

Observed changes in climate over the last century were summarised by Nicholls et al. (1996) and are shown in Figure 2.6. It can be seen from Figure 2.6a that an overall warming trend is noticeable since the beginning of the 20th century. If global warming is indeed occurring, as some of the preceding discussion might suggest, then possible causes need to be identified.

Humans are releasing large quantities of so called 'greenhouse gases' into the atmosphere due to industrial and other anthropogenic activities. It is believed that this is causing global warming and climate change. An understanding of the Earth's energy balance is central to understanding the link between greenhouse gases and the global temperature.

2.3.1 The Earth's Energy Balance

The Sun's radiation falls on the Earth's atmosphere and some of this so called 'short-wave' radiation is reflected back into space by either aerosols, clouds or the Earth's surface, which leaves the remainder to warm the Earth's surface and atmosphere (see Figure 2.7). The Earth must re-radiate this energy back into space in order to balance the incoming energy. It achieves this by emitting the so called 'long-wave' infra-red radiation. The amount of long-wave radiation emitted depends on the Earth's surface temperature and its radiation absorbing ability. To balance the incoming energy, the Earth's average surface temperature must be about -19°C (Trenberth et al., 1996). However, the global average temperature is 34°C warmer than this - averaging around 15°C. The blanketing effect of certain atmospheric gases can explain why the Earth is on average much warmer than dictated by the energy balance.

2.3.2 The Natural Greenhouse Effect

In 1827, Jean-Baptiste Fourier first recognised the similarity between what happens in the glass of a greenhouse with what happens in the atmosphere and hence the term 'greenhouse effect' was conceived. Some of the long-wave thermal radiation leaving the surface of the Earth escapes into space while some of it is absorbed by atmospheric

gases such as water vapour, carbon dioxide and some additional trace gases. These so called 'greenhouse gases' have a blanketing effect upon the Earth and keep it on average about 34°C warmer than it would otherwise be. This is known as the natural greenhouse effect because this process has been ongoing and pre-dates humans.

2.3.3 The Enhanced Greenhouse Effect and Global Warming

Atmospheric concentrations of carbon dioxide have increased by nearly a third over the last 250 years (IPCC, 2001a) due to increased industrial activity during the Industrial Revolution. The problem has been exacerbated by mass deforestation resulting in the loss of a major carbon dioxide sink. Historical evidence indicates that rapid global warming in the past has been associated with unusually large concentrations of atmospheric concentrations of carbon dioxide. This would imply that the rising concentrations of carbon dioxide will lead to a warmer world. Moreover, additional greenhouse gases such as methane, nitrous oxide and chlorofluorocarbons (CFCs) have been discharged. Relatively speaking, nitrous oxides and CFCs are more capable of hindering the release of the long-wave radiation than carbon dioxide and methane. However, their effects may be largely offset by their ability to deplete atmospheric ozone (Schimel et al., 1996). Furthermore, during the last decade, sulphate aerosols have entered the global warming debate. It is argued their cooling effects may slow the rate of warming (Arnell, 1996). However the cooling effects may be limited by their survival time in the atmosphere which only amounts to about a week compared with decades to centuries for the principal greenhouse gases. Consequently, attempts to curb sulphur emissions will be felt far more rapidly than reductions in greenhouse gas emissions.

2.4 Detecting Human-Induced Climate Change

The Earth's climate is dependent upon a whole range of natural processes (summarised in the introduction to this chapter) hence the range of natural climate variability is large. Trying to separate possible anthropogenic climate change *signal* from natural climate variability *noise* is a difficult task. Moreover, complex ocean-atmosphere interactions such as the El Niño and Southern Oscillation (ENSO) and North Atlantic Oscillation (NOA) phenomena add to the climate noise.

ENSO is a major source of natural inter-annual climate variability in the tropics and is also an important source of inter-annual variability in some regions at the higher latitudes (Rasmussen, 1985). El Niño is the term given to the anomalous warming of the Pacific Ocean off the coast of South America. The Southern Oscillation refers to fluctuations in sea surface pressure between the tropical eastern Pacific and the west Pacific-Indian Ocean and is associated with a global trend in inter-annual climate variability.

The NOA is a large scale fluctuation in atmospheric mass which alternates between the polar and subtropical regions. Changes in the mass and pressure fields lead to variations in the magnitude and direction of storm systems crossing the Atlantic from the US east coast to Europe which results in warm and wet winters in Europe (Nicholls et al., 1996).

Because of global warming concerns, hydroclimatological records are increasingly being analysed for trend (see e.g. Yoshino, 1999; Olsen et al., 1999, and Foster et al., 1997) to determine whether global warming is manifest in the records. For example,

Yoshino (1999) analysed runoff data for trends from 103 major world catchments and identified trends in some regions. He noted trends in runoff in the Sahel and other rivers in arid and semi-arid regions, with increasing trends observed in Western Europe and Eastern North America.

Foster et al. (1997) examined variations in rainfall and runoff in Scotland and Northern Ireland in an effort to determine whether the extreme climatic conditions of the 1990s were unusual or simply within the range of natural climate variability. They used both simple and more advanced trend detection techniques to reveal trends in rainfall and runoff data records at some locations. Foster et al. (1997) noted that trends in the data records could be explained by the influence of the Westerly and Cyclonic weather types on rainfall. This led them to conclude that climate change in Scotland and Northern Ireland over recent years may be part of a greater natural climate variability rather than any anthropogenic influences. However, they also noted that observed annual rainfall at some stations (e.g. Fort William in Scotland) was unusually high during recent years.

While it is difficult to attribute trends in data records solely to human-induced climate change, the results are nonetheless important. They suggest that water resources assessments carried out on the assumption that the time-series data are stationary may not be wholly adequate.

Although trend detection tests are useful in revealing statistically significant shifts in a data record, they are unable to identify the causes of such shifts. Distinguishing between the two is important because if it can be shown that the origins of climate change are human, then measures can be taken to avert its most serious detrimental impacts. General Circulation Models (GCMs) have recently emerged as a reliable tool

to aid in the complex task of discovering the origin of climate change (e.g. Stouffer et al., 1994; Hasselmann et al., 1995; Tett et al., 1997). GCMs have been developed to model the climate system and are first calibrated with current climate conditions and then used to simulate future climate. A more complete discussion on GCMs - highlighting their role in simulating future climate - will be presented in Chapter 3.

In an effort to try and ascertain the extent of human-induced climate change during the 20th century, Tett et al. (1997) used a 1000-year temperature record based on a GCM simulation experiment. The temperature record is based on a forcing of the UK Hadley Centre's HadCM2 GCM with a constant carbon dioxide concentration representative of pre-industrial times. Because a constant pre-industrial carbon dioxide forcing is used, the corresponding temperature is attributable solely to natural processes. The processes incorporated within the model structure include changes in solar and volcanic activity. Tett et al. (1997) extracted the maximum range of temperature variability in any 137-year period from the 1000-year record. A 137-year period was selected so that a comparison could be made with the 137-year (1860-1996) observational global average temperature record. The likely natural climate variability, along with the observed global mean temperature is shown in Figure 2.8. Providing the climate model is adequately reproducing the natural variability of the observed climate - which, on the basis of model validation, is true (Tett et al., 1997) - then it is clear from Figure 2.8 that the temperature extremes of the last decade have fallen outside the likely range of natural climate variability.

2.4.1 Human Influence on Global Warming

Some of the evidence presented so far in this chapter clearly points to global warming. However, whilst results from one study (Tett et al., 1997) summarised above point to anthropogenic causes, a careful examination of countless climate change studies would be required to form a strong conclusion. Fortunately, this task was given to the IPCC which was established in 1990. Nearly a thousand experts from across the world examined evidence such as the information in Figure 2.3 and Figure 2.8, and recently summarised their main findings (IPCC, 2001a):

- *an increasing body of observations gives a collective picture of a warming world and other changes in the climate system;*
- *emissions of greenhouse gases and aerosols due to human activities continue to alter the atmosphere in ways that are expected to affect climate;*
- *there is new[1] and stronger evidence that most of the warming observed over the last 50 years is attributable to human activities;*
- *human influences will continue to change atmospheric composition throughout the 21st century;*
- *anthropogenic climate change will persist for many centuries.*

2.5 Future Global Warming and Possible Effects on Hydrological Processes and Water Resources

The implications of global warming for hydrology (the natural system by which precipitation makes its way into rivers and eventually the oceans) and water resources

[1] since the Second Assessment Report (IPCC, 1996)

(the "built" or managed system that makes freshwater available for human uses) are among the most important to communities. Whilst some countries currently with surplus water resources may benefit in the future, it looks likely that the prospect of global warming will only increase pressure on regions with dwindling water resources. In other words, the water rich will become richer and the water poor will get poorer. Many parts of the world are already facing water shortages. This is because the demand for consumptive (e.g., domestic water supply) and non-consumptive (e.g., navigation, hydroelectric power generation, industrial cooling, compensation flow) supplies of water is barely met by the relatively slow rate of replenishment of the surface and groundwater resources.

It is therefore important to identify regions vulnerable to climate change. However, the complexity of the Earth's climate system makes the prediction of any long-term climate change highly uncertain. Nonetheless, efforts are being made to understand future climatic changes using the best tools currently available. Such tools include GCMs that are used to simulate the possible spatial patterns and magnitude of future climate change under both the natural and enhanced greenhouse effect. To begin with, when global climate modelling was in its early stages, little confidence could be placed in climate change simulations. More recent GCMs, however, are a great improvement on their predecessors, due mainly to faster computers and the better modelling of physical processes in both the oceans and atmosphere.

The first step in ascertaining the extent of future climate change requires an understanding of the sensitivity of global temperature to increases in greenhouse gases.

2.5.1 Future Levels of Greenhouse Gases and their Effects on Global Temperature

If carbon dioxide continues to be pumped in to the atmosphere at the current rate (termed the *'business as usual'*), there will be a carbon dioxide doubling by between 2050-2100. GCM experiments reveal that this would lead to an estimated global mean temperature rise of between 1.4°C and 5.8°C (IPCC, 2001a).

Moreover, recent evidence suggests that the global warming potential of the various greenhouse gases is 10%-30% higher than previously assumed because of complex feedback mechanisms. For example, as the Earth warms, more water - an important greenhouse gas - will be evaporated from the oceans and atmosphere. This will lead to a further increase in temperatures - which will increase evaporation and hence the development of a feedback mechanism. This suggests that a temperature rise of closer to 5.8°C than 1.4°C is more likely.

Despite an increase in global temperatures, there are concerns that feedback processes could lead to cooling in Western Europe, especially in the UK. It is possible that melting icebergs in the north Atlantic might release cooler water down the Atlantic disrupting the Gulf Stream (Hulme and Jenkins, 1998). There are additional feedback processes that will also affect the degree of global warming and its likely effects on climate change, and some of these will be discussed in the next chapter.

2.5.2 Effects of Global Warming on Hydrological Processes

Precipitation is the principal driving force behind the hydrological system. Any change in the intensity, duration and quantity of precipitation will have a direct effect on runoff

and groundwater. It is likely that under global warming, the world will be wetter on average (IPCC, 2001b). It is estimated that a global mean temperature rise of between 1.5°C and 4.5°C would lead to a 3%-15% rise in global mean precipitation (Arnell et al., 1996). There is less certainty regarding regional changes in precipitation. GCM simulations reveal that during the latter half of the 21st century it is likely that there will be an increase in precipitation over mid-northern to high-latitudes and Antarctica in winter. The lower latitudes are likely to see both regional increases and reductions over land areas. Furthermore, inter-annual variability in precipitation is set to rise over many areas experiencing increases in precipitation (IPCC, 2001b). In the dry subtropics, no significant change in precipitation is expected. There is no agreement as to how precipitation intensity and distribution is expected to change in the humid tropical regions. In the UK, pronounced increases in precipitation over northern England and Scotland in winter, and slight decreases in precipitation over Wales and Central England in summer are expected (Parry, 2000).

The process of evaporation converts liquid water from open water bodies, exposed soil or vegetation with underlying soil, into water vapour. Transpiration is defined as the proportion of total evaporation entering the atmosphere via soil and vegetation (Shuttleworth, 1993). Evapotranspiration is a combination of both processes and potential evapotranspiration takes place when there is no limitation in available soil moisture. It is likely that increased air temperatures will lead to an increase in evaporation. The increase would be dependent on additional factors such as changes in net radiation, humidity, wind speed and precipitation.

GCMs coupled with vegetation models (GVMs) are increasingly being used to simulate plant response to global warming (Nielsen, 1998). However, estimating future changes

in transpiration is complicated by vegetation feedback arising as a result of changes in plant properties (e.g. surface roughness, albedo, root depth and stomatal properties).

Arnell and Reynard (1993) showed that with appropriate changes in radiation and humidity, it is possible that a 2°C temperature rise could cause an increase in potential evapotranspiration by up to 40% in a humid temperate region. They also showed that smaller increases were to be expected in a drier region where changes in humidity are relatively insignificant. A significant omission from their study was the role of vegetation feedback.

Despite some of the uncertainties, it is possible to draw some conclusions regarding changes in evapotranspiration. In the UK, it is expected that potential evapotranspiration will generally increase across all regions apart from in the north west due to increased humidity. Actual rates of evapotranspiration are limited by the amount of available water and so a reduction in precipitation would reduce the amount of available water leading to reductions in actual evapotranspiration.

2.5.2.1 Soil Moisture

Changes in soil moisture will have important implications for evapotranspiration. Climate models indicate that soil moisture is set to increase in the higher latitudes in winter with decreases in some areas. Reductions in soil moisture are likely in the summer in northern mid-latitudes and southern Europe. More regular soil moisture deficit is expected due to warmer, drier summers. Reductions in soil moisture in North America are possible but there is uncertainty about the effects in northern Europe and northern Asia.

2.5.2.2 Groundwater Recharge

Groundwater recharge is dependent up on the balance between a change in the recharge season or the number of recharge events and the quantity of available water for recharge during the season. In semi-arid and arid areas, where recharge takes place after flood events, a change in rainfall occurrence and intensity frequency will alter the number of recharge events. Where winter precipitation is set to rise, there is uncertainty whether the higher rates of precipitation would restore the imbalance as a result of a shorter recharge due to higher temperatures and evaporation during spring and autumn (Arnell et al., 1996).

2.5.2.3 Runoff

Changes in precipitation and evaporation will invariably affect runoff. Mean annual runoff is likely to increase in the higher latitudes and Southeast Asia due to increased precipitation. Increase in runoff is also likely in the Mediterranean, South Africa and Australia (IPCC, 2001b). However, high evaporative losses could cause reductions in runoff even where precipitation increases. Since runoff is particularly sensitive to precipitation (Boorman and Sefton, 1997; Chiew et al., 1995), only relatively high evaporative losses would lead to such a reduction.

Mountainous regions could see significant disruptions to seasonal runoff patterns. Presently, in the colder climes, water stored in snow packs in the winter is released as runoff during the spring thereby providing natural storage. Warmer temperatures could lead to precipitation instead of snowfall during the winter. This would give rise to increased winter runoff and reduced spring and summer runoff. Such a scenario could

have major impacts on communities that have not had to consider development of water resources because of a reliance on natural water storage.

In the UK, runoff is likely to increase across most parts except in the south and east. Increases are likely during winter whilst decreases in the summer, especially in the north are expected.

2.5.2.4 Flooding

GCM experiments suggest that flood frequencies are likely to increase in a warmer world though there is uncertainty for various reasons. Flooding will be influenced by changes in the direction and severity of depression and storms. Tropical cyclone activity, which is expected to increase as a result of global warming, may lead to increased flooding. It is also likely that warming at the mid latitudes would give rise to flooding due to El Niño. Catchment characteristics will be an important factor in buffering against potential flooding. Larger catchments with high soil permeability will be less prone to flooding than smaller catchments with relatively impermeable soils.

2.5.2.5 Drought

A reduction in mean precipitation, the number of wet days and an increase in potential evapotranspiration as a result of higher temperatures can lead to increased drought frequency and severity. More droughts are to be expected in a warmer world but there is uncertainty regarding regional drought patterns. It is possible that the relatively greater warming at the higher latitudes would lead to more droughts. This is because as temperatures rise, the atmosphere is able to hold more moisture and evaporate more

water from the surface. In addition, precipitation derives mainly from evaporation at the ocean, and because the rate of evaporation is slower on the ocean (because of a larger heat capacity) it follows that in a warmer world, precipitation will not increase as quickly as evaporation thus leading to drought.

In contrast, It is possible that increases in the frequency and severity of rainfall events may reduce the likelihood of drought - especially if the rainfall events lead to higher soil moisture content and greater groundwater recharge (Whetton et al., 1993).

2.5.3 Effects of Global Warming on Water Resource Systems

2.5.3.1 Impounding Reservoirs

Water resource facilities such as impounding reservoirs provide numerous benefits to communities. They are often operated as a network of multiple reservoirs to maximise their efficiency (Adeloye and Nawaz, 1997; Adeloye and Montaseri, 1998). Their ability to store water during times of plenty for supply during times of drought is amongst the most important to society. In regions subject to increased instances of prolonged drought periods combined with an increase in evaporation, reservoirs will come under increasing stress.

In addition to catchment precipitation and evaporation, reservoirs are also affected by evaporation from the surface and precipitation on to the surface (Adeloye and Nawaz, 1998). Evaporation is significantly influenced by wind speed, humidity and temperature. Therefore, any change in future wind speed, humidity and temperature will affect evaporation. Surface evaporation from reservoirs in arid and semi-arid

catchments in particular, may be significant (Adeloye and Montaseri, 1999). In instances where reservoirs are prone to stress, management options would need to address reductions in deployable yield failing which the storage capacity would have to be increased, either by dredging or by raising dam height.

2.5.3.2 Climate Change and the Demand for Water

About 1.7 billion people (almost a third of the world's population) currently live in water stressed countries - where a water stressed country is defined as a country using more than 20% of its renewable water resources (IPCC, 2001b). This figure is expected to reach 5 billion by 2025. Global warming is likely to have a major impact on irrigation demand because higher temperatures would lead to larger crop water requirements. Domestic and industrial demands may not be significantly affected by climate change if measures are designed to increase the efficiency of water use.

In the UK, higher temperatures in southern and eastern England in the 2020s will lead to increased demand for water for domestic, agricultural and commercial purposes. It is estimated that the demand for water required for domestic and agricultural purposes will increase by 4% and 12%, respectively, by the 2020s in the UK (Herrington, 1996). This will exacerbate the pressures on water resources, particularly during the hot summer growing seasons.

Table 2.1 summarises expected changes in temperature, precipitation and drought occurrence across Europe, and has been compiled using information provided by Parry (2000). Figure 2.9 summarises the effects of a changing climate on UK water resources based on projections by the UK Climate Impacts Program (UKCIP).

2.5.4 Climate Change Effects and Uncertainties

Throughout this section, terms such as '*likely*' and '*expected*' have been used to represent the possibility of climate change and its effects. The use of such terms is rather vague and does not provide any real measure of likelihood. It is however possible to employ Monte Carlo simulation experiments to assess the sampling uncertainties in impacts on water resources of projected climate changes. This approach to risk analysis will enable the 'population of impacts' to be obtained, which will allow risks of having different levels of impacts to be quantified. This methodology has been adopted in the research and will be discussed in more depth in the next chapter.

2.6 Summary

The Earth has experienced global warming and global cooling throughout the ages which has led to widespread climatic changes in the past. The changes took place as a result of natural processes that are both external and internal to the Earth. External processes include changes in the Sun's output whereas internal natural processes contributing to climate change include volcanic activity and the ENSO phenomenon. Reconstructed and historical temperature records indicate that the Earth is currently undergoing a rapid warming period.

Climate models such as General Circulation Models (GCMs) have recently emerged as reliable tools in simulating the historical global climate - temperature in particular. Once calibrated, GCMs can be used to simulate future climate. GCM experiments reveal that the global mean temperature observed during the last decade has reached beyond the range of natural variability. It is now certain that anthropogenic activities

are responsible for global warming. The major contributors have been the release of large quantities of carbon dioxide in to the atmosphere and mass deforestation. It looks unlikely that the greenhouse gas emissions will be reduced significantly in the near future and so global warming will continue.

Global warming will lead to widespread climatic changes. A warmer world, on average will be a wetter world and liable to more extreme hydrological events. Increased rainfall variability, even in a slightly wetter climate, could lead to more droughts.

There is uncertainty regarding the regional impacts of global warming. Precipitation is the major driving force behind the hydrological cycle and any change in future precipitation will affect runoff and groundwater. In drier regions, an increase in evaporation and transpiration could also be significant. There is uncertainty in future changes in transpiration due to uncertainties in plant response to carbon dioxide changes. Higher temperatures will change the timing of snowmelt and this would have implications for regions reliant on natural water storage.

Changes in river regimes will affect water resource facilities such as impounding reservoirs. In areas with an increase in precipitation, water resources would generally be expected to benefit. In contrast, warmer summers with longer growing seasons and increased evaporation in the future would lead to greater pressures on water resources. Reservoir surface evaporation and precipitation fluxes would exacerbate the affects of climate change on large reservoirs. Reservoirs subject to stress as a result of high evaporative losses and reductions in precipitation could be further stressed by a rise in the demand for water.

Table 2.1: A summary of expected climatic changes in Europe (Parry, 2000).

Climatic Variable	Expected Change
Temperature	• Annual temperatures will increase at a rate of between 0.1°C and 0.4°C each decade; • There will be fewer cold winters by the 2020s and these will be almost non-existent by the 2080s; • Almost every summer by the 2020s will be warmer than the warmest summer experienced once a decade at present.
Precipitation	• An increase in rainfall and snowfall in northern Europe by 1-2% each decade, whereas southern Europe will experience rather smaller decreases; • Extreme precipitation events will increase in frequency, especially during winter.
Drought	• Increased summer drought risk in central and southern Europe.

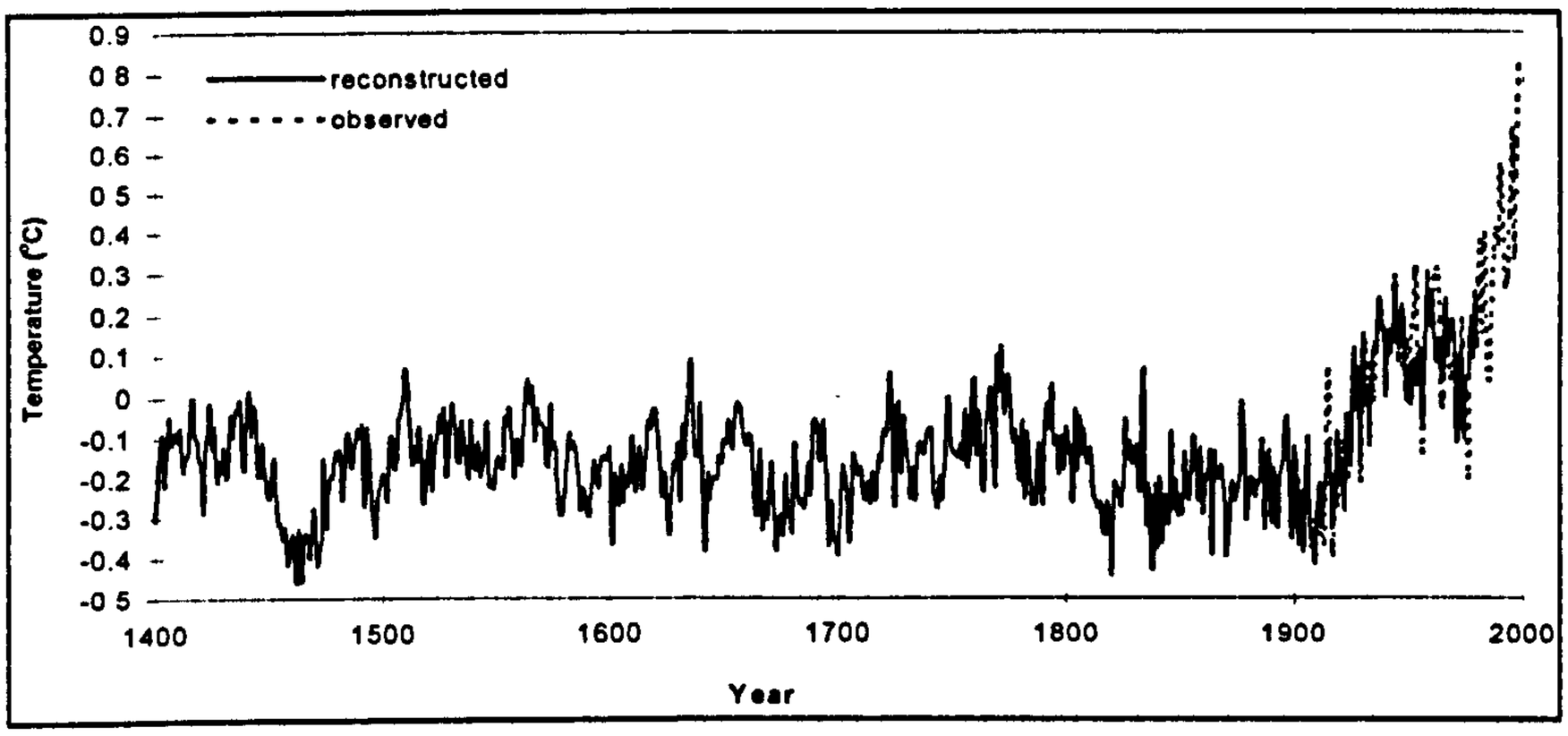

Figure 2.1: Annual average surface temperatures for the Northern Hemisphere (Mann et al., 1998).

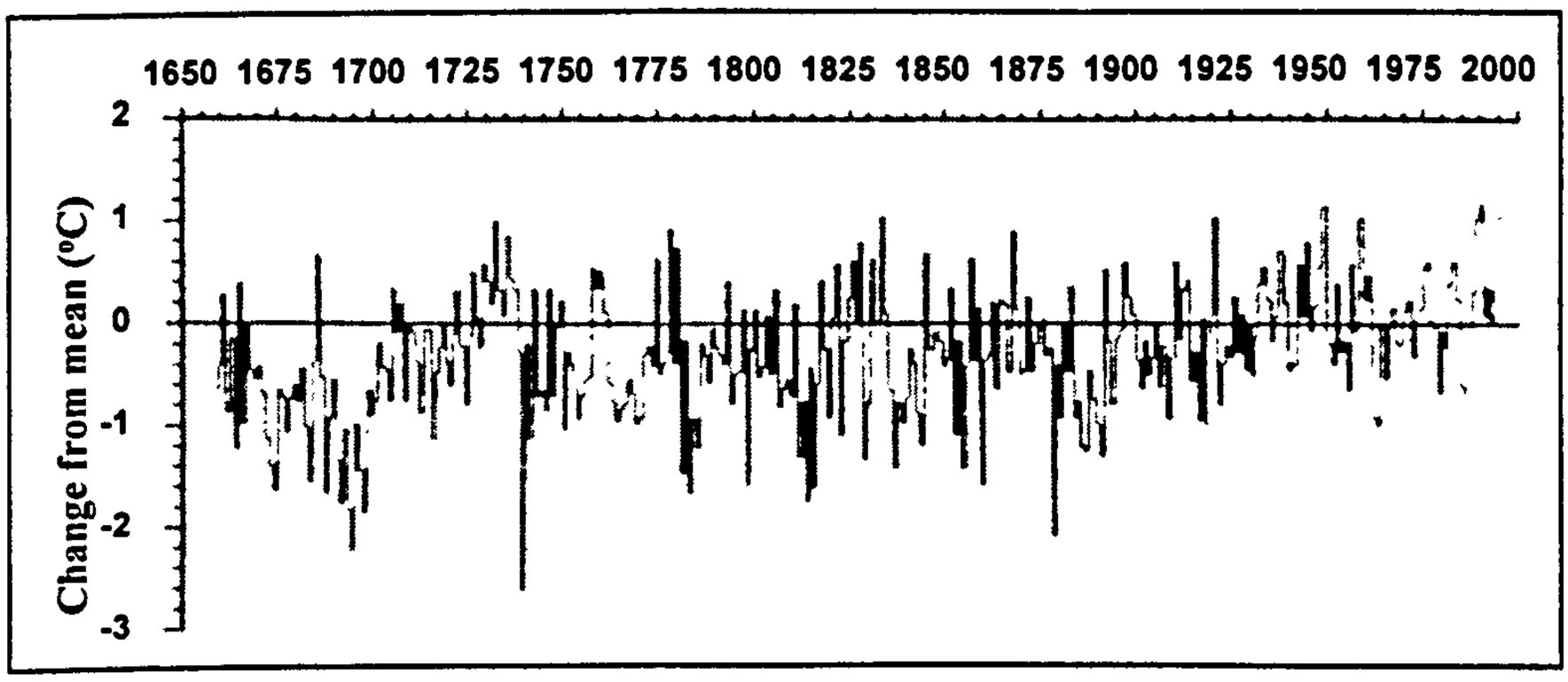

Figure 2.2: Central England temperature between 1659 and 1995 expressed as the difference from the 1961-1990 mean (Climate Research Unit, University of East Anglia).

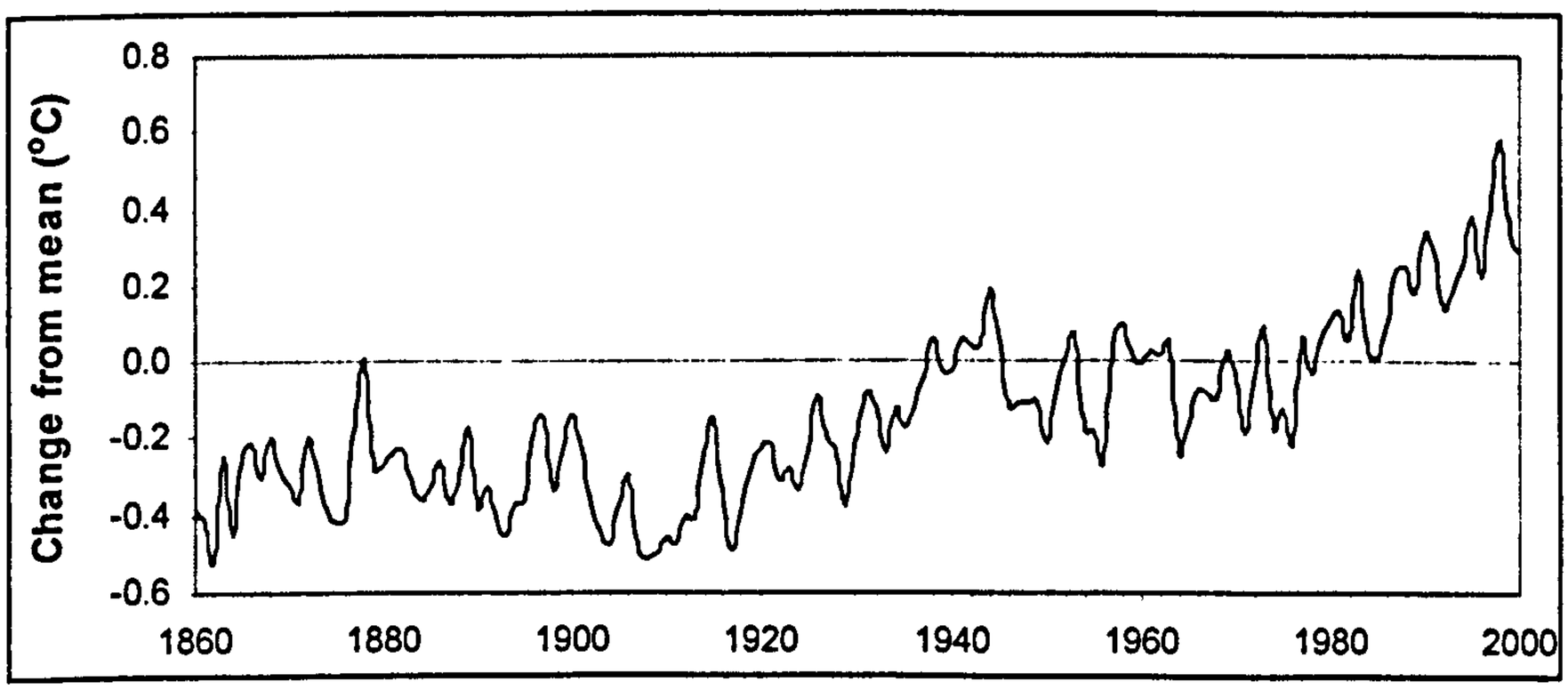

Figure 2.3: Changes in annual global mean surface temperature (surface air temperature over land and sea surface combined) from 1860 to 2000 relative to the baseline (1961-1990) period (Climate Research Unit, University of East Anglia).

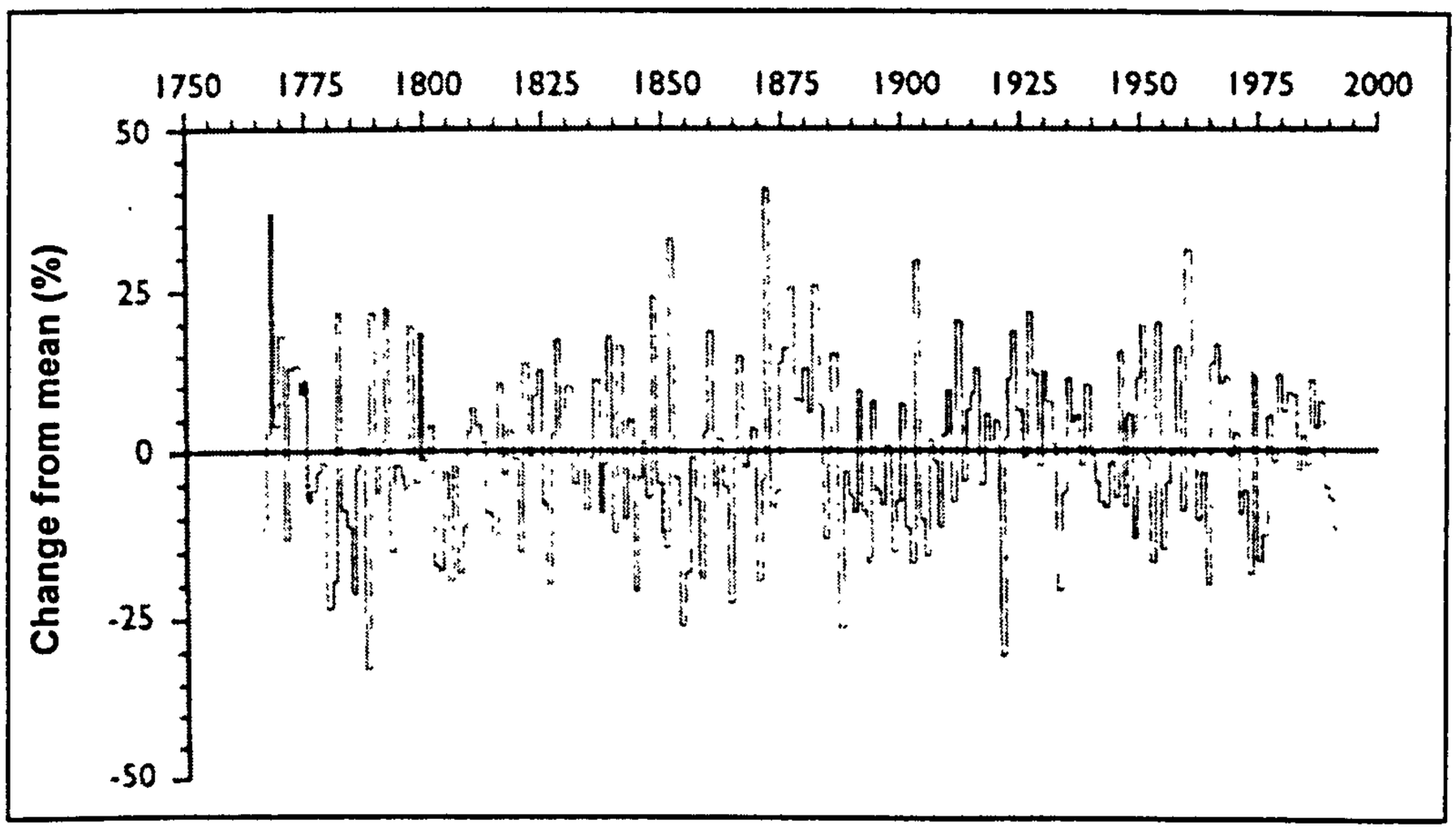

Figure 2.4: Change in England & Wales precipitation between 1766 and 1992, expressed as the difference from 1961-1990 mean (Climate Research Unit, University of East Anglia).

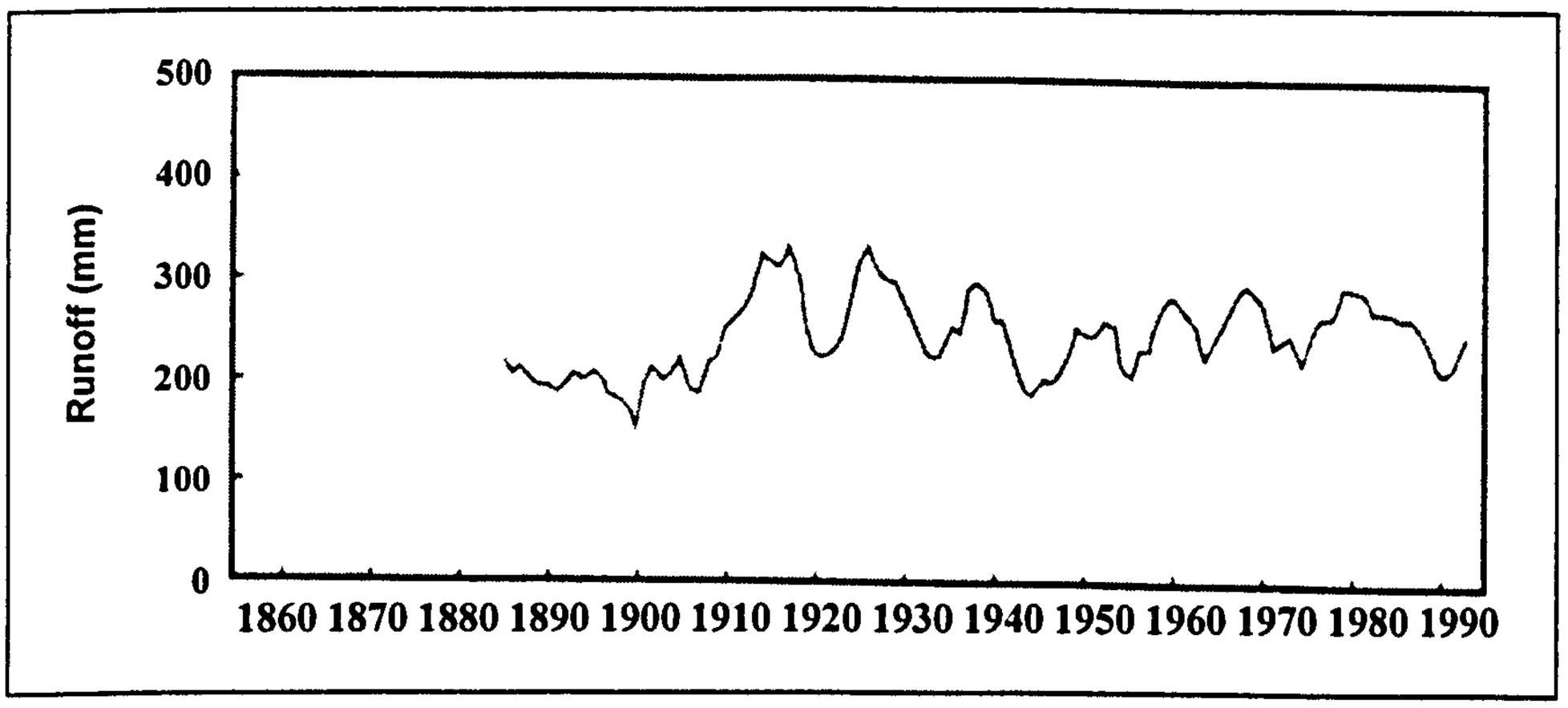

Figure 2.5: Observed runoff for River Thames at Teddington since 1882 (Environment Agency).

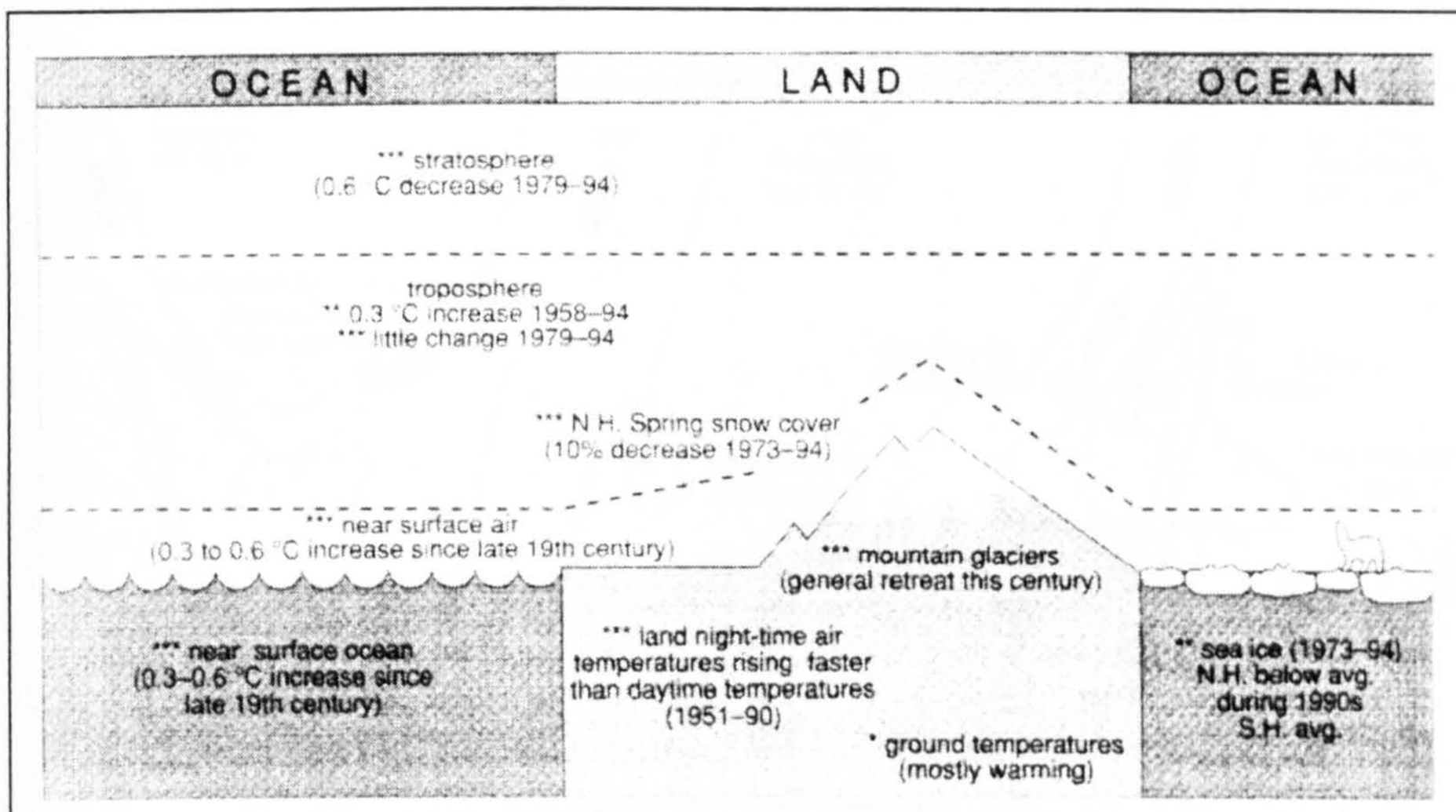

(a) Temperature indicators

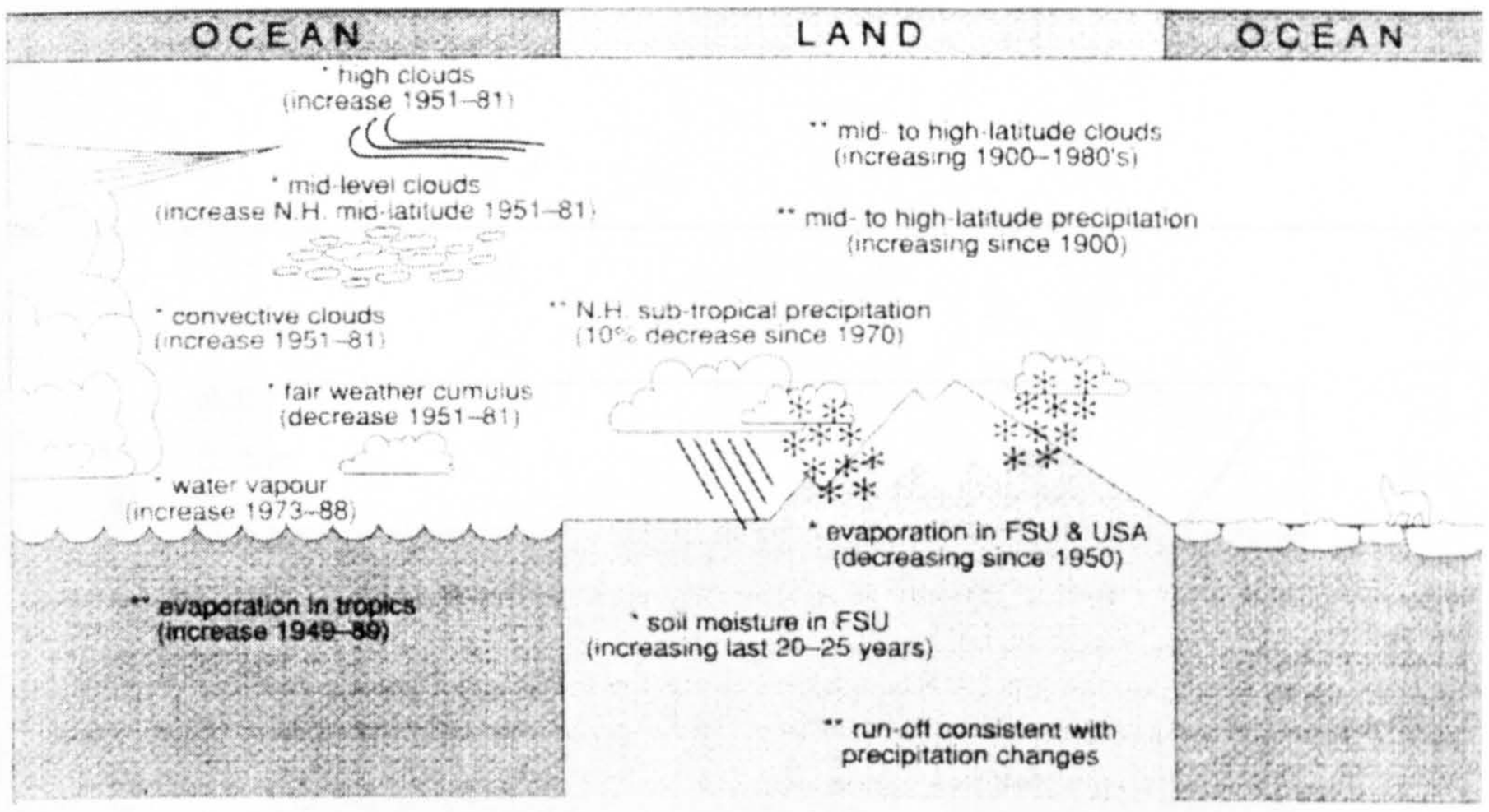

(b) Hydrological indicators

Figure 2.6: Summary of observed climatic trends over the instrumental period of record (Nicholls et al., 1996).

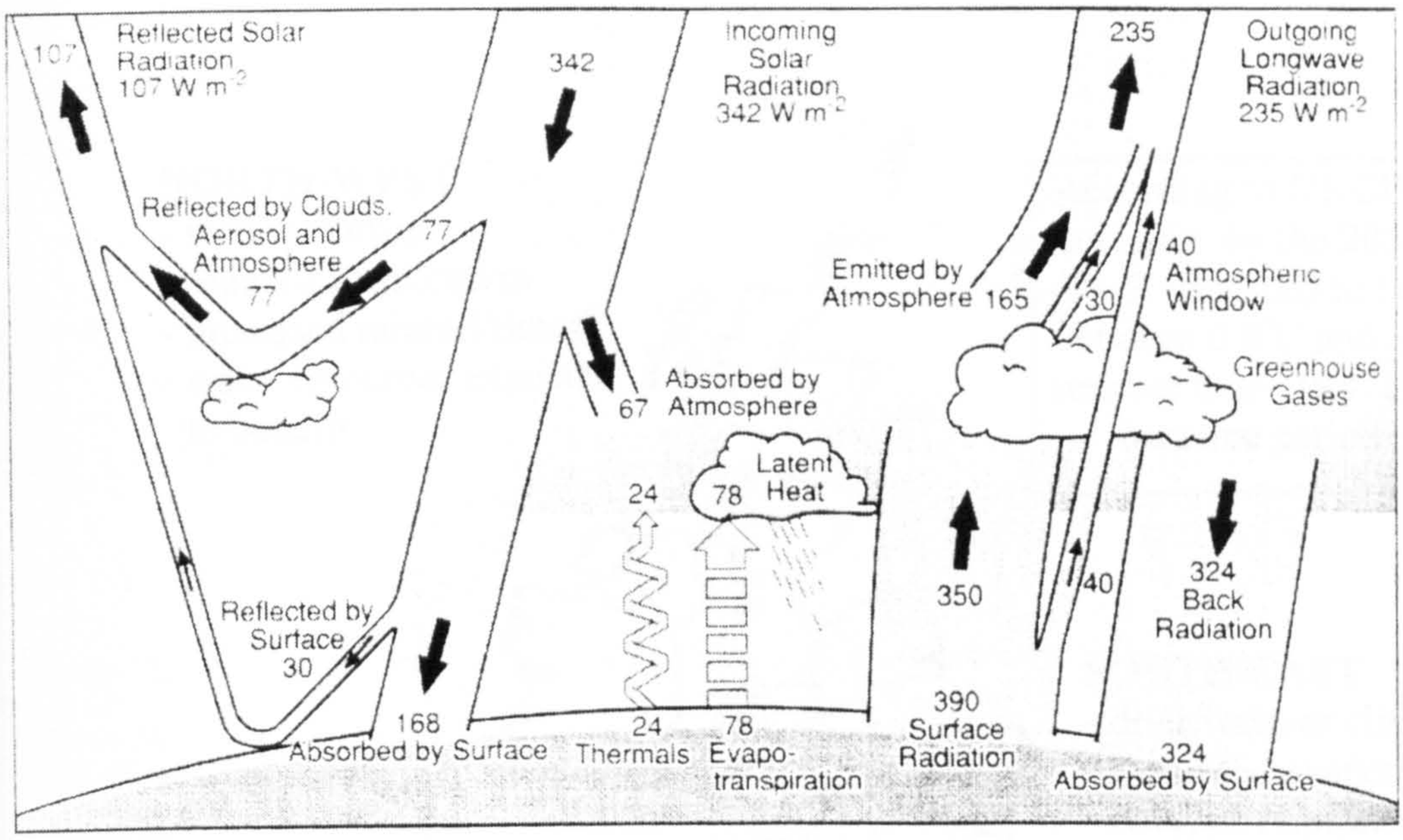

Figure 2.7: The Earth's radiation and energy balance (Trenberth et al., 1996).

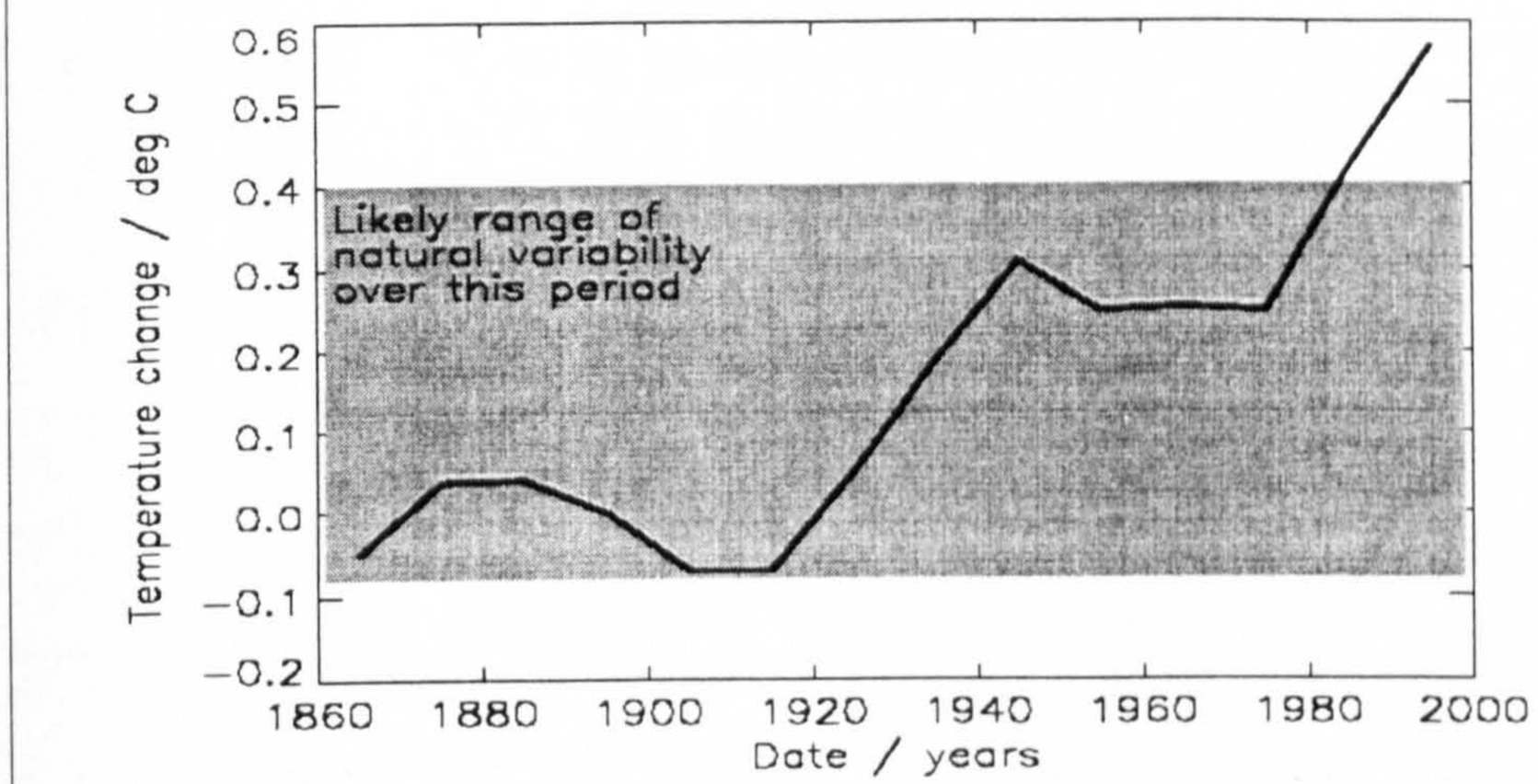

Figure 2.8: Observed change in mean global mean, decadal-average, temperature since 1860 shown by solid line. The shaded area shows the likely range of natural climate variability (Tett et al., 1997).

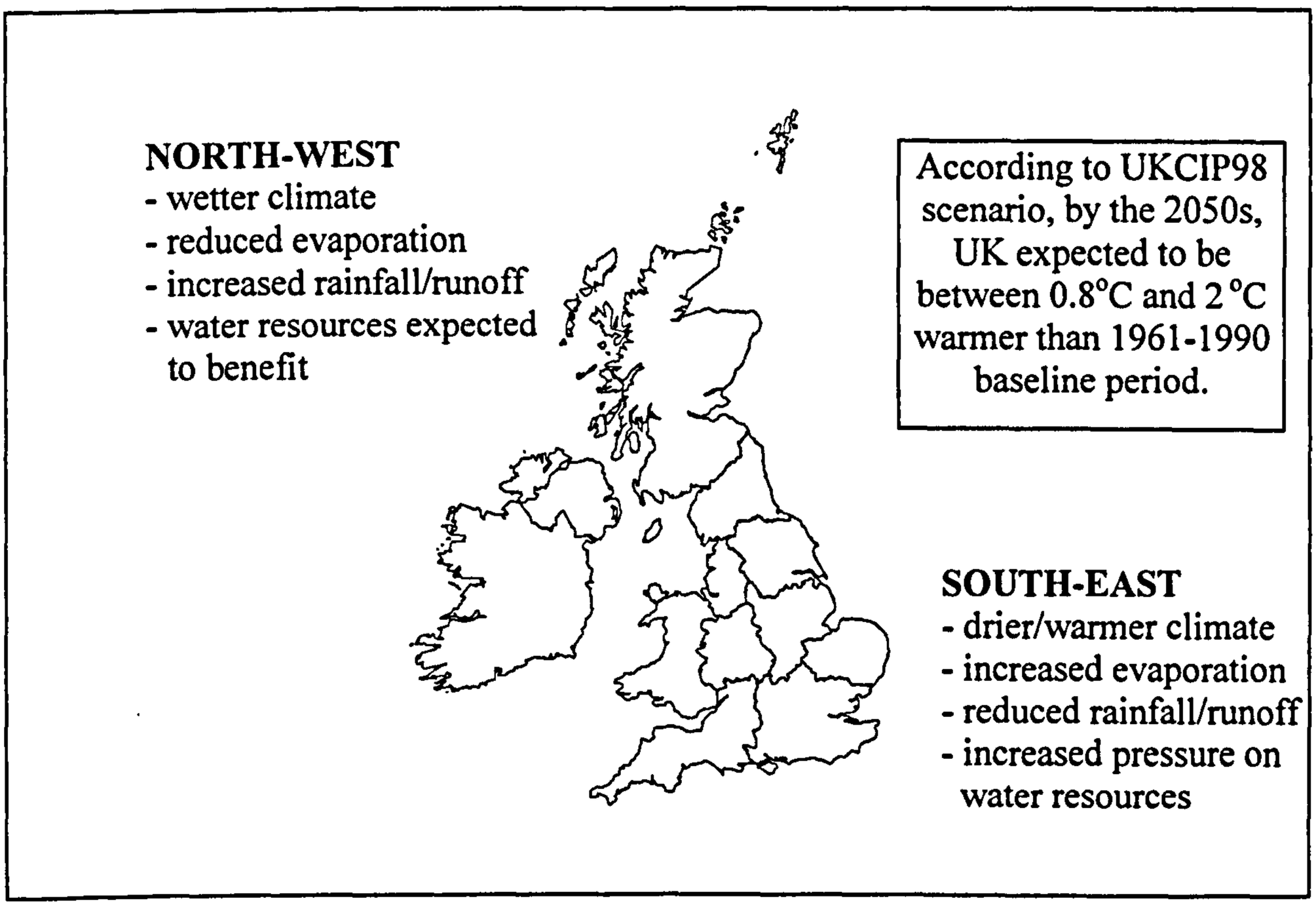

Figure 2.9: A changing UK climate.

CHAPTER THREE

CLIMATE CHANGE WATER RESOURCES IMPACTS ASSESSMENT AND UNCERTAINTIES

3.1 Introduction

There is no doubt that human-induced rapid global warming will bring about major changes to the Earth's climate system. Any large changes to the climate will also have implications for one of nature's most precious resource - water. Therefore, there is the need to ascertain the extent of climate change, assess its likely effects on water resources, and plan mitigating measures.

To this end, numerous studies have been carried out over the last decade or so to assess the impact of climate change on water resource systems (see Chalecki and Gleick, 1999 for a review). Impact assessment often involves three distinct stages: The first stage is to construct catchment-scale GCM-based climate change scenarios and use these to perturb baseline (current) climate to obtain future climate. This is then followed by forcing a catchment response model with both the current and future climate to obtain the corresponding runoff records. Finally, the hydrological data series are then input into a water resource simulation model to obtain possible impacts. Because of uncertainties introduced at successive stages of the assessment, it is important that the assessed impacts are viewed with caution (Hulme et al., 1999a).

As previously mentioned in section 1.1, uncertainties arise because of errors in global climate modelling and in 'downscaling' climate to the catchment scale, the imprecision

in hydrological and water resource systems modelling, and the limitation caused by using only single records for the impacts assessment (sampling uncertainty). It is possible that if the problem is posed in a sensitivity analysis context rather than prediction, which is commonplace (Arnell, 1996; Wood et al., 1997), then climate modelling errors and possibly downscaling errors are largely removed (Wood et al., 1997). Similarly, where both the baseline and future hydrology are based on the hypothesised rainfall-runoff scheme, the uncertainty due to this should also cancel out, leaving only the sampling uncertainty of the hydroclimate. By employing Monte Carlo simulation experiments, it is possible to assess the sampling uncertainties in impacts on water resources of projected climate changes. Such an approach enables the 'population of impacts' to be obtained as opposed to the single realisation of impact possible with traditional methods of assessment.

In section 3.2, the methodologies available for climate change water resources impacts assessment are described, with a particular emphasis on the traditional 'impacts' approach. Section 3.3 describes the ways to construct climate change scenarios, and details the role of climate models and their uncertainties. The discussion in section 3.4 focuses on methods for assessing the effects of climate change on hydrological processes such as streamflow. Some of the possible uncertainties arising during this stage of impacts assessment are also discussed. In section 3.5, methods of assessing the effects of climate change on water resource systems such as reservoirs are discussed. A particular emphasis is placed on Monte Carlo simulation techniques that allow the water resources impacts to be investigated within an uncertainty context. Section 3.6 reviews some notable climate impacts studies and discusses their main strengths and limitations. An extension of the traditional method for climate change water resource impacts assessment is also discussed.

3.2 Climate Impact Study Methodology

3.2.1 Impacts Study Approaches

There are three general approaches for conducting climate impact assessments (Kates, 1985; Carter et al., 1994): impact, interaction and integrated approaches. Each approach has its strengths and weaknesses, and these must be carefully examined before adopting a particular approach.

The impact approach is a relatively straightforward approach, and uses a specified change in climate to obtain the resultant impact. It can be thought of as an *'if-then-what'* scenario (Carter et al., 1994) - *if* the climate changes by certain amount, *then what* will be the likely impact? The approach assumes the effects of non-climatic factors to remain constant which is a significant limitation of the methodology. Despite this drawback, the impact approach is the most commonly adopted approach in climate change impacts assessments because of its simplicity.

The interaction approach also allows climate change impacts assessment to be carried out within a quantitative framework. However, it is more realistic than the relatively simple impact approach in that it incorporates the effects of non-climatic factors, such as land-use changes and feedback between climate and hydrological processes. This approach is becoming increasingly attractive particularly because of a greater understanding of some of the feedback processes.

The integrated approach is an attempt to improve on the interaction approach by incorporating the complex interactions of climate and society. For example, water

resource systems do not work in isolation but are typically linked to several sectors. Consequently, the effects of climate change on water resources may also have implications for agriculture, human health and coastal zones and fisheries (Strzepek, 1998). Also, some of the negative hydrological impacts can be mitigated by careful changes in the way water resource systems are operated. Therefore a holistic approach needs to be adopted that attempts to include the various sectors in the assessment. Investigators have used the Integrated Approach for assessments in the USA (Rosenberg et al., 1993), Egypt (Yates and Strzepek, 1998) and Canada (Cohen, 1991) and the UK (Loveland et al., 2000). However, small-scale research projects tend not to use this approach mainly due to time and budgetary constraints.

A climate change impact assessment methodology recommended by the United Nations Intergovernmental Panel on Climate Change (Carter et al., 1994) is shown in Figure 3.1. The first step requires identification of the goals of the assessment, the resource under investigation (e.g. water resources), the study area, a suitable time horizon, relevant data needs and the wider implications of the work. Step 2 involves the selection of a suitable method for impact assessment from a range of analytical methods. Methods utilising quantitative modelling are often preferred in impact assessments. Step 4 requires definition of future state of the climate with respect to the present conditions. Steps 5 and 6 involve the assessment of the effects of climate change on biophysical systems (such as rivers) and socio-economic systems (such as reservoirs), respectively. Step 7 is carried out in conjunction with steps 5 and 6 by incorporating feedback processes and management changes in the face of climatic change (e.g. a change in reservoir operational practices). Once the possible impacts of climate change on a water resource system are ascertained, it is essential to provide some adaptation strategies. For

example, possible adaptation strategies within a water resources context may include promoting more efficient use of water to cut demand.

3.3 Climate Change Scenarios

Climate change scenarios form the basis for climate impact studies. A climate change scenario can be defined as *'a coherent, internally-consistent and plausible description of a possible future (climatic) state of the world'* (Carter et al., 1994). It is worth noting that climate change scenarios are not predictions like weather forecasts. Weather forecasts make use of large quantities of meteorological data to predict the weather several days in advance. In contrast, a climate scenario provides an indication of what the future mean climate might be over decades or centuries depending on certain assumptions. These assumptions include future levels of greenhouse gas emissions, land use changes, and changes in climate system behaviour over long periods of time.

3.3.1 Types of Climate Scenarios

There are a number of available techniques for the construction of climate change scenarios. These include hypothetical scenarios, spatial and temporal analogues, and scenarios based on climate models. Hypothetical scenarios consist of arbitrary changes in climate. The use of hypothetical scenarios in sensitivity studies is a great advantage and, combined with the relative simplicity of the technique, have been widely used to assess the effects of arbitrary changes in climate on water resources (Nemec and Schaake, 1982; Bultot et al., 1988; McCabe and Hay, 1995; Mehrotra, 1999). However, a major limitation is that given their arbitrary nature, these scenarios do not present a realistic picture of likely future climate.

Spatial and temporal analogue scenarios are based on the assumption that the future climate in one region is analogous to current climate in another region, or from another time-period. For instance, given that the future climate of south east England is expected to become like the present climate of the Mediterranean, this technique could be used to construct scenarios for south east England. Nawaz et al. (1999) used a variant of this approach to construct future climate for a region in Iran. The main problem with this technique is that the causes of climates of the past or from different regions are different to the causes underlying future, greenhouse gas induced climate change. The only credible tool currently available for simulating future climate is the use of complex numerical climate models referred to as General Circulation Models or GCMs (Carter et al., 1999).

3.3.2 Climate Modelling and Uncertainties

To ascertain the extent of future climate change due to greenhouse gases, a climate model must first be formulated, calibrated and validated against current climate. Modelling the climate requires a mathematical formulation of the Earth's energy balance (depicted in Figure 2.7). In addition, a representation of the exchange of energy and water vapour between the atmosphere and land surface is required (see Figure 3.2). Therefore, while it is accepted that rising concentrations of greenhouse gases will lead to global warming, feedbacks in the climate system, in addition to the inherent uncertainty in future levels of greenhouse gases, make it difficult to predict climate change, especially at the regional scale (Stone, 1992). Some of these uncertainties are examined in more detail below.

3.3.2.1 Climate System Feedback Uncertainties

The major climate system feedback mechanisms are water vapour, cloud-radiation, ocean-circulation and ice-albedo feedback (Houghton, 1997). Feedback is termed positive if it accelerates global warming while negative feedback tends to buffer the warming effect. Water vapour feedback is the most significant. A warmer atmosphere has a higher moisture capacity because of an increase in evaporation. This results in a positive feedback (i.e. global warming is accelerated) because water vapour is a potent greenhouse gas. The role of cloud-radiation feedback in the climate system is more uncertain because several processes are in operation. Clouds reduce the incident solar radiation by reflecting a proportion back into space (i.e. negative feedback). They also have a blanketing effect on the Earth, in much the same way as greenhouse gases. The effects of clouds on solar radiation depend on a number of factors including their composition and height. Therefore, cloud radiation feedback may be either positive or negative. The most probable average value of cloud-radiation feedback is estimated as slightly positive - although there are likely to be significant regional variations (Houghton 1997).

The oceans too play a large role in determining the climate hence the importance of ocean-circulation feedback. Oceans are a major source of atmospheric water vapour. They also have a large heat capacity and they redistribute this heat through their internal circulation. Only an accurate representation of ocean structure and dynamics can lead to adequate simulation of climate change, especially at the regional scale.

At the higher latitudes, sea ice-albedo feedback is another potentially significant process that might lead to accelerated warming. This would occur because the thaw of sea ice

in a warmer world would lead to less solar radiation being reflected back into space. This would then have the effect of further decreasing the sea ice extent thus leading to further warming (Trenberth et al., 1996). However, increased open water would result in more evaporation and hence increased atmospheric water in the form of fog and low cloud cover thus offsetting the reduction in surface albedo (Trenberth et al., 1996).

The greatest uncertainty in climate change prediction arises from such feedback mechanisms, especially those relating to the behaviour and characteristics of clouds in warmer world (Hulme and Jenkins 1998).

3.3.2.2 Uncertainty in Greenhouse Gas Emissions

In addition to uncertainty in feedback processes, the prediction of climate is hampered by the uncertainty in predicting future levels of greenhouse gases. Since greenhouse gases are largely held responsible for climate change, then the prediction of future greenhouse gases is central to climate change projections. However, predicting future levels of greenhouse gases is an extremely difficult, if not impossible, task. This is because greenhouse gas emissions depend on a number of factors such as population, economic growth, energy use, energy resource development and the influence of efforts to curb emissions.

Atmospheric carbon dioxide levels are also influenced by natural processes such as biosphere feedback. For example, as increasing amounts of greenhouse gases are released into the atmosphere, biological or other natural biosphere processes could disrupt the carbon cycle and lead to a more rapid build up of atmospheric carbon dioxide. This would be followed by the release of large quantities of carbon dioxide

into the atmosphere resulting in positive feedback. Goulden et al. (1998) provide a good example of this. They warn that even a small amount of warming in the northern hemisphere could be enough to trigger thawing and subsequent decomposition of the frozen soil bases of the vast boreal forests of the northern hemisphere. This would lead to large quantities of CO_2 being released to the atmosphere. This is especially worrying given that an estimated one-quarter of all the world's terrestrial carbon is locked in the frozen soil bases.

As well as the input of CO_2 to the atmosphere, the issue is further complicated by the natural processes that remove CO_2 from the atmosphere. For example, photosynthesis of trees and other vegetation on land, and absorption by phytoplankton in the oceans (Jones, 1999).

Because no single assumption on future emissions can be made, it is necessary to make a variety of different assumptions to get an idea of the range of possibilities in future levels of greenhouse gases, termed emissions '*scenarios*'.

The IPCC produced six emissions scenarios (IS92a-f) in 1992 and one scenario in particular - the IS92a - has been adopted as a standard scenario for impacts assessments (Wigley and Raper, 1992). This is despite the IPCC's recommendation that all six IS92a scenarios be used to represent the range of uncertainties in emissions (Alcamo et al., 1995). The IS92a is termed the '*business-as-usual*' scenario and its popularity in impact assessments stems from the fact that it is considered the most likely scenario in the absence of strong pressure to curb greenhouse gas emissions.

Despite strong efforts to curb emissions, it looks likely that emissions will continue to

rise (IPCC, 2001a), especially considering that emissions in developing countries are rising. Although many nations have set emissions reduction targets, they are not being met, primarily because of the effects on the economy. At the Rio Earth Summit in 1992, a hundred and thirty-seven countries signed up to the UN Framework Convention on Climate Change (UNFCCC). The developed countries agreed to take the lead and reduce carbon dioxide emissions to below 1990 levels by 2000. However, the treaty was not honoured by most nations and the countries met again in 1997 in Kyoto. This time they agreed on reducing emissions to below 1990 levels by 2008-2012. USA, a major contributor of greenhouse gas emissions, recently declined to honour the Kyoto Protocol stating that it was not in the country's economic interest to do so. This put the entire Kyoto treaty under threat and the world's nations met again in July 2001, this time in the German city of Bonn. During this meeting the 1997 Kyoto protocol was modified, largely due to Japanese pressure, and agreement was reached after much deliberation. However, USA - producer of 25% of the world's greenhouse gas emissions - remained unperturbed and did not ratify the treaty.

The IS92a scenario is an intermediate scenario compared to other IPCC 1992 scenarios (IS92b-IS92f). It is based on a World Bank projected global population of 11.3 billion by 2100, an average annual global economic growth rate of 2.3% between 1990 and 2100 and assumes a combination of renewable and non-renewable energy sources in the future. The scenario assumes that the cost of nuclear energy will increase in the future and that the price of solar power will drop until they are at roughly the same level. Under the scenario, carbon dioxide *emissions* are expected to rise from about 7 Giga-tonnes of carbon per year (Gt C/yr) in 1990 to around 20 Gt C/yr by 2100 (see Figure 3.3a). This will lead to atmospheric CO_2 *concentrations* to double from 354 parts per million by volume (ppmv) in 1990 to 708 ppmv by around 2100 (see Figure 3.3b).

Although the IS92a scenario continues to be used in forcing climate models, the IPCC have recently produced another set of emissions scenarios based on current understanding of future changes in factors that affect emissions. These are a total of 40 scenarios and are defined in the Special Report on Emissions Scenarios or SRES (IPCC, 2000). The 40 SRES scenarios are grouped into four 'scenario families', each with its own projection of demographic, socio-economic and technological futures. For a scenario comparable to the IS92a, (SRES-B2) population growth is more modest and is expected to reach 10.4 billion by 2100 compared to IS92a projection of 11.3 billion. Carbon dioxide emissions are expected to rise to 680 ppmv by 2100. Figures 3.3a and 3.3b show the changes in carbon dioxide emissions and concentrations, respectively, under the IS92a and SRES-B2 scenarios. It can be observed that a slow down in carbon dioxide emissions is expected between 2020 and 2080 according to both scenarios.

3.3.2.3 Climate Change Impacts on Evapotranspiration and their Uncertainties

In water resources impact assessments, changes in precipitation along with evaporation and transpiration are the most important requirement (Arnell, 1996). The investigation of the effects of climate change on river flows may require changes in potential evapotranspiration (evaporation and transpiration), while changes in open water evaporation will be required to assess the effects of changes in reservoir surface fluxes on reservoir systems which may be significant (Fennessy, 1995; Gan et al., 1991; Nawaz and Adeloye, 1999; Nawaz et al., 1999).

Evaporation from an open water surface is dependent on net solar radiation, temperature, wind speed and humidity. Evaporation from the land surface consists of *evaporation* from soil and vegetation surface, and the *transpiration* through small

openings in plants called *stomata* (Chow et al., 1988). Evaporation from the land surface and transpiration from vegetation is termed the *evapotranspiration.*

Actual evapotranspiration is affected by the supply of available water at the evaporative surface (i.e. the soil moisture) in addition to the factors influencing open water evaporation. For climate impact assessments, the changes in potential evapotranspiration - the evapotranspiration taking place with an unlimited supply of available moisture - are usually required. Determining the change in potential evapotranspiration under global warming therefore requires changes in the factors that influence potential evapotranspiration.

The most comprehensive method for calculating evapotranspiration is by using the expression developed by Penman and Monteith (Monteith, 1965). This expression relates potential evapotranspiration ET_o (mm) to a number of parameters and is defined as (Monteith, 1965; Shuttleworth, 1993):

$$ET_o = \frac{1}{\vartheta}\left[\frac{\Lambda R_n + \rho_a c_p (e_s - e_d)/r_a}{\Lambda + \varpi(r_s + r_a)/r_a}\right] \qquad (3.1)$$

where,

ϑ = latent heat of vapourisation of water (MJ/kg) = $2.501\times10^6 - 2370\Omega$ where Ω is the temperature in $^\circ$C;

$\Lambda = 4098e_s/(237.3+\Omega)^2$, e_s is saturation vapour pressure at air temperature in kilopascals (kPa);

R_n is the net incoming solar radiation (MJ/m^2/day);

ρ_a = density of moist air (kg/m^3);

c_p = specific heat of moist air (=1.013 kJ/kg/$^\circ$C);

e_d = saturation vapour pressure at dew point temperature (kPa);

r_a = net resistance to diffusion through the air from surfaces to height of measuring instruments - it is also known as the aerodynamic resistance and is inversely proportional to wind speed and dependent on the height of the vegetation covering the ground;

r_s = net resistance to diffusion through the surfaces of the plant leaves and soil (stomatal resistance);

ϖ = psychometric constant dependent on specific heat of moist air, atmospheric pressure, molecular weight of moist and dry air and latent heat of vapourisation of water, values of ϖ for a given air temperature can be found in published tables.

In addition to its completeness, the Penman-Monteith Equation (3.1) has other advantages such as being able to provide good estimates of evapotranspiration from crops and forests (Beven, 1979). However, it is clear from Equation (3.1) that substantial data are required to obtain estimates of potential evapotranspiration. Often, such data may be difficult to obtain and hence, alternative expressions may be adopted.

One approach is to use the combined energy balance and aerodynamic method technique (*Bowen ratio* method) to determine the evaporation rate in mm (E_o) (Chow et al., 1988) as follows:

$$E_o = \frac{R_n}{(\vartheta \rho_w)(1 + b_r)} \tag{3.2}$$

where,

R_n and ϑ are defined above;

ρ_w = water density (kg/m^3) = 1000 kg/m^3 for temperatures between 0 °C and 10 °C and reduces by 1 kg/m^3 for every 5 ° C rise in temperature;

b_r = Bowen ratio - which is the ratio of sensible heat flux and water vapour heat flux.

As with Equation (3.1), the application of Equation (3.2) requires measurements of net solar radiation which are often unavailable. In such instances, measurements of sunshine hours may be used in conjunction with meteorological tables (see Doorenbos and Pruitt, 1975) to estimate solar radiation. In contrast, evaluation of the Bowen ratio might not be so straightforward since it requires the specific heat capacity at constant pressure, heat diffusivity, temperature, latent heat of vapourisation and vapour pressure. This implies that although Equation (3.2) is not as complex as Equation (3.1), large amounts of data are nonetheless required for estimating evaporation. Once the evaporation has been evaluated, it can be converted to potential evapotranspiration using various methods (see e.g. Shuttleworth, 1993; Shaw, 1994).

In addition to the well documented factors influencing evapotranspiration, the implications of rising carbon dioxide concentrations may be significant. It is understood that carbon dioxide influences evapotranspiration in two main ways by causing changes to vegetation. The first is that elevated levels of carbon dioxide can lead to full or partial plant stomatal closure (Cure and Acock, 1986; Rosenberg et al., 1990). Kimball and Idso (1983) reviewed nine experiments concerning the effects of elevated carbon dioxide concentrations on plant stomata. They concluded that a carbon dioxide doubling would lead to an increase in stomatal resistance of 34%. In a review of 21 experiments, Cure (1985) concluded that 51% increase in stomatal resistance was to be expected under carbon dioxide doubling. Morrison (1987) showed that a carbon

dioxide doubling could lead to a 60% increase in stomatal resistance. It should be noted that a large increase in stomatal resistance will not necessarily lead to a large reduction in transpiration. This is because, as transpiration begins to reduce due to stomatal closure, leaf temperature tends to increase, which subsequently increases transpiration (Cure and Acock, 1986). For example, Cure and Acock (1986) found that carbon dioxide doubling led to an average increase in stomatal resistance of 34%. The resulting impact on transpiration was slightly less - averaging around a 23% reduction. Aston (1984) found that a doubling of stomatal resistance (i.e. 100% increase) resulted in a 20-40% reduction in transpiration depending on ambient conditions. Other investigators (e.g. Kimball and Idso, 1983; Rogers et al., 1983; Morrison, 1987; Parry, 1992) have reported a 33% reduction in transpiration due to carbon dioxide doubling.

Another way in which carbon dioxide affects evapotranspiration is by increasing plant foliage due to vegetation feedback. Vegetation feedback would be initiated by the increased growth rate of some plant species due to higher concentrations of atmospheric carbon dioxide. An increase in plant bio-mass would lead to a rise in transpiration and a higher leaf area index (i.e. leaf area/ground area) would result in more evaporation. Kimball (1986) estimated that doubling of carbon dioxide concentration, assuming all else to remain constant, will increase the growth of plants such as root crops, grains, beans and most trees by $34 \pm 6\%$ (95% confidence level). Kimball et al. (1993) noted that, based on many greenhouse and growth chamber studies, plant growth typically increased by over 30% with carbon dioxide doubling. The degree of plant growth may also depend on temperature. If the climate warms by 3°C for instance, the relative increase in plant growth caused by carbon dioxide doubling could be as high as 56% instead of the 34% mentioned previously (Rosenberg et al., 1990). Idso et al. (1987) showed that under carbon dioxide doubling, plant growth reduced by 60% at a

temperature of 12°C. However, as the temperature was increased to 34°C, the corresponding plant growth increased by a phenomenal 134%.

It is possible, however, that the changes in evapotranspiration due to the two kinds of plant response, may, to some extent, cancel each other out (Rotter and van de Geijn, 1999). For example, Kimball et al. (1993) showed that for a wheat crop, potential evapotranspiration increased by 24% due to a 3.3°C temperature rise alone. When other climate scenarios were incorporated such as changes in radiation, vapour pressure, and wind speed, evapotranspiration was estimated to increase by 9%. When the effects of carbon dioxide doubling were included, the combined effects of stomatal conductance and increased foliage and leaf area index caused evapotranspiration to rise by only 2%. In other words, a 7% reduction in evapotranspiration was observed due to carbon dioxide doubling because increased plant foliage had largely offset the effects of stomatal resistance on evapotranspiration.

There appears to be more confidence in the effects of carbon dioxide doubling on stomatal resistance than on vegetation growth because the latter is also influenced by temperature.

The totality of the effect of carbon dioxide doubling on evapotranspiration can be expressed as (Wigley and Jones, 1985):

$$E_2 = c_f r_s g_p E_1 \tag{3.3}$$

where,

E_2 = changed evapotranspiration caused by a doubling of CO_2 concentrations;

E_1 = evapotranspiration under current carbon dioxide concentration;

c_f = climatic factors (excluding carbon dioxide);

r_s = stomatal resistance factor;

g_p = increased plant foliage factor.

Equation (3.3) can be used to carry out a sensitivity study of changes in CO_2 emissions and other factors on evaporation. For example, to assess the effects of a rise in stomatal resistance alone on evapotranspiration (E_s), the following Equation (3.4) can be used (Idso and Brazel, 1984):

$$E_s = E_1\left(1-\frac{1}{3}f\right) \tag{3.4}$$

where r_s = 1-1/3f, f is the fractional area of catchment covered by vegetation ($0 \le f \le 1$) and c_f and g_p are both equal to unity. If the entire catchment is covered with vegetation then f=1 and the reduction in evapotranspiration is 33%, i.e. a linear relationship. Where climate change scenarios are simultaneously being considered, then the appropriate scenario for term c_f in Equation (3.3) is evapotranspiration. There are currently no established formulations for g_p - therefore the only option available is to assess its impact on evapotranspiration by arbitrarily changing its value. However, recent GCMs can simulate the effects of changing atmospheric CO_2 concentrations on plant stomatal closure and plant growth (see Cox et al., 1998). This would imply that such GCM experiments might well lead to more realistic evapotranspiration scenarios.

The GCM-based evapotranspiration simulation is carried out via a land-surface scheme embedded in the GCM. The land-surface model is coupled to vegetation properties (such as leaf area index, height, and canopy conductance), based on climate, soil carbon

and nitrogen content and the atmospheric carbon dioxide concentrations. The coupling to the GCM is two-way, with the GCM providing climatic data to the vegetation model and the land-surface model predicting the vegetation properties from which the GCM land surface parameters can be derived. However land-surface schemes are limited in their ability to simulate vegetation changes due to uncertainties in future levels of carbon dioxide concentrations (Gates et al., 1996).

3.3.3 Scenarios based on Climate Models

Climate models of varying degrees of complexity have been developed by climate modelling centres throughout the world. These range from simple climate models (SCMs) to the more complex general circulation models (GCMs). The main driving force behind the models are similar but the incorporation of some important processes are handled differently by different models. Some important processes may be incorporated in one model but not another. Common to all GCMs is their ability to represent the atmospheric and oceanic processes that drive the climate. However, although atmospheric processes were well represented in early GCMs, the ocean was modelled in a rather simplistic way, considering it as a simple slab about 50-100m thick. In these early models, adjustments needed to be performed to allow for heat transport by the ocean current. However, when the model was forced with carbon dioxide, it was not possible to incorporate any changes in that transport that may occur (Houghton, 1997).

To capture the climatic processes more realistically, the ocean circulation must be directly coupled to the atmospheric circulation. The latest GCMs have been developed with this in mind and are known as coupled atmosphere-ocean models (AOGCMs).

The coupling is important because, by representing the ocean circulation, AOGCMs are able to simulate the time lags between a change in atmospheric composition and the corresponding climatic response (Carter et al., 1999). Moreover, AOGCMs can provide realistic simulations of the climate since they represent the exchange of heat, water and momentum at the ocean-atmosphere interface. The models have primarily been developed to simulate the effects of the enhanced greenhouse effect on climate up until the end of this century. Climate models are usually forced with carbon dioxide or its greenhouse gas equivalent to obtain an estimate of future climate.

3.3.3.1 GCMs

GCMs are complex mathematical models that solve equations of conservation of mass, momentum and energy that describe the processes in the atmosphere, ocean and land (Gates et al., 1996). The models portray the Earth as a three-dimensional grid, typically having a spatial resolution of between 250-600 km. The atmosphere is usually divided into 10 to 20 vertical layers and the oceans may be divided into up to 30 layers (Carter et al., 1999). The atmospheric layers are evenly distributed with a typical thickness of about 1000m (Houghton, 1997). In contrast, ocean layer thickness may range from 50m at the surface to 900m in deep ocean.

To simulate past and present climate, and estimate future climate, a GCM is usually run for many hundreds of years (e.g. 1400 years in the case of a UK Hadley Centre GCM) to provide a control climate (Hulme and Jenkins, 1998). The carbon dioxide forcing used is kept constant, usually at pre-industrial levels. Then, starting from some arbitrary point on the control run, the carbon dioxide forcing is increased. The starting point is taken to represent the start-point of industrialisation when human influences would have been relatively small. 1860 is usually selected as the point to introduce the

rise in carbon dioxide concentrations since recorded global temperature records are available for model validation.

The carbon dioxide forcing increases at the observed rate of increase between 1860-1990 (or more recently, 1860-2000) to simulate the climate to the present. From 1990 (or 2000) until 2100, the model is forced with one or more future carbon dioxide emissions scenarios (see section 3.3.2.2) to provide a future simulated climate. The simulation from 1860-2100 is known as the 'simulation run'.

GCM experiments adopting a gradual greenhouse gas forcing outlined above are referred to as transient experiments. All recent GCM experiments are transient experiments (e.g. see Gordon and O'Farrell, 1997; Gordon et al., 2000) and have superseded the older, equilibrium experiments. In an equilibrium experiment, the CO_2 forcing was doubled instantaneously and was therefore not representative of the gradual rise observed in reality. Equilibrium experiments were common when climate modelling was in its infancy largely due to limitations in computing power. Another advantage of transient experiments over the equilibrium experiments is that they can be used to assess the negative forcing effects of sulphate aerosols in addition to the positive forcing of greenhouse gases.

In the transient experiments, the greenhouse gas forcing is usually based on a 1% per year compound rise in carbon dioxide concentrations which leads to carbon dioxide doubling by about 2020 and a quadrupling by 2090. This is equivalent to the combined effect of all the greenhouse gases in the IS92a emissions scenario (see section 3.3.2.2).

Model projections of future climate might be sensitive to the point of introduction of rising carbon dioxide concentrations on the control run. Consequently, several identical model experiments, each with the same historical and future changes in carbon dioxide, are started from several different points on the control run; this is commonly referred to as an '*ensemble*' of projections (Hulme and Jenkins, 1998). The mean climate change projected by these ensembles is essentially the same proving that long term climate change is insensitive to initial conditions. However, there are major interannual and interdecadal differences as a result of natural climate variability, especially at a regional level such as over Britain. Climate modelling centres therefore usually provide an average of ensembles. Output from GCMs can be applied in a variety of ways and this will be discussed later in the chapter.

Great advances in climate modelling have been made during the last decade, especially with coupled models incorporating more processes. However, it should be emphasised that this will in itself, not necessarily lead to accurate projections of future climate unless the processes are fully understood before implementation. Indeed, inadequate representations of these processes could lead to climate projections of the scientifically superior models being less accurate than the projections made by some of the older generation of climate models (Jones, 1999). Other significant limitations of GCMs include (Stone, 1992; Lins et al., 1997; Shackley et al., 1998):

(i) poor simulation of certain climatic variables such as daily precipitation compared to other variables such as mean air temperature;

(ii) inability to simulate atmospheric, land and oceanic processes that determine small-scale climates thus making the direct use of their outputs at the (micro) catchment scale rather dubious;

(iii) difficulty in rapidly implementing new processes as new scientific facts and understandings emerge;

(iv) inability to perform extensive uncertainty analysis - uncertainties in model parameters and inputs such as greenhouse gas forcing - primarily due to the requirement for massive computational resources.

Despite some of these drawbacks, much progress has been made in recent years in the physical basis and spatial resolution of GCMs. The models are able to simulate these processes largely due to the exponential rise in computational power. Recently, it has been possible to incorporate the effects of variations in solar activity and volcanic eruptions in some GCMs (e.g. Gordon et al., 2000). In addition, GCMs have seen vast increases in spatial resolution. The newer generation models are run at nearer 250 km spatial resolution with up to 20 vertical layers compared to 1000 km and 2-10 layers, respectively, for some of the older GCMs. For catchment scale studies, this resolution is still too coarse, and techniques are available to 'downscale' GCM output to a finer spatial scale. Downscaling techniques will be discussed in section 3.3.5.2.

As advances continue to be made in climate modelling, only GCMs have the potential to give geographically and physically consistent estimates of regional climate change (Carter et al., 1994).

3.3.4 GCM Selection for Impact Assessment

As implied previously, there are a number of GCMs available for use in climate impacts assessments; the selection of appropriate models will be dictated by the ease of GCM

data access and whether the required climatological variables are available. GCM selection therefore requires a consideration of the following (Smith and Hulme, 1998):

(i) whether to restrict choice only to the latest models;

(ii) GCM spatial resolution;

(iii) GCM performance in simulating observed climate;

(iv) representativeness of results, e.g. a selection of three GCMs, giving, average, low and high-end range of all GCM experiments.

Based on these and other criteria, the IPCC recommended seven GCMs for impact assessments. These are (Carter et al., 1999):

(i) CCSR - Japanese Centre for Climate Research Studies model (Emori et al., 1999);

(ii) CGCM1 - Canadian Centre for Climate Modelling and Analysis GCM no. 1 (Boer et al., 2000);

(iii) CSIRO1 (also known as CSIRO-mk2b)- Australian Commonwealth Scientific and Industrial Research Organisation, first generation atmosphere-ocean coupled GCM (Hirst et al., 2000);

(iv) ECHAM4 (also known as MPI) - German Climate Research Centre, European Centre/Hamburg Model no. 4 (Zhang et al., 1998);

(v) GFDL-R15 - US Geophysical Fluid Dynamics Laboratory, R-15 resolution model (Manabe and Stouffer, 1996);

(vi) HadCM2 - UK Hadley Centre for Climate Prediction and Research Coupled Model no. 2 (Mitchell and Johns, 1997);

(vii) NCAR-DOE - US National Centre for Atmospheric Research model, DOE version (Meehl et al., 2000).

The main features of five of the recommended models (i.e. American, Australian, British, Canadian and German) are provided in Table 3.1. A summary of the HadCM3 model (a successor to the HadCM2 model) released after the IPCC's recommendation is also given. Further details of experiments conducted using three GCMs: HadCM3, CSIRO1 and CGCM1, developed in the UK, Australia and Canada, respectively, will be provided in section 3.3.4. Indeed, Carter et al. (1999) emphasised using more than one GCM in impacts assessments to investigate differences in model output.

3.3.4.1 Canadian Centre for Climate Modelling and Analysis' first Generation AOGCM (CGCM1)

A summary of the main features of CGCM1, adopted from Flato et al. (2000), are presented here. The atmospheric model has a horizontal resolution of 3.7° x 3.7° (approximately 411km x 411km at the Equator) and 10 equally spaced vertical layers. The oceanic component has a resolution of 1.8° x 1.8° (approximately 200km x 200km at the Equator) and 29 layers. The upper four layers are equally spaced at 50m intervals whilst the spacing increases to 200m at greater depths. This is in order to capture the important circulation and mixing processes occurring close to the ocean surface.

CGCM1 is unable to incorporate the direct coupling (by fluxes of heat, salinity and wind stress) of the atmosphere to the oceans. This is because of a different response rate of the ocean to temperature. Consequently, the model relies on artificial corrections known as flux-adjustments to reproduce observed climate over a validation period. The

technique is to run the ocean and atmosphere models independently and compute (i) the fluxes required by the ocean model when driven by observed sea-surface temperature (SST), sea-surface salinity (SSS) and wind stress, and (ii) the heat fluxes generated by the atmospheric model with observed SST and SSS. The difference between (i) and (ii) gives the flux adjustment.

The radiation scheme does not account for the different greenhouse gases but instead uses a higher carbon dioxide concentration as a surrogate. The cooling effects of sulphate aerosols can be accommodated by changes to the surface albedo. The land-surface scheme uses a modification of the simple bucket method (see section 3.4). A single soil layer with spatially varying field capacity and soil properties is used. This scheme has no mechanism for surface storage or subsurface flow. Consequently, any runoff from enclosed surfaces is transferred to the ocean via a virtual link.

3.3.4.2 Australian Commonwealth Scientific and Industrial Research Organisation's (CSIRO) first Generation AOGCM (CSIRO1)

A summary of the main features of the CSIRO1, adopted from Gordon and O'Farrel (1997) are presented here. Both the atmospheric and oceanic models have a horizontal resolution of 3.2° x 5.6° (approximately 356km x 623km at the Equator). The atmosphere is divided into 9 layers whilst the ocean has a finer vertical spatial resolution comprising 21 layers. The ocean model uses a heat transport scheme which reduces considerably, the problems related to extreme mixing in the Southern Ocean. The model requires flux adjustments for reasons mentioned in the previous section.

As with CGCM1, the radiation scheme does not account for the different greenhouse gases and instead, uses carbon dioxide as a surrogate. The cooling effects of sulphate aerosols can be accommodated by alterations to surface albedo.

The land-surface scheme is more detailed than the one used in CGCM1, and is parameterised by using a soil-canopy model. This representation allows for the inclusion of soil types, infiltration, deep soil percolation, runoff, surface albedo, canopy interception of moisture, plant stomatal resistance, snow accumulation and melting. A major feature is that the formulation of evapotranspiration includes the effects of temperature, water vapour pressure and carbon dioxide on plant stomata.

3.3.4.3 UK Hadley Centre's third Generation of Coupled AOGCM (HadCM3)

This is the UK Hadley Centre's third generation of coupled AOGCM. The following model description has been adopted from Gordon et al. (2000). The atmospheric model has a horizontal resolution of 2.5° x 3.75° (approximately 417km x 278km at the Equator) and 19 vertical levels. The oceanic component of the model has a horizontal resolution of 1.25° x 1.25° (approximately 139km x 139km at the Equator) and 20 vertical layers which are staggered for reasons already discussed. The oceanic horizontal spatial resolution is higher than that of any other GCM in use. The model is therefore able to adequately represent important details in oceanic current structures such as the Gulf Stream.

Compared to its HadCM2 predecessor and its contemporaries described previously, the major breakthrough in HadCM3 is that it does not require flux adjustments. This is due to improved simulation of sea-surface temperature (SST) and sea-ice. Therefore,

HadCM3 can be categorised as a truly coupled model. Moreover, the model is one of very few GCMs able to incorporate directly, the effects of minor greenhouse gases in addition to carbon dioxide. The trace gases include methane, nitrous oxides, CFC11, CFC12 and HCFC22. It is also able to include the effects of water vapour and ozone. A simple parameterisation of background aerosols is also included. The transport, oxidation and removal out of anthropogenic sulphur emissions by physical deposition and rain can also be selectively included. This enables the direct and indirect forcing effects of sulphate aerosols to be simulated with specific scenarios of sulphur and oxide emissions. The land surface scheme is similar to the one used by CSIRO1 and also includes the freezing and thawing action of soil moisture.

3.3.5 Applying Scenarios in Impact Assessments

After suitable GCMs have been selected for impact assessments, the GCMs' output can be processed and applied in a variety of ways. Because GCM output is too coarse at the catchment scale (see section 3.3.3.1), it cannot be used directly to represent current and future climate. The unreliability of some GCM simulated variable time-series such as daily precipitation at a particular catchment for instance, also rule out the direct use of GCM output time-series data. Instead, it is common to apply the mean changes to observed data. The normal procedure first involves defining the current climate by obtaining the observed daily or monthly climate data (e.g. precipitation and potential evapotranspiration, or precipitation and temperature, radiation or sunshine hours) over a period such as 1961-1990 - termed the 'baseline' period. In instances where there is difficulty adjusting this baseline (e.g. lack of consistent data), other baseline could be used (e.g. 1951-1980 or 1931-1960).

The baseline period of 1961-1990 is recommended by the World Meteorological Organisation (WMO) for the following reasons (Carter et al., 1994, 1999):

(i) it encompasses a range of climatic extremes such as droughts and floods;

(ii) it is a period for which there are large number of observational data-sets at the monthly or daily scale for a number of key climatological parameters;

(iii) it represents the recent climate to which many present day anthropogenic or natural systems have become well adapted to;

(iv) its end period (1990) coincides with the IPCC's common reference year used for climate projections;

(v) its use ensures consistency in impact assessments thus providing a basis for inter-study comparisons.

Once observational baseline data are collected, these are perturbed to obtain future climatology. The perturbation of observed baseline data can be carried out by using climate change scenarios derived from either the GCM 'simulation' run or both the 'simulation' and 'control' runs (see section 3.3.3.1 for explanation of both of these). If the change in climate since pre-industrial times is of interest then the latter approach should be used. However, if climate change from current (baseline) conditions is of interest then output from only the GCM simulation run is used.

Use of only the simulation run in constructing climate change scenarios has been adopted by the IPCC (Carter et al., 1999). Scenario construction involves using 30 year climatologies centred on the baseline (1961-1990), 2020s (2010-2039), 2050s (2040-2069) and the 2080s (2070-2099), from the simulation run to derive differences relative to the baseline (Carter et al., 1999). As mentioned already, this approach is preferred

because it allows climate impacts assessments to be carried out on the basis of current (baseline) climate conditions. This is so that adequate adaptation strategies can be developed. It should be noted that the climate change scenarios are assumed to be representative of anthropogenic climate change only. However, natural climate variability may also be responsible for the change and therefore it might be useful to ascertain the extent of this natural variability. Studies by Hulme et al. (1999b) and Hulme and Jenkins (1998) have addressed this issue.

Once the mean differences are obtained, they now have to be used to obtain future climate. It is common to apply the mean differences in climate derived from the GCM simulation experiment (i.e. twelve mean monthly factors) to observational baseline data directly. However, a critical limitation of this 'simple perturbation' technique is that the temporal structure (such as length of dry periods and interannual variability) of the perturbed records will be the same as the historic record. In other words, it is assumed that only mean annual or mean monthly variables such as temperature and precipitation change. Each day within a month or year is assumed to have the same absolute change in temperature and the same percentage change in precipitation (Smith and Hulme, 1998). Consequently, the pattern of daily climate and the interannual variability of future climate is similar to the historical climate. It could therefore be argued that the new future climate is effectively the same as the historic climate except for the scaling. A stochastic weather generator can be employed to combat this shortcoming - these will be discussed in section 3.3.6.

3.3.5.2 Downscaling GCM Output

A limitation of GCMs discussed in section 3.3.3.1 was their coarse spatial resolution

hence the inability to provide scenarios at the catchment scale. Therefore, while GCM output can be applied directly to hydroclimatological data for preliminary studies, 'downscaling' to a finer spatial scale is often preferred. There are three main ways of downscaling GCM output and these include 'unintelligent', statistical and dynamical downscaling.

'Unintelligent' Downscaling

These are interpolation-based techniques. The methods are termed 'unintelligent' because no new methodological insight going beyond the GCM-based change is introduced (Hulme and Jenkins, 1998). Jones and Hulme (1996) provide a review of a number of unintelligent downscaling methods. In the most basic approach, four GCM grid points nearest to the catchment are used for interpolation (von Storch et al., 1993). The interpolation can be carried out on the basis of linear averaging by the inverse of distance between the catchment and the four GCM grid points (Smith et al., 1992). The advantage of this approach is that it allows regional climate change scenarios to be defined that would otherwise be difficult or costly to obtain. The simple linear interpolation can be defined as (Smith et al., 1992):

$$VAR_D = \frac{\sum^{i}\left(\frac{1}{D_i^s}\right)VAR_i}{\sum\left(\frac{1}{D_i^s}\right)} \qquad (3.5)$$

where,

VAR_i is the value for the variable (temperature, precipitation) at grid point i;

D_i^s is the distance from the site to the GCM grid point i;

VAR_D is the downscaled variable.

Statistical Downscaling

Another way to downscale GCM grid point climate to the catchment scale is by using regression methods or circulation typing. Regression methods develop the statistical relationships between large-scale and catchment-scale surface climate (e.g. Wigley et al., 1990). For example, the relationship between catchment-scale mean surface temperature or precipitation and large-scale upper air geopotential temperature and height could be used (e.g. Winkler et al., 1997; Crane and Hewitson, 1998). Circulation-based downscaling relates catchment scale climate data to a synoptic weather or circulation classification scheme (von Storch et al., 1993; Wilby, 1997). In the UK, the Lamb (1972) synoptic classification is widely used.

Despite being able to provide climate at spatial resolutions as high as 1 km^2 (e.g. Bardossy and Platte, 1992) at a relatively low computational cost, statistical downscaling techniques suffer from several deficiencies. The disadvantages are that they are based upon the assumption that the observed statistical relationships will continue to be valid under greenhouse gas induced climate change (Wilby, 1997). However, Huth (1997) and Wilby (1997) warn that the relationships obtained between circulation and local-scale climate variables may not be valid in a future changed climate. Another disadvantage is that very long observational climate data, often at a daily or hourly temporal resolution, are required.

Downscaling techniques do not include atmospheric moisture therefore they should be viewed with caution. Wilby and Wigley (1997) suggest that statistical downscaling methods could be further improved by including atmospheric moisture in the formulation. Charles et al. (1999) downscaled climate to the catchment scale by

including atmospheric moisture. They showed that the downscaled climate was in good agreement with the observed climate.

Dynamical Downscaling

Dynamical downscaling methods use output from high resolution numerical models known as Regional Climate Models (RCMs). RCMs are nested regional limited-area models embedded within GCMs to simulate regional climate at a higher spatial resolution (eg. Leavesley, 1999; Hoestetler and Giorgi, 1993; McGregor and Walsh, 1994). However, despite their high spatial resolution, RCMs are dependent ultimately on boundary conditions extracted from GCM experiments. It is therefore likely that RCM simulations may be contaminated by errors in boundary conditions simulated by the GCM (Robock et al. 1993, from Lins et al. 1997). Moreover, the typical resolution of around 50km is still insufficient for small catchment scale studies. Presently, RCMs require large computational resources but as the exponential growth in computing continues, it is inevitable that RCMs would be able to downscale to a resolution higher than 50km.

Table 3.2 summarises some downscaling techniques and their strengths and weaknesses.

3.3.6 Stochastic Weather Generators as Perturbators of Current Climate

As mentioned in section 3.3.5, a stochastic weather generator can be used to introduce variability into future climate time-series (see e.g. Cole et al., 1991; Chiew et al., 1996). Consequently, a weather generation approach can be used to investigate changes in extremes as well as in long term means. Additionally, the simulations can also be used

to estimate the effects of climate change on daily peak flows, return period of floods, low flow characteristics, frequency, severity and duration of droughts and reservoir storage estimates because it takes into account changes in the timing, frequency and magnitude of changes in the climate variables (Chiew et al., 1996).

A stochastic weather generator is calibrated using baseline climate data and the parameters, including the variability parameter, are then perturbed using the climate change scenarios (e.g. Wilks, 1992; Buishand and Beckmann, 2000). A new sequence of daily climatic variables representing the future is thus produced. It is possible to generate a large number of climate time-series at a single-site or multiple-sites by ensuring the spatial correlation of the different climate variables.

Stochastic weather generators have not seen extensive use in climate impacts water resources studies due to some of their disadvantages. The main problem is that they require very large climatic input data which may be difficult to obtain. These data typically include daily historical minimum and maximum temperature, radiation (or sunshine hours) and precipitation. Furthermore, GCM simulated daily precipitation and temperature data are required to determine wet and dry days, and the standard deviation, respectively. Another limitation of weather generators is that low frequency aspects of climate such as changes in interannual or interdecadal variability is not captured very well (Wilby, 1997).

Two types of daily stochastic weather generators may be used in impacts assessments and these are the autoregressive (Markov chain) models (e.g. Richardson, 1981; Coe and Stern, 1982) and the Long Ashton Research Station Weather Generator (LARS-WG) developed by Rackso et al. (1991).

A first-order Markov chain model is formulated by considering the precipitation process as a Markovian chain consisting of two states - a wet day and dry day, where a day with 0.1mm or more precipitation is defined as a wet day (Faulkner et al., 1997; Mavromatis and Jones, 1998). For each successive day, the precipitation occurrence is conditioned on the state of the previous day. A second-order Markov chain model is formulated by considering (Faulkner et al., 1997) (i) the probability of a wet day following two others, (ii) the probability of a wet day given that the previous day was wet and the one before was dry, (iii) the probability of a wet day given that the previous day was dry and the one before was wet and (iv) the probability of a wet day following two dry days.

The LARS-WG has the advantage of having a 'long memory' of rare events since it simulates precipitation occurrence on the basis of distributions of the length of continuous sequences of wet and dry days. Hence it overcomes the limited memory of Markov chain models, which are poor at reproducing the persistence of weather conditions. Indeed, Racsko et al. (1991) noted that a Markov chain model grossly underestimated the frequency of long dry series at site in Hungary. LARS-WG has been applied in impacts studies by Semenev and Porter (1994) and Semenev and Barrow (1997).

Faulkner et al. (1997) compared the performance of a first-order and second-order Markov chain model with LARS-WG at three sites in the UK. The comparison was based on the mean and standard deviation of (i) monthly rainfall, (ii) monthly maximum 1-day rainfalls and (iii) lengths of dry spells. An additional test was to compare the number of dry spells with a minimum 10-day duration. On the basis of these tests, Faulkner et al. (1997) concluded that LARS-WG was the best model overall for reproducing statistics of observed rainfall. Consequently, LARS-WG was used in

the current work and is described in more detail below (description adopted from Racsko et al., 1991 and Semenov and Barrow, 1997).

LARS-WG uses observed daily precipitation, minimum temperature, maximum temperature, and net solar radiation to generate data. In the absence of radiation measurements, sunshine duration data may be supplied which are used internally by LARS-WG to obtain estimates of radiation. The model uses the formula of Prescott (1940):

$$R_n = R_a (a + b\, n/N) \tag{3.6}$$

where,

R_n = total daily incident net solar radiation (W/m^2);

R_a = total short-wave radiation received at the top of the atmosphere (W/m^2);

n = observed number of sunshine hours;

N = theoretical maximum sunshine hours at a specified location;

a = percentage of R_a reaching the Earth's surface on a completely cloud-covered day;

b = percentage of R_a absorbed by the clouds on a completely cloud-covered day.

Meteorological tables are used by the model to estimate R_a and n, and regression methods are implemented to develop a relationship between n/N and N/n with the coefficients a and b, respectively. The expressions of Rietveld (1978) defining a = 0.10 + 0.24 n/N and b = 0.38 +0.08 N/n are used by the model.

The simulation of precipitation, minimum and maximum temperature, and solar

radiation by LARS-WG is conditioned on occurrence of continuous series of wet or dry days. Wet series are defined as continuous sequences of days with rainfall equal to or greater than 0.1mm. The lengths of wet and dry series are modelled with mixed exponential distributions. The amount of rain on days in a wet series is simulated from a mixed exponential and uniform distribution. The parameters of the distributions are a function of only the day of the year, and not of the duration of the wet series or the position of the day within the series. The distribution of other climate variables, i.e. maximum and minimum temperature and solar radiation is based on the present status of the wet or dry series. Further details of climatological time-series modelling by LARS-WG (carried out in four steps), adopted from Racsko et al. (1991) are provided below:

Step 1: Wet and dry series modelling

If $P_w(d)$ and $P_d(d)$ are used to represent the probability distribution of wet and dry series lengths on day d, respectively then, for d=1 (first day) - the procedure is to (i) generate system status - i.e. wet or dry series, (ii) generate length of series, n_w, (iii) consider the period $[d, d+n_w]$ to be wet (by definition, each wet series is followed by a dry series), (iv) generate a value from $P_w(d)$ and consider the period $[d+n_w, d+n_w+n_d]$ to be dry, and (iv) repeat the process until the end of the year (d = 365, 366).

The probability distributions of $P_w(d)$ and $P_d(d)$ are defined as:

$$P_w(d) = \text{Geom}[\Phi(d)] \tag{3.7}$$

$$P_r(d) = \begin{cases} \text{Geom}[\Phi_{r,s_t}(d)] & \text{with probability } 1-\rho \\ \text{Geom}[\Phi_{r,l_g}(d)] & \text{with probability } \rho \end{cases} \tag{3.8}$$

where Geom[ ] is a geometric distribution for a series, $\Phi(\ )$ is a fitted parameter of the distribution, w = wet series, r = dry series, s_t = short series, and l_g= long series. After generating the wet-dry sequences, the precipitation is modelled.

Step 2: Precipitation modelling

The distribution of precipitation $P_p(\ )$ is dependent on d but not on the length of series or position within the series (l). It can be defined as:

$$P_p(d) = \begin{cases} D_{us_m}(0,0.3) & \text{with probability} \quad q_{s_m}(d) \\ D_{em_d}\{f(d)\} & \text{with probability} \quad q_{m_d}(d) \\ \Gamma_{l_e}(d) & \text{with probability} \quad q_{l_e}(d) \end{cases} \tag{3.9}$$

where D_{us_m} = uniform distribution of 'small' precipitation, D_{em_d} = exponential distribution of 'medium' precipitation, Γ_{l_e} = average 'large' precipitation, and $q_{s_m}(d) + q_{m_d}(d) + q_{l_e}(d) = 1$ for each day (d), the probability of occurrence of small (s_m), medium (m_d) and large (l_e) precipitation.

Step 3: Temperature modelling

The distribution of temperature ($P_t(\ )$) is modelled using a normal distribution with parameters $\Pi_{\kappa,t}(d,l)$ and $\Theta_{\kappa,t}(d,l)$, where κ = wet (w) and dry (d) series. The distribution of temperature $P_t(d)$ is given by:

$$P_t(d) = \Pi_{\kappa,t}(d,l) + \Theta_{\kappa,t}(d,l)\Psi_t(d) \tag{3.10}$$

where Ψ_t is the correlation coefficient between two continuous days defined by $\Psi_t(d) = a\Psi_{t-1}(d) + bG_f(0,1)$, where $G_f(0,1)$ is the Gauss function with parameters 0 and 1, a and b ($a^2 + b^2 = 1$) are parameters providing the standard normal distribution Ψ_t.

Step 4: Modelling sunshine hours

The distribution of sunshine hours ($P_n(\ )$) is also modelled using the normal distribution with parameters that are a function of the type series of day d, and position l within the series. The expression for $P_n(d)$ is:

$$P_n(d) = \Pi_{x,n}(d,l) + \Theta_{x,n}(d,l)F(0,1) \geq 0 \qquad (3.11)$$

where $\Pi_{x,n}$ and $\Theta_{x,n}$ are parameters of the distribution of sunshine hours.

3.4 Assessing the Hydrological Impacts of Climate Change

As shown in Figure 3.1, once climate scenarios have been defined (step 4), the biophysical (hydrological) impacts need to be assessed (step 5). Catchment hydrologic response to climate change can be assessed in two ways, (i) obtaining direct GCM derived hydrological output and (ii) using downscaled climate change scenarios in hydrological models.

It was briefly mentioned in section 3.3.2.3 that some GCM land-surface schemes are able to simulate evapotranspiration. Additionally, the land-surface schemes are able to simulate runoff at the GCM grid-point scale. The first numerical representation of the hydrological cycle within a GCM used a simple bucket model (Manabe, 1969). This

model assumes runoff to take place after a soil 'bucket' is filled by precipitation. The simple bucket model does not consider the effects of evapotranspiration. More complete land-surface representations are included in the more complex GCM land-surface models.

Miller and Russell (1992) used a GCM to determine runoff for 33 major world rivers for the present and carbon dioxide doubled climate. They concluded that there were large errors in GCM based estimates of runoff. Nash and Gleick (1991) showed that coupling hydrological models to GCMs produces better estimates of runoff than direct GCM based runoff estimates. They also concluded that GCM based runoff cannot reproduce small-scale runoff. This is because the GCM land-surface models cannot adequately simulate the land-surface processes at the catchment scale (Rowntree and Lean, 1994; Pitman and Chiew, 1996).

Pitman and Chiew (1996) compared runoff simulated by the Australian Bureau of Meteorology Research Centre (BMRC) GCM coupled to a land surface process model with observed runoff, and with runoff from a daily conceptual rainfall-runoff model (MODHYDROLOG). While the comparison showed reasonable GCM model performance for a large wet catchment in Northern Australia (2500 km^2), it performed poorly in a smaller, drier catchment (540 km^2) in Western Australia. Therefore, whilst perhaps GCM runoff data could be applied directly in some large catchments, the use of hydrological models is an alternative used by most investigators.

Hydrological models can be classed in two categories, (i) deterministic models and (ii) stochastic models. Deterministic models are developed to mimic certain physical processes occurring in a catchment during the transformation of precipitation in to

runoff. However, the physical uniformity of the catchment surface and subsurface usually requires a gross simplification, and a lack of understanding of some of the processes involved introduces a degree of empiricism. Furthermore, although the movement of water entering a catchment may follow a deterministic path, the magnitude and timing of the resultant processes will partly be random. Therefore, deterministic models have a stochastic component accounting for some of the processes that the physical component is unable to reproduce.

Stochastic models are calibrated directly to historical streamflow data in order to reproduce their statistical properties such as serial correlation, mean, and coefficient of variation. They can be used to generate a large number of equally likely sequences of streamflow data based on historical data. The main limitation is that the models do not explicitly account for the water balance since they do not utilise hydroclimatalogical data. Stochastic models will be discussed within an uncertainty context later in the chapter (section 3.5.3).

The majority of water resources impact studies have used deterministic models and a further discussion of these is provided in section 3.6. There are a variety of deterministic approaches available for hydrological modelling that range from simple water balance models to the more complex physically based models.

To ascertain the hydrological response of a catchment under climate change, the normal procedure is to calibrate and validate a hydrological model under baseline climate and then to run the model using future hydroclimatological data.

3.4.1 Hydrologic Models

Dooge (1992) described hydrological modelling as '*being concerned with the accurate prediction of the partitioning of water among the various pathways of the hydrological cycle*'. Hydrological models aim to simulate runoff (R) using hydroclimatological data such as precipitation (P) and evapotranspiration (E). This can be achieved using the water balance equation:

$$R = P - E \pm \Delta S_T \tag{3.12}$$

where,

ΔS_T is the change in catchment storage.

Various hydrological modelling techniques are available depending on the objective. However, the most widely used hydrological models can be categorised into three groups (Xu and Singh, 1998), (i) empirical models, (ii) conceptual models, and (iii) theoretical (physically-based) models.

Empirical models aim to establish a statistical relationship between runoff and precipitation, temperature or potential or actual evapotranspiration for baseline conditions using a regression approach (Revelle & Waggoner, 1983; Arnell, 1992; Duell, 1992). The regression equations then estimate runoff under a changed climate by using perturbed values of the hydro-climatic factors. An example of an empirical model is the Wright's model that has been developed for streamflow record extension in the

UK (see Wright, 1978; Jones and Lister, 1995). The model was used by Arnell and Reynard (1989) to assess effects of climate change on streamflow in the UK.

Water-balance models conceptualise the movement of water from the time it falls onto a catchment as precipitation to the time it exits as runoff. They can be applied on a daily, weekly, monthly or annual basis. The complexity of the models vary depending on the detail of the components of the water balance. An example of a simple water balance model is the runoff coefficient equation (also known as the annual water balance budget equation) of Glantz and Wigley (1987). More complex water-balance models include the monthly model of Xu (Xu et al., 1996), and daily models MODHYDROLOG (Chiew and McMahon, 1994) and HYSIM (Manley, 1975). HYSIM (HYdrologic SImulation Model) is a daily model that is used by some Water Companies in Britain to generate streamflow records (e.g. Mott MacDonald, 1995).

HYSIM has twelve basic parameters and internally simulates (i) interception store, (ii) runoff from impermeable areas, (iii) overland flow, (iv) interflow, and (v) slow and fast runoff response from groundwater and the hydraulics of flow in river channels (Manley and Water Resource Associates Ltd, 2001). The main drawbacks in using the more sophisticated models such as HYSIM are the large number of parameters for optimisation and the large amount of data needed for catchment characterisation and model input. Moreover, the limitation of most water balance models is that the parameters need to be calibrated. Indeed, as the model becomes more complex and hence more realistic in its representation of catchment dynamics, the number of parameters needing calibration increases; this will in turn lead to a reduction in the 'information content' of such parameters (Dooge, 1977). Furthermore, monthly or

annual water balance models are unable to account for possible changes in storm runoff characteristics in sufficient detail.

Both the empirical and conceptual modelling approaches assume that model parameters remain valid under a changed climate. Consequently, the applicability of the model under a different climate and time period is questionable (Leavesley, 1999). Physically based models perhaps offer the best hope of overcoming this limitation.

Physically based models have a structure similar to the real-world system and hence any changes to the system (e.g. land use changes or climatic changes) may be incorporated into the model. Physically based models are also commonly used to simulate the detailed spatial patterns of hydrologic response within a catchment, (Xu, 1999). For example, Running and Nemani (1991) used a physically based ecosystem model to investigate forest response (in a 1540 km^2 region) to climate change using a spatial resolution of 1 km^2. The limitation is that there is lack of good quality catchment and climate data at the fine spatial scale needed for validation. An example of a physically based model is the Systeme Hydrologique European (SHE) model (Abott et al., 1986). To describe the spatial variability of hydrologic processes, SHE uses a rectangular grid of (x,y) points in the horizontal plane. The vertical variation in properties is represented by a series of horizontal planes of various depths. SHE has been successfully applied to catchments with areas ranging from 30km^2 to 5000 km^2 (Bathurst and O'Connell, 1992).

3.4.2 Uncertainties in Hydrological Modelling

The effects of climate change on a catchment will depend on catchment characteristics and inter-relationships between the different parts of the system. Catchment response models therefore need to be calibrated and validated for each particular catchment. However, since there is no such thing as a perfect model, errors are bound to be introduced into the modelling process. Consequently, much work over the years has focused on attempting to minimise such uncertainties (e.g. Franchini et al., 1998; Kuczera, 1997; Yapo et al., 1996, 1998).

3.4.2.1 Model Calibration

Hydrological models usually require an estimation of their parameters. Depending on the degree of sophistication, these may range from just a few to more than twenty. For example, Xu and Singh (1998) note that 3 to 5 parameters may be adequate to describe the hydrological processes (at a monthly time-step) in a humid region. However, they state that a more complex model may be required for simulating the response of catchments located in arid and semi-arid regions. Eeles (1994) states that for a conceptual model, between 8 and 20 parameters should be sufficient in modelling catchment rainfall-runoff response. The parameters of physically based models can be related to catchment and climate characteristics while the parameters of water balance models and some conceptual models are not well defined and therefore need to be optimised.

Calibration involves minimising an objective function. The following objective function (OBJ) is commonly used:

$$OBJ = \sum_{i=1}^{n}\left[(SIM_i)^{\frac{1}{2}} - (OBS_i)^{\frac{1}{2}}\right]^2 \quad (3.13)$$

where,

SIM_i and OBS_i are the simulated and recorded flows, respectively, at time i.

Parameter optimisation can be carried out in a variety of ways. Until recently, nearly all methods of optimisation used 'local-search' procedures (Yapo et al., 1996) such as the simplex technique (Nelder and Mead, 1965), the pattern search method (Hooke and Jeeves, 1961), and the Rosenbrock (1960) rotating directions method. These so-called automatic optimisation procedures are search algorithms that try and minimise a particular objective function by a trial-and-error change to model parameters. However, Yapo et al. (1996) argue that such methods are unreliable since the 'optimised' parameter values which they provide are highly dependent on starting conditions. Indeed it is known that the objective function response plane contains hundreds, if not thousands, of local optima (Beven, 2001). Therefore, much effort has been geared towards avoiding a large number of local solutions whilst proceeding towards the global optimum. In this regard, the shuffled complex evolution (SCE-UA) algorithm has been developed and has generally been consistent, efficient and effective in locating the region of the global optimum (Yapo et al., 1996). Indeed, the SCE-UA has shown superior performance to a number of other optimisation algorithms including the simplex method and genetic algorithms (Tanakumara and Burges, 1996). Details of the SCE-UA algorithm are provided in Duan et al. (1994).

Given some of the uncertainties in locating the global optima, Beven (2001) states that the idea of an 'optimal' model is flawed and recommends that it should be replaced with

an 'equifinality' of models. It is then possible to weight the predictions of each model according to its past performance. On the basis of the weighting, a model that is not deemed adequate is given a zero weight and rejected. Beven and Binley (1992) put forward the Generalised Likelihood Uncertainty Estimation (GLUE) approach to hydrological modelling to allow for this. The GLUE methodology rejects the concept of a single, global optimum parameter set and instead considers equally plausible multiple parameter sets (Beven, 1993). Recently, Cameron et al. (2000) adopted the GLUE methodology for the assessment of the effects of climate change on flood frequency in a small upland catchment in Wales, UK. This study will be summarised in section 3.6.

A number of basic checks for identifying whether parameters have stabilised are available. One way is to view plots of parameter values against the number of iterations. However, results from such an exercise should be viewed with caution because stabilisation in itself does not mean that global minima has been achieved. Further plots are required, such as plots of sum of squares against parameter values at the region of optimised values. Checking whether all parameters are necessary can be done by sensitivity studies (e.g. Reungoat, 2000).

Some of the problems encountered in parameter optimisation include, (i) the limited length of historical data, (ii) lack of information on reasonable values or a range of appropriate values, (iii) model and data errors in parameter values, and more crucially (iv) the non-uniqueness of parameter values, i.e. different combinations of parameter estimates give the same evidence of model performance.

3.4.2.2 Model Validation

Numerous tests are available for assessing model performance and these include, (i) statistical parameters (ii) graphical plots, and (iii) dimensionless coefficients. Statistical parameters include well known expressions used to describe the characteristics of a specific time-series data such as mean, standard deviation, skewness and lag-one auto-correlation. Graphical methods may include hydrographs, x-y scatter plots, and flow duration curves, showing simulated and observed flows. For reservoir analysis purposes, an estimate of low flow measures such as Q_{95} (flow exceeded 95% of the time) obtained from duration curves is a good indication of model performance (Adeloye and Nawaz, 1998).

Dimensionless coefficients can be determined by linearly relating observed streamflow to simulated streamflow. A popular dimensionless coefficient for assessing model performance is the coefficient of determination (R^2):

$$R^2 = \frac{\left(\sum_{t=1}^{n}\left(OBS_t - \overline{OBS}\right)^2 - \sum_{t=1}^{n}\left(OBS_t - \hat{Y}_t\right)^2\right)}{\left(\sum_{t=1}^{n}\left(OBS_t - \overline{OBS}\right)^2\right)} \qquad (3.14)$$

where,

$\hat{Y}_t$ is obtained from the regression line relating the simulated flow (SIM) to the observed (OBS) flow. The coefficient of determination is always between 0 and 1. Good model performance is shown with the coefficient value closer to unity. The terms $\sum(OBS_t - \overline{OBS})^2$ and $\sum(OBS_t - \hat{Y}_t)^2$ are respectively referred to as the initial variance and the residual or unexplained variance. It can be seen from Equation (3.14)

that R^2 measures the proportion of the initial variance that is accounted for by the best-fit line relating the observed and simulated flows. A more complete performance measure would be one that describes explicitly the difference between the observed and simulated flows (Chiew and McMahon, 1993). Nash and Sutcliffe (1970) replaced $\hat{Y}_i$ in Equation 3.14 with OBS_i to obtain a variant of R^2 termed the coefficient of Efficiency (E_c):

$$E_c = \frac{\left(\sum_{t=1}^{n}\left(OBS_t - \overline{OBS}\right)^2 - \sum_{t=1}^{n}\left(SIM_t - OBS_t\right)^2\right)}{\left(\sum_{t=1}^{n}\left(OBS_t - \overline{OBS}\right)^2\right)} \qquad (3.15)$$

In contrast to R^2, the coefficient of efficiency represents the proportion of variance of the observed flows which can be accounted for directly by a model (without any subsequent correction by a regression model as is the case with R^2).

By definition, the value of E_c is always less than R^2 - an exception to this is when the best-fit line relating observed and simulated flows is SIM=OBS (i.e. Y=X) - in which case R^2 and E_c have the same value. As in the case of R^2, a value of E_c close to 1 is indicative of good model fit. An E_c value of 1.0 suggests that all simulated flows (at a particular time-step) are the same as the observed flows. In contrast to R^2, E_c can have a negative value which is indicative of rather poor model performance.

Chiew and McMahon (1993) state that for typical hydrological and water resources investigations, a hydrological model can be deemed to be performing exceptionally if $E_c \geq 0.93$ or $R^2 \geq 0.97$, or if $R^2 \geq 0.93$ with a mean simulated flow within 10% of mean observed flow. The model is showing acceptable performance if $E_c \geq 0.80$ or $R^2 \geq$

0.90, or $R^2 \geq 0.77$ with a mean simulated flow within 10% of mean observed flow. Simulations with $E_c \geq 0.60$ are generally satisfactory. Adeloye and Nawaz (1998) stress that model performance should be assessed based on the models' intended purpose. For example, Nawaz and Adeloye (1999) used observed flows and the flows simulated by the empirical model of Wright (Wright, 1978) to assess performance in regard to storage-yield assessments. They found that while commonly used statistical measures showed the model to be performing well during validation, there were large differences in reservoir storage derived using observed and simulated flow records.

As already mentioned, an important requirement in hydrological modelling is to assess the adequacy of the model using observational data. However, for future changed climatic conditions, observational data are obviously unavailable. Moreover, physical catchment characteristics, in addition to climate may be significantly different in the future. In such instances, the Split Sampling approach can be used (Wood et al., 1997). The approach dictates that given a hydrological model is to be used for simulation in a drier climate, calibration should take place over a wet period and validation over a dry period, and vice-versa (Klemes, 1986).

3.4.3 Selecting Hydrological Models for Climate Impact Assessments

Klemes (1985) provides criteria for selecting suitable models for climate impact assessment. He notes that the model structure must have an adequate physical basis and the model must be sufficiently robust to be applicable to different regions and climates. The applicability to different regions can be achieved by modifying model parameters, and the applicability to a different climate can be achieved by modification of input data. Based on Klemes (1985) criteria, physically-based models would seem to be the

most appropriate for impact assessment. However, as already discussed, these models are complex, have a large number of parameters, extensive data requirements, and subject to uncertainty because of a current lack of knowledge of catchment processes and process parameterisations at this level of detail (Leavesly, 1994; Beven, 1989).

Yates and Strzepek (1994) compared two conceptual water balance models and three empirical models at five catchments. They concluded that the conceptual water balance models were most adequate for climate impacts investigation based on their ability to reproduce runoff over calibration and validation period. The conceptual models were also more consistent in estimating changes in climatological variables.

In another review, Gleick (1987) concluded that the use of monthly water balance models have some important advantages over other methods in accuracy, flexibility and relative simplicity.

3.4.4 Some Models for Catchment Response Assessments

3.4.4.1 A Simple Water Balance Equation

A relatively straightforward method of climate impact assessment is to use a simple, percentage-runoff coefficient technique (Wigley and Jones, 1985; Glantz and Wigley, 1987). Starting from the annual water balance equation (and ignoring any non-evaporative losses such as infiltration-percolation for the moment and storage), Equation (3.12) can be re-written as:

$$R = P - E' \tag{3.16}$$

where R is annual runoff (mm), P is the annual precipitation (mm) and E' is the annual actual evapotranspiration (mm). Defining the runoff ratio, $\gamma_b = R_b / P_b$, then the sensitivity of mean annual runoff could be calculated as:

$$\frac{R_f}{R_b} = \frac{c_p - (1-\gamma_b)c_e}{\gamma_b} \tag{3.17}$$

where subscripts *f* and *b* denote future and baseline values respectively; c_p and c_e are factor changes in the annual precipitation and actual evapotranspiration, respectively, as a result of climate change, i.e. $P_f = c_p P_b$ and $E_f^{'} = c_e E_b^{'}$.

Equation (3.17) is a simple way to assess the relative sensitivity of annual runoff to changes in annual precipitation and actual evaporation. However, while it is not unreasonable to ignore the non-evaporative losses in the annual model, such losses must be accounted for in monthly models. Glantz and Wigley (1987) extended the above approach to incorporate non-evaporative losses to obtain:

$$\frac{\Delta R}{R_b} = \frac{1}{\gamma_b}\frac{\Delta P}{P_b} - \frac{\Delta E^{'}}{E_b^{'}}\left\{\frac{1-\xi_b}{\gamma_b} - 1\right\} - \frac{\xi_b}{\gamma_b}\frac{\Delta L}{L_b} \tag{3.18}$$

where the Δ refers to increment; L is the sum total of all other losses (e.g. infiltration, seepage and deep percolation) and $\xi = L/P$. (Note that $E^{'}$ in Equation (3.18) now refers to the monthly actual evapotranspiration.) Equation (3.18) can be re-written in the form of Equation (3.17) as:

$$\frac{R_f}{R_b} = \frac{1}{\gamma_b}\left\{(c_p - 1) - ([c_e - 1][1 - \xi_b - \gamma_b]) - (\xi_b[\theta - 1])\right\} + 1 \tag{3.19}$$

where $\theta = L_f / L_b$. ξ_b can also be written as:

$$\xi_b = 1 - \gamma_b - \frac{E_b'}{P_b} \tag{3.20}$$

If a further assumption is made that non-evaporative losses remain unchanged with time, then L_f/L_b becomes unity and hence the monthly changes in runoff become:

$$\frac{R_{f_i}}{R_{b_i}} = \frac{1}{\gamma_{b_i}}\left\{\left(c_{p_i} - 1\right) - \left(\left[c_{e_i} - 1\right]\left[1 - \xi_{bi} - \gamma_{b_i}\right]\right)\right\} + 1; \qquad i=1,2,...,12 \tag{3.21}$$

To apply Equation (3.21) will require $\gamma_{b_i}, c_{p_i}, c_{p_i}$ and ξ_{b_i}. Both c_{p_i} and c_{e_i} are provided by the climate change scenarios for rainfall and evapotranspiration, respectively for each month i. γ_{b_i}, the baseline runoff coefficient for month i, will be obtained by dividing the corresponding mean monthly runoff by the corresponding rainfall for that month. ξ_{b_i} is evaluated according to Equation (3.20) using estimates of the mean actual evapotranspiration and the mean rainfall for month i. The method used to calculate the actual evapotranspiration was described in section 3.3.2. It should be noted that Equation (3.21) is a gross simplification of the complex processes occurring in the transformation of rainfall to runoff. Equation (3.21) is very simple to use, does not have any parameters (and hence does not need calibration) and is directly applicable to any catchment in any region, which is a significant consideration given the fact that data from different climatic regions are to be investigated.

The assumption underpinning Equation (3.21), i.e. that θ is unity, is necessary to avoid the problem associated with quantifying L_f which is not an output of GCMs and hence

for which scenarios are not available. Admittedly, the dominant component in L, i.e. infiltration, will be greatly affected by land use changes. However, until climate has actually changed and we then have the benefit of measuring L under the new climate, there will be no other way of knowing by how much L has been affected.

3.4.4.2 Monthly Water Balance Model of Xu

This is a single store model (Vandewiele and Xu, 1991; Xu et al., 1996) and is illustrated in Figure 3.4, which, in its basic form, has three parameters controlling respectively, actual evapotranspiration (AE), slow and fast runoff. The model has been successfully calibrated for many catchments from ten countries with satisfactory results (Vandewiele and Ni-Lar-Win, 1998). An extended version of the model can simulate snow accumulation and melting and has six parameters. Together with monthly runoff, both models can accept as inputs different combinations of monthly precipitation, potential evapotranspiration (PE), temperature and humidity. In general, time series data of monthly PE are preferred but where these are unavailable, the PE is estimated internally from temperature and/or humidity using empirical relationships. The snow module is also driven by the temperature. Monthly runoff and other water balance components are the outputs. Tables 3.3 and 3.4 summarise the equations of the model with and without the incorporation of the snow module. The model uses a combination of Newton-Raphson, steepest descent and Marquardt methods to minimise the (sum of squares) objective function in Equation (3.13).

This model is suitable for catchments with areas between 10-5000 km^2. The main reason for this is that the model has only one store and has no mechanism for fast runoff transfer from one month to the next (see fast runoff Equation (3.25) in Table

3.3). As a consequence, time of concentration must be much less than one month (about two to three days), and this restricts the applicability of the model to catchments with an area smaller than about 5000 km^2. The model can be used on larger catchments by (i) applying the model on each sub-catchment or (ii) modifying the fast flow equation by considering a transfer term. The fast flow equation can then be written as

$$R_t^f = \left(a_6\left[M_{t-1}^s\right]^+\right)^{b_2}(M_t + P_t^a) + a_7\left(\left[M_{t-2}^s\right]^+\right)^{b_2}(M_{t-1} + P_t^a) \qquad (3.38)$$

where $P_t^a = \left\{P_{t-1} - E'_{t-1}\left[1 - e^{(-P_{t-1}/E'_{t-1})}\right]\right\}$.

Based largely on experience, the model is recommended for use in catchments located in humid catchments (Xu, pers. comm.). However, slight modifications to fast and slow flow equations can lead to its applicability to arid and semi-arid climates. For example, in some small and very dry catchments, the ground water table is very deep, and in such cases, the slow flow equation could be omitted.

3.4.4.3 A Conceptual Daily Rainfall-Runoff Model - MODHYDROLOG

MODHYDROLOG is a conceptual daily rainfall-runoff model structured around five moisture stores shown in Figure 3.5. All five stores are inter-related by catchment processes shown in Figure 3.5 and formulated in Table 3.5. The model requires daily precipitation and potential evapotranspiration as input and simulates groundwater recharge in addition to runoff. The model has 19 parameters (see Table 3.6) which simulate soil moisture and surface water movement. Two of the parameters - LOCATE and RMD can be fixed, leading to only 17 parameters for optimisation. LOCATE can be set to 7 in the Northern Hemisphere and RMD can be set to 1 because there is no

information on how depression storage fills. A pattern search optimisation routine is used to minimise the objective function (defined in Equation 3.13). Reungoat (2000) showed that even when the parameters requiring optimisation are reduced to seven, the model performs adequately. Indeed, Reungoat's (2000) study highlights precisely the problem of non-uniqueness mentioned in section 3.4.2.1 in rainfall-runoff model parameter estimation. MODHYDROLOG has been extensively tested in arid and temperate climates (Chiew and McMahon, 1994; Reungoat, 2000) and used in a number of climate impacts investigations. A limitation of the model is that it is unable to simulate snowmelt that may be of significance in climate change impact studies.

3.5 Assessing the Water Resources Impacts of Climate Change

As shown in Figure 3.1, once the hydrological impacts of climate change have been assessed (step 5), the impacts on water resource systems such as reservoirs (socio-economic impacts) need to be investigated (step 6).

As already mentioned in section 2.5.3.1, The ultimate purpose of a reservoir is to stabilise the flow of water by retaining water during times of plenty and releasing it during times of drought. Therefore, the possibility of rapid climate change could have all sorts of adverse effects on reservoirs. Consequently, water resource impacts assessment must investigate the implications for storage facilities and their performance.

3.5.1 Reservoir Performance Criteria and Planning Analysis

Reservoir planning involves determination of the storage size of the facility which will satisfy the demand placed on it with an acceptable level of performance. Three reservoir performance criteria have been defined by Hashimoto et al. (1982), (i) reliability, (ii) resiliency, and (iii) vulnerability.

3.5.1.1 Reservoir Performance Criteria

Reliability is a measure of reservoir failure occurrence and can be either time-based (δ) or volumetric reliability (υ), defined respectively as (Hashimoto et al., 1982):

$$\delta = \left(1 - \frac{f_p}{T_p}\right) \qquad (0 \le \delta \le 1) \qquad (3.49)$$

$$\upsilon = 1 - \frac{\left(\sum_{t \in f} R_t^* - \sum_{t \in f} R_t^D\right)}{\sum_{t \in T_p} R_t^*} \qquad (0 \le \upsilon \le 1) \qquad (3.50)$$

where,

f_p = total number of failure periods;

T_p = total number of time periods in the streamflow record;

R_t^D = drought release of reservoir system during the t-th failure periods;

R_t^* = target demand during the t-th period.

The resilience ($\Re$) is a measure of reservoir system recovery following failure and a number of definitions have been reported (Fiering, 1982). However, the most widely applied definition is due to Hashimoto et al. (1982):

$$\Re = \frac{1}{\left(\frac{f_p}{f_s}\right)} \qquad (0 < \lambda \leq 1) \qquad (3.51)$$

where f_s is the number of continuous sequences of failure periods and f_p is the total number of failure periods.

The ratio f_p/f_s in Equation (3.51) represents the average duration of the continuous failure periods and hence the resilience can be referred to as the inverse of the average duration of continuous failure periods. It therefore follows that the longer the average duration of the failure periods, the smaller the resilience, which makes it more difficult for a reservoir to recover to a normal state following failure.

As mentioned previously, other definitions of resilience have also been reported. For instance, Moy et al. (1986) used the duration of the longest continuous sequence of failure rather than the average. The longest sequence was used because it could more readily be included as a constraint in a linear programming optimisation model used by Moy et al. (1986) than Equation (3.51).

Another performance measure sometimes used in water resources investigations is vulnerability (η). This is a measure of the severity of reservoir failure, and as with resilience, a number of definitions are reported in the literature (e.g. Simonovic, 1992;

Loucks, 1997; Zongxue et al., 1998). The definition due to Zongxue et al. (1998) is as follows:

$$\eta = \frac{\left(\sum_{t \in f} R_t^* - \sum_{t \in f} R_t^D\right)}{\sum_{t \in f} R_t^*} \qquad (0 \le \eta \le 1) \qquad (3.52)$$

Loucks (1997) combined all the above three performance indices - reliability, resilience and vulnerability - into a single expression termed the sustainability index (φ) which is defined as:

$$\varphi = \delta \Re (1 - \eta) \qquad (3.53)$$

where $\delta, \Re$ and η are the time-based reliability, resilience and vulnerability, respectively.

According to Equation (3.53), a reservoir system is highly sustainable if it has a high reliability and resilience and a low vulnerability.

3.5.1.2 Reservoir Planning Analysis

While there are many reservoir planning techniques (see McMahon and Mein, 1986; ReVelle, 1997) only a few of these specified targets for the performance criteria discussed in section 3.5.1.1. Those that do belong to two broad groups: (i) simulation models, and (ii) optimisation models. Simulation models are based on reservoir water balance and can be further categorised into (i) behavioural approach and (ii) Sequent Peak Algorithm (SPA). Behaviour analysis is based on reservoir storage whereas the SPA uses storage deficits. While the behavioural approach is much more versatile and can easily accommodate storage dependent phenomena such as reservoir surface

evaporation and seepage and can design for any reliability, it requires an operating policy for its implementation. Apart from where a heuristic operating policy is used, this is generally unavailable during reservoir planning. Moreover, the initial state of the reservoir has a significant impact on the outcome of a behaviour analysis (Pretto et al., 1997; McMahon & Mein, 1986). The behavioural approach also has the limitation that it uses a trial and error technique for reservoir analysis. Another limitation is that it is difficult to control the level of shortfall during a failure period, i.e. when the reservoir is unable to supply the target demand (see Pretto et al., 1997). However, Adeloye et al. (2001) have shown that a modification of the basic SPA can lead to a curing of the so called misbehaviour found in the behavioural approach. Because the SPA was used as the planning technique in the study, it will be described in more detail in the next subsection.

Reservoir optimisation can be formulated using linear programming, non-linear programming and dynamic programming (ReVelle, 1997). Optimisation models require the formulation of an objective function such as minimising reservoir storage capacity for a given yield, or maximising reservoir yield for a fixed storage capacity. The disadvantage of optimisation is that reservoir performance criteria apart from the reliability, such as vulnerability and resiliency cannot be designed for. The main strength of optimisation models are that they do not require an operating policy to implement.

Dandy et al. (1997) compared optimisation and simulation approaches for reservoir yield assessment in Australia. They concluded that the optimisation approach produced unrealistically high yield estimates when compared to yield estimates from the simulation approach.

3.5.1.3 SPA and its Modifications

The basic SPA (Thomas and Burden, 1963) estimates the failure-free capacity of an initially full single reservoir as the maximum of all the sequential deficits obtained using (Loucks et al., 1981):

$$K_{t+1} = \begin{cases} K_t + D_t + \hat{E}_t - Q_t; \text{if} > 0.0 \\ 0.0; \text{otherwise} \end{cases} \quad ; t = 1,2\ldots,T_p,\ T_p+1,\ T_p+2,\ldots,2T_p \qquad (3.54)$$

where K_t and K_{t+1} are the volumetric sequential deficits at the beginning and end of period t respectively; Q_t is the volumetric inflow during t; D_t is the volumetric demand during t; $\hat{E}_t$ is the volumetric reservoir surface net evaporation (i.e. direct evaporation less direct rainfall) during t; and T_p is the total number of periods. Because $\hat{E}_t$ depends on the exposed surface area of the reservoir, which in turn depends on storage, cannot be explicitly included in the basic SPA and is thus ignored.

Given some of the limitations of the basic SPA, modifications have been carried out by Lele (1987), and Adeloye and Montaseri (1998). Lele's (1987) modifications enabled both surface net evaporation losses and different reliability levels to be considered explicitly using an iterative procedure. Unlike the behavioural approach (Nawaz and Adeloye, 1999; McMahon & Mein, 1986; Pretto et. al., 1997), the determination of storage-yield for a desired reliability is no longer a trial and error procedure in the modified SPA. Furthermore, because the SPA by default uses two cycles of the historical record, the usual problems associated with the choice of the starting state of the reservoir is no longer an issue.

Moreover, being able to impose a limit on supply shortfall during failure periods with the modified SPA also means that system's vulnerability or volumetric failure risk (Hashimoto et al., 1982) can be selected *a priori*. According to Adeloye et al. (2001), restricting the amount of water shortfall during any failure period to fixed amounts also brings another, quite important benefit. Adeloye et al. (2001) showed that if no restriction is placed on water shortfall during any failure period (which is the basis of the behavioural approach), then it could lead to storage estimates 'misbehaving'. The misbehaviour of certain statistics of reservoir storage capacity estimates obtained using a behavioural approach were first reported by Pretto et al. (1997). Pretto et al. (1997) showed that statistics of storage estimates such as mean and higher quantiles (based on behaviour analysis) for medium record lengths (i.e. 100 years) exhibit a hump in their functional relationships with the runoff data record length. Adeloye et al. (2001) showed that this apparent misbehaviour was largely cured by using the modified SPA which allows restrictions to be placed on the shortfall.

As mentioned previously, Adeloye and Montaseri (1998) extended the modified SPA to be applicable to multiple reservoir systems. They showed that in the absence of any formal operating policy the use of the Space Rule (Maass et al., 1962; Oliveria and Loucks, 1997; Nalbantis and Koutsoyiannis, 1997) could be used to minimise spills from each of a group of reservoirs. The Space Rule is based on equalising, as much as possible, the ratio of the predicted flow into each reservoir during the remainder of the drawdown-refill cycle to that in all the reservoirs, and the ratio of space available in each reservoir to that in all the reservoirs at the beginning of that cycle.

3.5.2 Characterising the Uncertainty in Reservoir Planning Variables

Uncertainty in reservoir design stems primarily from the inability to predict future inflow that a reservoir is likely to encounter during its operational life. Indeed, Nemec and Schaake (1982) argue that '*it will almost never be possible to forecast a long sequence of actual flows equal to the life of a project in real time....*' Consequently, analysts must learn to cope with this source of uncertainty. Even if it were possible to accurately predict future flows, it would not eliminate the uncertainties in reservoir design. The reason for this given by Klemes (1980) is provided below.

Klemes (1980) states that '*in most practical situations, the differences in performance (of a reservoir) are lower than the noise level in reliability computations. This is so because reliability and storage capacity are highly non-linear. Thus it may happen, for example, that while a reservoir with a storage capacity K is capable of ensuring the release of outflow with a (near) 100% reliability over a period of 30 years, a reservoir with storage capacity equal to only 50% of K does not reduce the reliability to anything close to 50% but, in terms of failure years to (say) 90%, in terms of the time to (say) 93.7% and in terms of volume of water supplied to (say) 99%.*'

Most of the available techniques for reservoir analysis make use of a single data record (baseline or future) at sites of the proposed reservoir to estimate the capacity for a given yield and reliability. Such an analysis of a reservoir system using a single data record will give a single estimate of the yield or storage capacity for the reliability. This single estimate will have the required reliability as long as a drought sequence severer than the design sequence does not occur during operation of the reservoir (Adeloye, 1994). Where this happens not to be the case, then the realised reliability during operation

could be significantly different from the intended reliability. In other words, the use of single streamflow records in water resource studies does not allow for the testing of alternative designs and policies against a range of sequences that are likely to occur in the future. By testing designs and policies against a range of possible sequences that could occur, the variability and range of possible future performance is better understood and better system designs and policies can be selected. Stochastic hydrology techniques are usually applied for this purpose.

3.5.3 Stochastic Hydrology

Stochastic streamflow models are employed to generate alternate sequences of streamflow having the same statistical properties as the historical data. The alternate sequences can then be used in reservoir models to obtain a range of reservoir system characteristics such as yield and performance measures. The streamflow process is part deterministic and part random (stochastic) and therefore its magnitude and timing cannot be predicted with certainty. This behaviour is more appropriately described by stochastic models because their outputs are random to some extent. In other words, for a stochastic streamflow model, a given input produces different outputs as opposed to a single output in deterministic models.

As far as stochastic streamflow generation is concerned, a number of models of varying complexities now exist (Loucks et. al., 1981; Frick and Salas, 1991). These models fall into two broad types for annual flow generation: the relatively simple, short-term persistence models, such as the auto-regressive (AR) process; and the more complex long-term persistence models, such as the fractional Gaussian noise (FGN) process.

It is often argued that because streamflow is a natural process, then any valid model must preserve the persistence in streamflow. Persistence of a hydrological process refers to the tendency of an extreme event being followed by an even more severe event, e.g. long periods of consistently low flows or long periods of consistently high flows. Long term persistence introduces non-stationarity into a hydrological time series in that parameters estimated using different segments of the data will be statistically different. The usual measure of long term persistence is the Hurst coefficient (h) defined as:

$$h = \frac{\log(\varsigma/\sigma_u)}{\log(n_u/2)} \tag{3.55}$$

where ς is the range of cumulative departures from the mean value in a time series, σ_u is standard deviation of the series and n_u is the number of observations in the series data. The Hurst coefficient tends to an average of 0.7 for most natural time series data (Salas, 1993). The characteristic departure from 0.7 of the h for random processes is often termed the Hurst phenomenon. The significance of the Hurst phenomenon is that since streamflow process is a natural process, then any stochastic model to describe streamflow process must be capable of preserving the 'h' coefficient at 0.7.

As already mentioned in section 2.4, the prospect of human-induced climate change calls into question the assumption of a stationary hydrologic time-series. Consequently, analysts might be better served by examining a time-series for trend. If there is trend in the record, this needs to be incorporated into stochastic data generation. Broken Line models (Bras and Rodrigues-Iturbe, 1985), FGN (Mandelbrot and Wallis, 1968), and the fractionally differenced ARIMA model known as FARIMA (Montanari et al., 1997) are all examples of long-term persistence models which have been used to model non-stationary time series and preserve the Hurst coefficient. More recently, Strupczewski

and Mitosek (1996) provided a method to incorporate non-stationarity. Their recommended approach is based on a constant streamflow probability distribution with a variation in parameters over time. Because of the difficulty involved in estimating model parameters, long-term persistence models have not seen widespread use.

Extensive studies have shown that for reservoir storage-yield analysis, the complexity of the stochastic model is unimportant; what is more important is the accuracy of parameter estimates (Klemes et al., 1981). Thus very little information will be lost by using a simple AR process model instead of FGN process model, so long as there is an adequate streamflow data record with which to estimate the parameters of the model. Adeloye (1996) demonstrated that records of at least 20 years are required to provide parameter estimates of sufficient accuracy. The simple AR model was used for stochastically generating streamflow data in the study with the sampling uncertainties in the parameters of such models being explicitly incorporated.

3.5.3.1 Lag-one Autoregressive Model

The lag-one auto regressive model, AR(1), also known as the Markov model has been extensively applied in water resources to generate annual streamflow (e.g. Vogel and Stedinger, 1988; Adeloye and Nawaz, 1997). This is a relatively simple model that reproduces the desired persistence of annual flows and is defined as:

$$q_i = \alpha + \beta q_{i-1} + v_i; \quad i = 1, y \tag{3.56}$$

where,

q_i, q_{i-1} = annual flows for the i-th and (i-1)-th years, respectively;

β = lag-one serial correlation coefficient of annual flows;

$\alpha = \mu_q(1 - \beta)$ where μ_q is mean of annual flows;

v_i = independent zero mean normal random variable with variance $\sigma_v^2 = \sigma_q^2(1-\beta^2)$;

σ_q^2 = variance of annual flows.

Equation (3.56) is a single-site data generation technique. The multiple site model can be written as:

$$Z_i = AZ_{i-1} + BV_i \qquad (3.57)$$

where,

Z_i, Z_{i-1} = vector (N x 1) of annual flows at the different sites for the i-th and (i-1)-th years, respectively;

A,B = (N x N) coefficient matrix whose elements are chosen to reproduce the lag-zero and lag-one cross-correlations between annual flows at the different sites;

V_i = (N x 1) vector of independent standard normal random variables

To estimate the two model parameters in Equation (3.56), i.e. α and β, in addition to the variance of the random error σ_v^2, the single (baseline or future) data record is used. However, given that such records are finite, these estimates will be affected by sampling errors and therefore, the uncertainty of model parameter estimates should be considered by stochastic data modellers (Grygier and Stedinger, 1988).

The following procedure has been recommended by Stedinger and Taylor (1982) to correct the annual streamflow parameters of AR(1) model such as the mean, standard deviation and serial correlation coefficient for uncertainty. Let α, β, and σ_v^2 be the true parameter values which are unknown. These values can conceptually be thought of as arising from the sum of two quantities, i.e. the sample estimates and their random component. Let the sample estimates of α, β, and σ_v^2 (which are random variables) be denoted by $\hat{\alpha}$, $\hat{\beta}$ and $\hat{\sigma}_v^2$, respectively. Using a matrix notation of the AR(1) model in Equation (3.56), i.e.,

$$G = U\theta + V \tag{3.58}$$

where,

$$\theta = (\alpha,\ \beta)^T; \tag{3.59}$$

$$G = \begin{bmatrix} q_1 & \cdots & q_y \end{bmatrix}^T; \tag{3.60}$$

$$U = \begin{bmatrix} 1 & \cdots & 1 \\ q_0 & \cdots & q_{y-1} \end{bmatrix}^T; \text{ and} \tag{3.61}$$

$$V = \begin{bmatrix} v_1 & \cdots & v_y \end{bmatrix}^T \tag{3.62}$$

The least squares solutions for θ and σ_v^2 is:

$$\hat{\theta} = (\hat{\alpha},\ \hat{\beta})^T = (U^T U)^{-1} U^T G \tag{3.63}$$

$$\hat{\sigma}_v^2 = \frac{1}{y-2}(G - U\hat{\theta})^T (G - U\hat{\theta}) = \frac{1}{y-2}\sum_{i=1}^{y}(q_i - \hat{\alpha} + \hat{\beta} q_{i-1})^2 \tag{3.64}$$

The symbols T and -1 in Equations (3.63) and (3.64) represent the transpose and inverse of a matrix, respectively. Since V is normally distributed, it follows that

$$\frac{(y-2)\hat{\sigma}_v^2}{\sigma_v^2} \sim \chi_{y-2}^2 \tag{3.65}$$

where χ_{y-2}^2 is the Chi-squared distribution having (y – 2) degrees of freedom (Montgomery, 1984). Likely values of σ_v^2 can thus be sampled with the Chi-squared distribution using the inverse, i.e.,

$$\tilde{\sigma}_v^2 = \frac{(y-2)\hat{\sigma}_v^2}{\chi_{y-2}^2} \tag{3.66}$$

According to Equation (3.58), for a given σ_v^2, the vector of possible values of $\theta = (\alpha, \beta)^T$, denoted by $\tilde{\theta}$, has a bivariate normal distribution with mean $\hat{\theta}$ and covariance matrix $\tilde{\sigma}_v^2(U^TU)^{-1}$, i.e.,

$$\tilde{\theta} \sim N(\hat{\theta},\ \tilde{\sigma}_v^2(U^TU)^{-1}) \tag{3.67}$$

Therefore, for each generated value of $\tilde{\sigma}_v^2$, a corresponding value of $\tilde{\theta}$ can be estimated by a vector $(\tilde{\alpha},\ \tilde{\beta})^T$ from a bivariate normal distribution with mean $\hat{\theta}$ and covariance matrix $\tilde{\sigma}_v^2(U^TU)^{-1}$. The stochastic annual data sequences which incorporate the uncertainty in the three parameters, i.e. mean, variance, and lag-one serial correlation, are generated using the following procedure (Stedinger and Taylor, 1982):

Step 1

The model parameters, $\hat{\theta} = (\hat{\alpha}, \hat{\beta})^T$ and $\hat{\sigma}_v^2$, are estimated using the available annual flow record.

Step 2

For i =1, y:

(i) A possible value of $\tilde{\sigma}_v^2$ is determined using Equation (3.66). Estimates for the Chi-squared function in terms of the standard normal are available in Abramowitz and Stegun (1972, p. 941):

$$\chi_v^2 = v\left\{1 - \frac{2}{9v} + k\sqrt{\frac{2}{9v}}\right\}^3 \qquad (3.68)$$

where v is (y-2) degrees of freedom and k is an independent standard normal random variable, i.e. $k \sim N(0, 1)$.

(ii) Possible true pair of α and β parameters, i.e. $\tilde{\alpha}$ and $\tilde{\beta}$, are drawn from the bivariate normal distribution according to Equation (3.67). A relatively straightforward method of generating multivariate normal distribution variables, using the Cholesky decomposition of the covariance matrix, is provided in Knuth (1988). The covariance matrix $C = \tilde{\sigma}_v^2(U^TU)^{-1}$ has (2 × 2) elements and is symmetric and positive definite or semi-definite. Given such a matrix C, there exists a lower triangular matrix L such that $LL^T = C$. If L is assumed to be a lower triangular matrix then a unique solution (i.e. Cholesky decomposition methods) can be applied to decompose matrix C and find such a matrix L (Lane,

1979). If v_1' and v_2' (elements of the vector V') are independent standard normal variables with zero mean and unit variance, and if

$$\tilde{\theta} = \hat{\theta} + LV' \quad \text{or} \tag{3.69}$$

$$\begin{bmatrix} \tilde{\alpha} \\ \tilde{\beta} \end{bmatrix} = \begin{bmatrix} \hat{\alpha} \\ \hat{\beta} \end{bmatrix} + \begin{bmatrix} l_{1,1} & 0 \\ l_{2,1} & l_{2,2} \end{bmatrix} \begin{bmatrix} v_1' \\ v_2' \end{bmatrix} \tag{3.70}$$

then $\tilde{\alpha}$ and $\tilde{\beta}$ are dependent random variables, normally distributed with mean $\hat{\alpha}$, $\hat{\beta}$ and covariance matrix C (Knuth, 1988).

(iii) Each set of parameters, $\tilde{\alpha}$, $\tilde{\beta}$ and $\tilde{\sigma}_v^2$, is then used to generate the annual flow using Equation (3.56).

The corresponding possible true mean and variance of the annual flows for each period i can be obtained using:

$$\mu_{q,i} = \frac{\tilde{\alpha}_i}{(1-\tilde{\beta}_i)} \tag{3.71}$$

$$\sigma_{q,i}^2 = \frac{\tilde{\sigma}_{v,i}^2}{(1-\tilde{\beta}_i^2)} \tag{3.72}$$

Equations (3.71) and (3.72) are useful for correcting flows generated without the consideration of uncertainty in parameter estimates. Such a situation could arise for example in the generation of monthly flows using the Valencia-Schaake disaggregation model (Valencia and Schaake, 1973) (see section 3.5.3.2) or the Thomas-Fiering seasonal model (Thomas and Fiering, 1962). In both cases although uncertainty in the

monthly flow mean and variance are not modelled explicitly, the generated monthly flows can be adjusted for uncertainty in the annual flow mean and variance. These adjustments are made by scaling the sample estimates of the monthly flow mean and variance parameters by $\mu_{q,i}/\overline{q}$ and $\sigma^2_{q,i}/s^2_q$, respectively, where $\overline{q}$ is the sample estimate of the annual mean and s^2_q is the sample estimate of the annual variance, and $\mu_{q,i}$ and $\sigma^2_{q,i}$ are given by Equations (3.71) and (3.72) respectively. For example, let the disaggregated, standardised flow, i.e. zero mean and unit variance, for month j, year i be $z_{i,j}$. Let the mean flow estimate for month j be $\overline{Q}_j$ and let the variance estimate be S^2_j, then the disaggregated flow for the month without correcting for parameter uncertainty is:

$$\hat{Q}_{i,j} = z_{i,j}\sqrt{S^2_j} + \overline{Q}_j \tag{3.73}$$

and when corrected for parameter uncertainty, it is:

$$Q_{i,j} = z_{i,j}\sqrt{S^2_j \frac{\sigma^2_{q,i}}{s^2_q}} + \overline{Q}_j \frac{\mu_{q,i}}{\overline{q}} \tag{3.74}$$

3.5.3.2 Seasonal Flow Generation

While annual models are much easier to handle, such a coarse time scale may not capture the significant within-year (or seasonal) behaviour of most water resources systems (Adeloye and Nawaz, 1997). In the least, monthly flows are required or where the system is of the type in which operational decisions are to be made on a daily or weekly basis, such as in regulating and pumped-storage reservoirs, then flows for such

finer time scales are required. For single sites, monthly flows can be generated directly using seasonal models, or models with periodic parameters. An example of a monthly stochastic streamflow generation model is the Thomas-Fiering Model (Thomas and Fiering, 1962). This model generates monthly flows directly by varying its parameters from one month to the next. Alternatively, annual flows generated with the AR(1) model for example, can be disaggregated via a number of disaggregation schemes. Any one of the following three methods can be applied for the disaggregation: (i) Method of Fragments (ii) proration of annual flows and (iii) the Valencia-Schaake model. A description of the Thomas-Fiering model along with the three disaggregation schemes is now provided. A relatively more detailed description of the Valencia-Schaake model is given since it was adopted in this work. It should be noted that in the following discussion, the term 'historical' data record is synonymous with terms single 'baseline' or 'future' data record.

The Thomas-Fiering (T-F) Model

The Thomas and Fiering (T-F) model is similar to the AR(1) model (Equation 3.56) except that in the T-F model, the three parameters α, β and σ_v^2 are varied according to the month under consideration. Consequently, the T-F model will require a much larger number of parameters (i.e. $12 \times 3 = 36$) to be estimated. Although the T-F model will adequately reproduce these 36 parameters in the generated sequences, it is unable to reproduce the annual flow statistics or the correlations between the monthly and annual flows in the historical record. Further details of the T-F model are provided in McMahon and Mein (1986).

Annual Flow Disaggregation by Proration

The proration disaggregation method is a simple technique in which the generated annual flows are disaggregated based on the historical monthly percentage of the long-term mean annual total flow volumes occurring in each month (Savic et al., 1989). In other words, the use of this method involves obtaining monthly mean flows from the historical data. If these are denoted by $\overline{Q}_j$; j=1,2,...,12 and the annual flow generated in the i-th period is denoted by q_i; i=1,2,...,n where n is the length of data record, then the disaggregated monthly flows are defined as:

$$\begin{bmatrix} Q_{1,1} & . & . & Q_{1,n} \\ Q_{2,1} & . & . & Q_{2,n} \\ . & . & . & . \\ Q_{12,1} & . & . & Q_{12,n} \end{bmatrix} = \begin{bmatrix} \overline{Q}_1 / \overline{q} \\ . \\ . \\ \overline{Q}_{12} / \overline{q} \end{bmatrix} \times \begin{bmatrix} q_1 & . & . & q_n \end{bmatrix} \qquad (3.75)$$

where $Q_{j,i}$ is the disaggregated flow in month j, year i and $\overline{q}$ is the mean annual flow. Owing to its formulation, the proration method will only reproduce the mean of the monthly flows.

Annual Flow Disaggregation by Method of Fragments

The Method of Fragments was proposed by Svanidze (1964) and later updated by Srikanthan and McMahon (1982). The method involves the following steps:

(i) Construct a new monthly time series $Q'_{j,i} = Q_{j,i} / q_i$; i=1,2....,n; j=1,2,...,12, from the historical data record, where $Q_{j,i}$ is the historic flow in month j, year i, and q_i is the annual flow in year i. These $Q_{j,i}$ are referred to as the 'fragments'.

(ii) Rank the annual flow volumes (carrying along the associated fragments) from the lowest value to the highest value so that $q_1 \leq q_2 \ldots\ldots \leq q_n$.

(iii) Using the ranked annual flow volumes, form n classes with defined upper and lower limits. Class 1 will have a lower limit of zero whereas there is no upper limit for class n. The intermediate class limits are obtained by averaging the two adjacent flows in the ranked series. Thus for example the upper limits of class 1 will be $0.5(q_1+q_2)$, which is also the lower limit of class 2, etc.

(iv) Assign the fragments to the classes. Class 1 is assigned to those fragments that are associated with smallest annual flow q_1 while those associated with the second largest annual flow q_2 are assigned to class 2 and so on.

(v) Generate the annual flow using an appropriate annual flow model such as the AR(1) model, check to see which of the class intervals it belongs and hence use the fragments associated with that class to dissagregate the generated annual flow.

It can be seen from step (v) above that the Method of Fragments is similar to the proration method except that unlike in the latter, the fragments used for distributing the generated annual flow are not constant but vary with the generated annual fow. Both of these simple methods use a purely deterministic approach to distribute annual flow to monthly flows, whereas streamflow data are the sum of deterministic and random components.

This inability to account for the stochastic component of streamflow may have been responsible for another problem of the Method of Fragments as noted by Adeloye and Nawaz (1997). In a study of storage-yield characteristics of some reservoirs, they used the Method of Fragments to disaggregate stochastic annual flows, which were then analysed to develop the probability distribution of storage capacities for various demands. They showed that the probability distribution of storage capacity is a step

function, especially for within-year reservoir systems. This is because the smallest annual flows of the generated sequences, which determine the critical twelve months (and hence the within-year storage requirement), often cluster together implying that a larger number of such flows will be disaggregated with the same fragment. Since the estimates of storage capacity for within-year systems are based on the smallest annual flow in the data record, such storage capacities obtained will also be clusters.

The Method of Fragments can easily be adapted to generate stochastic monthly flows at multiple reservoir sites and this is described in McMahon and Mein (1986).

Valencia and Schaake Disaggregation Model

The Valencia and Schaake (1973) model can be described as follows (Montaseri, 1999):

Let $Z_i = (Z_i^1, \ldots, Z_i^N)^T$ be the vector (N × 1) of transformed zero mean annual flows at sites n = 1, N. Let $X_i = (X_{1i}^1, \ldots, X_{M1}^1, \ldots, X_{1i}^N, \ldots, X_{Mi}^N)^T$, where N is the total sites and M is the total number of seasons per year, be the vector (MN × 1) of transformed zero mean seasonal flows X_{mi}^n for season m, year i, and site n, so that either $E[Z_i] = 0$ or $E[X_i] = 0$. The Valencia-Schaake model for the case of disaggregation of annual flows into seasonal flows is:

$$X_i = AZ_i + BV_i \tag{3.76}$$

where V_i is a (MN × 1) vector of independent standard normal random variables and independent of Z_i, and, A and B are (MN × N) and (MN × MN) coefficient matrices, respectively.

The elements of the parameter matrices A and B are determined using the matrices:

$$S_{ZZ} = E[Z_i Z_i^T] \tag{3.77}$$

$$S_{XX} = E[X_i X_i^T] \tag{3.78}$$

$$S_{XZ} = E[X_i Z_i^T] \tag{3.79}$$

$$S_{ZX} = E[Z_i X_i^T] \tag{3.80}$$

where,

S_{ZZ}, S_{XX} and S_{XZ} are (N × N), (MN × MN) and (MN × N) matrices, respectively, and have elements:

$$S_{ZZ} = E[Z_i^n X_i^T] \text{ for } n, k = 1, N \tag{3.81}$$

$$S_{XX} = E[X_{ji}^n X_{li}^k] \text{ for } n, k = 1, N \text{ and } j, l = 1, M \tag{3.82}$$

$$S_{XZ} = E[X_{ji}^n Z_{li}^k] \text{ for } n, k = 1, N \text{ and } j, l = 1, M \tag{3.83}$$

and S_{ZX} is clearly a transposed matrix of S_{XZ}.

The elements of matrix S_{XX} are the variances for the same season at each site, (i.e. n = k, and j = l), and lag zero cross-covariances between different seasons for either each site or various sites (i.e., j ≠ l). It is also symmetric in the same manner as S_{ZZ}. Matrix S_{XZ} contains the lag-zero cross-covariances between the annual flows and the seasonal flows at sites.

Using the standard transformation of annual and seasonal streamflow data, i.e. with zero mean and unit variance, the values of S_{ZX} and S_{XX} matrices for two sites and two seasons become:

$$S_{XX} = \begin{bmatrix} 1 & r(X_1^1, X_2^1) & r(X_1^1, X_1^2) & r(X_1^1, X_2^2) \\ r(X_2^1, X_1^1) & 1 & r(X_2^1, X_1^2) & r(X_2^1, X_2^2) \\ r(X_1^2, X_1^1) & r(X_1^2, X_2^1) & 1 & r(X_1^2, X_2^2) \\ r(X_2^2, X_1^1) & r(X_2^2, X_2^1) & r(X_2^2, X_1^2) & 1 \end{bmatrix} \tag{3.84}$$

$$S_{XZ} = \begin{bmatrix} r(X_1^1, Z^1) & r(X_1^1, Z^2) \\ r(X_2^1, Z^1) & r(X_2^1, Z^2) \\ r(X_1^2, Z^1) & r(X_1^2, Z^2) \\ r(X_2^2, Z^1) & r(X_2^2, Z^2) \end{bmatrix} \tag{3.85}$$

where $r(X_j^n X_l^k)$ is lag-zero cross-correlation between the flows of seasons j and l at sites n and k; and $r(X_j^n Z^k)$ is lag-zero cross-correlation between the annual flows at site k and the flows of season j at site n.

Using the term of S_{XX}, S_{XZ}, and S_{ZZ}, the values of A and B are obtained by:

$$A = S_{XZ} S_{ZZ}^{-1} \tag{3.86}$$

$$BB^T = S_{XX} - S_{XZ} S_{ZZ}^{-1} S_{ZX} \tag{3.87}$$

Clearly X_i will have a normal distribution with zero means if both Z_i and V_i are normally distributed.

The sum of the generated seasonal flows will equal the annual flows if both seasonal and annual historic streamflow records are normally distributed. However, once the monthly flows are transferred e.g. using logarithm to achieve normality, the sums of the generated seasonal flows will generally deviate from generated annual flows. This small distortion can be ignored, or the generated seasonal flows can be scaled for the specified values of the annual flows (Grygier and Stedinger, 1988).

In the case of spatial sub-sites disaggregation, the model equation may be written as:

$$Z_i = AY_i + BV_i \tag{3.88}$$

where Y_i is transformed zero mean total annual flows at sites during year i; and Z_i, A, B, and V_t are as defined previously.

Savic et al. (1989) analysed four synthetic streamflow generation schemes for use in the estimation of the required conservation storage for a single reservoir: Thomas-Fiering Seasonal Model and three types of Disaggregation Models (Proration of Annual Streamflow, method of fragments and Modified Valencia-Schaake). The comparisons were based on two criteria: the statistics of generated and historic streamflow; and a

comparison between the reservoir sizes obtained using generated and historical streamflow data. Savic et al.(1989) concluded that the performance of an AR(1) annual model followed by the Valencia-Schaake disaggregation model to obtain monthly flows on the basis of statistical agreement was better than a T-F model, the method of fragments or the proration method. Furthermore, Savic et al. (1989) state that the poor performance of the proration method in reproducing historical statistics may imply that this model is not suitable for use in reservoir analysis. Another advantage of disaggregation models is that they can be used to disaggregate also in space as well as in time (Frick and Salas, 1991; Firor et al., 1996).

3.6 Examples of Climate Change Impacts Assessment and Uncertainty Studies

Numerous studies investigating the possible impacts of climate change on water resources have been carried out to date. The proceedings from a climate and water conference (Lemmelä and Helenius, 1998) contains over 150 articles, and a comprehensive online bibliography of more than 920 climate change articles has been compiled by the US Pacific Institute (www.pacinst.org). To keep pace with the large number of studies being published, the database is continually updated. Furthermore, the UK Department of Environment Transport Regions reviewed climate impacts studies carried out in the UK between 1998 and 2000 (Hedger et al., 2000).

Given the vast literature on the subject, Chalecki and Gleick (1999) categorised these studies on the basis of specific criteria. The climate change water resource studies can

be classed as those investigating the impacts on runoff and groundwater, and those studying the impacts on reservoir systems.

Table 3.7 summarises some studies carried out over the years and shows that the first published study on the topic was by Nemec and Schaake (1982). They investigated the impact of climate change on runoff and as well as reservoir systems. They looked at two catchments, one large catchment is located in an arid region and the other, in a humid region. They used the Sacramento daily conceptual water balance model for catchment response modelling and noted that precipitation was the major variable influencing runoff. They used hypothetical climate change scenarios and found that a 25% precipitation rise and 1°C temperature rise increased the runoff by 250% and 70% for the arid and humid catchments, respectively. Next, they assessed the impacts on a very large hypothetical reservoir. They noted that a 1% change in precipitation produced a 2% change in reliable yield, and a 1% change in potential evapotranspiration produced a 0.5% and 1% change in yield for the arid and humid catchments, respectively. The effects of precipitation change on storage were much more pronounced than the effect on yield which may have been caused by the nearly flat shape of a typical, non-linear storage-yield function in the region of high yields, i.e. yields close to a full level of development. For example, the effects of a 25% reduction in precipitation (for a given demand) resulted in more than 400% and 200% increases in required storage capacity for the arid and humid cases, respectively.

Other notable studies include those of Cole et al. (1991), Idso and Brazel (1984), Shnaydman and Niemann (1996), Nawaz et al. (1999) and Hulme et al. (1999b). Cole et al. (1991) followed a similar approach to Nemec and Schaake (1982) except that interannual variability in precipitation was included by using a stochastic weather

generator. Idso and Brazel (1984) showed that different effects on runoff would be obtained by including evapotranspiration changes due to carbon dioxide doubling. Idso and Brazel (1984) found that for a 2°C rise in temperature and 10% reduction in precipitation, streamflow changed from -41% to +42% when carbon dioxide effects on plant stomata were incorporated. The study of Nawaz et al. (1999) differed from the other published studies at the time in that they investigated the effects of transient GCM based climate scenarios on multiple reservoir storage-yield. Moreover, they also included the effects of reservoir surface fluxes which may be significant in some of the arid regions (see Fennessey, 1995; Adeloye and Nawaz, 1998).

In another study, Shnaydman and Niemann (1996) investigated water resources planning strategies. They analysed the Terek River catchment in northern Russia. They used hypothetical scenarios and arbitrary changes in irrigation demand to determine the effects of climate change on the reliability and resiliency of a reservoir. They noted that reservoir reliability and resilience varied insignificantly when inflows and demands varied from -10% to +20%. However, there was a large reduction in reliability and resiliency when runoff was reduced by 20%.

Nawaz et al. (1999) stated that the inclusion of reservoir surface fluxes (precipitation and evaporation) should be incorporated into studies on the effects of climate change on reservoirs. They demonstrated that for reservoirs in arid or semi-arid regions, expected to become even drier in the future, ignoring net surface evaporation would lead to an under design for yield. In contrast, the omission of net evaporation from reservoirs in wetter catchments expected to become wetter in the future, might actually be beneficial. Hulme et al. (1999b) used results from a GCM experiment to investigate the effects of natural climate variability and those due to anthropogenic climate change. They found

that for some regions across Europe, the effects of human-induced climate change on runoff (and subsequently, wheat production) may be less pronounced than impacts caused by natural climate variability.

From Table 3.7, and based on numerous studies (see www.pacinst.org; Lemmelä and Helenius, 1998; Chalecki and Gleick, 1999), some general patterns and deficiencies in the published literature can be summarised as follows:

- earlier studies used hypothetical scenarios whereas GCM output is favoured in more recent investigations;
- UK Hadley Centre's GCM appears to be the most popular;
- GCM output is commonly downscaled using interpolation;
- baseline climate perturbation is carried out using mean changes rather than introducing interannual variability into future hydroclimatological time-series through the use of stochastic weather generators;
- water balance models are the preferred hydrological modelling tool;
- more emphasis is placed on the effects of climate change on runoff than on reservoirs or groundwater;
- relatively few studies have investigated climate change effects on low flow indicators such as Q_{95};
- only a single study (that of Kirshen and Fennessey, 1995) has investigated the impacts of carbon dioxide induced change in evapotranspiration (vegetation feedback) on reservoir systems;
- the role of natural climate variability in climate change impacts has received little attention;

- there have been relatively few attempts at quantifying the uncertainty in impacts assessment.

The present study has addressed most of these shortcomings of the traditional approach. In particular, it has focussed on characterising the uncertainty of climate change impacts by developing the statistical characteristics of the impacts through the use of extensive Monte Carlo simulation experiments.

The few attempts addressing the issue of uncertainty in climate impacts (see Figure 3.6 for range of uncertainties) have concentrated on the differences of impacts resulting from the use of different GCM scenarios. Because of the different parameterisation in the GCMs' (see section 3.3.3.1), different climate change scenarios result even when such models are forced with the same CO_2 emissions scenario. When such scenarios are used to force a catchment model, different impacts are obtained. However, this approach does not strictly speaking, provide the uncertainty of the impacts; rather, only the median levels of the impacts are produced. Such median impacts cannot be used to develop uncertainty limits for the impacts unless the complete statistical characteristics of the impacts are developed using a Monte Carlo simulation approach.

An example study applying a Monte Carlo simulation scheme was carried out by Shackley et al. (1998). In their study, Shackely et al. (1998) used a global carbon cycle model and historical carbon dioxide emissions levels to generate a large number of possible future carbon dioxide scenarios. Their output showed a greater variability in future carbon dioxide levels than those obtained using deterministic models. Although Shackley et al. (1998) did not subsequently use the stochastically generated emissions scenarios to force a climate model to obtain a large number of climate scenarios, such is

entirely feasible with the aid of a climate model. However, the use of a GCM for such a purpose would prove to be too computationally intensive (Arnell, 2000) and instead, a Simple Climate Model could be employed. Jones (2000) used a variant of this approach in a irrigation impact study.

Nikolaidas et al. (1994) used eight years of daily historical meteorological data from a catchment in Vermont, USA to stochastically generate 50 sequences of precipitation, air temperature, dew point, wind speed, solar radiation, and cloud cover. They then used these data in conjunction with a modified Enhanced trickle-Down (ETD) conceptual hydrological model (Nikolaidas et al., 1993) to determine the effects on runoff. They showed the range of input uncertainty in baseline mean annual runoff to be ±24.2%. They then compared these results with those obtained from deterministic modelling and climate change scenarios based on the GFDL (see Table 3.1) and the Goddard Institute for Space Studies (GISS) GCMs. The GFDL and GISS predicted reductions in annual runoff of 37.5% and 17.9%, respectively. The two GCMs impacts are both predicting reductions in runoff. However, when the sampling uncertainty in the inputs were incorporated by Nikolaidas et al. (1994) the results showed that the runoff could actually increase by 24%. Since the statistical description of the impacts is a natural end-product of the Monte Carlo simulation experiments, the probability of actually having the 24% increase in runoff can be estimated.

Mimikou et al. (2000) investigated a catchment in central Greece and used one scenario from the HadCM2 transient experiment and another from the UKHI equilibrium experiment - both representative of the 2050s. The impact assessment proceeded in two stages. The first stage involved using baseline historical data (1960-1996) to generate 50 sequences of precipitation and temperature data using respectively the lag-one and

lag-two stochastic autoregressive models (AR(1) and AR(2)). The second stage involved applying the climate change scenarios to the generated time-series data to obtain 50 sequences of future (1996-2050) precipitation and temperature. Both the baseline and future sequences were then fed in to the rainfall-runoff model to obtain the impacts on runoff.

Only mean monthly runoff changes were provided by Mimikou et al. (2000) as opposed to the changes between all fifty baseline and future runoff sequences. Results showed that future mean monthly runoff resulting from the HadCM2 scenario was less than baseline runoff in all months of the year. The pattern of change was for the largest runoff reductions to occur during the summer (especially in June and August when up to a 46% reduction was expected). The expected winter reductions (of about 13%) were more moderate, especially during January, March and December while the change in mean annual runoff was -18.4%.

Cameron et al. (2000) adopted the GLUE methodology (see section 3.4.2.1) to explore explicitly the uncertainties associated with the impacts of climate change on flood frequency for a small Welsh catchment in the UK. They used 1000 rainfall and streamflow model parameter sets to generate separate 1000 year continuous hourly rainfall and streamflow time series data. These data were used in conjunction with scenarios based on UKCIP98 scenario (developed by the UK Climate Impacts Programme using output from HadCM2) to investigate the impacts of climate change on the hourly annual maximum flood peaks of both short and long return periods (e.g. 10 to 100 years). They reported that the risk of a given streamflow as an element in the distribution of T year floods is changed under a different climate. Based on their study, Cameron et al. (2000) recommended that there is a need to account explicitly for

uncertainty within hydrological modelling, especially in estimating the impacts of climate change.

More recently, Sankarasubramanian et al. (2001) adopted a Monte Carlo simulation approach to investigate the influence of hydrologic model parameters on runoff. They investigated catchments in California, Colorado and Arkansas and adopted the concept of elasticity (i.e. proportional change in runoff divided by the proportional change in a climatic variable such as precipitation) for quantification of the sensitivity of streamflow to changes in climate.

Sankarasubramanian et al. (2001) used a Monte Carlo simulation technique to generate 10,000 50-year sequences of annual precipitation and potential evapotranspiration. These sequences were then fed into three different annual rainfall-runoff models, (i) a simple linear statistical model, (ii) a linear model and (iii) a non-linear model. Next, they used a nonparametric approach along with the generated precipitation and runoff data to evaluate the precipitation elasticity of streamflow. Use of 10,000 data sequences allowed evaluation of the bias and root-mean-square error associated with the elasticity. The main conclusion reached was that that in addition to being influenced by climate, streamflow is also sensitive to model parameters. Results from the study of Sankarasubramanian et al. (2001) along with those from some other studies summarised above would suggest the need for incorporating uncertainty analysis in climate change water resources impacts assessments.

The approach to uncertainty analysis used in this work and summarised in Figure 3.7 is similar to that employed by Mimikou et al. (2000). However, rather than just presenting the mean of the impacts, the complete probability distribution of the impacts are

developed. Furthermore, Mimikou et al. (2000) limited their study to the runoff, whereas in this study, the storage-yield-performance characteristics of reservoirs are also examined.

3.7 Summary

Various methods of assessing the effects of climate change on water resources are available. The most commonly used technique is to adopt an Impact approach. Central to this are climate change scenarios. Although different methods of scenario construction are available, the use of GCMs is the preferred option. Because of various uncertainties, a sensitivity analysis approach is usually adopted. In this approach, a number of climate change scenarios are used to perturb baseline climate to obtain several future climates. These are then input to hydrological models to obtain the hydrologic response of a catchment. In climate change water resource impacts studies, monthly or daily water balance models are usually employed to assess the hydrologic impacts. The next stage in an impact study requires an assessment of changing hydrological conditions on water resource systems such as reservoirs. There are a number of techniques available for this but simulation is most widely used.

A review of published literature reveals that while impacts studies are many, only few of such studies have quantified the sampling uncertainties of the impacts. The sensitivity approach, commonly utilising no more than five or ten, equally likely states of the future climate can be extended to take account of sampling uncertainties. The extended methodology proposed in this work uses a combination of stochastic and deterministic models to derive a large number (e.g. 1000 possibilities) of equally likely

states of the future climate. These data, when fed into a water resource systems response model will provide a large number of impacts on system characteristics (e.g. yield, reliability, resiliency), which can then be subject to standard statistical tests. The results can then be used to construct box-plots, confidence limits and percentiles, thus enabling probability statements to be attached to the assessed impacts.

Table 3.1: Summary of GCMs from five Climate Modelling Centres.

Climate modelling Centre	**Canadian Climate Centre**	**Commonwealth Scientific & Industrial Research Organisation, Australia**	**Hadley Centre, UK**	**Hadley Centre, UK**	**Max Planck Institute, Germany**	**Geophysical Fluid Dynamics laboratory, USA**
Model name	CGCM1	CSIRO1	HadCM2	HadCM3	MPI	GFDL
Atmospheric horizontal resolution (latitude by longitude)	3.75° X 3.75°	3.2° X 5.6°	2.5° X 3.75°	2.5° X 3.75°	2.8° X 2.8°	3.75° X 2.25°
Atmospheric vertical resolution (layers)	10	9	19	19	19	14
Oceanic horizontal resolution (latitude by longitude)	1.8° X 1.8°	3.2° X 5.6°	2.5° X 3.75°	1.25° X 1.25°	2.8° X 2.8°	1.875° X 2.25°
Oceanic vertical resolution (layers)	29	21	20	20	9	18
Treatment of land-surface processes	Modified bucket for soil moisture	Soil layers, plant canopy, and leaf stomatal resistance included	Soil layers, plant canopy, and leaf stomatal resistance included	Soil layers, freezing and thawing of soil layers, plant canopy, and leaf stomatal resistance included	Soil layers, plant canopy, and leaf stomatal resistance included	Simplified bucket for soil moisture
Treatment of atmosphere-ocean coupling	Flux-adjusted	Flux-adjusted	Flux-adjusted	Not flux-adjusted	Flux-adjusted	Flux-adjusted
Treatment of multiple greenhouse gases	No, CO_2 used as surrogate	No, CO_2 used as surrogate	No, CO_2 used as surrogate	Yes	No, CO_2 used as surrogate	No, CO_2 used as surrogate
Treatment of sulphate chemistry	Albedo change only	Albedo change only	Albedo change only	Parameterisation includes the transport, oxidation and removal out of anthropogenic sulphur emissions by physical deposition and rain.	Albedo change only	Albedo change only
Equilibrium climate sensitivity °C	3.5	4.3	2.6	3.3	2.6	3.4
Year when results between 1900-2100 were made available[a]	1998	1999	1998	2000	1998	1999

[a] Refers to GCM monthly data, the release of daily data often takes longer

Table 3.2: Scenario construction methods and requirements (adopted from Smith and Hulme, 1998, with slight modifications) - continued overleaf.

Scenario method	Assumptions	Type of result[a]	Limitations	Required data	Cost[b]	Time demand	Computing demand	Required analyst skills
Non-model based								
Synthetic	A sensitivity scenario; result may be implausible	Typically, uniform climate change across a region and seasons	Climate will most likely not change uniformly across regions and seasons	Need to obtain observed data (min 30 year)	Zero	Low	Zero	Low
Analogue - spatial	Climate in another location can serve as a plausible scenario of future climate	Description of mean M climate	Topography is unimportant in shaping climate	Extensive continental or global climate data	Low	Low/medium	PC	Some understanding of climate diagnostics
Analogue - temporal	Historical or paleoclimate periods can serve as scenarios of climate change	Description of climate patterns and D or M variability	Past warm periods not caused by human activities, e.g., greenhouse gas emissions	Extensive historic climate data series for the region concerned	High for collecting paleoclimate data; low for historical data	Low for historical data, can be high for paleoclimate data		
Model-based								
Simple Climate Models (SCMs)	Reduced-form models can mimic the behaviour of GCMs	Global-mean temperature and sea-level	SCMs do not give regional variation	Combine with 30 years observed data	Very low	Low	PC	Low
General Circulation Models (GCMs)	The model simulates the important climate processes well	300-600 kilometres resolution; M or D data; mean of time-series	Grid boxes have low resolution	Maybe some data for validation purposes; combine with 30 years observed data	Low/medium	Medium	PC or workstation (maybe large data storage requirement)	Modest
Regional climate models (RCMs)[c] - existing	The models have higher resolution than GCMs so they simulate the important climate processes well	25-100 kilometres resolution; M or D data; mean or time series	RCMs use boundary conditions from GCMs, so may not correct for errors	May be some data for validation purposes; may need to combine with 30 years observed data	Low/medium	Medium	PC or workstation (maybe large data storage requirement)	Modest

Table 3.2 (continued): Scenario construction methods and requirements (adopted from Smith and Hulme, 1998, with slight modifications)

Scenario method	Assumptions	Type of result[a]	Limitations	Required data	Cost[b]	Time demand	Computing demand	Required analyst skills
Regional climate models (RCMs)[c] - new	The models have higher resolution than GCMs so they simulate the important climate processes well	25-100 kilometres resolution; M or D data; mean or time series	RCMs use boundary conditions from GCMs, so may not correct for errors	Extensive data for initialization and validation; may need to combine with 30 years observed data	Very high	Very high	High; workstation or mainframe computer	Extensive knowledge of climate modelling
Statistical downscaling[c] - regression methods	Use existing relationships to calculate small-scale climate	Site or catchment specific time series; D or M data	Synoptic-scale relationships are constant over time	Extensive D or M series of synoptic and/or surface climate variables	High, if data to be purchased	High	Substantial; PC or workstation	Some understanding of climate dynamics
Statistical downscaling[c] - circulation typing	Founded on sensible physical linkages between climate at the large scale and weather at the catchment scale.	Site or catchment specific time series; D or M data	Established relationships between a weather pattern and corresponding baseline catchment scale climate remain constant under climate change	Extensive D or M series of surface climate variables	High	High	Substantial; PC or workstation	Some understanding of climate dynamics

[a] D = daily data; M = monthly data.
[b] Costs for obtaining observed data are generally low to medium.
[c] These methods must all be used in conjunction with GCM results.

Table 3.3: Main equations of Xu's conceptual monthly water balance model - without snow module (Vandewiele and Xu, 1991).

Potential evapotranspiration:	$E_t = a_4(\Omega_t^+)^2$	(3.22)
Actual evapotranspiration:	$E_t^{'} = \min\left\{W_t\left(1-e^{-a_1 E_t}, E_t\right)\right\}$	(3.23)
Slow runoff:	$R_t^s = a_2\left(M_{t-1}^+\right)$	(3.24)
Fast runoff:	$R_t^f = a_3\left(M_{t-1}^+\right)P_t^a$	(3.25)
Total runoff:	$R_t = R_t^s + R_t^f$	(3.26)
Complete water balance equation:	$M_t = M_{t-1} + P_t - E_t^{'} - R_t$	(3.27)

Where $W_t = P_t + M_{t-1}^+$ is the available water; $M_{t-1}^+ = \max(M_{t-1}, 0)$ is the available storage; $P_t^a = P_t - E_t\left(1-e^{P_t/\max(E_t,1)}\right)$ is the active rainfall; P_t and Ω_t are monthly precipitation and air temperature, respectively; E_m and Ω_m are long-term average potential evapotranspiration and air temperature, respectively; a_1 parameter is a function of soil permeability; a_2 and a_3 are the storage constant and fast runoff parameters, respectively.

Table 3.4: Main equations of Xu's conceptual monthly water balance model - with snow module (Xu et al., 1996).

Snowfall:	$S_t^f = P_t\left\{1-e^{[-(\Omega_t-a_5)/(a_5-a_6)]^2}\right\}^+$	(3.28)
Snowpack:	$S_t^p = S_{t-1}^p + S_t^f - M_t$	(3.29)
Snowmelt:	$S_t^m = S_{t-1}^p\left\{1-e^{[(\Omega_t-a_6)/(a_5-a_6)]^2}\right\}^+$	(3.30)
Rainfall:	$P_t^r = P_t - S_t^f$	(3.31)
Potential evapotranspiration:	$E_t = E_m[1+a_7(\Omega_t-\Omega_m)]$	(3.32)
Actual evapotranspiration:	$E_t^{'} = \min\left\{E_t\left(1-a_8{}^{W_t/E_t}\right), W_t\right\}$	(3.33)
Slow runoff:	$R_t^s = a_9\left[M_{t-1}^s\right]^+$	(3.34)
Fast runoff:	$R_t^f = a_{10}\left[M_{t-1}^s\right]^+\left[M_t + P_t^a\right]$	(3.35)
Total runoff:	$R_t = R_t^s + R_t^f$	(3.36)
Complete water balance equation:	$M_t^s = M_{t-1}^s + P_t^r - M_t - E_t^{'} - R_t$	(3.37)

Where $W_t = E_t^{'} + \left(M_{t-1}^s\right)^+$ is the available water; $\left(M_{t-1}^s\right)^+ = \max\left(M_{t-1}^s, 0\right)$ is the available storage including snow; $P_t^a = P_t^r - E_t\left(1-e^{-P_t^r/E_t}\right)$ is the active rainfall; P_t and Ω_t are monthly precipitation and air temperature, respectively; E_m and Ω_m are long-term average potential evapotranspiration and air temperature, respectively; a_j (j = 5,6,....10) are model parameters.

Table 3.5: The main equations of MODHYDROLOG (Chiew and McMahon, 1994).

Infiltration:	$I_{ft} = \min\{(a_{coeff}\, e^{-a_{sq} M/a_{smsc}}), (P - a_{rinsc})\}$	(3.39)
Overland flow:	$R_{over} = P - a_{rinsc} I_{ft}$	(3.40)
Depression flow:	$R_{dep} = e^{-a_{md} a_{dsc}/R}(a_{dsc} - a_{ads} M_{dep})$	(3.41)
Surface runoff:	$R_{sur} = R_{over} - R_{dep}$	(3.42)
Interflow:	$R_{int} = a_{sub}(M/a_{smsc}) I_{ft}$	(3.43)
Groundwater recharge:	$R_{gw} = a_{crak}(M/a_{smsc})(I_{ft} - R_{int})$	(3.44)
Soil moisture flow:	$R_m = I_{ft} - R_{int} - R_{gw}$	(3.45)
Actual evapotranspiration:	$E' = \min\{a_{em}(M/a_{smsc}), E\}$	(3.46)
Deep seepage:	$R_{seep} = a_{vcond}(M_{gw} - a_{dlev})$	(3.47)
Baseflow/river recharge:	R_{bf} or $R_r = a_{rk1} M_{gw}^{+} + a_{rk2}\left(1 - e^{-a_{rk3} M_{gw}^{+}}\right)$	(3.48)

Where M is the soil moisture store; P, E, R are precipitation, potential evapotranspiration and runoff, respectively; M, M_{dep} and M_{gw} are respectively the soil moisture store, depression store and groundwater store; a_{coeff}, a_{md}, a_{dsc} etc. are model parameters defined in Table 3.6.

Table 3.6: 19 MODHYDROLOG parameters.

Parameter	Description
a_{rinsc}	Interception storage capacity
a_{coeff}	Infiltration loss parameter
a_{sq}	Exponent in infiltration capacity equation
a_{ads}	Fraction of total catchment area with depressions
a_{dsc}	Depression storage capacity
a_{rmd}	Exponent in depression flow equation
a_{sub}	Constant of proportionality in interflow calculation
a_{crack}	Constant of proportionality in groundwater recharge calculation
a_{smsc}	Soil moisture store capacity
a_{em}	Maximum vegetation controlled rate of evapotranspiration
a_{locate}	Parameter fixing origin in cycle of seasonal fluctuation of COEFF, CRAK and SUB
a_{seas}	Parameter fixing amplitude in seasonal fluctuation of COEFF, CRAK and SUB
a_{power}	Routing exponent
a_{co}	Routing coefficient
a_{rk1}	Constant of proportionality in linear component of stream-aquifer flow equation
a_{rk2}	Constant of proportionality in exponential component of stream-aquifer flow equation
a_{rk3}	Exponent in exponential component of stream-aquifer flow equation
a_{vcond}	Constant of proportionality in deep seepage equation
a_{dlev}	Deep seepage parameter

Table 3.7: Summary of some studies investigating the impact of climate change on water resources (continued overleaf).

Region/Country	Year	Investigators	Approach	Impacts	Climate change scenarios	Downscaling method	Perturbation method	Hydrological Model	Water resource systems model
Texas and Mississippi, USA	1982	Nemec and Schaake	Impact	Runoff, hypothetical single reservoir	Hypothetical	N/A	Mean climate only	Daily Sacremento soil moisture accounting model	Simulation
Arizona, USA	1984	Idso and Brazel	Interaction (CO_2 effects on stomatal resistance included)	Runoff	Hypothetical	N/A	Mean climate only	Langbien empirical model	
Belgium	1988	Bultot et al.	Impact	Runoff, groundwater	Hypothetical	N/A	Mean climate only	Daily IRMB conceptual rainfall-runoff model	-
UK	1991	Cole et al.	Impact	Runoff, hypothetical single reservoir	Average of 5 GCMs	GCM output used directly	Climate variability included	Daily water balance model	Not specified
Australia	1995	Chiew et al	Impact	Runoff, soil moisture	Hypothetical, BMRC, CCC, CSIRO9, HadCM1, GFDL	GCM output used directly	Mean climate only	MODHYDROLOG Daily conceptual rainfall-runoff model	
British Columbia, Canada	1996	Loukas and Quick	Interaction (CO_2 effects on stomatal resistance included)	Runoff	CCC 2nd generation atmospheric	Interpolation	Mean climate only	UBC Watershed model	-
UK	1997	Arnell et al.	Impact	Runoff, groundwater	HadCM1, HadCM2	Interpolation	Mean climate only	Moore's daily conceptual water balance model	
Sweden	1997	Xu and Halldin	Impact	Runoff	Hypothetical	N/A	Mean climate only	Monthly water balance model of Xu	-
Nile, north east Africa	1998	Yates and Strzepek	Impact	Runoff	HadCM1, GFDL, GISS, MPI, CCC	Interpolation	Mean climate only	WBNILE simple monthly lumped parameter water balance model	-
Czech Republic	1997	Dvorak et al.	Impact	Runoff, existing single reservoir	Hypothetical, GISS, GFDL, CCC	Not specified	Mean climate only	BILAN monthly water balance model	Not stated
West Yorkshire, UK & Urmia, Iran	1999	Nawaz et al.	Impact	Runoff, existing multiple reservoirs	HadCM1, HadCM2, spatial analogue	GCM output used directly	Mean climate only	Monthly water balance equation	simulation model

Table 3.7 (continued): Summary of some studies investigating the impact of climate change on water resources.

Region/Country	Year	Investigators	Approach	Impacts	Climate change scenarios	Downscaling method	Perturbation method	Hydrological Model	Water resource systems model
Central India	1999	Mehrotra	Interaction (CO_2 effects on stomatal resistance included)	Runoff, soil moisture, hypothetical single reservoir	Hypothetical	N/A	Mean climate only	Divya's conceptual rainfall-runoff model	Simulation
Uruguay River, South America	1999	Braga and Molion	Impact	Runoff	HadCM1, GISS, GFDL	GCM output used directly	Mean climate only	IPM-III daily conceptual water balance model	
USA	1999	Lettenmaier et al.	Impact	Runoff, existing multiple reservoirs	HadCM1,GFDL, MPI	Interpolation	Mean climate only	VIC-2L semi-distributed 2 layer variable infiltration daily model; lumped NWSRFS Sacramento daily soil moisture accounting model	HEC-PRM simaultion model; optimisation model
Europe	1999b	Hulme et al.	Impact	Runoff	HadCM2, natural climate variability	Interpolation	Mean climate only	Daily water balance model	-
Severn Trent, UK	2000	Crookall and Bradford	Impact	Runoff, groundwater, existing multiple reservoirs	HadCM2	Interpolation	Mean climate only	HYSIM daily conceptual water balance model	ResSim Simulation model
New York, USA	2000	Blake et al.	Impact	Runoff, extreme events	CCC, HadCM2, GISS	GCM output used directly	Mean climate only	WatBal daily water balance model	-
Upper Wind Catchment, USA	2000	Stonefelt et al.	Interaction (CO_2 effects on stomatal resistance included)	Runoff	NCAR	NCAR RCM	Mean climate only	Soil Water Assessment Tool (SWAT), physically based daily model	-
USA	2000	DeWalle and Swistock	Interaction (land use changes)	Runoff	Hypothetical	-	Mean climate only	Simple annual regression model	-
Sweden	2001	Bergstrom et al.	Impact	Runoff	HadCM2, MPI	RCM	Mean climate only	HBV daily model, distributed lumped sum daily hydrological model	-

HadCM: Hadley Centre for Climate Prediction and Research, UK; CCC: Canadian Climate Centre; GISS: Goddard Institute for Space Studies, USA; NCAR: National Centre for atmospheric Research, USA; GFDL: Geophysical Fluid Dynamics Laboratory, USA; MPI: Max Planck Institute for Meteorology, Germany; BMRC: Australian Bureau of Meteorology Research Centre; CSIRO: Australian Commonwealth Scientific and Industrial Research Organisation; RCM: Regional Climate Mod

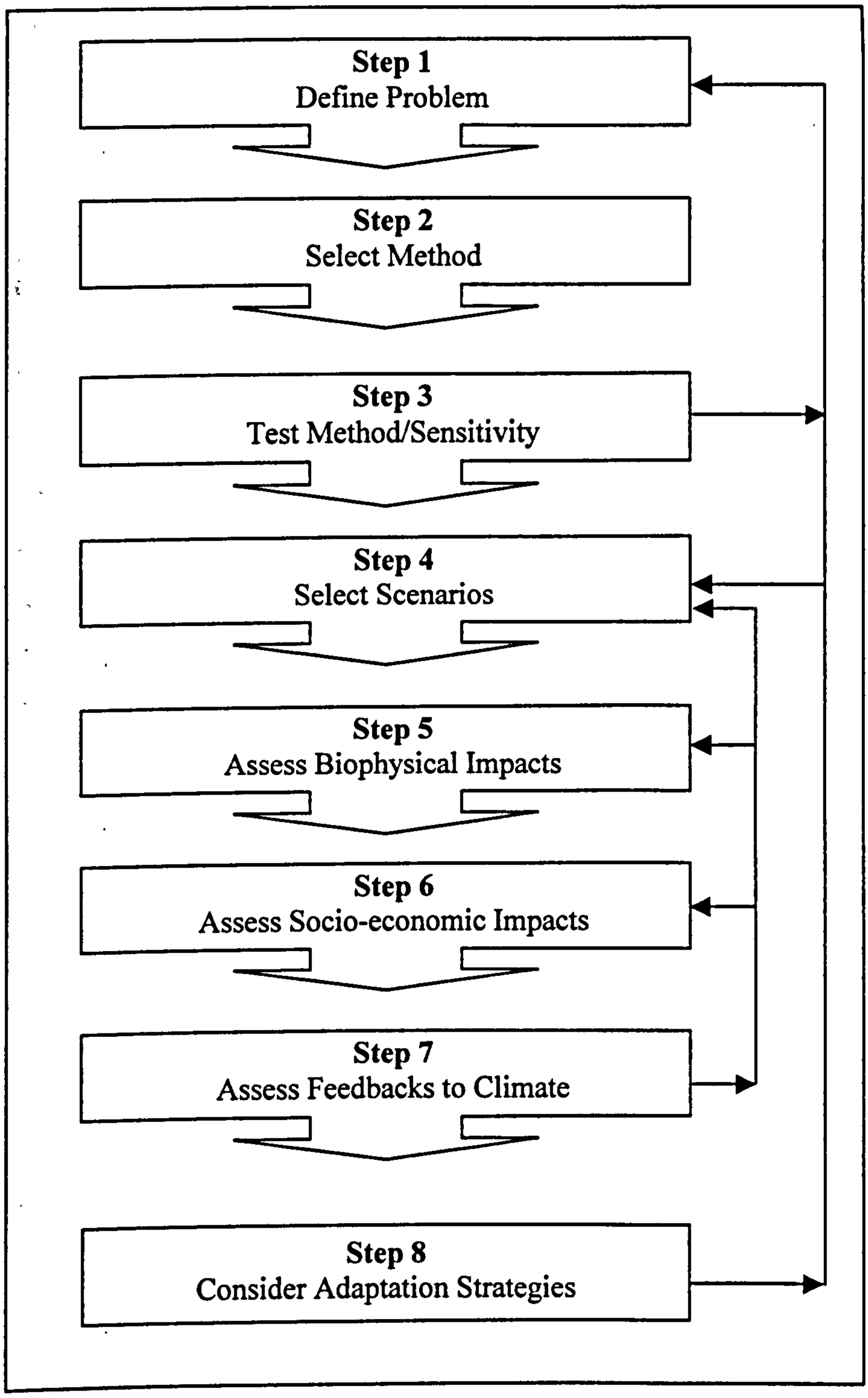

Figure 3.1: Climate Impact Assessment Methodology (Carter et al., 1994).

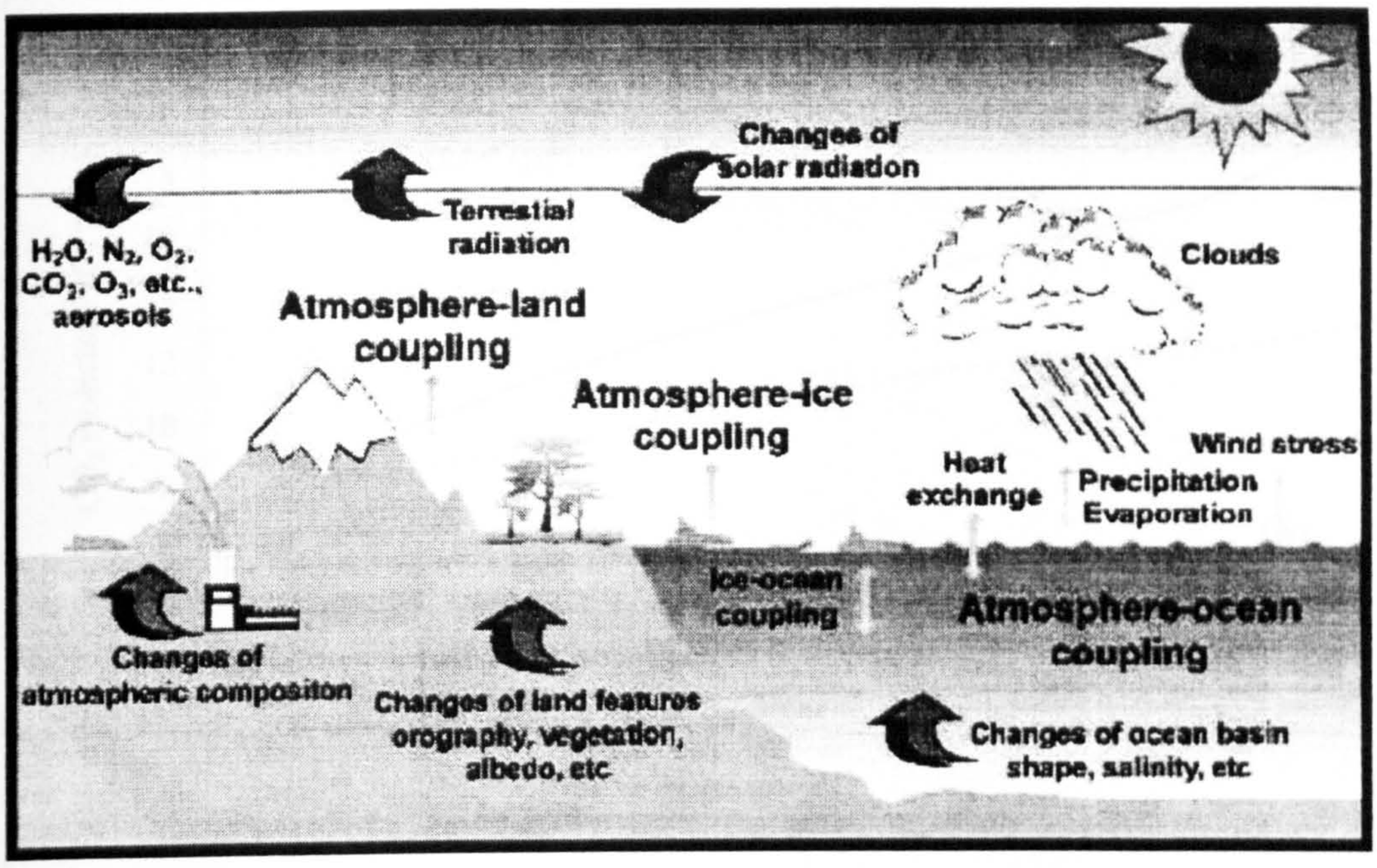

Figure 3.2: Land-surface, oceanic and atmospheric processes simulated by a GCM (http://www.dar.csiro.au/res/cm/default.htm).

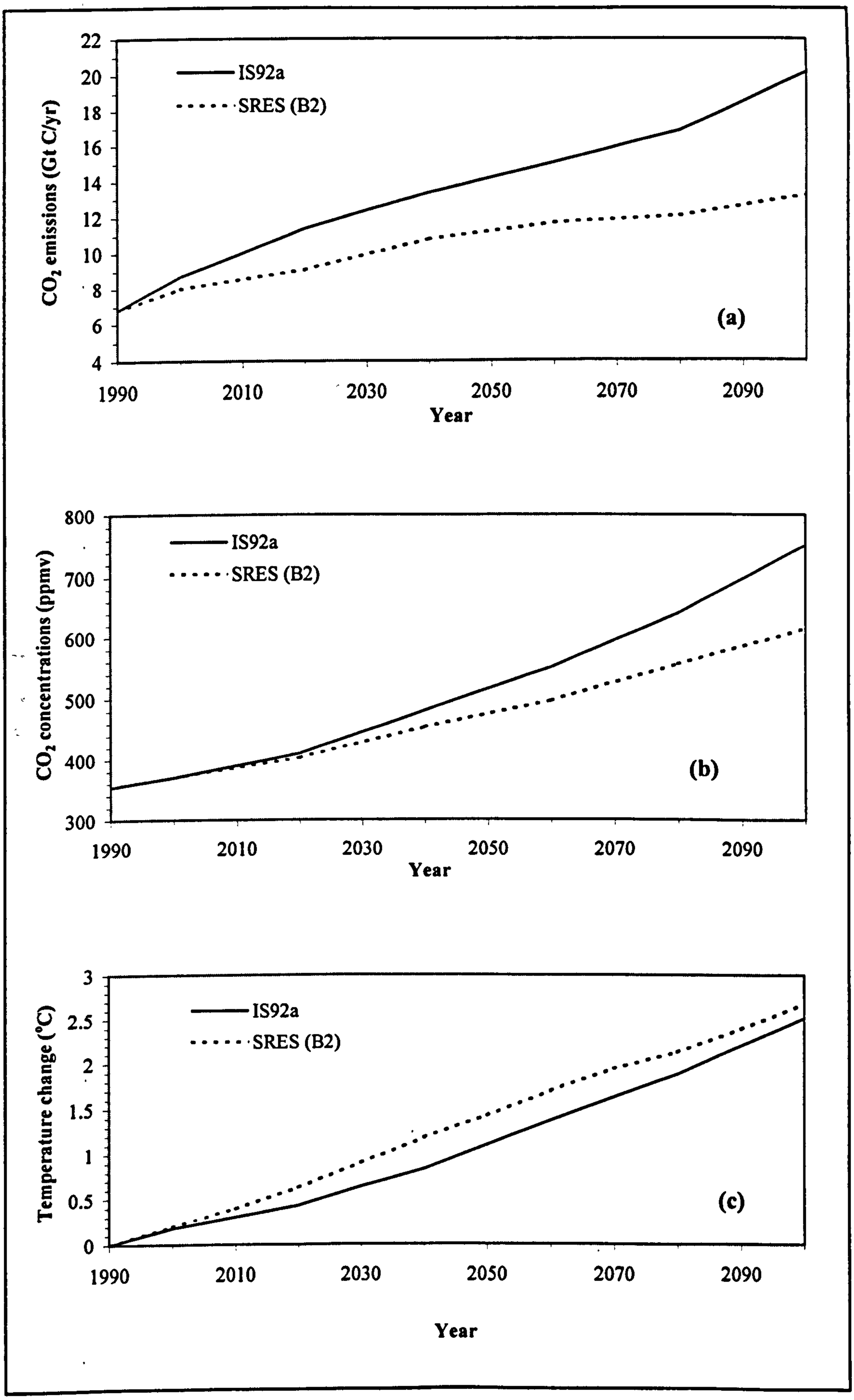

Figure 3.3: Projected global CO_2 levels and temperature change based on IS92a and SRES(B2) scenarios (IPCC, 2001a)
((a) = CO_2 emissions; (b) = CO_2 concentrations; (c) = temperature change).

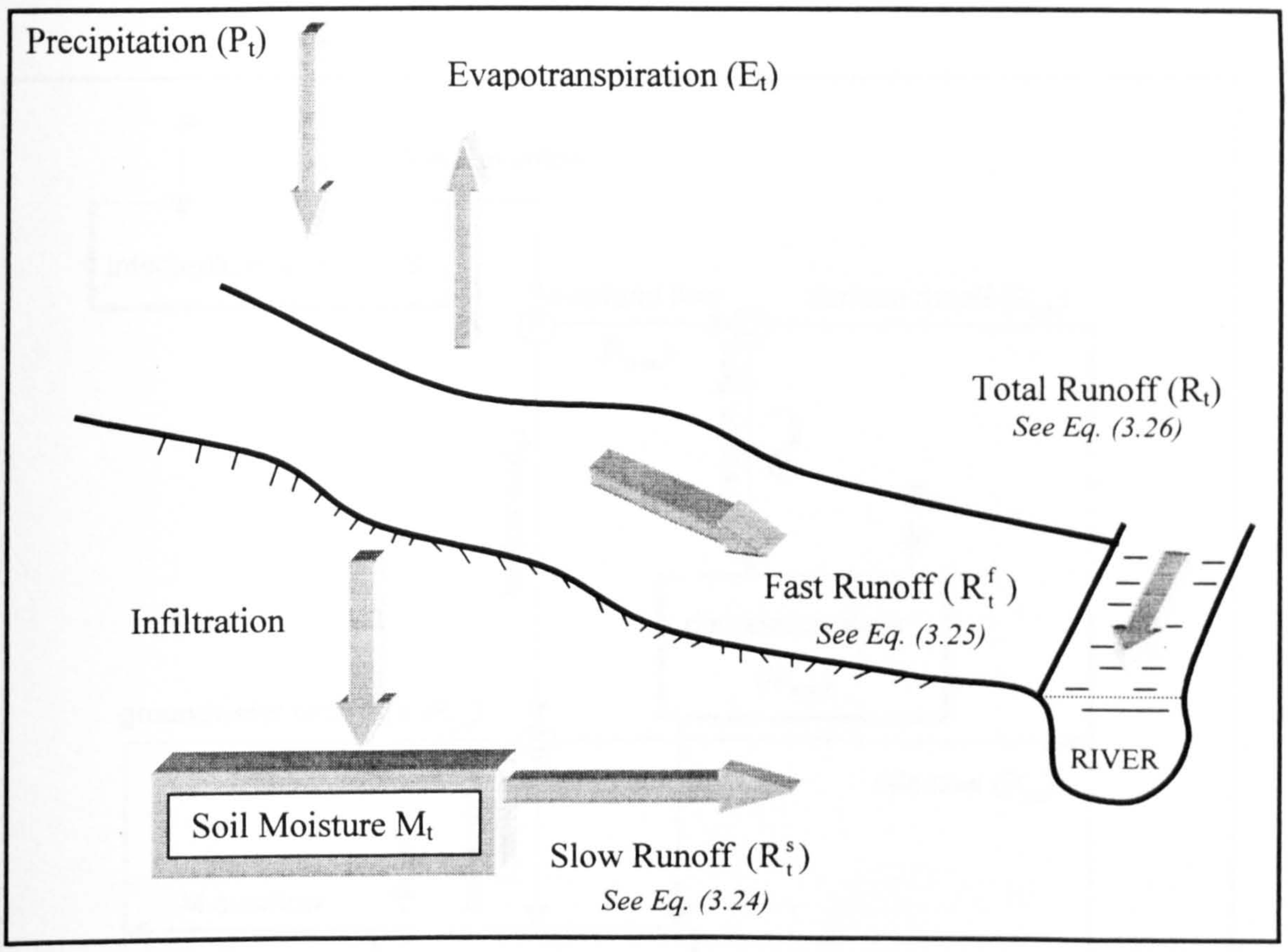

Figure 3.4: Schematic of Xu's conceptual monthly-water balance model (adopted from Xu and Vandewiele, 1991, with modifications).

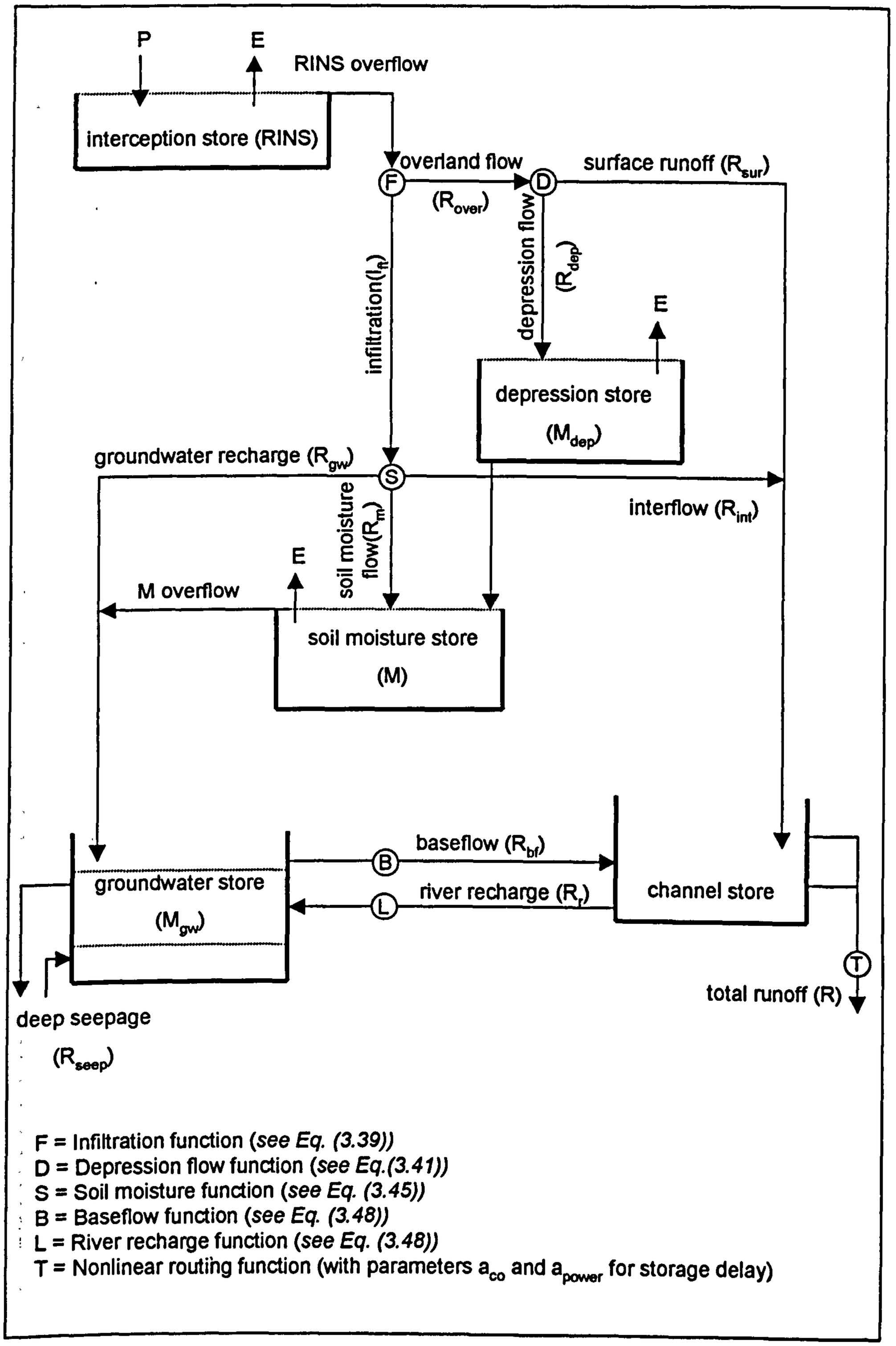

Figure 3.5: Schematic of MODHYDROLOG (adopted from Chiew and McMahon, 1994, with modifications).

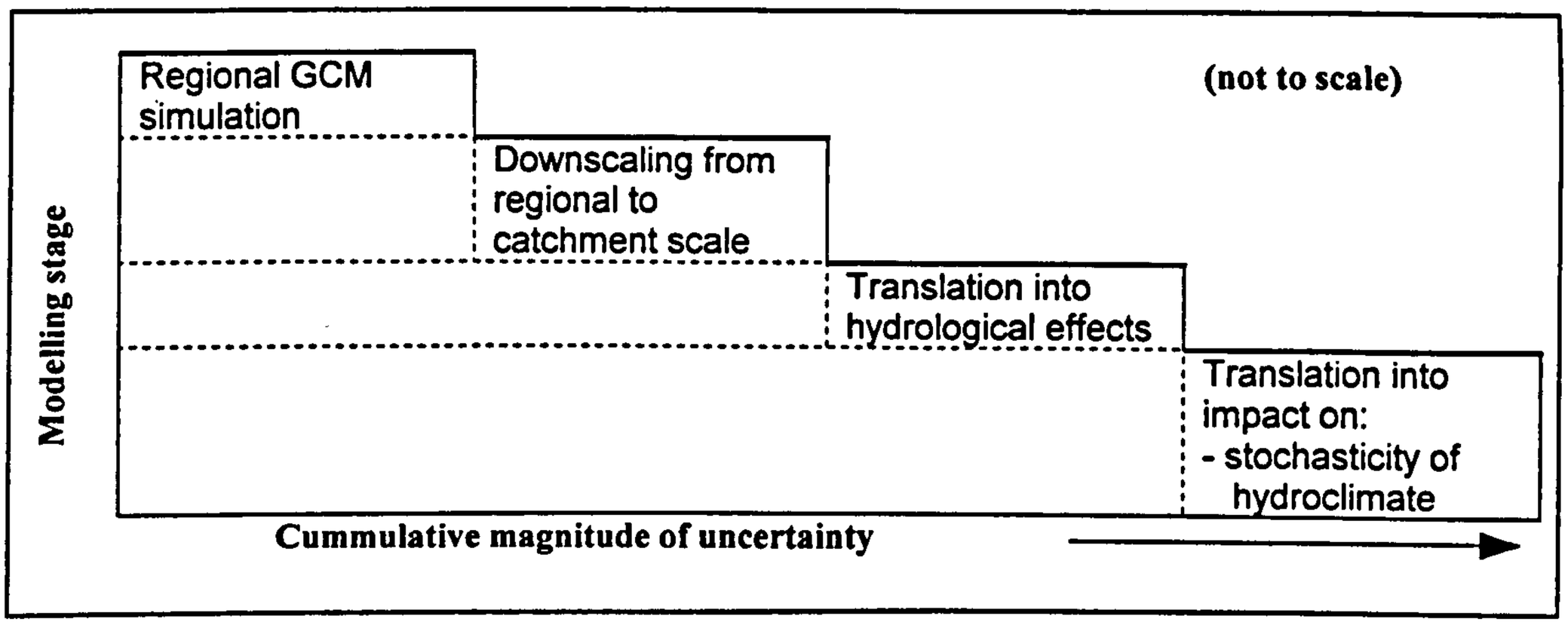

Figure 3.6: Schematic of the levels of uncertainty in successive stages of climate impact assessment (note the incremental uncertainties are not necessarily equal).

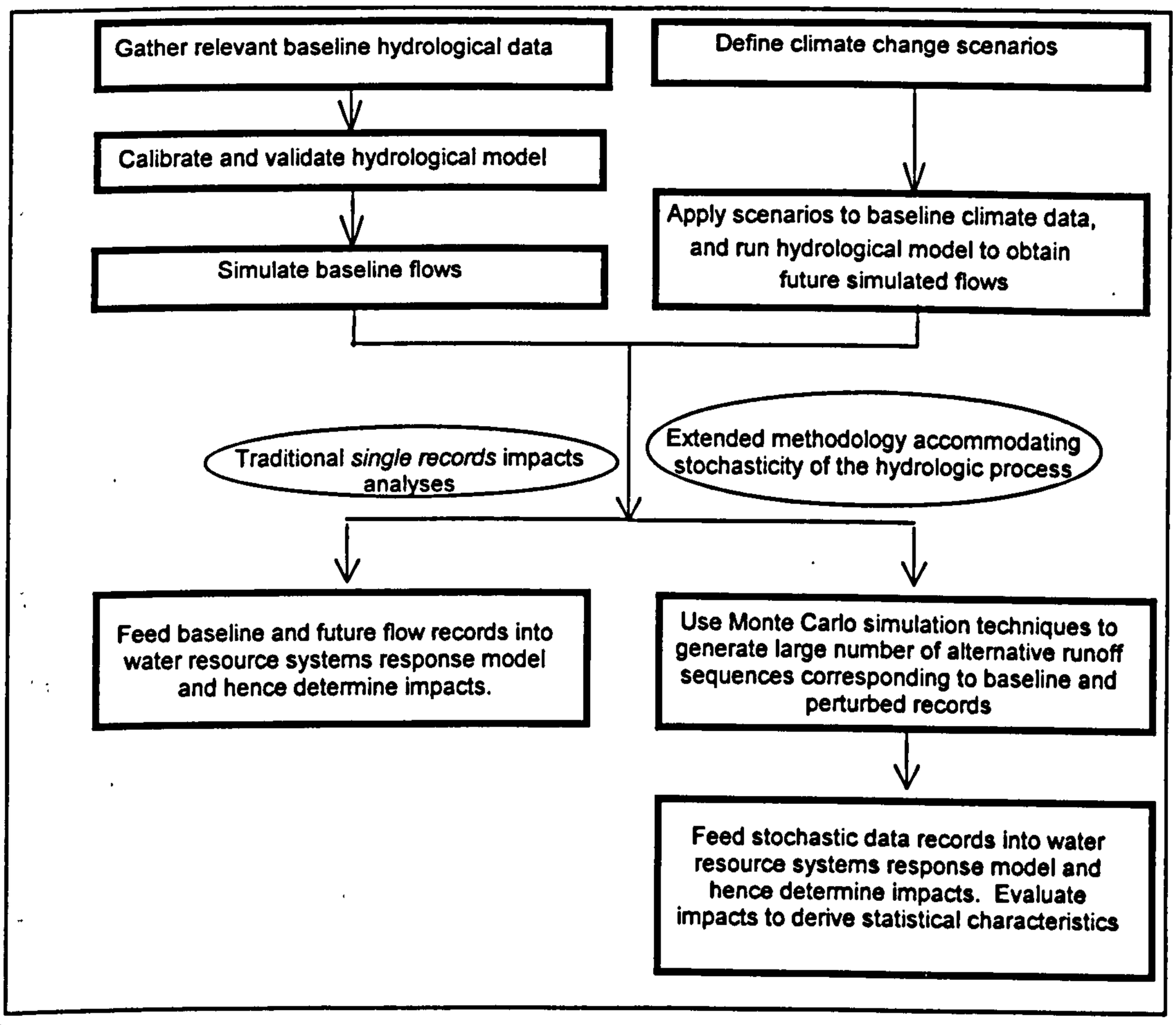

Figure 3.7: Deterministic and stochastic methodologies for climate change water resources impacts assessment (note the stochastic methodology enables sampling uncertainty of the impacts to be characterised).

CHAPTER FOUR

ANALYSES FOR CLIMATE CHANGE IMPACTS: THE YORKSHIRE (ENGLAND) AND IRANIAN CASE STUDIES

4.1 Introduction

The previous chapters introduced the objectives of the present work and discussed two approaches to climate change water resource impacts assessment. These are the traditional approach, and an extended approach that takes account of sampling uncertainties in hydrological data. This chapter presents the application of these approaches to investigate the likely impacts of climate change on multiple reservoir systems. Both methodologies will be applied to two different reservoir systems, one in the northeast of England (Yorkshire) and the other in the northwest of Iran (Urmia) to form case studies covering two different climates.

The Yorkshire system will then be re-analysed in greater detail. The re-analysis will involve perturbing baseline climate using the LARS stochastic weather generator which will allow variability to be incorporated into the future hydroclimatological data. It may be recalled from section 3.3.5 that there are two ways of perturbing baseline climate. The simple perturbation approach applies GCM based mean monthly changes in the hydroclimate to baseline data and so does not allow for the incorporation of variability into the future hydroclimatological data.

The catchments and reservoir systems are described in section 4.2. The baseline hydroclimatological data records are presented in section 4.3. It is important to include net reservoir surface-fluxes in reservoir analysis and therefore reservoir surface area-storage relationships adopted for the Yorkshire and Urmia analyses are also presented in this section. The analysis discussed in this chapter will be carried out in three stages, i.e. preliminary, intermediate and final detailed investigations. The preliminary investigation adopts the traditional single records approach and uses the simple perturbation method to determine the future hydroclimate for both the Yorkshire and Urmia catchments. The intermediate investigation is an extension of the preliminary investigation by combining the simple perturbation method with a Monte Carlo simulation approach. The final detailed investigation focuses on the Yorkshire system and uses a stochastic weather generator as the basis for perturbing baseline hydroclimate within a Monte Carlo approach. The various models and climate scenarios employed in the preliminary and intermediate investigations are summarised in section 4.4. A similar summary of the final detailed investigation is presented in section 4.5.

4.2 Catchments

4.2.1 English Catchments

The first system is located in the Calderdale area of northwest Yorkshire in England and consists of four direct catchments namely Gorpley, Hebden, Luddenden, and Ogden. These catchments are located between 53° 41′ and 53° 50′ northern latitude, and 1° 53′ and 2° 10′ western longitude as shown in Figure 4.1. The catchments are upland in character with minimum and maximum altitudes of 250 and 510 meters above sea level,

respectively. Land cover is mainly grass with some trees, and the surface soil mainly consists of hill peat. The mean annual temperature over the baseline period for the region is about 8.2°C and the average annual precipitation is about 1438 mm. Some relevant catchment characteristics are summarised in Table 4.1.

The Yorkshire system comprises twelve inter-linked reservoirs and is therefore a fairly complex system as shown in Figure 4.1. Consequently, a four-reservoir simplified configuration of the system (see Figure 4.2) was first considered in the analysis. Monthly data were available for the four reservoir sub-systems namely the Gorpley group, the Hebden valley group, the Luddenden valley group and the Ogden group.

Subsequently, Hebden, Luddenden and Ogden reservoirs were analysed as an 11-reservoir complex system (see Figure 4.3) using the available daily data. Figure 4.3 excludes the single reservoir of the Gorpley system (with a storage capacity of < 5% of the complete multiple-reservoir system) since it is not hydraulically linked to the Hebden, Luddenden and Ogden grouped reservoir system (see Figure 4.1). Nonetheless, such a detailed study when compared with the lumped four-reservoir system analysis should permit the evaluation of the effects of system and data aggregation on the assessed impacts. Some of the reservoirs have been photographed as part of this work and are shown in Figure 4.4.

The reservoirs provide water for domestic and industrial purposes, as well as compensation releases, and they are operated to satisfy the full demand at all times, although during extreme droughts, reductions in releases can be made. Information provided by Yorkshire Water (Yorkshire Water RRDY, 1991) has been used to present

relevant baseline (i.e. 1961-1990) annual flow statistics along with some reservoir system characteristics in Table 4.2.

Values of the standardised demand parameter *m* (see Table 4.2) can provide information as to whether a reservoir is likely to exhibit within-year or over-year behaviour (Vogel and McMahon, 1996; Adeloye and Nawaz, 1998; Montaseri and Adeloye, 1999). Reservoirs that are, on average, likely to fill and spill several times a year are known as within-year systems whereas reservoir storage carried over from one year to the next constitutes an over-year system. Being able to predict the behaviour of a reservoir system prior to analysis is advantageous because then an appropriate time-step can be adopted for analysis. Over-year systems could be adequately analysed using annual time-series data whilst monthly time-series data would be necessary for the analysis of purely within-year systems.

The *m* parameter is defined as (1-yield)/CV where yield is expressed as a ratio of mean annual flow, and CV (coefficient of variability) is a dimensionless measure of the variability in the streamflow data, defined as $CV = \sigma/\mu$; where μ and σ are respectively the mean and standard deviation of the streamflow data record. Hurst (1951) was the originator of the concept of the *m* parameter and subsequent analysists (Adeloye and Nawaz, 1998; Montaseri and Adeloye, 1999) have implied that values of m = 1 represents the transition between a point where over-year storage predominates (m<1) to where within-year storage predominates (m>1). According to this definition, the Yorkshire reservoirs are within-year systems which would suggest that monthly streamflow data must be used for analysing this reservoir system.

4.2.2 Iranian Catchments

The second reservoir system, located in Urmia region of northwest Iran, comprises three catchments: Baranduz, Shahr, and Nazlu. These catchments are located between 37° 6′ and 38° 0′ northern latitude, and 44° 19′ and 45° 5′ eastern longitude as shown in Figure 4.5. The catchments are situated in the mountainous areas of the region where the minimum altitude is approximately 1300 meters above sea level.

Urmia region can be classified as semi-arid based on the study of McMahon et al. (1992), and because it is located at a high altitude, it is generally cold. Although the average annual temperature of about 9°C is a little higher than in Yorkshire, the temperature in winter is much lower, averaging about -2°C. There are on average 125 freezing days annually in the region (MWP, 1995). Average annual precipitation for the catchments is about 430 mm and around 96% of this falls from October to July, with approximately half of this falling as snow (MWP, 1995). Consequently, snowmelt plays a major role in the hydrology of the catchments. However, temperatures during summer can reach as high as 29°C; hence catchment evaporative losses are quite high.

The Urmia catchments have a total area of 2751 km^2 that is drained by a number of tributaries of the main drainage channels of the Baranduz, Shahr, and Nazlu rivers (see Figure 4.5). These three rivers are the major water supply source for Urmia City and the surrounding agricultural land. At present, about 60% of the mean annual runoff in these rivers takes place between November and May when the irrigation demands are very low. Without the presence of any dams, this water is simply lost to the saline Urmia Lake. Consequently, three reservoir systems are proposed by the Iranian

Ministry for Water and Power to control and regulate the rivers at the location of the reservoirs.

The planning of the Urmia reservoirs will consider different levels of reliability and the shortfall in the demands during failure will be limited to 30%. This shortage level is quite similar to that currently used in Yorkshire. Relevant characteristics of the Baranduz, Shahr and Nazlu catchments are summarised in Table 4.1 and a simplified schematic for the Urmia system is shown in Figure 4.6. Relevant baseline (i.e. 1961-1990) annual flow statistics along with some reservoir system characteristics for the reservoirs are given in Table 4.2.

The *m* values in Table 4.2 for Urmia reservoirs indicate that the proposed Shahr and Nazlu reservoirs are likely to exhibit over-year behaviour. On the other hand, Baranduz reservoir is just beyond the over-year to within-year transition point. In general, the *m* values indicate that annual streamflow data would be sufficient for the analysis of the Urmia systems. However, for reasons of consistency and given that monthly hydroclimatological data were available for Urmia, it was decided to use monthly data in the reservoir analysis.

4.3 Hydroclimatological Data

The principal data requirements in climate change impact assessments are precipitation, potential evapotranspiration (PE) and runoff. Moreover, open water evaporation data are also important for assessing their effect on reservoir storage-yield requirement, which may be significant in arid and semi-arid regions. The data may be applied at the monthly or daily time-step. However, when assessing the hydrological effects of climate

change, daily hydrological models may be preferable to mimic the behaviour of a catchment more realistically. This is probably the major reason why a majority of climate change studies summarised in Table 3.7 preferred the use of a daily model. As mentioned previously, for modelling the water resource systems' response (e.g. reservoirs), a monthly time-step is usually sufficient for within-year systems.

4.3.1 Yorkshire Data

Both monthly and daily hydroclimatological baseline data (1961-1990) were available at the Yorkshire catchments. Monthly precipitation data over the baseline period were available at two gauging stations; one at Ramsden station near Gorpley reservoir and the other at Widdop station at Hebden group (see Figure 4.1). Mean monthly and annual precipitation at these sites are given Table 4.3. The coefficient of variation (CV) values are also provided in the table.

Daily baseline precipitation data were available at a total of five sites, namely Gorple, Widdop, Walshaw Dean, Luddenden and Ogden. The daily data were aggregated to monthly data with which to calculate the seasonal averages. These averages, along with the annual averages are presented in Table 4.3. The data indicate a gradual decrease in precipitation from the west (Gorple reservoir) to the east (Ogden reservoir) of west Yorkshire.

Baseline monthly potential evapotranspiration (PE) data taken from the Meteorological Office Rainfall and Evaporation Calculating System (MORECS) database (Thompson et al., 1981) were available. The MORECS database contains rainfall and PE data for each of the 188, 40km × 40km grid squares covering the UK for the baseline period. The PE

data available for this study were for Calder in west Yorkshire. All the Yorkshire catchments are located within this region. As shown in Table 4.4, the annual average PE for the region is 412 mm with a maximum of 70 mm in July and a minimum of about 7 mm in January. Daily PE data were also available at the Gorple site and the average monthly values are given in Table 4.5. These data have been derived by Mott MacDonald (1995) using the Penman equation (Penman, 1948; MAFF, 1967). The annual PE (545 mm) is somewhat higher at the Gorple site than the regional average based on MORECS. This is because PE at Gorple is derived using catchment-scale climatic variables such as sunshine hours, temperature, wind speed etc. Indeed, these data at Gorple site, which are of a higher spatio-temporal resolution than the MORECS data will be appropriate for use in the detailed investigation of the Yorkshire system. It should be noted that whether based on daily or monthly data, the annual PE is generally much lower than the annual precipitation (see Table 4.3) at Yorkshire.

As previously discussed in section 3.3.6, the LARS weather generator uses the daily observed number of sunshine hours (n) and internally converts these to net solar radiation if measurements of the latter are unavailable. The sunshine data are converted to radiation using Equation (3.6). According to this equation, calculation of net solar radiation also requires the total short-wave radiation received at the top of the atmosphere (R_a) and the maximum number of sunshine hours (N). Values of n, along with values of N and R_a for Yorkshire (53.8^0 northern latitude) obtained from relevant meteorological tables (Shaw, 1994) are provided, for the baseline period (1961-1990) in Table 4.5. Minimum and maximum daily temperature data are also available for the baseline period and the average monthly and annual values are provided in the same table.

Monthly historical inflow data records were available over the baseline period (1961-1990) for Gorpley, Hebden, Luddenden and Ogden reservoir sub-systems. These were based on daily inflows derived for Yorkshire Water by Mott MacDonald (1995) using the HYSIM model. A brief description of HYSIM was provided in section 3.4.1. Although Mott MacDonald (1995) aggregated daily inflows to monthly data, the daily values were not made available to this study by Yorkshire Water Ltd. Thus, for the purposes of this research, daily inflows for the more detailed five-reservoir group configuration illustrated in Figure 4.3. were simulated. The simulation was carried out using the HYSIM model during a visit to Yorkshire Water Services Ltd. It was necessary to obtain the daily inflow records to allow the climate change reservoir impacts assessment to be carried out at a higher spatio-temporal resolution.

The mean monthly and annual inflows, converted to runoff, are presented in Table 4.6. Comparing the annual runoff in Table 4.6 with the annual precipitation and PE in Tables 4.3, 4.4 and 4.5 reveals that for the Yorkshire catchments, annual precipitation is considerably higher than annual PE. Annual runoff ratios (i.e. annual runoff/annual precipitation) are therefore quite large. For example, the runoff ratio for Widdop catchment is 0.73.

4.3.2 Urmia Data

Temperature data for Urmia region were available for the period 1963-1990 and mean monthly values and the annual average value are given in Table 4.7.

Precipitation from Mir-Abad and Hashem-Abad precipitation stations located nearby the Urmia catchments have reliable data records (MWP, 1995) spanning the baseline period

which were used. Mir-Abad precipitation station is located at 37° 26′ northern latitude and 44° 52′ eastern longitude at an elevation of 1525 m, and Hashem-Abad station is situated at 37° 17′ northern latitude and 44° 55′ eastern longitude at an elevation of 1480 m (see Figure 4.5). The lengths of precipitation record at the Mir-Abad and Hashem-Abad stations are 25 years (1965-1990) and 27 years (1963-1990), respectively. The mean and coefficient of variation of the monthly and annual precipitation (given in Table 4.8) at the Mir-Abad are 440.0 mm and 0.24, and the corresponding values for Hashem-Abad station are 420.5 mm and 0.34. Table 4.8 also shows that seasonal precipitation variability in these catchments is quite high. For example, the minimum and maximum average monthly precipitation at Mir-Abad station is about 3 mm (August) and 83 mm (December). Indeed, the precipitation CV during August is a staggering 2.15 at Mir-Abad station.

Mean monthly open-water evaporation data (E_0) derived from Class A Pan evaporation measurements were available for the Urmia catchments for the period 1953-1993 and are presented in Table 4.7. Also provided in Table 4.7 are the mean monthly PE data for the same period. These data have been made available by the Iranian Ministry of Water and Power (MWP, 1995) and are based on the Penman-Monteith Equation (3.1). Along with precipitation data, E_0 data will be used to assess the effects of reservoir net surface-fluxes on storage-yield.

Baseline monthly inflow data for each of the Urmia sites were also available. Statistical properties of baseline annual and monthly runoff are shown in Table 4.9. The data indicate a marked seasonal difference in runoff and the range of annual flow CV varies between 0.32-0.40. Comparing the annual runoff in Table 4.9 with the annual precipitation and PE in Tables 4.8 and 4.7 reveals that for the Urmia catchments, annual

PE is considerably high. This could be the cause for a relatively small runoff ratio (of 0.53) at the Nazlu catchment for instance.

4.3.3 Reservoir Surface Area-Storage Data

A reservoir surface area-storage functional relationship is required for converting net evaporation flux (mm) into volumetric unit for use in the reservoir simulation. Using capacity and surface area data from a total of twelve reservoirs at Gorpley, Hebden, Luddenden and Ogden reservoir groups, together with similar data from two further reservoirs from a reservoir group to the south of the study catchments, an empirical storage relationship function was developed using regression techniques. Although actual relationship between surface and reservoir surface is typically non-linear (see Takeuchi and Hamlin, 1998), it is customary to approximate this relationship using a linear function particularly in regions beyond the dead storage zone (Loucks et al., 1981; ReVelle, 1997). This makes it possible to incorporate such functions in reservoir simulation and optimisation models which for simplicity are normally formulated as linear functions of the storage and other decision variables (Loucks et al., 1981).

The linear approximation to the storage-area relationship was adopted in the study, although as noted by Adeloye et al. (2001), the modified Sequent Peak Algorithm used for the reservoir simulation could be used with a non-linear reservoir-area relationship. The resulting linear relationships for the Yorkshire catchments is $A_s = 0.0877S + 0.0056$ ($R^2 = 0.84$), where A_s is the reservoir area (km^2) and S is the storage ($10^6\ m^3$).

The area-storage relationship for Urmia has been approximated (Montaseri, 1999) by $A_s = 0.0317S + 1.688$ ($R^2 = 0.99$) and is based on area-storage data for three Urmia

reservoirs. Each of the Urmia reservoirs had ten measurements of area and corresponding storage, giving a total of thirty data points for deriving the average area-storage relationship.

4.4 Case Studies using Data from England and Iran

The present work involved three studies: the 'preliminary', 'intermediate', and 'detailed final' studies. Each of the three studies was uniquely different in a number of ways as summarised in Table 4.10. The preliminary study investigated both the Yorkshire and Urmia systems and was based on the traditional 'single records' approach. For the catchment rainfall-runoff response modelling, it used the simple water balance Equation (3.21) described in section 3.4.4.1 whose main strength lies in its relative simplicity since there is no need for extensive time-series data; indeed, only average monthly hydroclimatological data are sufficient.

The intermediate study, which also investigated reservoir systems from the two different regions, used an extension of the traditional approach to quantify the sampling uncertainties of assessed climate change water resource impacts. This study also differed from the preliminary study in that a monthly rainfall-runoff water balance model was used. The final detailed study investigated the Yorkshire system in more detail by using a daily water balance model for catchment response and a stochastic weather generator to perturb baseline climatic data. Each of these studies is now presented in greater detail.

4.4.1 Preliminary Study

The impact assessment was carried out using the traditional single records approach described in section 3.6 (see Figure 3.7). The catchment rainfall-runoff response model used was the monthly runoff-coefficient Equation (3.21) presented in section 3.4.4.1. Only mean monthly precipitation, actual evapotranspiration and runoff data are used in this expression.

The preliminary study investigated the effects of climate change on reservoir storage and yield for both the Yorkshire system (reservoir configuration I - shown in Figure 4.2) and Urmia system (see Figure 4.6).

The precipitation data provided in Table 4.3 was used for the Yorkshire catchments. For the Urmia catchments, the precipitation record at Mir-Abad station was used for the Nazlu catchment whilst the Hashem-Abad record was used for the Baranduz and Shahr catchments.

Assuming Mir-Abad (altitude 1525m) precipitation at Nazlu (altitude 2000m) and Hashem-Abad (altitude 1480m) precipitation at Baranduz (altitude 1900m) and Shahr (altitude 1800m) may not be necessarily correct due to the different altitudes. However, given that there are no precipitation stations in the study area, precipitation data from these two stations has been used.

Actual evapotranspiration (AE) with which to estimate the monthly means with sufficient accuracy were not available for the Yorkshire reservoir catchments; only the PE data were available as noted in section 4.3.1. It is necessary to obtain the needed AE

from the PE data. However, there was a 4-year (1993-1996) monthly data record of MORECS-based (Thompson et al., 1981) actual and potential evapotranspiration for a 40km by 40km square grid which encompasses all the studied reservoir groups. These 4-year AE and PE records were used to derive the baseline AE data corresponding to the period of the available PE data record, as follows. First, using the four year grid data, the ratio of the mean actual to the mean potential evapotranspiration for each month of the year was obtained. These ratios were then used to scale the available PE time series data to obtain the time series data of actual evapotranspiration, whence derive the monthly mean estimates (see Table 4.4). This approach assumes that the ratio of AE to PE at the catchments is equal to that for the much larger grid, which is reasonable given that all the catchments are located within the MORECS grid. Despite this, however, the preferred option was not to use the grid's monthly mean AE directly because of the potentially large sampling variability of such small sample (i.e. four years) estimates. On the contrary, the sampling variability of the monthly means derived with the longer baseline record will be much lower, implying that such estimates will be more reliable and hence more representative of the true mean actual evapotranspiration.

Open water pan evaporation measurements (E_o) were also not readily available at the Yorkshire sites and these were also obtained from the available PE data. PE was converted to E_o using $E_p = kE_o$ where E_o is the open-water surface evaporation (mm); E_p is the potential evapotranspiration (mm) and k has the value of 0.6 for November-February; 0.7 for March, April, September and October and 0.8 for the remaining months based on European conditions (Shaw 1994).

Both mean monthly and annual values of actual evapotranspiration and E_o as obtained using the above approaches are presented in Table 4.4. The data show the mean annual,

minimum and maximum values of E_o are 552 mm, 12.5 mm (January) and 87 mm (July), respectively. These values are generally considerably less than the corresponding precipitation (see Table 4.3) implying that a net inflow flux of water from any reservoir surface in the region is inevitable.

As stated in section 4.3.2, mean monthly open-water and PE data were available for the Urmia catchments. As in the Yorkshire case, however, the mean monthly AE data were required by the runoff-coefficient equation. In the absence of relevant MORECS data for Urmia, the AE data were derived using the same monthly ratios derived for the Yorkshire catchments to scale the PE data at the Urmia catchments (in Table 4.7).

The mean monthly and annual values of AE and E_o are presented in Table 4.7. It can be noted that the mean monthly open-water generally exceeds precipitation in Urmia (compare Tables 4.7 and 4.8) suggesting that a net outflow flux of water from any reservoir surface in the region is inevitable.

The perturbation of baseline hydrology was achieved using climate change scenarios and the simple runoff coefficient technique. A total of five climate change scenarios were used for the Yorkshire system; two from the UK Hadley Centre's first generation coupled GCM HadCM1 and three from HadCM2 (see Table 3.1 for HadCM2 model description). Both GCMs use a transient (i.e. gradual) greenhouse gas forcing and the main differences between the two are that HadCM2 uses a larger number of atmospheric and oceanic layers (19 and 20 respectively) compared with HadCM1 (11 and 17 respectively). The scenarios, presented in Tables 4.11-4.13, are representative of the 2020s climate with the exception of one of the HadCM1 scenarios which is for the 2050s. H120, H150 and GG1m include the effects of CO_2 only whereas the two GS1

scenarios include, in addition, the cooling effects of sulphate aerosols. In the absence of climate scenarios for Urmia, the GS1t was applied as a spatial analogue (GS1t).

The extended SPA (Adeloye and Montaseri, 1998) was used for multiple-reservoir analysis. An important aspect of the study involved assessing the effects of net reservoir fluxes on reservoir storage-yield under a changed climate. The area-storage relationships presented in section 4.3.3 were used for the analysis. Only average monthly precipitation and mean monthly open water evaporation rates were used. Fennessey (1995) found this approach to give almost the same results as using time series data of precipitation and evaporation.

Monthly time-based reliabilities of 100%, 98% and 90% were used in analysis. For reasons of consistency, two annual demand levels of 30% and 70% of the mean flow were considered for both reservoir systems. The monthly demands for the Yorkshire system were assumed to be uniform throughout the year whereas the monthly demands for the Urmia system varied in accordance with the estimated monthly municipal and irrigation demand from the system (MWP, 1995). This distribution of demands within the year is shown in Table 4.14.

The supply deficits during failure periods were taken as current deficits allowed for in the Yorkshire system and these are 32%, 41%, 27%, and 37% for Gorpley, Hebden, Luddenden, and Ogden reservoirs respectively (Yorkshire Water RRDY, 1991). For the Urmia reservoirs, an initial uniform deficit of 30% was assumed throughout in accordance with the information contained in the project report (MWP, 1995).

Storage-yield curves derived from the extended SPA (see section 3.5.1.3 for details of the SPA) output were used to assess the effects of climate change on reservoir yield. To determine the yields, existing storage for the grouped Yorkshire system of 30% and 70% of mean flow was used. Again, for reasons of consistency, the yield corresponding to arbitrary storages of 30% and 70% of the mean flow was investigated for the Urmia reservoir system.

4.4.2 Intermediate Study

The main details of this study are summarised in Table 4.10. The intermediate study extended the preliminary investigation by evaluating the sampling uncertainties of impacts. Other distinguishing features of the intermediate study include the use of two additional climate change scenarios and a monthly water balance model developed by Xu et al. (1996).

For the Yorkshire sites, Xu's model requires monthly time-series of precipitation, PE and runoff data. For the Urmia sites, temperature was also input to model both the PE and snowmelt/accumulation. As remarked in section 4.2.2, snowmelt plays an important role in the hydrology of Urmia region.

Three climate change scenarios for the 2020's based on the UK Hadley Centre GCM, HadCM2 (see Table 3.1 for model description) were used in Yorkshire. Two of the scenarios, GS1m and GS1t were the same as those used for the preliminary study. The third scenario - UKCIP98 - developed by the UK Climate Impacts Programme - does not incorporate the cooling effects of sulphate aerosols. This is essentially due to a limited understanding of how sulphate aerosols influence climate (Hulme and Jenkins,

1998). Published scenarios for Urmia were not readily available; consequently a simple climate model called MAGICC (Model for the Assessment of Greenhouse Gas Induced Climate Change) and the SCENGEN (SCENario GENerator) regional climate change scenario generator were used to generate the needed precipitation and temperature scenarios.

MAGICC comprises a gas model and upwelling diffusion-energy balance (UD/EB) climate model and an ice melt & thermal expansion (IM/TE) model. The gas model converts each of the main greenhouse gases into atmospheric concentrations and uses this to calculate radiation forcing. The UB/EB climate model calculates global mean temperature response to a given radiation forcing and the IM/TE model computes sea-level change. The gas model was used by the IPCC (Houghton et al., 1997) to derive some of the greenhouse gas emissions scenarios described in section 3.3.2.2.

SCENGEN is able to generate global and regional scenarios of climate change using results from MAGICC and a wide range of GCM's (Hulme et al. 1995). It achieves this by scaling output from MAGICC to agree with output from a particular GCM by (i) determining the change in regional climate (temperature, precipitation etc.) per degree of global warming as simulated by a GCM (known as the climate sensitivity), and (ii) by applying this change to the global mean temperature simulated by MAGICC. The scaling factor (S_f) can be expressed in mathematical terms as $S_f = \Delta T_{year} / \Delta T_{2x}$, where ΔT_{2x} is the climate sensitivity for the particular GCM and ΔT_{year} is the global temperature change for the year simulated by MAGICC.

Using output from the so-called Simple Climate Models such as MAGICC to obtain regional climate change scenarios has proved quite popular (e.g. IPCC, 1990; 1992; CCIRG, 1996) over recent years. This is because this technique allows regional climate change scenarios (that are in broad agreement with GCM output) to be determined in a significantly shorter time frame than a GCM. Consequently, the SCM can be forced with numerous greenhouse gas scenarios to obtain a wide range of regional climate change scenarios.

To generate climate change scenarios for Urmia region, two IPCC emissions scenarios were used by MAGICC. These are the reference ('business as usual') scenario and the policy (reduced emissions) scenario. Different emissions scenarios IS92a-IS92f (Wigley and Raper, 1992; IPCC, 1996) can be selected and for this study, the IS92a (medium) formed the reference scenario (see section 3.3.2.2) and the IS92d (medium-low) was used as a policy scenario. A climate sensitivity of 2.5°C which is the 'best estimate' IPCC value (Hulme, 1996) was specified and SCENGEN was used together with results from MAGICC and HadCM2 GCM. The resulting scenario was named IRHAD, connoting Iranian scenario based on a Hadley Centre GCM.

Tables 4.11 and 4.12 summarise the changes in monthly precipitation and PE by the 2020's for Yorkshire. Table 4.11 also contains the precipitation scenarios for Urmia. The monthly temperature scenario for Urmia are contained in Table 4.13.

4.4.2.1 Rainfall-Runoff Modelling

As mentioned previously, the monthly water balance model of Xu (Vandewiele and Xu, 1991; Xu et al., 1996) was used for catchment rainfall-runoff response modelling. A complete description of this model was presented in section 3.4.4.2.

Model calibration and validation periods for Yorkshire were between 1980-1986 and 1987-1990, respectively. For Yorkshire, since snow routing was not carried out, only three parameters needed to be optimised (see Table 3.3); a_1, a_2 and a_3; the optimised parameters are given in Table 4.16. Figures 4.7-4.9 provide a comparison of observed and simulated monthly runoff during calibration and validation at the Yorkshire sites. Relevant performance measure statistics during calibration and validation of the model are summarised in Table 4.16. Results indicate that model performance for the Yorkshire catchments during calibration and validation was generally very good (with performance during calibration a little better than during validation) with a coefficient of determination (R^2) range of 0.84-1.00. The coefficient of efficiency (E_c) range over calibration and validation for the Yorkshire catchments are also provided in Table 4.16.

In Urmia, the respective calibration and validation periods were 1970-1980 and 1981-1985. The six optimised parameters used for snow routing at the Urmia catchments are provided in the Table 4.15. Figures 4.10-4.12 provide a comparison of observed and simulated monthly runoff during calibration and validation at the Urmia sites. Relevant performance measure statistics during calibration and validation of the model are summarised in Table 4.16. Results indicate that model performance during calibration was generally very good with a coefficient of determination (R^2) range 0.94-0.97. However, the model did not perform so well during validation with an R^2 range of 0.70-

0.95. The coefficient of efficiency (E_c) range over calibration and validation are also provided in Table 4.16.

On the basis of model performance criteria of Chiew and McMahon (1993) (see section 3.4.2.2), the models are generally showing an acceptable level of performance during calibration and validation. However, the slightly lower levels of performance in Urmia during both calibration and validation may stem from the fact that the model is intended for use in relatively small humid catchments. The relatively lower level of performance of the model during validation in Yorkshire is probably due to the model's inability to accurately simulate the prolonged period of low flows during the 1988-1992 drought. As noted in section 3.4.4.2, a possible remedy for this is to exclude the slow runoff Equation (3.24) from the overall model formulation.

4.4.2.2 Monte Carlo Experiments

Once both baseline and future streamflow records had been simulated, they were fed into a stochastic streamflow model. The parametric, multivariate annual lag-1 auto-regressive AR(1) model followed by disaggregation to monthly flows using a Valencia-Schaake (VS) scheme was utilised for this purpose. A description of both the AR(1) and VS models was provided in section 3.5.3. The multivariate AR(1) model scheme will ensure that both the spatial correlations between the annual flows at the sites in the multiple reservoir systems, as well as the at-site serial correlations, are preserved. The VS scheme, parameterised independently for the baseline and future runoff, helps to preserve correlations between the monthly and annual flows. The coupled multivariate annual AR(1)-VS model was used to generate 500 replicates of monthly runoff (baseline and perturbed) having the same length as the assumed baseline or future record.

An important step in generating stochastic streamflow using models such as AR(1) and Valencia-Schaake disaggregation schemes is the distribution selection of the streamflow data. There are various techniques to select the most appropriate distribution for streamflow data. These include the use of histograms and other more formal goodness-of-fit tests such as the probability plot correlation coefficient (PPCC) test, the Chi-Squared test, the Kolmogorov-Smirnov test and the L-moments diagram test (Stedinger et al., 1993).

It was decided to test the Yorkshire and Urmia monthly and annual flows for five distributions using the PPCC test which has been coded in Fortran by Montaseri (1999). The five distributions under consideration were the normal, two-parameter log-normal (LN2), the three-parameter log-normal (LN3), Gamma and the log Pearson type 3 (LP3) distributions. In the PPCC test, the degree of agreement between an observed streamflow data record and an assumed theoretical distribution is indicated by a correlation coefficient. Values of the correlation coefficient from the PPCC test for the Yorkshire and Urmia baseline (1961-1990) monthly and annual historical streamflow records are provided in Tables 4.17-4.23. The bold underlined values in the table represent the maximum values of the correlation coefficient.

The results in Tables 4.17-4.23 reveal that the normal distribution is the most suitable distribution for modelling annual flows at all the Yorkshire sites whereas the LN3 distribution is most appropriate for modelling annual flows at all the sites in Urmia. Consequently, the normal and LN3 distributions were used in the AR(1) stochastic streamflow generator to model annual flows at the Yorkshire and Urmia sites, respectively.

Probability plots (based on output of the PPCC test coded by Montaseri (1999)) of baseline annual flows are also shown in Figures 4.13 and 4.14 for Yorkshire and Urmia, respectively. Also included in the plots are the upper and lower boundary values of the confidence interval at the 5% significance level. The plots indicate that the normal and LN3 distributions are suitable for modelling the annual flows at Yorkshire and Urmia, respectively. This further reinforces the selection of these distributions for modelling annual flows.

As far as the monthly flows are concerned, selecting the most appropriate distribution is not so straightforward. This is because, as shown in Tables 4.17-4.23, different distributions are appropriate in each particular month. Ideally, therefore, the best distribution should be selected for each month. Clearly, such an approach would be rather tedious. An alternative approach is to assign a score to a particular distribution by summing the total number of occasions it yielded the highest correlation coefficient. The distribution which resulted in the highest score would then be used in modelling all the twelve months of the year (see Tables 4.17-4.23). According to Tables 4.17-4.23, the LP3 and LN3 distributions are most suitable for modelling monthly flows at the Yorkshire and Urmia sites, respectively. Fitting methods for both the LP3 and LN3 distributions are provided by Stedinger et al. (1993).

After determining appropriate probability distributions for generating streamflow, the performance of the stochastic model was assessed. This is important since the stochastic streamflow model must be able to reproduce important statistical characteristics of the observational (baseline) data. The model adopted in the work was the multiple-site lag-one autoregressive model, AR(1) of annual flows coupled to the Valencia-Schaake disaggregation model incorporating parameter uncertainty (see section 3.5.3). The

stochastic model was used to generate 500 sequences of monthly streamflow data. A comparison of selected statistical parameters (e.g. mean flow, CV etc.) of the baseline data and data generated by the stochastic model at both Yorkshire and Urmia is provided in Table 4.24. It should be noted that the statistics for the generated annual flows were averaged over the 500 replicates of stochastic data.

As shown in Table 4.24, the stochastic data generation model is preserving all the statistics of the historical baseline data adequately. The agreement of the mean, CV and Hurst coefficient is particularly good.

The final stage of the assessment involved using the perturbed baseline streamflow records (representing future climatic conditions) to generate 500 sequences of stochastic streamflow data records. These data were then fed into the SPA to obtain 500 reservoir yields for a fixed reservoir storage capacity (see Figure 3.7). Burges and Linsley (1971) recommend that 500 samples are sufficient to accurately define monthly streamflow data derived reservoir distribution. Yields were evaluated for fixed storages of 30% MAF for both the Yorkshire and Urmia systems. The 30% MAF storage capacity selected for Urmia was done for reasons of consistency. After determining the 500 yields, they were then subjected to standard statistical analysis to determine mean, standard deviation and various quantiles.

4.5 Final Study: A Detailed Investigation of the Yorkshire System

Both the preliminary and intermediate studies described so far will offer valuable insight into the effects of climate change on reservoirs located in two different climatic regions.

However, it could be argued that these studies suffer from several deficiencies. Some of the main limitations are that:

(i) they used only the UK Hadley Centre GCM scenarios and ignore scenarios from other GCMs;

(ii) the simple factored approach to perturbing baseline climate implies that the variability of the baseline and future climate is the same;

(iii) the temporal resolution of (monthly) water balance models in simulating catchment response to climate change may be insufficient.

Moreover, a further minor limitation of the previous studies is that potential evapotranspiration scenarios ignored the vegetation response to changes in CO_2 discussed in section 3.3.2.3.

Consequently, it was thought appropriate to carry out a final, more detailed investigation of the Yorkshire system. Such a study is likely to form the basis of a valuable comparison with the previous, less rigorous investigations carried out for the Yorkshire system. The final detailed study adopted a similar methodology to the one in the intermediate study but there were some important differences. These are that (i) climate scenarios based on three different GCMs were considered, (ii) a more statistically robust technique of perturbing baseline climate was adopted, and (iii) a daily water balance model allowed more detailed analysis of catchment response. Other issues were also briefly investigated; (i) the impacts on water resources of changes in PE due to CO_2 induced changes in vegetation, (ii) climate change impacts on groundwater recharge, one-month flow frequency curves and reservoir control curves, and (iii) the effects on water resources resulting from a rise in the demand for water.

4.5.1 Climate Change Scenarios

Outputs from CGCM1, CSIRO1 and HadCM3, described in section 3.3.3.1, representative of the climate in the 2020s, 2050s and 2080s compared to the 1961-1990 baseline were used. This resulted in a total of nine climate change scenarios for radiation, temperature and precipitation. Additionally, the GCM temperature and radiation data were used to construct PE scenarios that will be described later.

The CGCM1 simulation experiment is based on observed carbon dioxide and sulphate aerosol forcing from 1850 to 1989 and a 1% per year compound increase from 1990-2100 based on the IS92a emissions scenario (see section 3.3.2.2). The effects of carbon dioxide doubling (plus sulphate aerosol effects) lead to a 1.9° C global mean surface air temperature rise - known as the climate sensitivity. The CSIRO1 simulation experiment is based on observed carbon dioxide forcing (sulphate aerosol forcing is excluded) from 1880 to 1989 and a 0.9% per year compound increase from 1990-2100 based on the IS92a emissions scenario. The effects of carbon dioxide doubling without sulphate aerosol effects gives a climate sensitivity of 2.2° C. The HadCM3 simulation experiment is based on observed carbon dioxide forcing (sulphate aerosol forcing is excluded) from 1860 to 1989 and a 1% per year compound increase from 1990-2100 based on the IS92a emissions scenario. Only the equilibrium climate model sensitivity (3.3° C) is currently available.

Table 4.25 summarises the historical and projected future greenhouse gas emissions scenarios used for forcing the above three GCM experiments. Also given in Table 4.25 are the CSIRO1 and CGCM1 climate sensitivity, i.e. global average temperature response to CO_2 doubling.

Since GCM output is at a relatively coarse spatial scale, it was downscaled to the Yorkshire catchments' scale using linear interpolation described in section 3.3.5.2. GCM climate variables were used at four grid points (VAR_i, i=1,4) nearest the Yorkshire catchments whose average location was taken as 2°W longitude and 53.8°N latitude. The locations of four grid points at which GCM climate was available are given in Table 4.26. It can be observed that only two grid points (i.e. 1 and 2) will be required for downscaling CGCM1 output. This is because the line joining the two grid points intersects the Yorkshire sites. Figure 4.15 provides a schematic of the 4 GCM grid points used for downscaling by linear interpolation, where VAR_i (i=1,4) are the climate variables at the four GCM grid points, VAR_D is the downscaled variable for a specific catchment, and D_i (i=1,4) are the distances from the catchment to the respective grid points.

Using Equation (3.5) and the grid point locations given in Table 4.26, three individual downscaling expressions were derived for each of the GCMs. These are defined as follows:

$$VAR_{CGCM1} = 0.533VAR_1 + 0.4667VAR_2 \quad (4.1)$$

$$VAR_{CISRO} = 0.203VAR_1 + 0.330VAR_2 + 0.278VAR_3 + 0.188VAR_4 \quad (4.2)$$

$$VAR_{HadCM3} = 0.258VAR_1 + 0.236VAR_2 + 0.241VAR_3 + 0.265VAR_4 \quad (4.3)$$

where VAR_{CGCM1}, VAR_{CISRO} and VAR_{HadCM3} are the downscaled variables (i.e. radiation, temperature, precipitation and PE) for the Yorkshire catchments based on the CGCM1, CSIRO and HadCM3 GCMs.

Scenario construction required a definition of GCM based simulated climate for Yorkshire sites over the baseline period. This also allowed for an assessment of GCM performance to be made over the baseline period. Observed and GCM simulated hydroclimate variables over the baseline period are shown in Figure 4.16. According to the figure, CSIRO1 appears to be reproducing the observed baseline solar radiation most adequately. Observed temperature is being modelled well by HadCM3 while CGCM1 is performing most adequately in reproducing observed precipitation.

The reason for the superior performance of the CGCM1 in modelling precipitation is because the CGCM1 simulation experiment includes the effects of sulphate aerosols. It is usually the case that GCM experiments carried out without sulphate aerosol forcing tend to under-estimate precipitation. However, aerosol effects are often ignored because of a lack of understanding in how they influence the climate. Consequently, a lot of research effort is geared towards understanding the link between sulphate aerosols and the climate system (Hulme and Jenkins, 1998). A comparison of HadCM3 PE with observational data shows good model performance during the summer months in particular. This model's much improved land-surface process formulation (see section 3.3.4.3) will no doubt be largely responsible for this.

The complete range of climate change scenarios (applied to all the Yorkshire sites) expressed as percentage change from the baseline are presented in Figures 4.17 - 4.22. The corresponding absolute monthly changes in temperature, precipitation and PE from the baseline are provided in Tables 4.27-4.29. Also, the annual percentage and absolute changes in temperature, precipitation and PE are summarised in Table 4.30. It should be noted that the PE scenarios in Figure 4.22 were determined using GCM radiation and temperature time-series data in conjunction with the Bowen ratio method described in

section 3.3.2.3. As discussed in section 3.3.2.3, the Bowen ratio method (Equation (3.2)) requires, in addition to radiation and temperature data, the specific heat capacity at constant pressure and the heat diffusivity data. These data were however unavailable with which to calculate the Bowen ratio, therefore an alternative approach, utilising baseline observed PE data (see Table 4.5) was employed. This involved (i) evaluating evapotranspiration based on GCM baseline radiation and temperature data by setting the Bowen ratio to 1 and, (ii) varying the Bowen ratio in a trial-and-error manner in order to synchronise the calculated evapotranspiration with the observed baseline evapotranspiration.

The climate change scenarios in Figures 4.17-4.22 are generally presented twice in the same figure but in two different formats. One group of bar charts provides a comparison of change in climate resulting from the same GCM but for different future time periods. The second group of charts provide a comparison of climate change resulting from different GCMs for the same future time-period. Such a presentation scheme allows each group of scenarios based on a specific GCM to be viewed in isolation, as well as allowing inter-model comparisons.

All temperature scenarios (see Figure 4.17 and Table 4.27) indicate a gradual warming at the Yorkshire sites. Seasonal changes suggest the warming to be more pronounced during winters and at its greatest by the 2080s. For example, the HadCM3 scenario shows an average temperature rise of 76% in January by the 2080s. The smallest rise in temperature predicted by HadCM3 is about a 6% rise by the 2020s in December. The largest and smallest rise in average temperature projected by CSIRO1 is in the months of February and December (2080s), and August (2020s), respectively. A similar pattern of enhanced winter warming and moderate summer warming is observed in the

CGCM1. An inter-model comparison suggests that both the HadCM3 and CSIRO1 are predicting the most severe warming. This is because both of these models, unlike the CGCM1, use only greenhouse gas forcing and ignore the effects of sulphate aerosol cooling. Table 4.27 shows that absolute changes in temperature range from 0.2°C (HadCM3 - December 2020s) to 2.9°C (HadCM3 - June 2080s).

Precipitation scenarios expressed as percentage change from the baseline are presented in Figure 4.18 and the corresponding absolute changes are provided in Table 4.28. There is a general reduction in precipitation during the summer for the CGCM1 and HadCM3 scenarios. In contrast, precipitation is expected to increase in nearly all the months under the CSIRO scenarios. The opposite changes in summer precipitation predicted by CSIRO1 (for the same region) compared to the other two models is an important observation. It highlights current gaps in climate modelling and further reinforces the need for a sensitivity approach to impact assessment. The largest increases and reductions in precipitation are predicted by CGCM1 for March in the 2080s (33%) and HadCM3 for July 2080s (44%), respectively. An inter-model comparison reveals the HadCM3 to be predicting the biggest changes in summer precipitation.

Unlike the temperature scenarios, the change in precipitation does not vary uniformly during the century. Indeed, precipitation may increase in the 2020s, reduce by the 2050s and rise again by the 2080s (e.g. the HadCM3 scenario for April). What is being observed in this case are the effects of natural internal climate variability in the system, which may arise as a result of the North Atlantic Oscillation (NOA) for instance (see section 2.4). It is these natural variations, rather than any human-induced climate

change that might be responsible for the fluctuations observed in some of the precipitation scenarios.

Precipitation scenarios were used to define changes in dry and wet days which are given in Figures 4.19 and 4.20, respectively. According to these, HadCM3 and CSIRO1 predict more dry days over the summer whilst the reverse is true for the CSIRO scenarios.

Net solar radiation scenarios are presented in Figure 4.21. Solar radiation is affected directly by cloud cover. Therefore, on the basis of the precipitation scenarios, there should be a general increase in solar radiation reaching the Earth during the summer for CGCM1 and HadCM3. However, according to the CSIRO1, there should be a reduction over much of the year. This pattern is true to some extent for some of the scenarios. However, Hulme et al. (1999a) note that precipitation increases do not necessarily lead to increases in cloud. A closer inspection of the scenarios reveals some general patterns. CGCM1 is showing an increase in solar radiation throughout most of the year. The exceptions are during January to March, and in July and August towards the middle to end of this century. The differences in radiation from the baseline are much smaller than temperature differences with maximum increases and reductions of about 8% and 4.5%, respectively. The magnitude of changes is similar in CSIRO1 but there is a reduction in radiation more often in the year. The biggest increase and reduction in radiation occur during the months of June (2050s) and November (2080s), respectively. HadCM3 shows a greater consistency with increases in radiation from about April to November and reductions during the remainder of the year. An inter-model comparison shows the HadCM3 estimated changes in radiation to be greater than those predicted by the other two models.

PE scenarios expressed as percentage change from the baseline are presented in Figure 4.22 and the corresponding absolute changes are provided in Table 4.29. The PE changes seem to follow a similar pattern to changes in solar radiation (see Figure 4.21) except that the PE changes are somewhat bigger. For example, the maximum increase in HadCM3 2050s PE in August is 16% compared to about a 12% rise in radiation for the same month (see Figure 4.22).

It was previously mentioned in section 3.3.2.3 that in addition to being influenced by a number of climatic parameters, PE is also dependent on the concentration of atmospheric CO_2. Therefore PE scenarios incorporating CO_2 effects also need to be considered. Consequently, PE scenarios were constructed using Equation (3.4) and land cover information provided in Table 4.1. This resulted in a constant 32% reduction in PE throughout the year. This PE scenario has been termed the H5T scenario and the corresponding absolute annual change from the baseline is provided in Table 4.30. It should be noted that this change represents only the well documented reduction in PE due to plant stomatal closure. As mentioned in section 3.3.2.3, it is also possible that CO_2 will result in increased PE due to increased vegetation growth. However, such scenarios were not derived due to a limited understanding of the effects of CO_2 on vegetation growth.

It was however possible to obtain PE scenarios that include both forms of plant response to rising CO_2 concentrations. As mentioned in section 3.3.4.3, the land-surface scheme within the HadCM3 GCM allows for the simulation of plant response to changes in CO_2 concentrations. The subsequent scenarios should therefore ideally represent more realistic changes in PE than the scenarios based on GCM temperature and radiation data. The HadCM3 PE scenarios provided in Figure 4.23 show a rise in PE throughout most

of the year except July, August and September (2050s). The summer reductions may seem unusual considering that both temperature and the number of dry days are expected to rise in those months. However, given the changes are based on plant response to CO_2, they are entirely feasible. Many previous studies on the effects of CO_2 on PE (discussed in section 3.3.2.3) have been limited due to a lack of understanding in plant response to CO_2 changes.

Changes in PE in Yorkshire presented here offer insight into how PE is influenced by the combined effects of stomatal closure and vegetation growth. The results show that the inclusion of both these effects results in moderate changes in PE ranging from +10% to about -7%. These changes are in contrast to the more severe changes observed by investigators studying the effects of stomatal resistance on PE alone (see section 3.3.2.3). It is also interesting to compare the HadCM3 PE scenarios in Figure 4.23 with the radiation and temperature based HadCM3 PE scenarios in Figure 4.22. The bar charts indicate that whilst PE is expected to increase on the basis of temperature and radiation changes during the summer, reductions are expected when the effects of CO_2 induced changes on vegetation are included. These results are important and suggest that rising concentrations of CO_2 might lead to reductions in summer PE. This is contrary to the common belief that rising temperatures will cause a rise in PE. PE scenarios were unavailable for CGCM1 and CSIRO1 since they are not supplied by the respective modelling centres.

Although all the climate scenarios were used in most of the analysis, a detailed investigation of the water resource impacts used only a single scenario. This was necessary given the time constraints of the research. It could be argued that any one of the CGCM1 scenarios would be ideal since this model performed well in simulating

baseline precipitation (see Figure 4.16) - the major component driving the hydrological cycle. However, the HadCM3 scenario, representative of the 2050s climate was selected instead. This is because the Hadley Centre suite of GCMs (HadCM1 and HadCM2) are perhaps the most widely applied in impact assessments. Assuming a continuation of this trend, it is possible that the current study would form the basis for comparisons with future studies using HadCM3 scenarios. Indeed, using the HadCM3 scenarios will also allow comparisons to be made with the preliminary and intermediate studies that considered the HadCM1 and HadCM2 scenarios. Moreover, PE scenarios for HadCM3 are also available. These will enable the effects of CO_2 changes in PE on water resource systems to be assessed for the first time with the HadCM3 model. The 2050s period was chosen because this is increasingly becoming the standard period over which to investigate climate change impacts.

4.5.2 Applying Climate Change Scenarios to Baseline Climate Data using a Stochastic Weather Generator

The LARS stochastic weather generator (LARS-WG) (Rackso et al., 1991) described in section 3.3.6 was used for the purpose of perturbing baseline climate. To achieve this, baseline hydroclimate (i.e. minimum and maximum daily temperature, daily precipitation and solar radiation) first had to be generated by LARS-WG using the historical baseline records. Given that observational radiation data were unavailable at the sites, the model was supplied with observed sunshine hours data instead (see Table 4.5). These data are used internally by LARS-WG to obtain estimates of radiation. Other data computed internally by LARS-WG and not required as input are the total short-wave radiation received at the top of the atmosphere (R_a) and the maximum number of sunshine hours, N (see section 3.3.6). These data are actually computed

internally by LARS-WG using input latitude information, and are therefore not required as inputs to the model. However, for completeness, they have been obtained from meteorological tables (Shaw, 1994) and are reproduced Table 4.5. The LARS-WG estimated net solar radiation over the baseline period for Yorkshire is given in Table 4.31.

After determining the baseline radiation time-series data, these were converted to PE using temperature data along with the Bowen ratio method. The resulting PE and solar radiation are summarised in Table 4.31. It was necessary to simulate baseline PE because this PE rather than the observed PE would be used in subsequent analyses. This is to allow modelling errors in future and baseline PE to cancel each other out. A comparison of PE derived using LARS-WG simulated radiation and temperature with observational PE data over the baseline period is provided in Figures 4.24 and 4.25. A comparison is also made between LARS-WG simulated precipitation and observed precipitation over the baseline period at all five reservoir sites. This is given in Figures 4.26 and 4.27. The figures illustrating the mean monthly changes (Figures 4.26 and 4.27) show that LARS-WG tends to over-estimate precipitation during January-March at some of the sites. There is a general tendency to under-estimate precipitation in some of the summer months at some sites. PE is over-estimated by the model from March-August with under-estimations in the remaining months.

After simulating the baseline hydroclimate, climate scenarios were used by LARS-WG to generate future hydroclimate. The use of the weather generator enabled variability to be introduced in to the future time-series. One of the scenarios (HadCM3 2050s) was also applied directly in the perturbation of baseline climate. As mentioned previously, impacts assessments carried out with this much simpler 'factored approach' will prove

useful for making comparisons with assessed impacts determined using the more 'realistic' future climate incorporating inter-daily variability.

4.5.3 Hydrological Modelling

Having perturbed the baseline climate, the next step in the methodology required perturbation of baseline hydrology. The MODHYDROLOG daily water balance model was selected for this task. The model was calibrated for the period 1962-1975 and validated for the period 1976-1990. The calibration procedure optimised for 17 parameters but first the initial values of these parameters needed to be specified.

These were selected in accordance with the recommendation of Chiew and McMahon (1994). The recommendation is based on defining some of the initial parameter values on the basis of catchment characteristics such as soil type and land cover. This and other relevant information for the Yorkshire sites was presented in Table 4.1. Of the 17 parameters that required a specification of initial values, five were selected on the basis of soil type; a_{insc}, a_{sub}, a_{crack}, a_{smsc} and a_{coeff}. These five parameters are respectively (i) interception store capacity, (ii) constant of proportionality in interflow equation, (iii) constant of proportionality in groundwater recharge equation, (iv) soil moisture store capacity and (v) maximum infiltration loss parameter. Some other information in Table 4.1 was used for setting initial values of most of the remaining parameters. For example, land cover and stream length/slope information were used to set initial values of EM (maximum plant-controlled rate of transpiration) and CO (routing coefficient) parameters, respectively. The optimised parameter values are provided in Table 4.32.

Figures 4.28 and 4.29 show a comparison of observed and simulated mean monthly runoff during calibration and validation, respectively, at all sites. The various performance related statistics are summarised in Tables 4.33 and 4.34. It can be observed that model performance during calibration and validation was very good with an R^2 range of 0.96-1.00 and 0.87-1.00, respectively. The respective changes in the coefficient of efficiency (E_c) over calibration and validation are 0.83-0.91 and 0.74-0.97. As expected, these are somewhat lower than R^2 values owing to the formulation of E_c (see section 3.4.2.2). It can also be noted (Table 4.33) that with the exception of Widdop flow, the differences between observed and simulated mean annual runoff are within 5%. According to Chiew and McMahon's (1993) model adequacy test described in section 3.4.2.2, the models are generally performing exceptionally. Despite this however, further adequacy tests would ideally need to be performed. As discussed in section 3.4.2.2, a good test for model adequacy would be to compare reservoir storage-yield curves derived from observed and simulated flow records. Unfortunately it was not possible to undertake such an assessment in the current research due to time constraints.

A comparison of runoff simulated by MODHYDROLOG and Xu's monthly model used in the Intermediate study was however carried out. Mean monthly baseline runoff simulated by the two models, along with the observed runoff, are provided in Figure 4.30 for Hebden site. The baseline period selected is between 1962-1990 since both rainfall-runoff models discarded the 1961 runoff as part of their initialisation procedure. The MODHYDROLOG simulated runoff at Gorple, Widdop and Walshaw Dean sites were aggregated to give the Hebden runoff so that a comparison can be made with Xu model simulated runoff at Hebden site.

Figure 4.30 shows that MODYDROLOG simulated runoff is generally slightly higher than the observed runoff during most of the year. Runoff from Xu's model is slightly lower than the observed runoff from October-February and higher in the remaining months. Moreover, based on these results, it could be concluded that Xu's model is performing better than MODHYDROLOG during the winter. However, probably due to MODHYDROLOG's groundwater recharge component, it is showing better performance during the summer. Furthermore, a comparison of R^2 and E_c values in Tables 4.16 and 4.34 show both models are simulating runoff equally well. It could therefore be argued that using the much simpler monthly model of Xu would have given as good a result as the use of the more complex 17-parameter MODHYDROLOG.

To assess the hydrological response of the catchments to climate change, the baseline and future data were fed into MODHYDROLOG. The baseline was specified using LARS-WG data in place of observed baseline data. This was to allow any errors introduced in baseline and future hydroclimate data generation modelling to cancel each other out. In simulating the runoff, MODHYDROLOG discarded the first year hence shortening the original 30-year (1961-1990) data records to 29-year records. MODHYDROLOG also simulates groundwater recharge and baseflow. Therefore it was also possible to investigate the effects of climate change on groundwater recharge.

4.5.4 Water Resource Systems' Modelling

The single runoff records, baseline and future, were then input into a stochastic streamflow model to ultimately assess the effect of their sampling errors on water resource impacts. As in the intermediate study, the parametric, multivariate annual lag-one auto-regressive AR(1) model followed by disaggregation to monthly flows using a

Valencia-Schaake (VS) scheme was utilised for this purpose. The coupled multivariate annual AR(1)-VS model was used to generate 1000 replicates of monthly runoff (baseline and perturbed) having the same length as the assumed baseline or future record (i.e. 29 years). Although it was mentioned earlier that 500 replicates are sufficient, it was thought that this number is an absolute minimum. It was thought that for this detailed investigation, the 500 replicates should be doubled to reflect the detailed analysis in this study.

The water resource impacts assessment involved assessing the effects of climate change on reservoir storage-yield-performance in addition to reservoir operation. Surface fluxes were included in reservoir analysis in the same way as for the intermediate study and reservoir reliability and resilience were also investigated.

Another facet of the study was to assess the impact of a rising demand on reservoir storage by the 2050s. This required estimates of water demand under a changed climate. Such estimates have been documented in a UK Environment Agency report (NRA, 1994). Figures quoted for Yorkshire indicate a 23% rise in demand by 2021. This figure is based on a 'high' scenario and assumes leakage levels to be held at 1991 levels. Moreover, it assumes domestic consumption and non-household consumption to rise at compound annual rates of 1% and 0.75%, respectively. In the absence of a demand scenario for the 2050s in Yorkshire, a figure of 20% was adopted. This was selected partly for convenience but also because it is close to the projected demand rise in Yorkshire by 2021.

4.6 Summary

This chapter has described how the techniques introduced in previous chapters were applied to investigate climate change impacts on hydrological and water resource systems. The application used case studies from England and Iran. These reservoir systems are located in regions with two contrasting climates, i.e. a more moderate, temperate climate of Europe (the Yorkshire system) and the semi-arid climate of Iran (the Urmia system). The relevant characteristics of the two reservoir systems were presented and it was noted that the Urmia system is much larger than the Yorkshire system.

Hydroclimatic data for both Urmia and Yorkshire were then presented with the temperature data for Urmia indicating that snowmelt plays a significant role in the Hydrology of the region. Moreover, evaporation and precipitation data revealed that evaporation generally exceeds precipitation in Urmia whilst the reverse is true in Yorkshire. This information is important for including the effects of net-reservoir surface evaporation fluxes in the storage-yield analysis.

After presenting a description of the catchments and summarising the hydroclimatic data, details of three studies were provided. These studies are the (i) preliminary, (ii) intermediate and (iii) final detailed investigations. The preliminary study considered both the Yorkshire and Urmia systems and investigated the impacts of climate change on reservoir storage-yield. The study employed a simple factored approach to perturb baseline climate and used a simple runoff coefficient approach to assess the catchment rainfall-runoff response to climate change. Climate change scenarios from two GCM

experiments were applied which are the UK HadCM1 and HadCM2. Furthermore, this study adopted the traditional single records approach to impacts assessment.

The intermediate study also investigated both the Yorkshire and Urmia systems but differed from the preliminary study in a number of ways. Firstly, this investigation was conducted within a Monte Carlo framework in addition to applying the traditional methodology used in the preliminary study. The Monte Carlo framework will allow the sampling uncertainties in the runoff data records to be quantified. Secondly, a monthly water balance model was used as a basis for assessing catchment response. This approach also allowed the effects of snowmelt in the Urmia catchments to be incorporated in the analysis.

The final detailed study considered only the Yorkshire system but in a greater level of detail than the two previous investigations. The main aspects of this study were (i) climate scenarios based on three different GCMs were considered, (ii) a more statistically robust technique of perturbing baseline climate was adopted, and (iii) a daily water balance model allowed more detailed analysis of catchment response. Other issues were also briefly investigated; (i) the impacts on water resources of changes in PE due CO_2 induced changes in vegetation, (ii) climate change impacts on groundwater recharge, one-month flow frequency curves and reservoir control curves, and (iii) the effects on water resources resulting from a rise in the demand for water.

There was an extremely important purpose to carrying out the analysis in three phases in that it would enable comparisons between results of the more detailed investigation and those studies adopting a more simplified approach to climate change impacts assessment. Indeed, an important outcome of the analysis carried out in this chapter is

that the simulation of baseline runoff using a monthly water balance model is practically indistinguishable from that based on a much more involved daily water balance model. Results showed that the use of the relatively complex MODHYDROLOG daily water balance model does not necessarily result in a more accurate simulation of baseline runoff than Xu's monthly model. This result has implications for the climate impacts assessment and suggests that the extra effort expended in calibrating the daily water balance model may not be justified.

The results of the analysis and further discussion are presented in the next chapter.

Table 4.1: Characteristics of the catchments analysed.

	Yorkshire catchments						Urmia Catchments		
		Hebden Group							
	Gorpley	Gorple	Widdop	W. S. Dean	Luddenden	Ogden	Baranduz	Shahr	Nazlu
Area (km^2)	2.83	8.02	9.00	9.41	6.46	5.39	618	418	1715
Coordinates (lat, lon)	53° 42' N, 2° 9' W	53° 46' N, 2° 6' W	53° 47' N, 2° 6' W	53 ° 48' N, 2 ° 3' W	53° 47' N, 1° 57' W	53° 47' N, 1° 54' W	37° 20' N, 44° 57' E	37 ° 25' N, 44 ° 53' E	37° 40' N, 44° 50' E
Altitude (m)	450	400	350	420	370	400	1900	1800	2000
Stream length (m)	1370	2450	5140	2180	2890	2980			
Slope (m/km)	115.3	63.7	29.6	40.9	62.3	47.3			
PIMP*	3	5	4	4	6	4			
Soil type	Hill peat	Hill peat	Hill peat	Hill peat	Hill peat, shale, mudstone	Shale, mudstone			
Vegetation cover	Mostly grass	Mostly grass	Grass and some trees	Mostly grass	Mostly grass	Grass and some trees			

* Percentage impervious area.
Note: stream length, slope, PIMP, soil type and vegetation cover information for Yorkshire required for final detailed investigation

Table 4.2: Summary statistics of annual flow and characteristics of the reservoir systems under investigation.

Reservoir	Baseline annual flow				Reservoir system characteristics					
	Mean (10^6) m^3	CV	Skewness	Lag-one serial correlation	Storage capacity		Yield		Standardised demand parameter 'm'	Within-year (WY) or over-year (OY)
					$(10^6$ $m^3)$	(% MAF)	$(10^3$ m^3/day)	(% MAF)		
YORKSHIRE										
Gorpley	2.75	0.18	-0.08	0.26	0.56	20	2.73	36	3.6	WY
Gorple	7.93	0.19	-0.28	0.43	2.93	37	16.39	75	1.3	WY
Widdop	9.22	0.18	-1.32	0.28	2.77	30	15.50	61	2.2	WY
W. S. Dean	9.27	0.18	-1.30	0.26	2.58	28	14.45	57	2.4	WY
Hebden total	26.50	0.18	-0.11	0.37	8.28	31	46.34	64	2.0	WY
Luddenden	5.33	0.17	0.21	0.38	1.43	27	9.02	62	2.2	WY
Ogden	4.47	0.19	0.09	0.24	1.43	32	5.42	44	2.9	WY
Group total	38.97	0.18	-0.07	0.35	11.69	30	63.67	60	2.2	WY
URMIA										
Baranduz	285.454	0.32	1.43	0.03	n/a*	n/a*	516.16	66	1.06	WY
Shahr	171.798	0.35	1.37	0.06	n/a*	n/a*	357.72	76	0.69	OY
Nazlu	401.996	0.40	1.20	0.24	n/a*	n/a*	881.09	80	0.50	OY
Group total	859.248	0.34	1.07	0.15	n/a*	n/a*	1754.97	75	0.74	OY

Streamflow data record length = 30 years (1961-1990)
'm' parameter = (1-yield)/CV
MAF = mean annual flow
Gorple, Widdop & W.S. Dean belong to Hebden group
* reservoirs being planned

Table 4.3: Mean monthly precipitation characteristics for the Yorkshire catchments over the baseline (1961-1990) period.

Site	Parameter	Jan	Feb	Mar	Apr	May	Jun	Jul	Aug	Sep	Oct	Nov	Dec	Ann
Gorpley	Mean (mm)	147.8	103.4	119.3	104.4	84.6	94.1	92.1	122.0	118.0	140.8	156.4	179.4	1462.1
	CV	0.47	0.65	0.53	0.49	0.58	0.56	0.46	0.35	0.65	0.59	0.45	0.85	0.20
Gorple	Mean (mm)	154.1	110.8	125.0	98.2	90.8	90.8	92.1	124.9	126.1	143.7	153.1	160.5	1469.9
	CV	0.46	0.53	0.49	0.53	0.48	0.46	0.45	0.41	0.48	0.50	0.39	0.40	0.13
Widdop	Mean (mm)	144.7	102.8	121.5	93.7	83.8	89.1	91.9	123.8	121.0	139.5	146.6	155.1	1413.4
	CV	0.47	0.52	0.50	0.52	0.50	0.47	0.43	0.38	0.49	0.50	0.41	0.43	0.16
W. Dean	Mean (mm)	141.5	100.8	117.9	98.3	90.2	86.4	88.9	119.2	124.8	133.8	145.6	149.7	1397.1
	CV	0.45	0.53	0.44	0.51	0.44	0.49	0.49	0.41	0.45	0.49	0.38	0.41	0.12
Hebden average	Mean (mm)	146.4	104.5	121.3	96.7	88.2	88.7	90.9	122.5	123.9	138.7	148.2	154.8	1424.7
	CV	0.44	0.56	0.43	0.49	0.47	0.45	0.50	0.40	0.49	0.47	0.39	0.41	0.16
Luddenden	Mean (mm)	109.7	84.2	93.8	81.1	74.9	79.0	65.0	94.8	99.8	109.1	110.2	111.4	1112.9
	CV	0.43	0.58	0.42	0.50	0.49	0.60	0.50	0.43	0.58	0.48	0.40	0.49	0.14
Ogden	Mean (mm)	108.8	80.9	89.8	79.2	74.0	71.9	64.8	89.4	94.0	109.3	105.2	114.1	1081.4
	CV	0.44	0.57	0.43	0.51	0.48	0.62	0.49	0.41	0.52	0.52	0.43	0.48	0.13

Note: Gorple, Widdop & W.S. Dean belong to Hebden group

Table 4.4: Mean monthly evaporation at Calder in Yorkshire over baseline (1961-1990) period based on monthly time-series data.

Month	PE (mm)	AE (mm)	E_o (mm)
Jan	7.5	7.5	12.5
Feb	10.0	10.0	16.7
Mar	20.3	20.1	29.0
Apr	37.2	36.8	53.2
May	57.6	56.4	72.0
Jun	67.8	52.9	84.7
Jul	69.9	36.3	87.4
Aug	58.8	35.3	73.6
Sep	40.3	35.1	57.6
Oct	21.9	21.0	31.3
Nov	12.1	12.1	20.1
Dec	8.4	8.4	13.9
Ann	411.8	332.0	552.0

PE: Potential evapotranspiration
AE: Actual evapotranspiration
E_0: Open water evaporation

Table 4.5: Mean monthly historical climatological data for west Yorkshire (1961-1990).

Month	Observed number of sunshine hours (n)	Maximum theoretical number of sunshine hours (N)	Total short-wave radiation received at top of atmosphere, R_a (w/m^2)	Min. temp. (°C)	Max. temp. (°C)	Ave. temp. (°C)	PE# (mm)	E_o* (mm)
Jan	35.0	246.3	51.2	0.4	5.0	2.7	12.9	21.5
Feb	53.4	272.2	108.2	0.3	4.9	2.6	15.5	25.8
Mar	90.1	363.0	224.5	1.6	7.1	4.3	33.4	47.7
Apr	123.2	416.7	338.3	3.2	9.8	6.5	50	71.4
May	164.3	491.9	455.7	6.1	13.7	9.9	79.5	99.4
Jun	162.6	505.7	492.7	9.2	16.7	12.9	82.4	103.0
Jul	156.0	510.1	485.3	11.0	18.2	14.6	84.2	105.3
Aug	146.0	458.1	394.4	10.8	17.8	14.3	74.1	92.6
Sep	114.4	381.0	261.3	9.0	15.5	12.3	52	74.3
Oct	80.8	325.8	153.9	6.6	12.2	9.4	31.1	44.4
Nov	53.0	256.0	67.9	2.9	7.8	5.4	17.5	29.2
Dec	28.2	230.8	35.4	1.3	5.9	3.6	12.4	20.7
Annual	1206.9	4457.6	3068.7	5.2	11.2	8.2	545.0	735.3

Potential evapotranspiration based on daily time-series data at Gorple site
* Open water evaporation based on daily time-series data at Gorple site

Table 4.6: Monthly runoff characteristics for the Yorkshire catchments over the baseline (1961-1990) period.

Site	Parameter	Jan	Feb	Mar	Apr	May	Jun	Jul	Aug	Sep	Oct	Nov	Dec	Ann
Gorpley	Mean (mm)	135.9	96.1	91.9	60.4	41.4	28.8	30.1	53.3	69.4	101.4	123.9	137.9	970.4
	CV	0.45	0.50	0.59	0.52	0.67	0.70	0.73	0.76	0.68	0.54	0.39	0.44	0.18
Gorple	Mean (mm)	137.7	101.1	95.4	68.4	43.1	32.8	30.4	50.3	65.3	100.2	123.2	141.6	989.4
	CV	0.43	0.47	0.54	0.55	0.60	0.62	0.62	0.72	0.65	0.54	0.42	0.39	0.19
Widdop	Mean (mm)	141.1	103.0	98.4	73.0	45.3	34.3	32.1	52.7	68.1	104.3	127.0	145.8	1025.1
	CV	0.41	0.47	0.52	0.54	0.62	0.62	0.63	0.72	0.63	0.53	0.42	0.38	0.18
W.S. Dean	Mean (mm)	134.8	97.7	91.9	74.0	44.8	33.1	32.2	51.8	64.6	100.6	122.1	137.7	985.4
	CV	0.41	0.47	0.51	0.55	0.64	0.62	0.65	0.72	0.62	0.53	0.43	0.39	0.18
Hebden	Mean (mm)	137.4	99.8	97.0	71.5	44.6	33.9	32.0	52.7	67.1	102.3	124.0	141.7	1003.9
	CV	0.42	0.48	0.51	0.54	0.62	0.61	0.63	0.71	0.63	0.53	0.42	0.39	0.18
Luddenden	Mean (mm)	97.9	80.5	80.2	68.7	55.6	47.6	38.3	46.7	53.6	74.1	83.9	97.2	824.5
	CV	0.29	0.37	0.31	0.37	0.41	0.41	0.33	0.49	0.53	0.50	0.36	0.35	0.17
Ogden	Mean (mm)	114.0	88.3	78.1	64.2	41.6	30.6	20.7	34.1	49.5	85.8	102.8	119.2	828.9
	CV	0.40	0.51	0.49	0.60	0.77	0.79	0.87	0.92	0.84	0.66	0.49	0.48	0.20

Note: Gorple, Widdop & W.S. Dean belong to Hebden group

Table 4.7: Mean monthly evaporation and temperature data for Urmia sites.

	Baranduz			Shahr			Nazlu			All sites
Month	AE (mm)	PE (mm)	E_o (mm)	AE (mm)	PE (mm)	E_o (mm)	AE (mm)	PE (mm)	E_o (mm)	Temp. (°C)
Jan	13.3	13.3	21.0	15.0	15.0	21.3	15.5	15.5	20.3	-2.1
Feb	16.9	16.9	34.4	15.4	15.4	34.5	14.7	14.7	33.8	-1.5
Mar	15.4	15.6	62.6	15.3	15.5	59.7	14.9	15.0	58.7	4.0
Apr	12.5	12.6	93.5	12.7	12.8	92.4	12.1	12.2	91.4	9.6
May	20.2	20.6	134.8	20.3	20.7	130.1	19.9	20.3	127.6	14.4
Jun	33.9	43.4	173.6	32.3	41.4	167.5	31.7	40.7	165.6	19.2
Jul	33.7	64.8	198.1	33.3	64.0	193.5	32.9	63.3	191.2	23.4
Aug	63.4	105.7	181.5	61.2	102.0	187.2	60.1	100.1	184.8	23.4
Sep	94.3	108.4	155.2	90.9	104.5	150.3	89.9	103.3	148.2	19.7
Oct	79.1	82.4	109.1	77.3	80.5	104.2	76.3	79.5	102.0	13.2
Nov	27.1	27.1	61.5	29.9	29.9	59.0	31.0	31.0	57.8	7.0
Dec	17.5	17.5	25.9	16.0	16.0	25.8	14.0	14.0	25.0	1.2
Annual	427.3	528.3	1251.2	419.6	517.7	1225.5	413.0	509.6	1206.4	9.0

PE: Potential evapotranspiration
AE: Actual evapotranspiration
E_0: Open water evaporation
PE, AE & E_o data for 1953-1993 period and temperature data for 1963-1990 period.

Table 4.8: Mean monthly precipitation characteristics for the Urmia catchments over the baseline period.

Site	Parameter	Jan	Feb	Mar	Apr	May	Jun	Jul	Aug	Sep	Oct	Nov	Dec	Ann
Hashem Abad (Baranduz, Shahr: 1963-1990)	Mean (mm)	37.5	41.9	58.4	68.6	55.5	26.8	6.5	3.5	3.4	31.7	39.0	47.7	420.5
	CV	0.60	0.45	0.62	0.63	0.57	0.81	1.64	1.90	1.87	1.12	0.86	0.63	0.24
Mir Abad (Nazlu: 1965-1990)	Mean (mm)	26.9	33.7	56.8	82.9	73.3	37.8	8.3	3.4	9.2	31.3	44.5	31.8	440.0
	CV	0.61	0.73	0.84	0.55	0.79	1.10	1.76	2.15	1.69	1.07	1.12	1.07	0.34

Table 4.9: Mean monthly runoff characteristics for the Urmia catchments over the baseline (1961-1990) period.

Site	Parameter	Jan	Feb	Mar	Apr	May	Jun	Jul	Aug	Sep	Oct	Nov	Dec	Ann
Baranduz	Mean (mm)	21.7	21.2	31.0	64.7	102.3	85.5	45.1	19.0	9.5	12.8	23.8	25.2	461.9
	CV	0.26	0.30	0.45	0.40	0.36	0.43	0.59	0.85	0.60	0.58	0.44	0.32	0.32
Shahr	Mean (mm)	8.2	8.7	18.4	61.0	112.5	112.4	43.7	13.5	5.7	6.1	11.0	9.8	411.0
	CV	0.52	0.44	0.53	0.45	0.34	0.39	0.61	0.74	0.64	0.71	0.69	0.58	0.35
Nazlu	Mean (mm)	7.8	7.9	12.8	38.2	68.2	49.6	17.6	6.2	4.1	5.4	8.6	8.1	234.4
	CV	0.34	0.32	0.46	0.42	0.46	0.59	0.77	0.87	0.82	0.59	0.46	0.34	0.40

Table 4.10: Summary of main differences between three climate change water resources impacts studies.

Study	Region	Approach	Impacts	GCMs	Future time-periods under consideration	Downscaling method	Perturbation method	Catchment rainfall-runoff response model	Water resource systems response model
Preliminary	Yorkshire & Urmia	Traditional single records	Runoff and reservoir storage-yield	HadCM1 HadCM2	2020s, 2050s	GCM output used directly	Mean monthly changes only (simple perturbation)	Simple monthly water balance equation (simple runoff coefficient approach)	Extended SPA
Intermediate	Yorkshire & Urmia	Traditional & Monte Carlo	Runoff and reservoir storage-yield-performance	HadCM2	2020s	GCM output used directly/linear interpolation	Mean monthly changes only (simple perturbation)	Monthly water balance simulation model of Xu	Extended SPA
Final detailed	Yorkshire	Traditional & Monte Carlo	Runoff, reservoir storage and yield, groundwater, and reservoir (i) control curves, (ii) resilience and (iii) sustainability	CSIRO1 CGCM1 HadCM3	2020s, 2050s, 2080s	Linear interpolation	Daily stochastic weather generator to include variability in future hydroclimate	MODHYDROLOG daily water balance simulation model	Extended SPA

Table 4.11: Change in rainfall both in mm and % of baseline mean (% in parenthesis) based on the simple perturbation method.

Scenario	Jan	Feb	Mar	Apr	May	Jun	Jul	Aug	Sep	Oct	Nov	Dec
H120	25.3	10.0	17.1	-4.8	-7.1	7.9	12.8	-7.1	2.4	24.9	42.7	4.6
	(18)	(10)	(15)	(-5)	(-8)	(7)	(14)	(-6)	(2)	(18)	(30)	(3)
H150	12.6	5.0	10.3	-2.9	-3.5	5.7	7.3	-2.4	3.5	15.2	22.8	3.1
	(9)	(5)	(9)	(-3)	(-4)	(5)	(8)	(-2)	(3)	(11)	(16)	(2)
GG1m	2.8	8.0	4.6	5.8	7.1	-1.1	-2.7	5.9	7.1	15.2	15.6	9.3
	(2)	(8)	(4)	(6)	(8)	(-1)	(-3)	(5)	(6)	(11)	(11)	(6)
GS1m	5.7	2.0	3.5	4.9	4.4	1.1	-1.8	1.2	-1.2	8.3	4.4	3.2
	(4)	(2)	(3)	(5)	(5)	(1)	(-2)	(1)	(-1)	(6)	(3)	(2)
GS1t	5.7	4.0	5.8	12.8	14.0	-16.3	-8.2	-5.9	5.9	30.6	-1.5	0.0
	(4)	(4)	(5)	(13)	(16)	(-15)	(-9)	(-5)	(5)	(22)	(-1)	(0)
UKCIP98	5.7	11.1	3.5	3.9	5.2	-3.3	-3.7	2.4	5.9	11.1	11.7	8.0
	(4)	(11)	(3)	(4)	(6)	(-3)	(-4)	(2)	(5)	(8)	(8)	(5)
IRHAD	-1.1	-1.5	-1.6	-1.0	-1.9	-1.2	-0.5	-0.1	-0.3	0.8	0.6	-0.7
	(-3)	(-4)	(-3)	(-1)	(-3)	(-4)	(-7)	(-3)	(-6)	(3)	(1)	(-2)

H120: HadCM1-2020s, H150: HadCM1-2050s, GG1m, GS1m, GS1t, UKCIP98, IRHAD all based on HadCM2-2020s.

Table 4.12: Change in PE both in mm and % of baseline mean (% in parenthesis) based on the simple perturbation method.

Scenario	Jan	Feb	Mar	Apr	May	Jun	Jul	Aug	Sep	Oct	Nov	Dec
H120	0.0	4.0	3.0	9.3	0.0	18.3	0.0	4.1	9.3	2.2	6.1	-1.8
	(0)	(40)	(15)	(25)	(0)	(27)	(0)	(7)	(23)	(10)	(50)	(-22)
H150	-0.4	1.1	0.4	3.0	-0.6	2.7	-0.7	1.2	1.2	0.0	2.5	-1.7
	(-5)	(11)	(2)	(8)	(-1)	(4)	(-1)	(2)	(3)	(0)	(21)	(-20)
GG1m	-1.1	-0.9	-0.8	-0.4	0.6	0.0	2.1	0.6	0.8	-0.2	-2.1	-2.1
	(-14)	(-9)	(-4)	(-1)	(1)	(0)	(3)	(1)	(2)	(-1)	(-17)	(-25)
GS1m	-0.9	-0.7	-0.4	-0.4	0.0	-0.7	1.4	1.8	1.6	0.0	-0.6	-0.8
	(-12)	(-7)	(-2)	(-1)	(0)	(-1)	(2)	(3)	(4)	(0)	(-5)	(-10)
GS1t	0.4	-0.6	-0.2	-2.2	-4.0	3.4	4.2	8.8	4.8	1.3	-0.1	-0.4
	(5)	(-6)	(-1)	(-6)	(-7)	(5)	(6)	(15)	(12)	(6)	(-1)	(-5)
UKCIP98	0.2	0.9	0.0	0.7	2.3	2.7	5.6	3.5	14.5	2.6	0.7	0.3
	(3)	(9)	(0)	(2)	(4)	(4)	(8)	(6)	(36)	(12)	(6)	(3)

H120: HadCM1-2020s, H150: HadCM1-2050s, GG1m, GS1m, GS1t, UKCIP98, IRHAD all based on HadCM2-2020s.

Table 4.13: Rise in 2020s temperature in Urmia (°C) based on the simple perturbation method.

Scenario	Jan	Feb	Mar	Apr	May	Jun	Jul	Aug	Sep	Oct	Nov	Dec
IRHAD	0.7	0.8	1.0	0.8	0.8	1.1	1.2	1.0	1.3	1.0	0.5	0.5

IRHAD based on HadCM2-2020s

Table 4.14: Percentage of annual demand during each month for Urmia reservoir system.

Reservoir	Jan	Feb	Mar	Apr	May	Jun	Jul	Aug	Sep	Oct	Nov	Dec
Baranduz	0.0	0.0	0.0	4.3	12.1	20.3	22.2	18.3	13.1	6.8	2.9	0.0
Shahr	2.1	2.1	2.1	5.4	10.8	17.1	18.8	16.2	12.1	7.1	4.1	2.1
Nazlu	0.0	0.0	0.0	4.2	12.6	20.5	22.3	19.1	13.0	6.0	2.3	0.0
Group total	0.4	0.4	0.4	4.5	12.0	19.7	21.6	18.3	12.9	6.5	2.9	0.4

Table 4.15: Parameter estimates of Xu's monthly water balance model from the Yorkshire and Urmia calibration exercises.

Param.	Yorkshire - excluding snow module (10^{-3})				Param.	Urmia - including snow module (10^{-2})		
	Gorpley	Hebden	Luddn.	Ogden		Baranduz	Shahr	Nazlu
a_1	6.501	6.223	5.603	13.28	a_4	1685.8	1873.0	1577.0
a_2	65.99	117.5	89.84	88.21	a_5	-294.61	357.98	439.82
a_3	5.718	6.041	1.295	5.391	a_6	5.5165	24.829	-0.0006
					a_7	0.1789	0.1678	0.0073
					a_8	0.4537	0.9459	0.2953
					a_9	0.7446	2.9067	480.30

a_1: soil permeability parameter; a_2: storage constant; a_3: fast runoff parameter (without snow module); a_4: evapotranspiration parameter; a_5: slow runoff parameter; a_6: fast runoff parameter (snow module)

Table 4.16: Rainfall-runoff model performance of Xu's monthly water-balance model during calibration and validation.

Catchment	Calibration		Validation		Percentage difference	
	R^2	E_c	R^2	E_c	Calibration	Validation
Yorkshire*						
Gorpley	0.98	0.85	0.97	0.79	11.5	11.4
Hebden	1.00	0.95	1.00	0.94	-0.7	1.9
Luddenden	0.99	0.89	0.96	0.81	3.9	7.13
Ogden	0.91	0.74	0.84	0.62	23.0	28.2
Urmia#						
Baranduz	0.94	0.71	0.70	0.54	-7.8	-10.8
Shahr	0.96	0.82	0.88	0.69	-7.2	-2.3
Nazlu	0.97	0.75	0.95	0.70	-2.0	4.7

* calibration: 1980-1986; validation 1987-1990
# calibration: 1970-1980; validation 1981-1985
R^2: coefficient of determination; E_c: coefficient of efficiency

Table 4.17: PPCC test based correlation coefficients for monthly and annual baseline (1961-1990) streamflow data record in the Gorpley catchment.

Month	Normal	Gamma	LN2	LN3	LP3
Jan	0.9822	0.9891	0.9856	0.9895	**0.9913**
Feb	0.9799	0.9917	0.9827	**0.9928**	0.9923
Mar	0.9101	**0.9933**	0.9734	0.9920	0.9895
Apr	0.9734	0.9788	0.9801	0.9815	**0.9877**
May	0.9407	0.9873	**0.9912**	0.9911	**0.9912**
Jun	0.9418	**0.9936**	0.9892	0.9891	0.9891
Jul	0.9298	0.9579	**0.9692**	**0.9692**	**0.9692**
Aug	0.9575	**0.9809**	0.9589	0.9658	0.9690
Sep	0.9618	0.9916	0.9776	0.9885	**0.9925**
Oct	0.9670	0.9905	0.9659	**0.9924**	0.9875
Nov	0.9811	0.9816	0.9762	0.9762	**0.9836**
Dec	0.9837	**0.9958**	0.9805	0.9943	0.9912
Total score*	0	4	2	3	7
Annual	**0.9861**	0.9845	0.9833	0.9833	0.9845

* Number of underlined PPCC. The maximum PPCC for each month is indicated in bold underline.

Table 4.18: PPCC test based correlation coefficients for monthly and annual baseline (1961-1990) streamflow data record in the Hebden catchment.

Month	Normal	Gamma	LN2	LN3	LP3
Jan	0.9841	0.9917	0.9825	**0.9940**	**0.9944**
Feb	0.9810	0.9904	0.9802	**0.9916**	0.9914
Mar	0.9378	0.9915	0.9928	0.9939	**0.9952**
Apr	0.9606	0.9683	0.9735	0.9723	**0.9757**
May	0.9427	0.9916	0.9934	**0.9936**	0.9935
Jun	0.9591	**0.9881**	0.9802	0.9827	0.9813
Jul	0.9203	0.9672	0.9804	**0.9816**	0.9815
Aug	0.9397	**0.9830**	0.9792	0.9809	0.9822
Sep	0.9460	0.9794	0.9786	0.9868	**0.9906**
Oct	0.9603	0.9850	0.9729	**0.9913**	0.9890
Nov	0.9737	0.9766	0.9782	0.9778	**0.9808**
Dec	0.9814	0.9873	0.9767	0.9872	**0.9876**
Total score*	0	2	0	5	6
Annual	**0.9954**	0.9945	0.9881	0.9881	0.9943

* Number of underlined PPCC. The maximum PPCC for each month is indicated in bold underline.

Table 4.19: PPCC test based correlation coefficients for monthly and annual baseline (1961-1990) streamflow data record in the Luddenden catchment.

Month	Normal	Gamma	LN2	LN3	LP3
Jan	0.9934	**0.9938**	0.9774	0.9933	0.9914
Feb	0.9871	0.9945	0.9894	**0.9945**	0.9943
Mar	0.9577	0.9927	0.9893	0.9904	**0.9930**
Apr	0.9645	0.9789	0.9799	**0.9812**	0.9801
May	0.9551	0.9799	0.9801	0.9814	**0.9856**
Jun	0.9722	**0.9915**	0.9909	0.9896	0.9909
Jul	0.9335	**0.9797**	0.9767	0.9765	0.9772
Aug	0.9591	0.9940	0.9943	0.9944	**0.9944**
Sep	0.9486	**0.9891**	0.9873	0.9886	0.9883
Oct	0.9495	0.9854	0.9918	0.9915	**0.9924**
Nov	0.9805	0.9820	0.9781	**0.9831**	0.9817
Dec	0.9669	0.9800	0.9878	0.9858	**0.9880**
Total score*	0	4	0	3	5
Annual	**0.9833**	0.9830	0.9832	0.9831	0.9787

* Number of underlined PPCC. The maximum PPCC for each month is indicated in bold underline.

Table 4.20: PPCC test based correlation coefficients for monthly and annual baseline (1961-1990) streamflow data record in the Ogden catchment.

Month	Normal	Gamma	LN2	LN3	LP3
Jan	0.9908	**0.9942**	0.9791	0.9928	0.9906
Feb	0.9761	0.9902	0.9815	0.9913	**0.9928**
Mar	0.9535	0.9916	0.9920	**0.9925**	**0.9925**
Apr	0.9535	0.9757	0.9790	**0.9796**	0.9791
May	0.9330	**0.9934**	0.9874	0.9929	0.9931
Jun	0.9537	**0.9909**	0.9814	0.9885	0.9901
Jul	0.8983	0.9882	0.9899	**0.9939**	0.9929
Aug	0.9183	**0.9935**	0.9833	0.9877	0.9899
Sep	0.9171	**0.9885**	0.9686	0.9879	**0.9885**
Oct	0.9474	0.9865	0.9736	0.9913	**0.9918**
Nov	0.9829	0.9920	0.9866	0.9918	**0.9922**
Dec	0.9653	0.9805	0.9892	0.9892	**0.9900**
Total score*	0	5	0	3	6
Annual	**0.9912**	0.9893	0.9896	0.9674	0.9883

* Number of underlined PPCC. The maximum PPCC for each month is indicated in bold underline.

Table 4.21: PPCC test based correlation coefficients for monthly and annual baseline (1961-1990) streamflow data record in the Baranduz catchment.

Month	Normal	Gamma	LN2	LN3	LP3
Jan	0.9490	0.9760	0.9768	0.9775	**0.9778**
Feb	0.9294	0.9892	0.9712	**0.9896**	0.9862
Mar	0.9287	0.9872	0.9841	**0.9928**	0.9923
Apr	0.9636	0.9895	0.9917	**0.9919**	0.9904
May	0.9756	0.9917	0.9939	0.9939	**0.9942**
Jun	0.9666	**0.9869**	0.9821	0.9858	0.9832
Jul	0.9276	0.9851	0.9854	**0.9887**	0.9859
Aug	0.8571	0.9887	0.9879	0.9911	**0.9938**
Sep	0.9463	**0.9852**	0.9277	0.9772	0.9369
Oct	0.9412	0.9875	0.9889	**0.9903**	0.9902
Nov	0.9747	0.9869	0.9896	0.9905	**0.9913**
Dec	0.9807	**0.9921**	0.9865	0.9911	0.9891
Total score*	0	3	0	6	4
Annual	0.9374	0.9875	0.9847	**0.9931**	0.9929

* Number of underlined PPCC. The maximum PPCC for each month is indicated in bold underline.

Table 4.22: PPCC test based correlation coefficients for monthly and annual baseline (1961-1990) streamflow data record in the Shahr catchment.

Month	Normal	Gamma	LN2	LN3	LP3
Jan	0.9609	0.9913	0.9881	**0.9947**	0.9930
Feb	0.9390	0.9857	0.9885	**0.9919**	0.9915
Mar	0.9389	0.9942	0.9901	**0.9947**	0.9941
Apr	0.9557	**0.9938**	0.9919	0.9920	0.9927
May	0.9741	0.9914	0.9928	0.9905	**0.9930**
Jun	0.9657	**0.9915**	0.9849	0.9879	0.9852
Jul	0.9037	0.9818	0.9833	0.9841	**0.9883**
Aug	0.9037	0.9838	0.9897	**0.9935**	0.9929
Sep	0.9665	0.9927	0.9538	**0.9949**	0.9896
Oct	0.9078	0.9728	0.9745	**0.9756**	0.9744
Nov	0.9472	0.9793	0.9803	0.9794	**0.9805**
Dec	0.8861	0.9534	0.9691	0.9705	**0.9712**
Total score*	0	2	0	6	5
Annual	0.9329	0.9896	0.9791	**0.9932**	0.9928

* Number of underlined PPCC. The maximum PPCC for each month is indicated in bold underline.

Table 4.23: PPCC test based correlation coefficients for monthly and annual baseline (1961-1990) streamflow data record in the Nazlu catchment.

Month	Normal	Gamma	LN2	LN3	LP3
Jan	0.9400	0.9807	0.9808	**0.9898**	0.9883
Feb	0.9641	**0.9878**	0.9838	0.9834	0.9861
Mar	0.9461	0.9896	0.9907	0.9907	**0.9907**
Apr	0.9630	0.9882	0.9915	0.9910	**0.9916**
May	0.9723	0.9897	0.9748	**0.9899**	0.9871
Jun	0.9426	0.9758	0.9841	0.9842	**0.9843**
Jul	0.8956	0.9796	0.9585	**0.9842**	0.9667
Aug	0.9254	0.9850	0.9792	**0.9928**	0.9909
Sep	0.9337	0.9951	0.9765	**0.9960**	0.9941
Oct	0.9533	**0.9885**	0.9827	0.9813	0.9827
Nov	0.9547	0.9679	0.9711	**0.9717**	0.9713
Dec	0.9728	0.9888	0.9909	**0.9909**	0.9909
Total score*	0	2	0	8	3
Annual	0.9521	0.9912	0.9905	**0.9929**	0.9926

* Number of underlined PPCC. The maximum PPCC for each month is indicated in bold underline.

Table 4.24: Comparison of the key statistical parameters for the baseline and stochastically generated annual streamflow data for the Yorkshire and Urmia rivers.

Site	Min. (10^3 m^3)	Max. (10^3 m^3)	Mean (10^3 m^3)	CV	Skewness	Serial correlation (lag-one)	h
Gorpley	**1760**	**3512**	**2746**	**0.177**	**-0.08**	**0.26**	**0.67**
	1550	*3565*	*2746*	*0.178*	*0.01*	*0.59*	*0.64*
Hebden	**16328**	**35976**	**26503**	**0.181**	**-0.11**	**0.37**	**0.73**
	12998	*36799*	*26488*	*0.183*	*0.02*	*0.24*	*0.67*
Luddenden	**3912**	**7174**	**5326**	**0.174**	**0.21**	**0.38**	**0.63**
	3367	*7427*	*5324*	*0.176*	*-0.01*	*0.18*	*0.61*
Ogden	**2820**	**6132**	**4468**	**0.193**	**0.09**	**0.24**	**0.68**
	2378	*6593*	*4467*	*0.195*	*-0.09*	*-1.20*	*0.69*
Baranduz	**158350**	**559370**	**285430**	**0.320**	**1.43**	**0.03**	**0.67**
	145252	*599730*	*287324*	*0.330*	*1.60*	*0.03*	*0.66*
Shahr	**96260**	**344040**	**171796**	**0.351**	**1.37**	**0.06**	**0.61**
	83574	*368770*	*173693*	*0.361*	*1.07*	*0.07*	*0.73*
Nazlu	**185020**	**914240**	**401985**	**0.402**	**1.20**	**0.24**	**0.66**
	178532	*955289*	*404673*	*0.420*	*1.43*	*0.11*	*0.68*

Bold font indicates values based on historical data over baseline (1961-1990) period
Values in italics are based on 500 replicates of streamflow generated using the stochastic streamflow generator.
h: Hurst coefficient

Table 4.25: Greenhouse gas and sulphate aerosol forcing scenarios used in three GCM experiments and the corresponding climate sensitivity.

	GCM Experiment		
	HadCM3	**CSIRO1**	**CGCM1**
Control CO_2 forcing (ppmv)	295 (1850 level)	330 (1975 level)	295 (1850 level)
Transient CO_2 forcing	1% pa compound	0.9% pa compound	1% pa compound
Greenhouse gases forcing	Historic, 1860-1989 IS92a, 1990-2100	Historic, 1881-1989 IS92a, 1990-2100	Historic, 1850-1989 IS92a, 1990-2100
Sulphate aerosol forcing	None	None	Historic, 1860-1989 IS92a, 1990-2100
Transient warming at CO_2 doubling (°C)	n/a	2.0	1.9

ppmv: parts per million by volume

Table 4.26: Co-ordinates of four grid points nearest to Yorkshire catchments based on three different GCMs used for downscaling climate to the Yorkshire catchment scale.

Grid point	**CGCM1**		**CSIRO1**		**HadCM3**	
	Western longitude	**Northern latitude**	**Western longitude**	**Northern latitude**	**Western longitude**	**Northern latitude**
1	3.75°	53.81°	5.63°	52.56°	3.75°	52.50°
2	0.00°	53.81°	0.00°	52.56°	0.00°	52.50°
3	0.00°	57.56°	0.00°	55.75°	0.00°	55.00°
4	3.75°	57.56°	5.63°	55.75°	3.75°	55.00°

Table 4.27: Absolute changes (from baseline) in temperature (°C) in Yorkshire.

Scenario	**Jan**	**Feb**	**Mar**	**Apr**	**May**	**Jun**	**Jul**	**Aug**	**Sep**	**Oct**	**Nov**	**Dec**	**Ann**
C2	0.3	0.5	0.2	0.3	0.5	0.8	1.1	0.8	0.7	0.9	0.4	0.5	0.6
C5	0.6	0.7	0.4	0.5	0.8	1.6	1.9	1.4	1.5	1.4	0.9	0.9	1.0
C8	1.4	1.1	1.0	1.1	1.5	2.1	2.6	2.7	2.6	2.3	1.5	1.5	1.8
A2	0.4	0.7	0.9	0.8	1.2	1.0	1.0	0.9	0.9	1.3	0.7	0.9	0.9
A5	0.7	0.9	1.4	1.5	1.8	1.6	1.7	1.6	1.6	1.8	1.6	1.3	1.5
A8	1.2	1.3	1.7	2.0	2.6	2.1	2.3	2.3	2.5	2.4	2.3	1.8	2.1
H2	0.7	0.8	0.7	0.7	0.7	0.9	0.9	1.2	0.9	0.9	0.6	0.2	0.8
H5	1.9	1.4	1.3	1.2	1.7	1.8	1.8	2.5	2.3	2.0	1.0	1.2	1.7
H8	2.1	1.8	1.7	2.0	2.5	2.9	2.8	3.5	3.2	2.6	1.8	1.3	2.4

C: CGCM1, A: CSIRO1, H: HadCM3, 2: 2020s, 5: 2050s, 8: 2080s.

Table 4.28: Absolute changes in precipitation (mm) in Yorkshire.

Scenario	Jan	Feb	Mar	Apr	May	Jun	Jul	Aug	Sep	Oct	Nov	Dec	Ann
C2	-5.0	19.0	33.3	2.1	-20.5	-4.6	-14.9	-6.8	-12.3	-21.1	-7.5	5.5	-33.1
C5	16.8	21.8	42.2	-2.1	-13.5	-13.9	9.1	8.0	-4.0	-29.2	2.9	10.3	46.2
C8	33.2	17.0	46.9	6.9	-8.9	-25.7	11.3	5.5	-1.4	-7.5	-6.5	7.3	78.1
A2	-2.0	27.1	28.9	3.3	7.4	7.0	9.1	18.6	16.3	-17.8	6.6	33.4	134.6
A5	-14.7	6.5	35.7	17.7	7.4	-5.2	4.8	17.4	12.1	-2.5	14.2	33.5	124.7
A8	18.0	7.3	52.7	17.5	30.2	-19.1	11.1	18.0	8.2	7.1	58.0	43.0	249.5
H2	11.5	-14.4	1.4	3.3	0.7	-30.0	-26.6	-21.6	-11.9	-7.4	8.6	16.1	-69.4
H5	37.8	1.8	22.3	-8.6	-20.2	-29.8	-44.8	-59.8	-60.3	5.8	-4.8	50.3	-105.9
H8	48.1	13.7	10.9	6.0	-9.4	-32.6	-53.2	-55.6	-46.7	12.9	18.6	36.3	-46.3

C: CGCM1, A: CSIRO1, H: HadCM3, 2: 2020s, 5: 2050s, 8: 2080s.

Table 4.29: Absolute changes in potential evapotranspiration (mm) in Yorkshire.

Scenario	Jan	Feb	Mar	Apr	May	Jun	Jul	Aug	Sep	Oct	Nov	Dec	Ann
C2	0.3	-0.3	-2.1	0.0	5.4	1.6	6.3	0.5	1.8	2.3	1.2	0.2	17.0
C5	0.3	-0.2	-2.9	0.3	5.2	4.0	0.7	-2.4	0.2	3.2	1.4	0.7	9.6
C8	0.1	0.2	-1.3	1.1	4.4	6.4	-1.1	-3.6	1.0	1.9	2.2	0.3	11.0
A2	0.3	-0.3	-1.2	-0.2	1.4	1.8	2.0	-4.4	-0.8	1.2	0.4	-0.3	0.0
A5	0.7	0.5	-2.1	-0.7	2.1	7.3	3.5	-1.6	-0.4	-0.1	0.1	-0.8	9.9
A8	0.2	0.5	-2.5	-0.5	-2.4	7.5	0.9	-2.5	-0.2	0.8	-0.4	-0.6	1.3
H2	-0.3	0.2	-1.4	-1.3	1.0	8.1	6.6	0.2	3.2	0.7	1.1	-0.8	18.2
H5	-0.9	0.4	-1.5	1.8	3.5	5.9	11.6	5.7	8.6	1.6	0.8	-1.1	37.7
H8	-0.8	-0.2	0.0	1.0	2.1	6.9	11.6	6.3	8.0	1.2	0.4	-0.3	37.5
H2M	0.1	1.1	1.0	0.1	2.0	2.5	-1.8	-2.2	0.3	0.4	1.4	0.6	7.0
H5M	0.0	0.3	-0.5	0.2	-0.5	-0.1	-0.5	-4.9	-3.1	2.3	0.4	0.3	2.2
H8M	1.2	-0.6	2.1	0.8	1.4	-0.7	-2.7	-2.5	3.2	-0.4	-0.1	1.2	6.8

C: CGCM1, A: CSIRO1, H: HadCM3, M: GCM simulated change, 2: 2020s, 5: 2050s, 8: 2080s.

Table 4.30: Annual changes in hydroclimate in Yorkshire.

Scenario	Temperature change		Precipitation change			PE change	
	%	Abs (°C)	%	Abs (mm)	CV (%)	%	Abs (mm)
C2	11.5	0.9	-0.7	-9.3	-2.2	3.1	16.9
C5	19.0	1.6	3.2	42.4	-6.9	2.1	11.4
C8	27.0	2.2	6.2	82.1	1.1	2.0	10.9
A2	7.5	0.6	5.4	71.5	14.6	0.0	0.0
A5	13.2	1.1	6.7	88.7	10.3	1.8	9.8
A8	22.7	1.9	13.1	173.4	2.8	0.2	1.1
H2	9.7	0.8	-4.7	-62.2	-20.6	1.3	7.1
H5	21.0	1.7	-5.7	-75.5	-26.3	0.4	2.2
H8	29.3	2.4	-1.7	-22.5	-13.6	1.3	7.1
H5M						0.4	2.2
H5T						-32.0	-174.3

C: CGCM1, A: CSIRO1, H: HadCM3, M: GCM simulated change, T: stomatal resistance effects, 2: 2020s, 5: 2050s, 8: 2080s.

Table 4.31: LARS-WG simulated baseline (1961-1990) net solar radiation and potential evapotranspiration based on the Bowen ratio Equation (3.2) at the Yorkshire sites.

Month	Solar radiation (w/m^2)	PE (mm)
Jan	17.4	8.0
Feb	37.0	15.1
Mar	74.1	38.1
Apr	122.7	59.0
May	169.0	91.6
Jun	181.7	92.5
Jul	169.0	86.7
Aug	143.5	74.6
Sep	99.5	42.4
Oct	52.1	22.1
Nov	25.5	9.5
Dec	12.7	7.4
Ann	1104.2	546.9

Table 4.32: 17 optimised MODHYDROLOG parameters during calibration (1962-1975).

Parameter	Site				
	Gorple	Widdop	W.Dean	Luddenden	Ogden
a_{rinsc}	1.1	2.1	2.5	2.3	1.9
a_{coeff}	190	180	165	182	179
a_{sq}	0.9	0.6	0.6	0.9	0.9
a_{ads}	1	0.5	0	0.5	0.5
a_{dsc}	39	50	33	33	18
a_{sub}	0.2	0.32	0.08	0.24	0.09
a_{crak}	1.38	1.7	0.02	1.28	1.66
a_{smsc}	90	230	170	200	190
a_{em}	13.5	11.5	13	13	13
a_{seas}	0	0	0	0	0
a_{power}	0.9	0	0	0	0
a_{co}	30	40	22	23	25
a_{rk1}	0	0	0	0	0.06
a_{rk2}	0.04	0.05	0.18	0.14	0.1
a_{rk3}	43	61	47	50	50
a_{vcond}	0.32	0.1	0.2	0.14	0.2
a_{dlev}	0.2	0.2	0.2	0.7	0.05

Table 4.33: Observed and simulated mean annual runoff over calibration and validation periods based on MODHYDROLOG.

Catchment	Calibration period (1962-1975)			Validation period (1976-1990)		
	Obs runoff (mm)	Sim runoff (mm)	% Error (%)	Obs runoff (mm)	Sim runoff (mm)	% Error (%)
Gorple	914	885	-3.1	1056	1060	0.4
Widdop	952	934	-1.9	1092	1296	18.7
WS Dean	921	925	0.3	1047	1003	-4.3
Luddenden	673	674	0.1	729	721	-1.0
Ogmix	670	656	-2.0	733	757	3.3

Table 4.34: MODHYDROLOG performance during calibration and validation.

Catchment	Calibration (1962-1975)			Validation (1976-1990)		
	RMSE (mm)	R^2	E_c	RMSE (mm)	R^2	E_c
Gorple	9.8	0.99	0.83	11.7	1.00	0.97
Widdop	17.1	1.00	0.89	32.5	0.87	0.74
WS Dean	17.4	0.96	0.88	18.3	0.96	0.91
Luddenden	11.0	0.99	0.83	13.9	0.97	0.80
Ogmix	12.8	0.98	0.91	17.2	0.99	0.88

RMSE: root mean square error; R^2: coefficient of determination; E_c: coefficient of efficiency

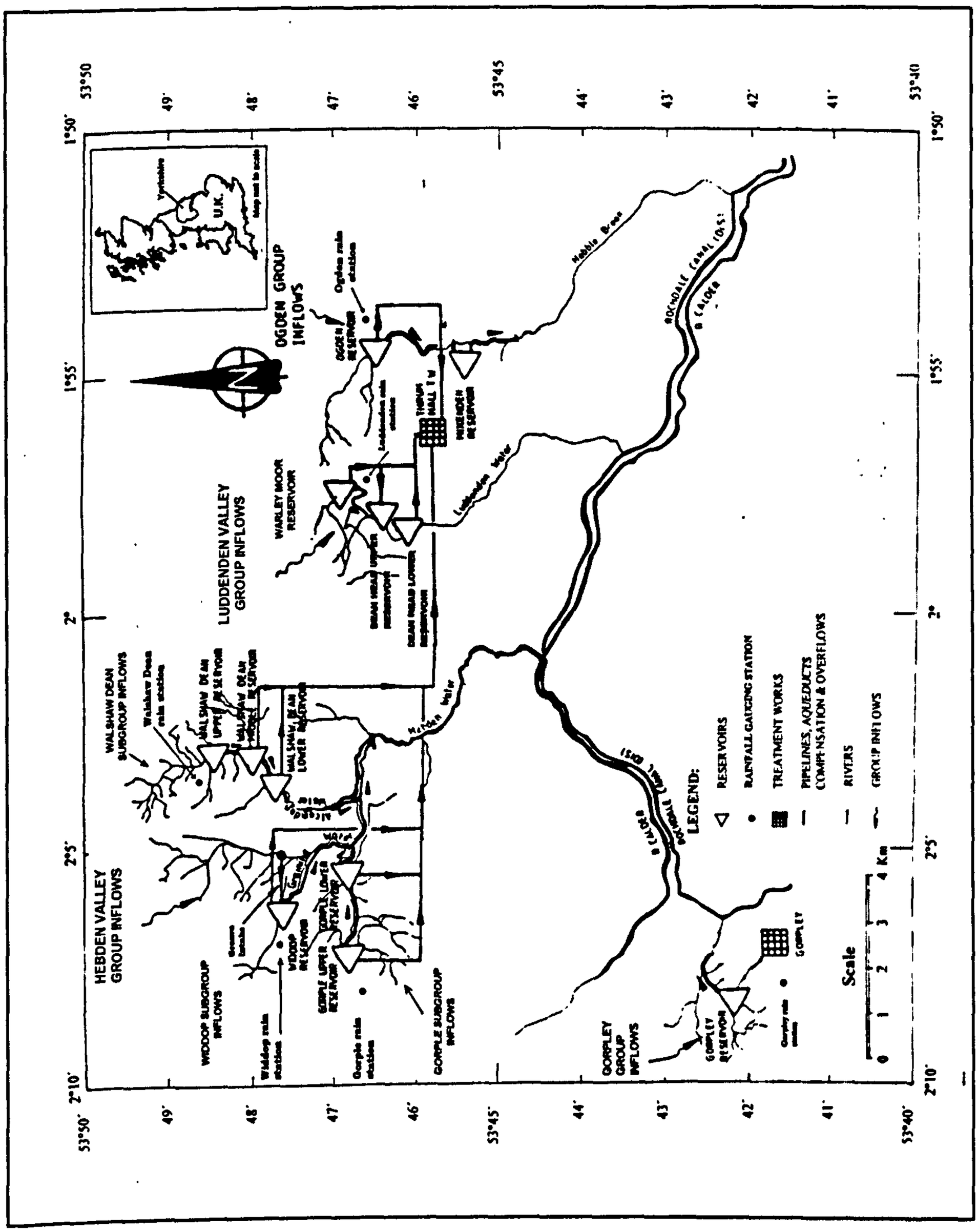

Figure 4.1: Detailed map of the Yorkshire reservoir system (adopted from Yorkshire Water RRDY, 1991, with modifications)

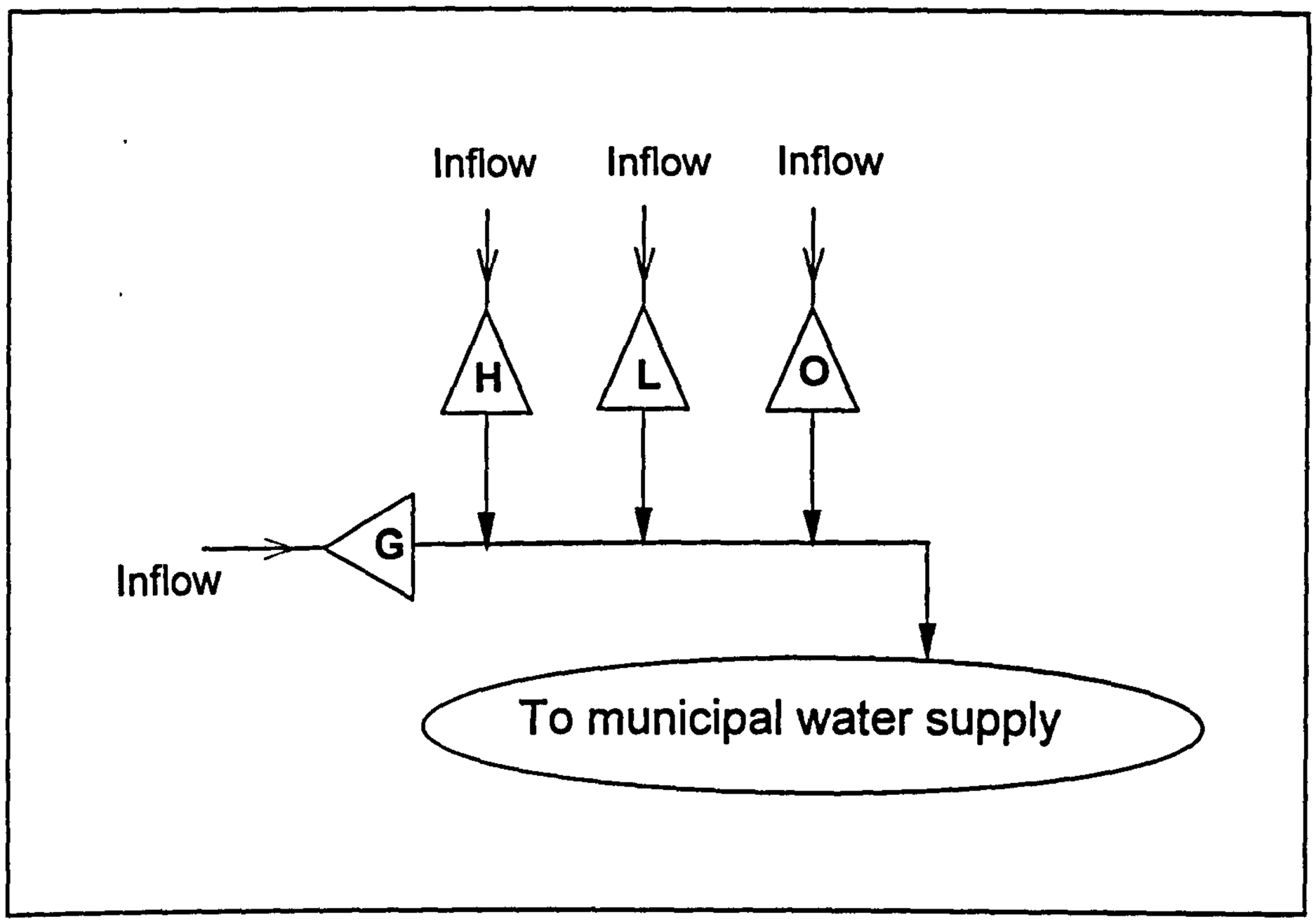

Figure 4.2: Simplified schematic of the Yorkshire multiple reservoir system (G: Gorpley, H: Hebden, L: Luddenden, O: Ogden)

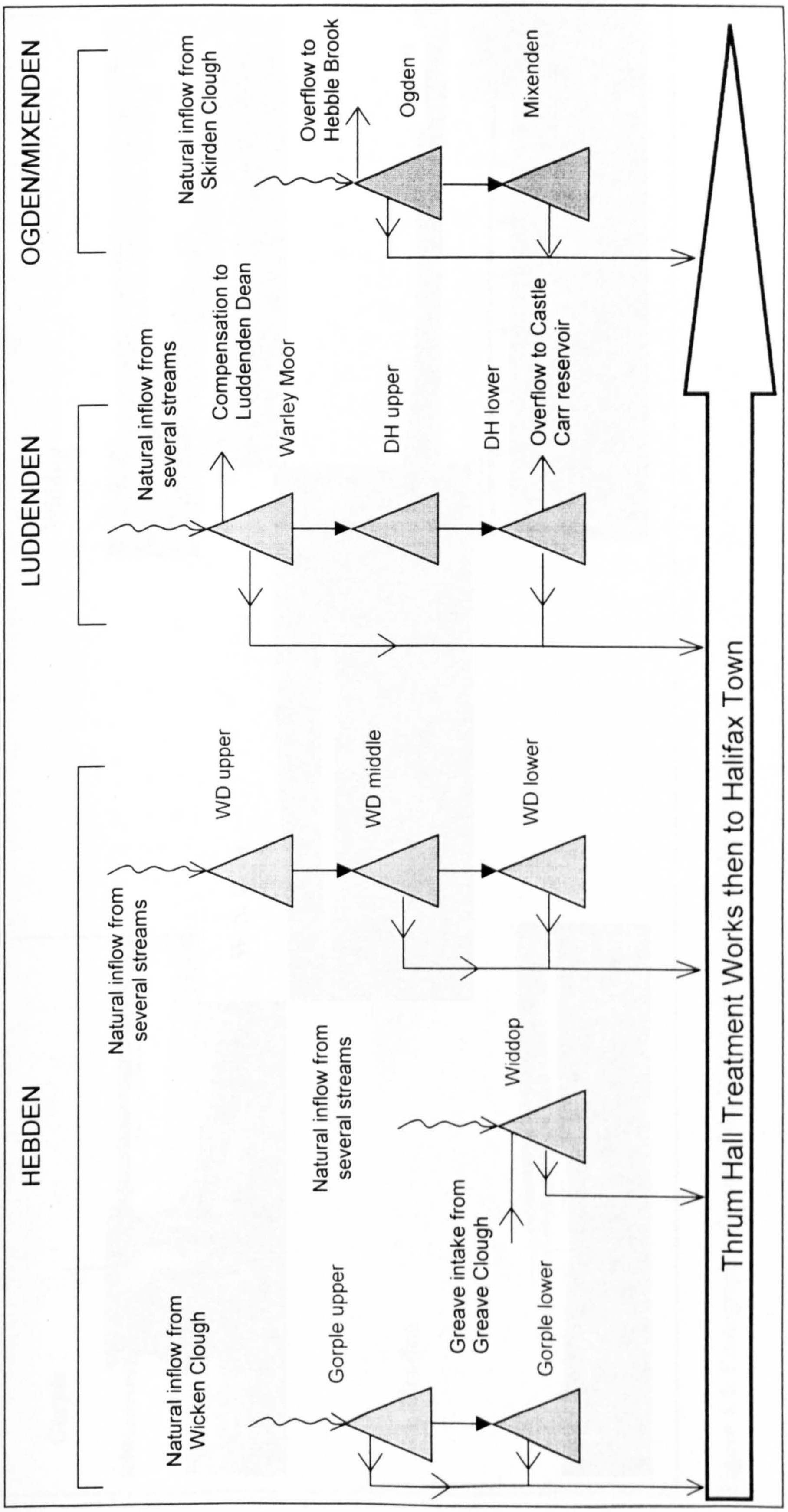

Figure 4.3: Schematic configuration of the Yorkshire reservoir systems.

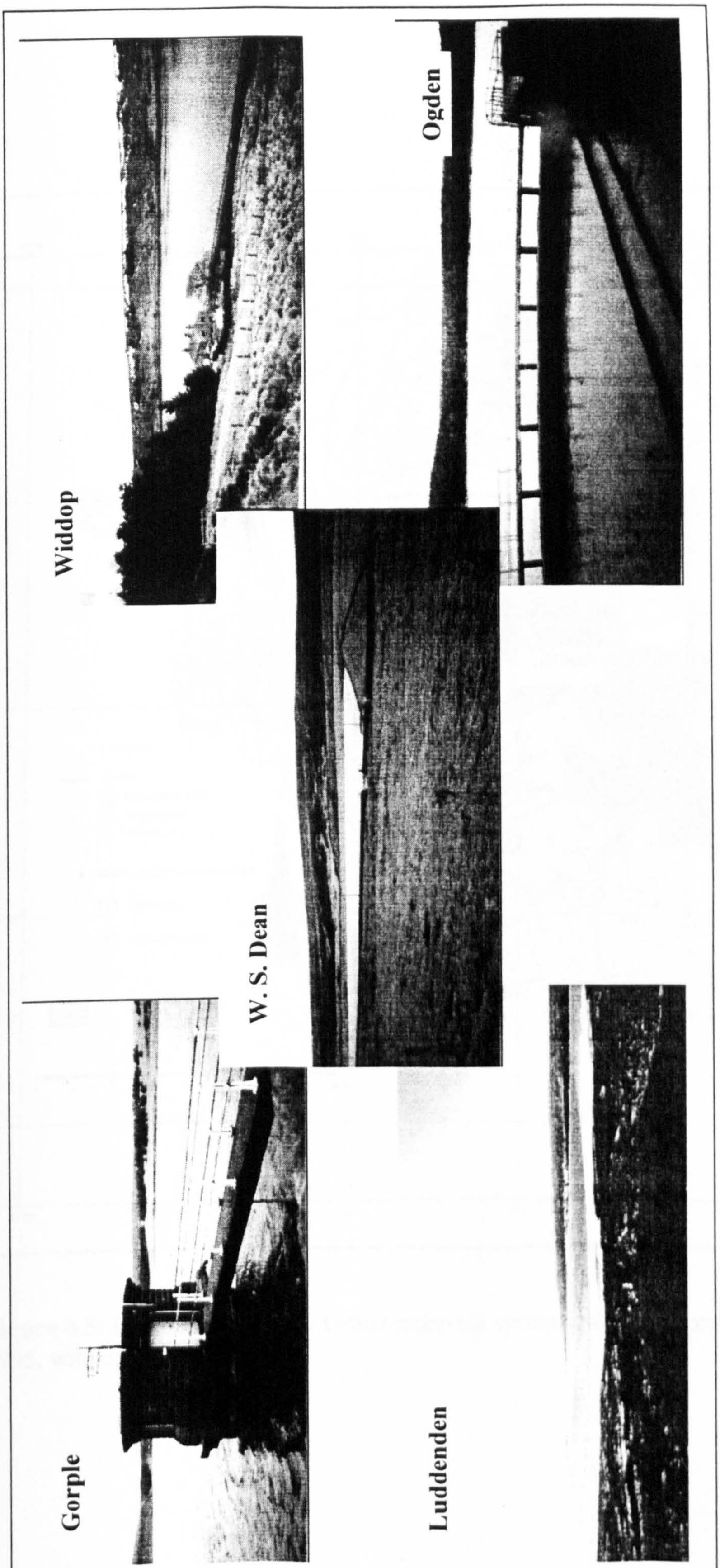

Figure 4.4: Photographs of some of the Yorkshire reservoirs under investigation.

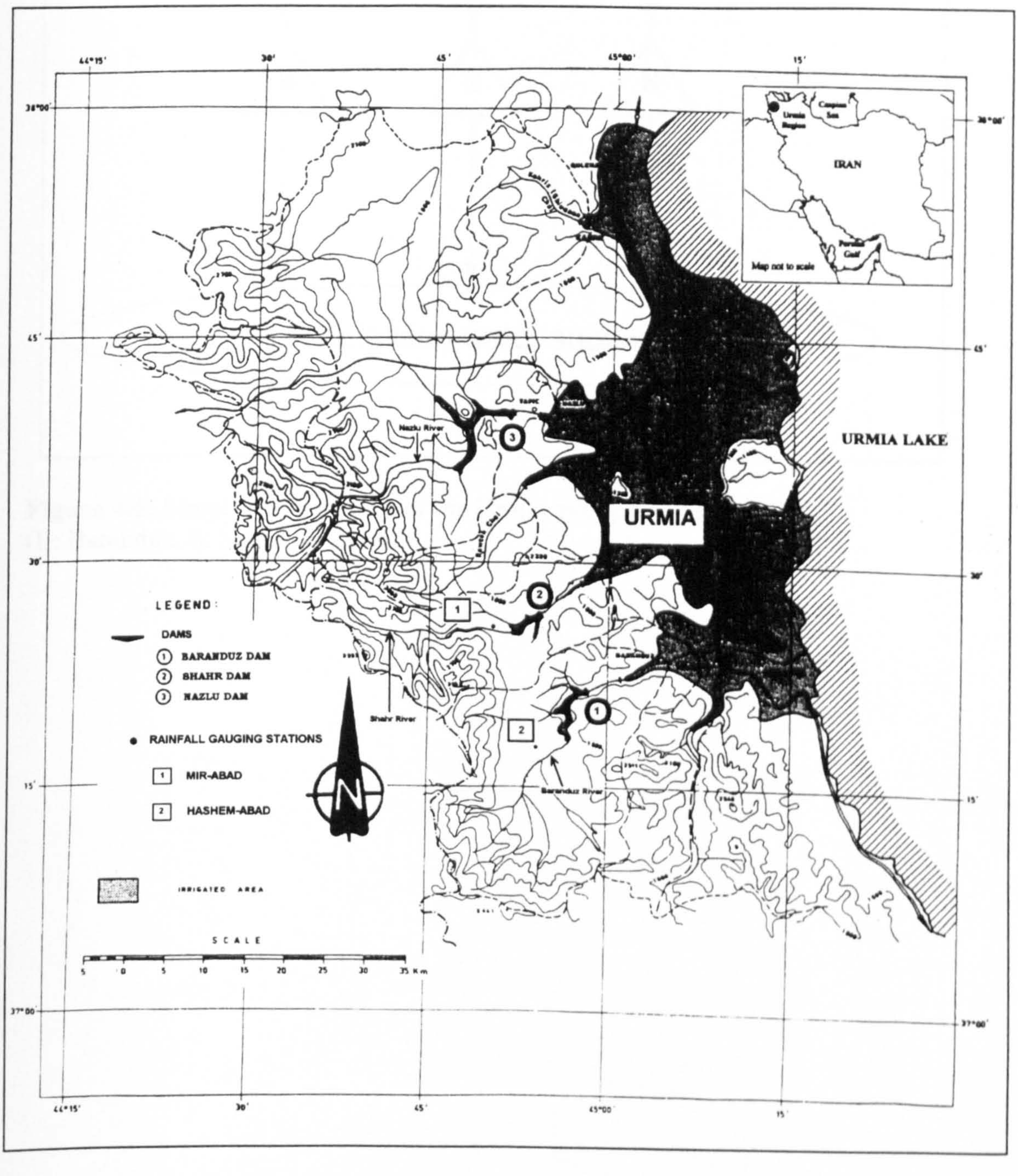

Figure 4.5: Detailed map of the Urmia reservoir systems (adopted from MWP, 1995, with modifications).

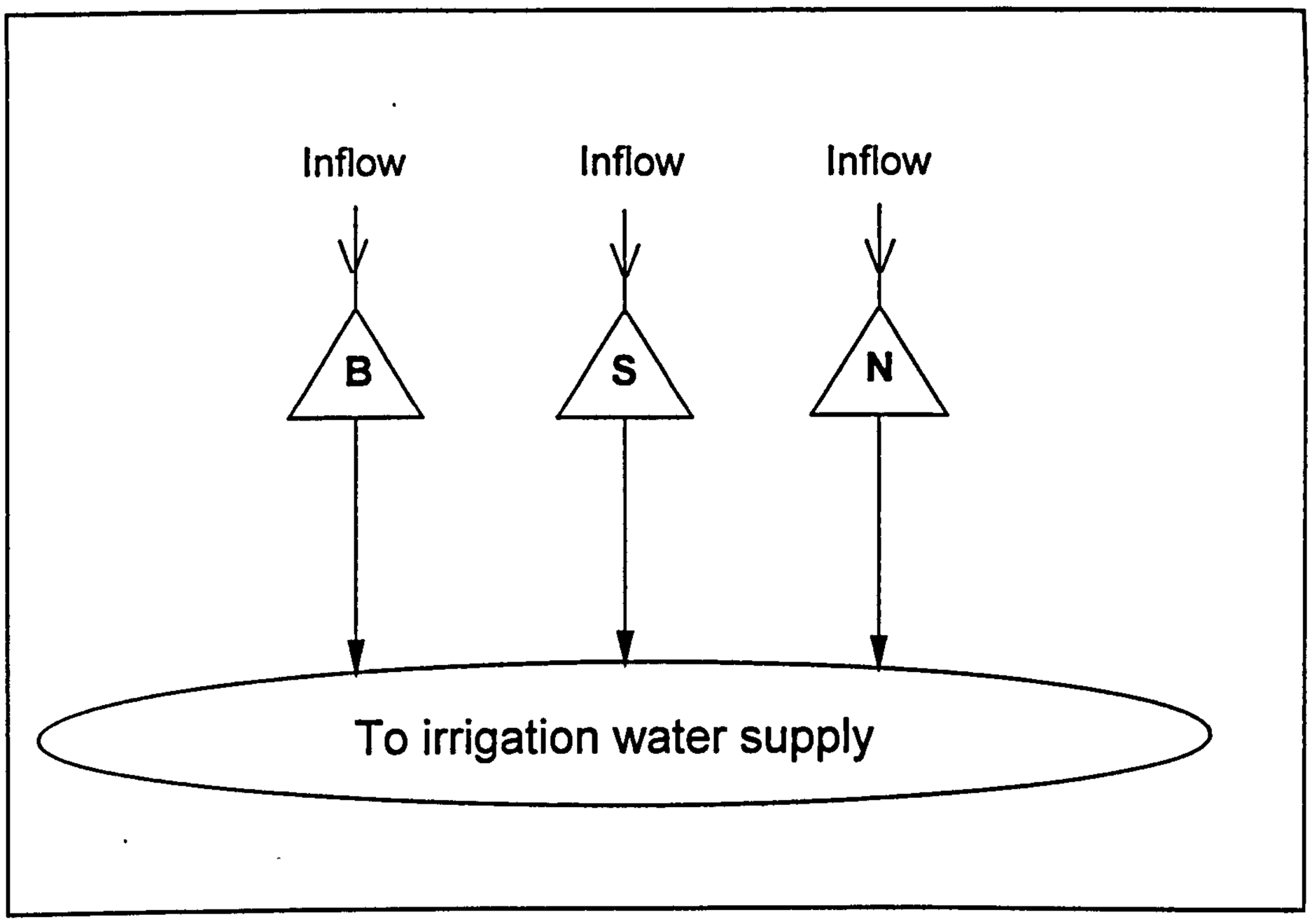

Figure 4.6: Simplified schematic of the Urmia multiple reservoir system (B: Baranduz, S: Shahr, N: Nazlu).

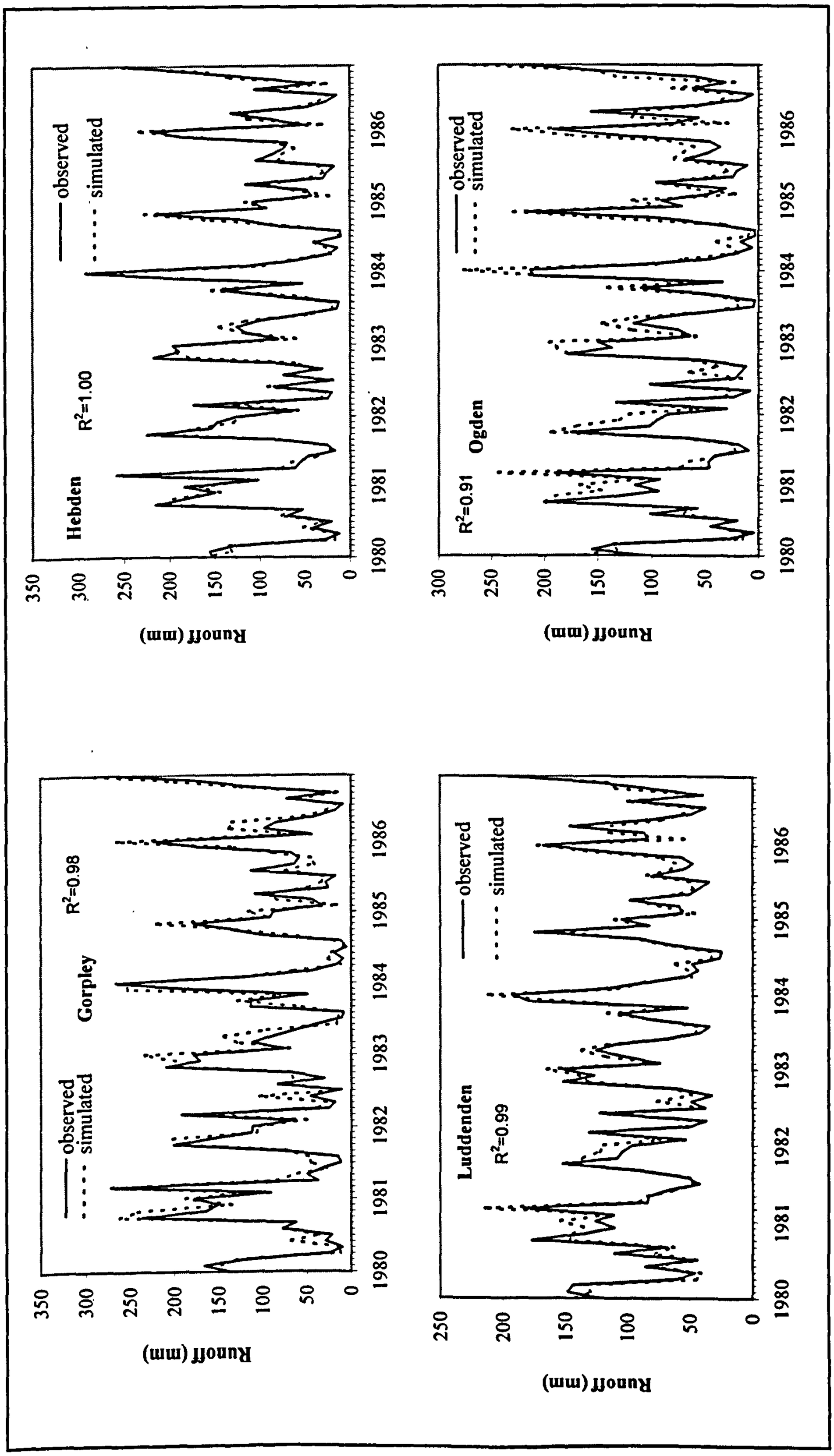

Figure 4.7: Hydrographs of Xu model monthly simulated and observed flows in Yorkshire over calibration period.

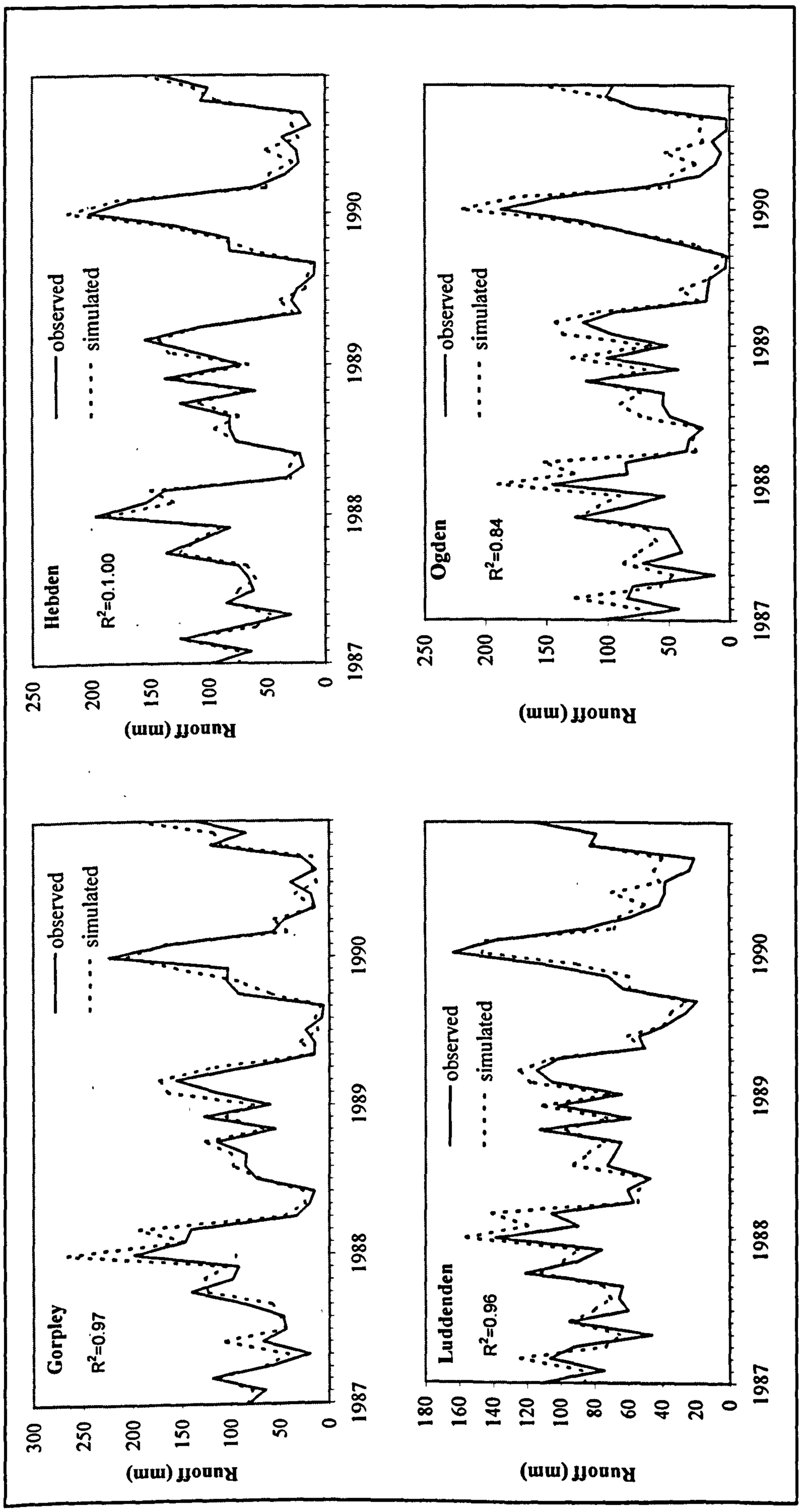

Figure 4.8: Hydrographs of Xu model monthly simulated and observed flows in Yorkshire over validation period.

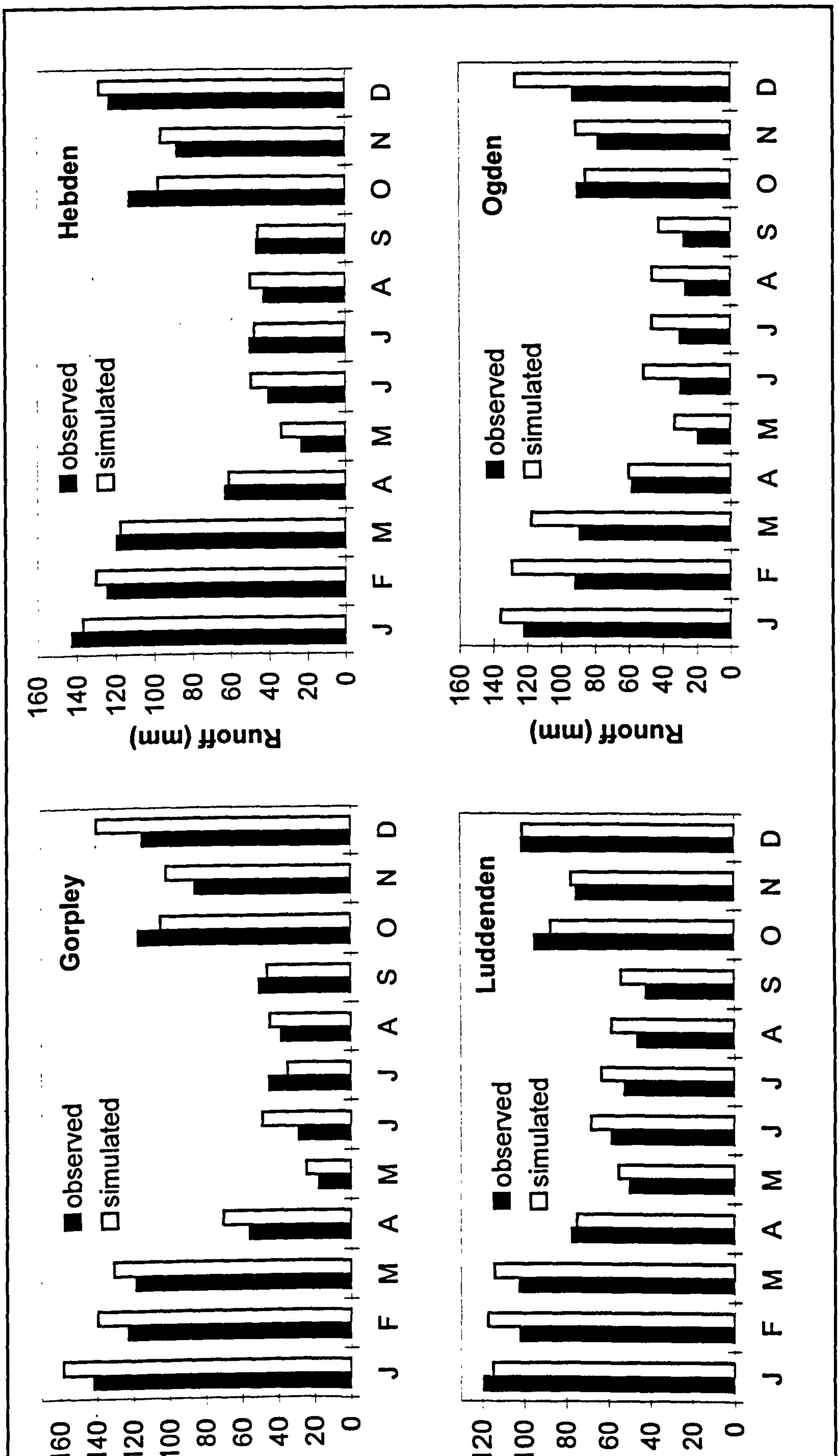

Figure 4.9: Monthly mean observed and Xu model simulated runoff for the validation period 1987-1990 (Yorkshire system)

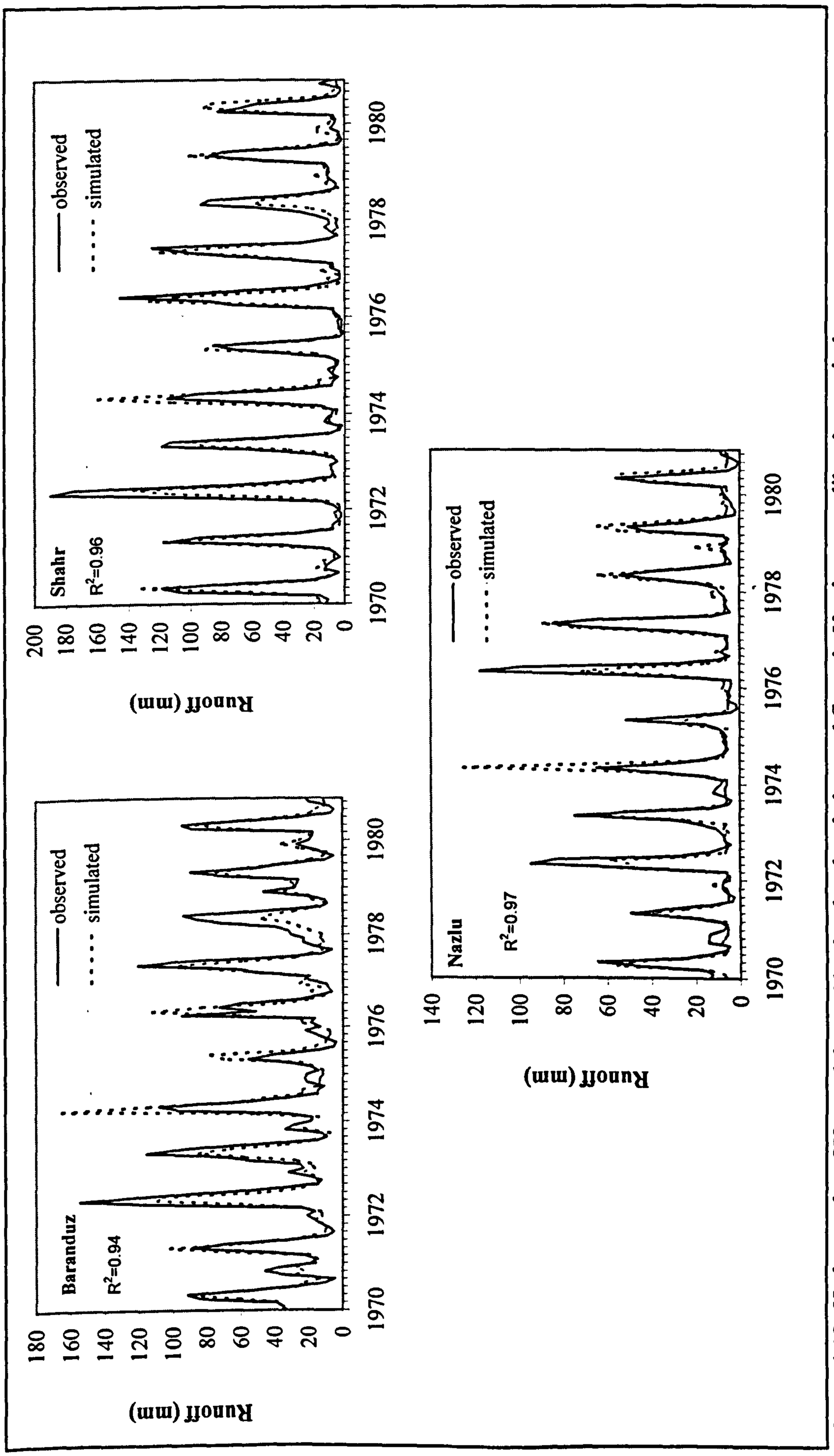

Figure 4.10: Hydrographs of Xu model monthly simulated and observed flows in Urmia over calibration period.

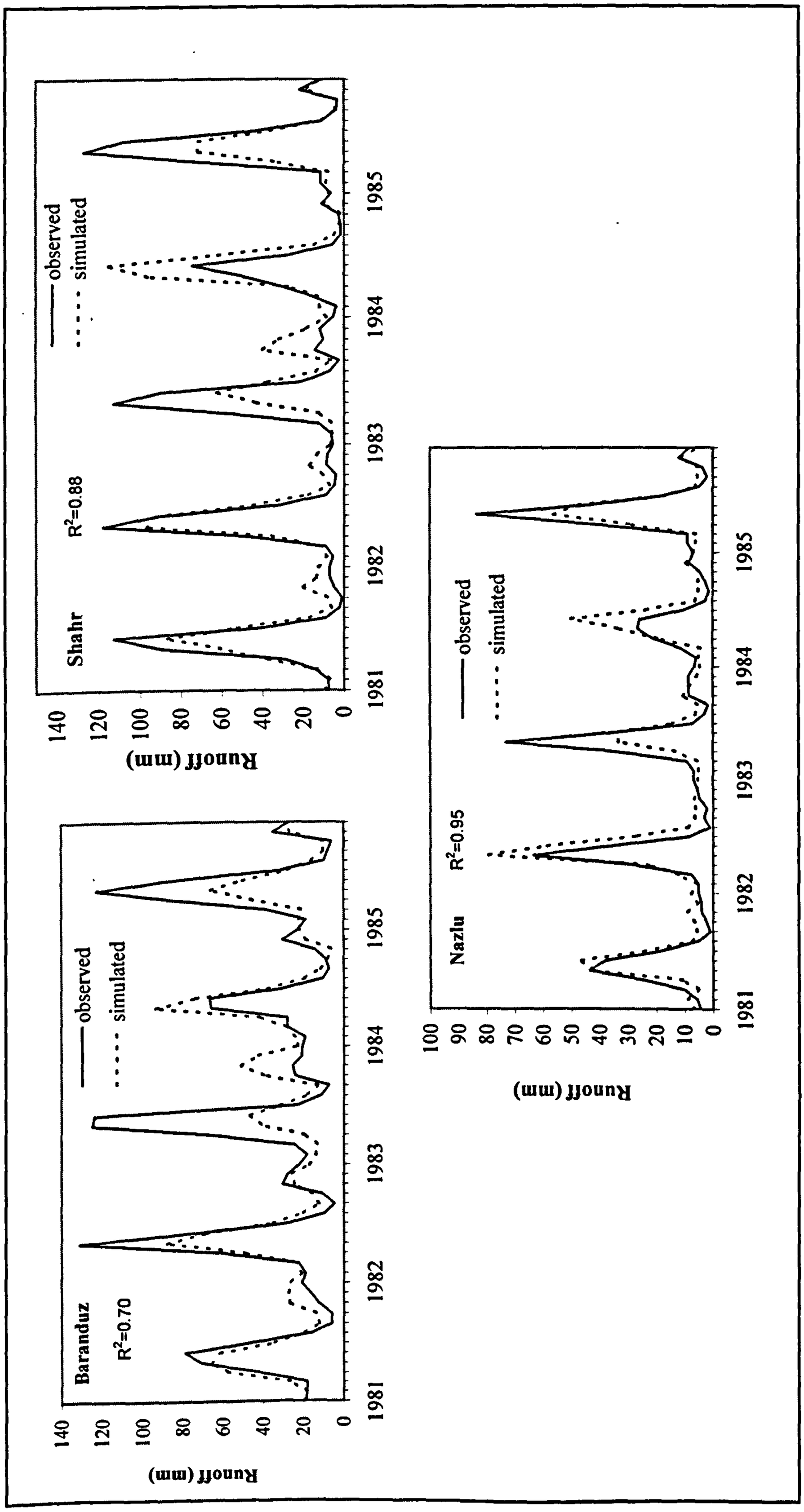

Figure 4.11: Hydrographs of Xu model monthly simulated and observed flows in Urmia over validation period.

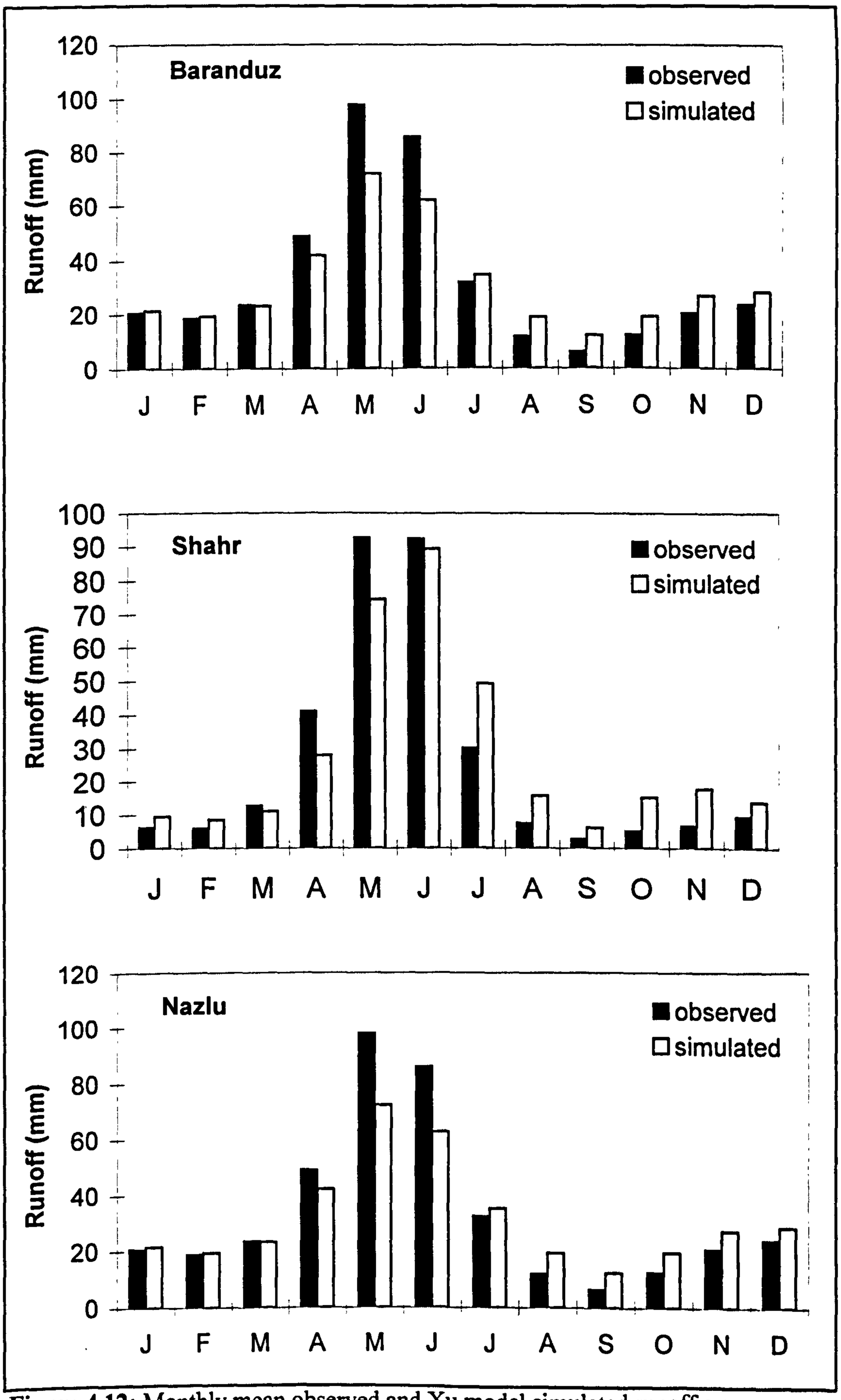

Figure 4.12: Monthly mean observed and Xu model simulated runoff over validation period 1981-1985 (Urmia system).

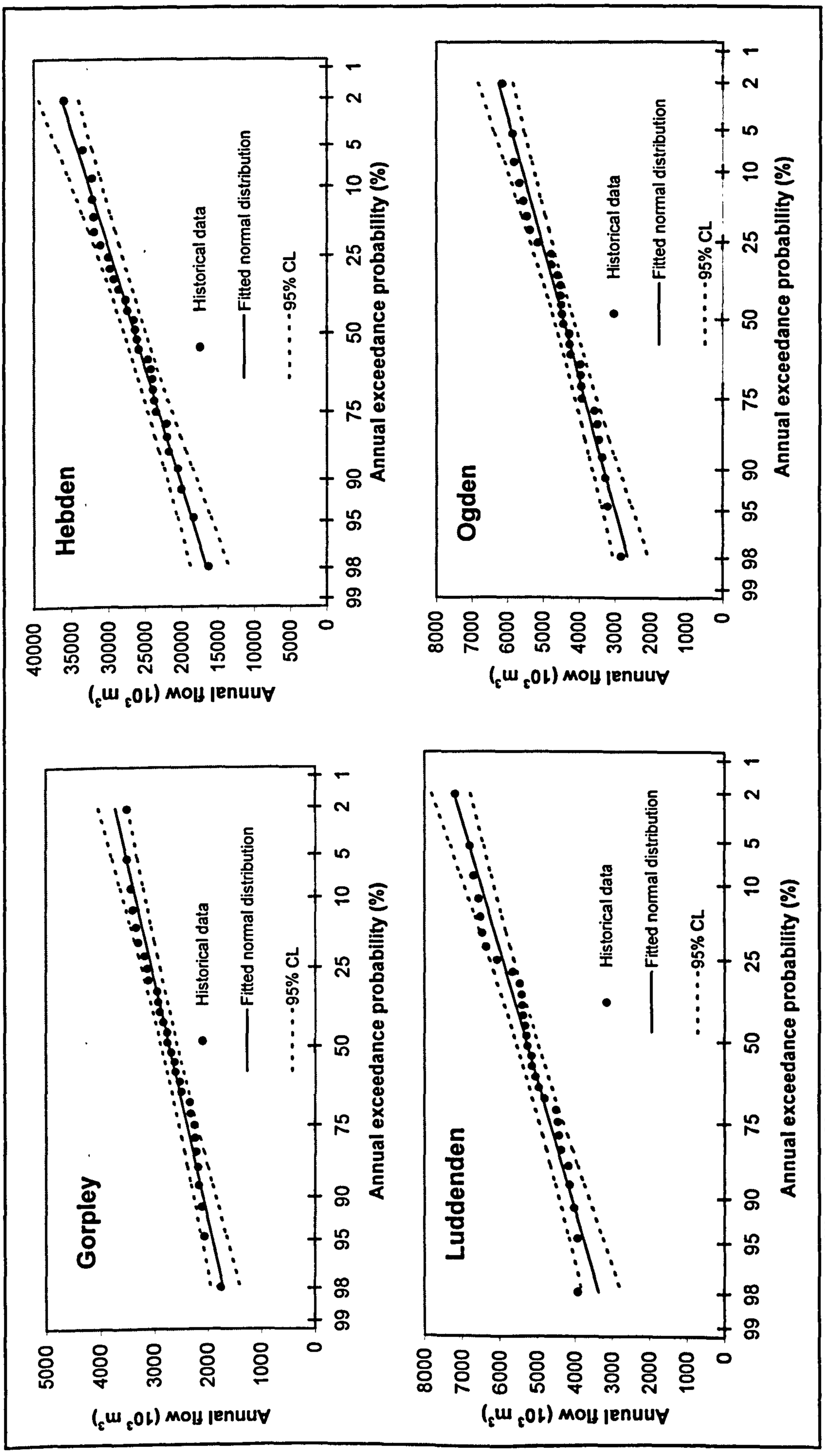

Figure 4.13: Probability plot of baseline (1961-1990) flow for the Yorkshire catchments (CL = confidence limit). Based on the Normal distribution hypothesis.

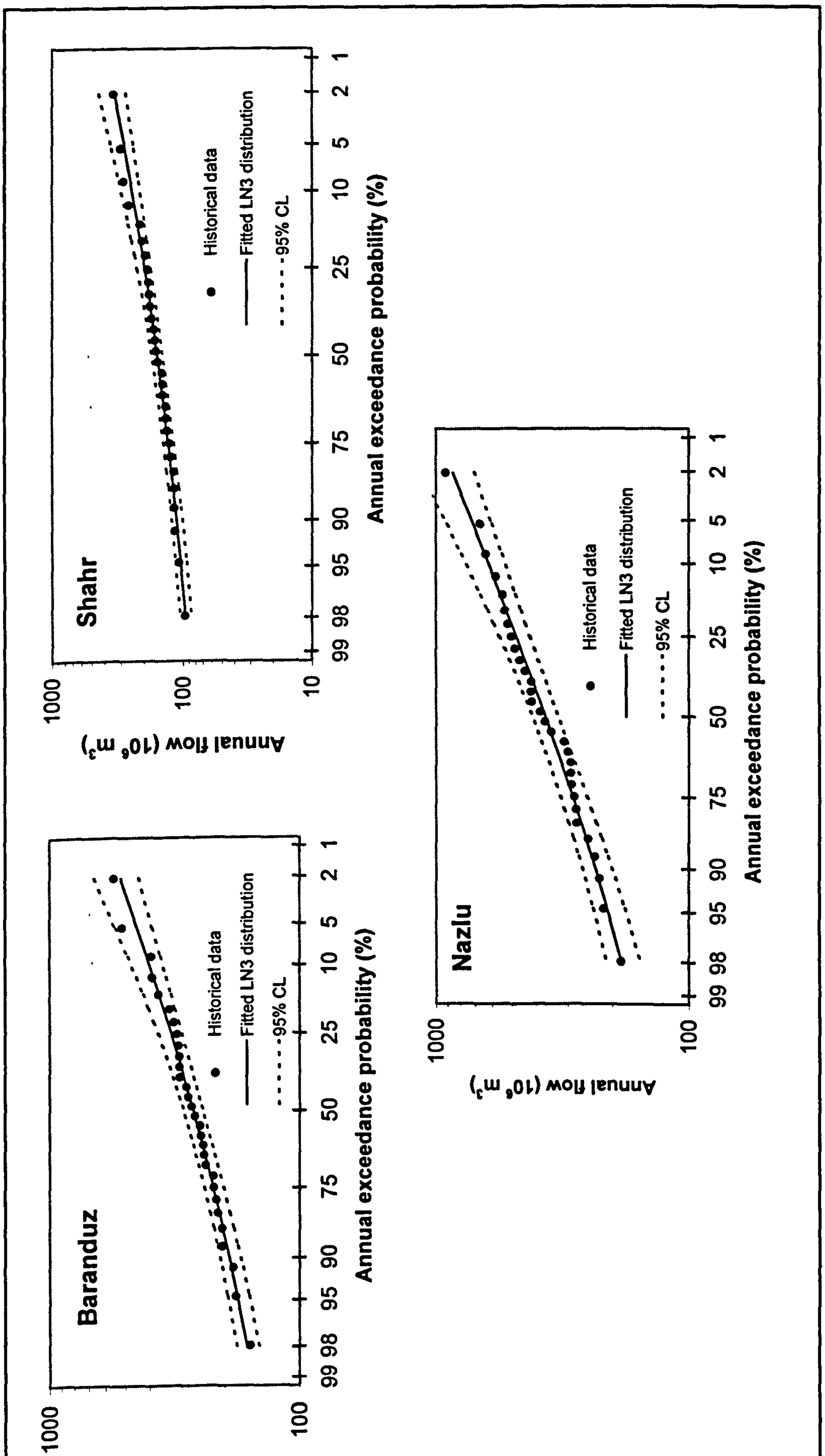

Figure 4.14: Probability plot of baseline (1961-1990) flow for the Urmia catchments (CL = confidence limit). Based on the 3-parameter log-normal distribution hypothesis.

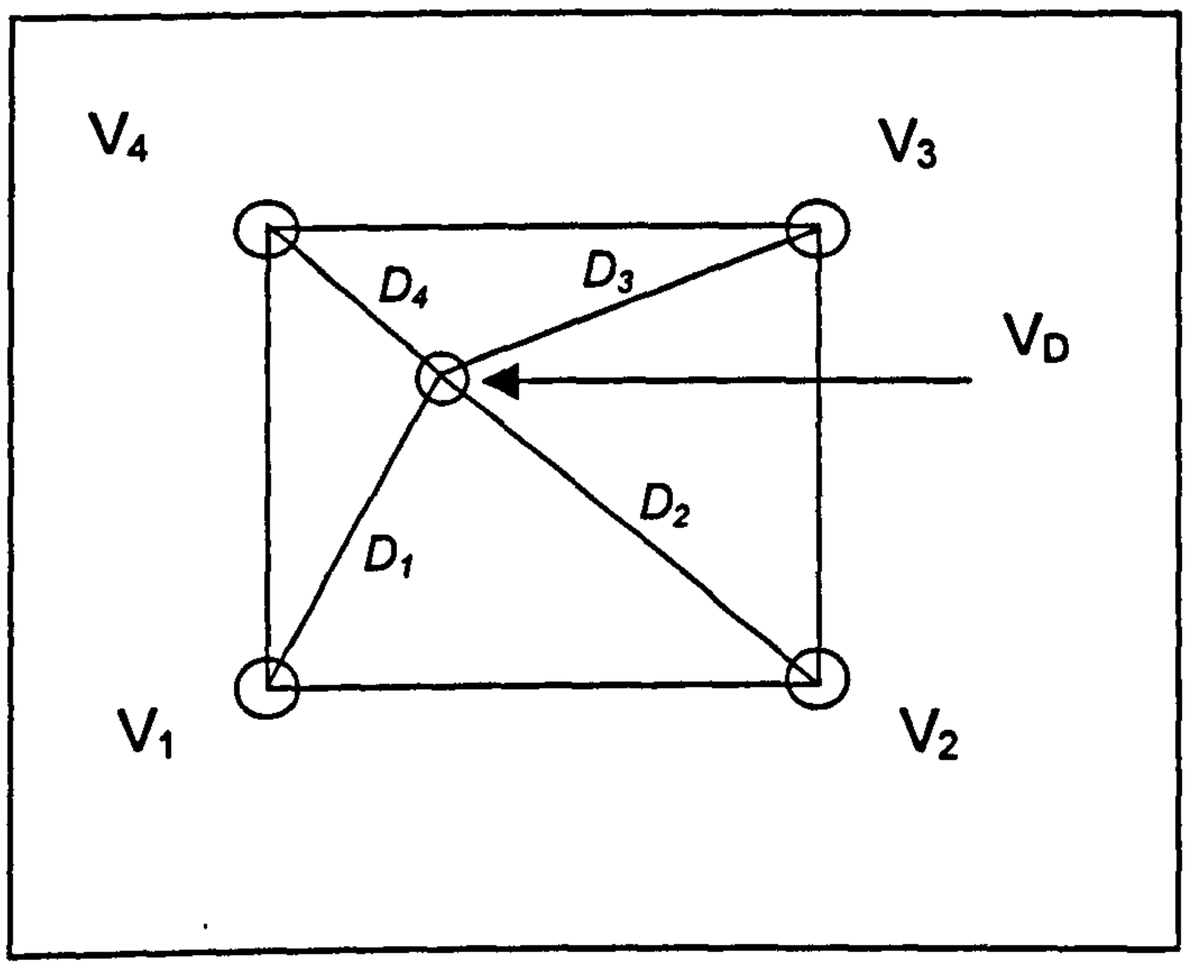

Figure 4.15: Schematic of 4 GCM grid points used for downscaling by linear interpolation.

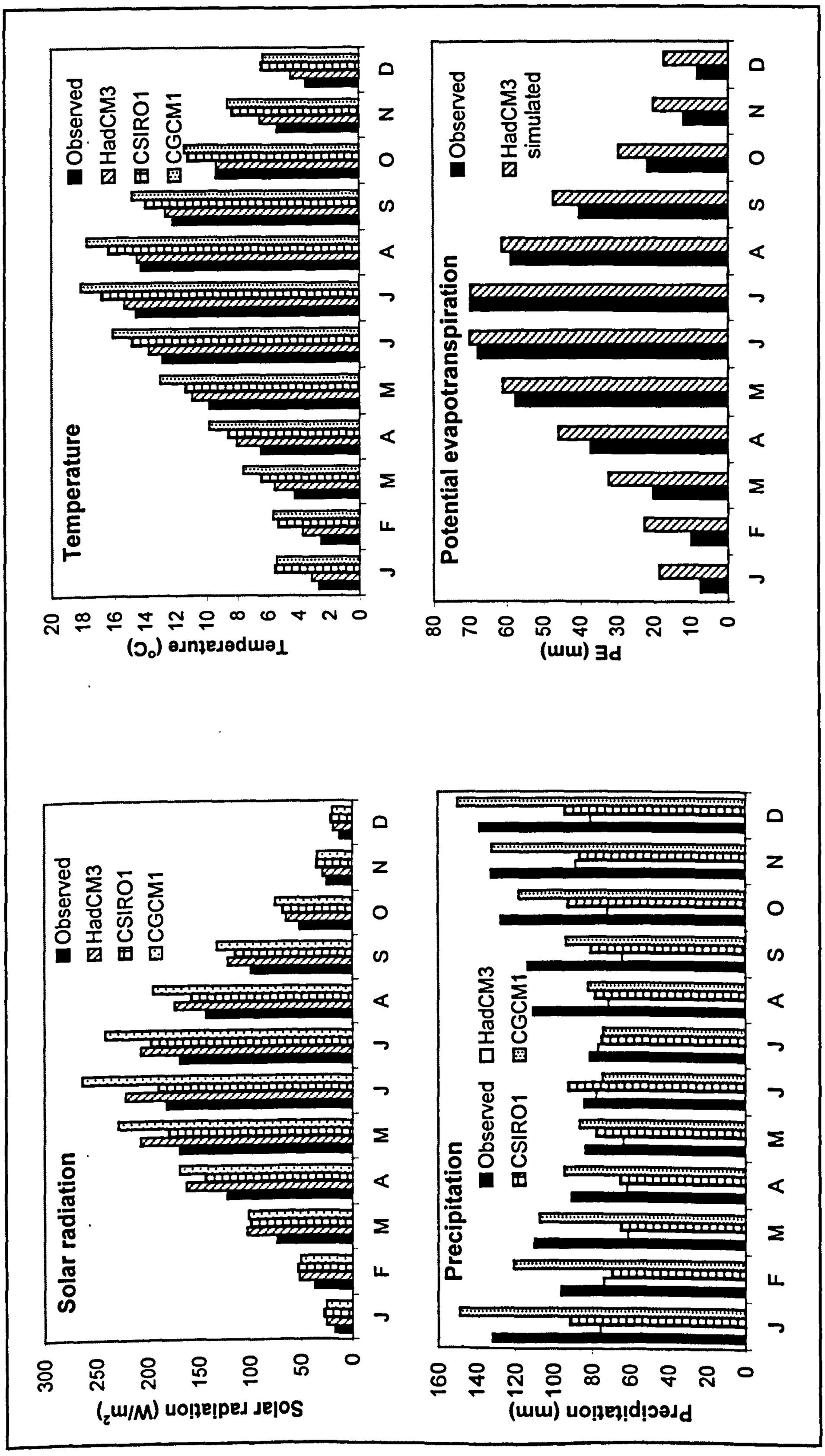

Figure 4.16: GCM performance over baseline (1961-1990) period (average at all Yorkshire sites).

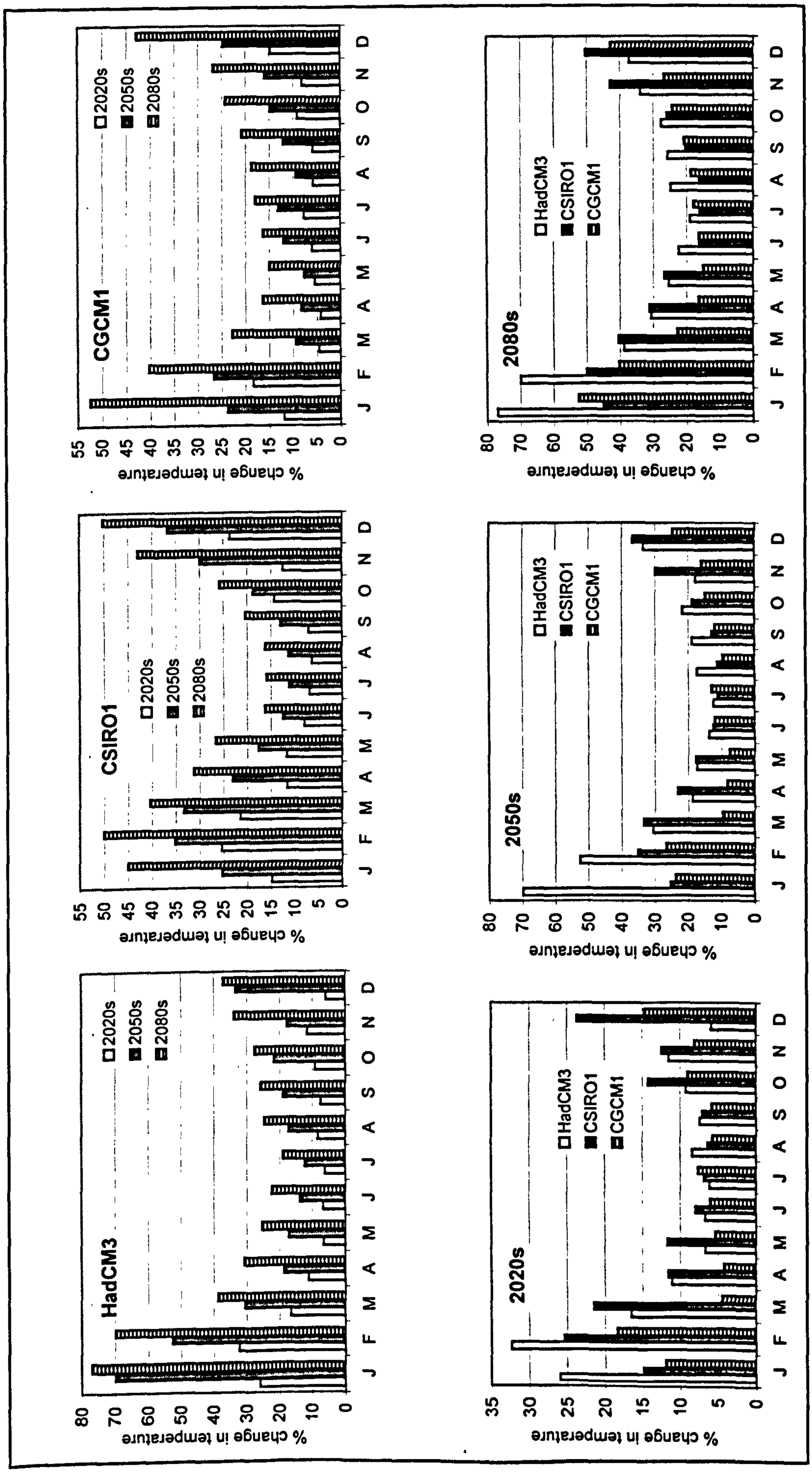

Figure 4.17: Change in future temperature at Yorkshire sites.

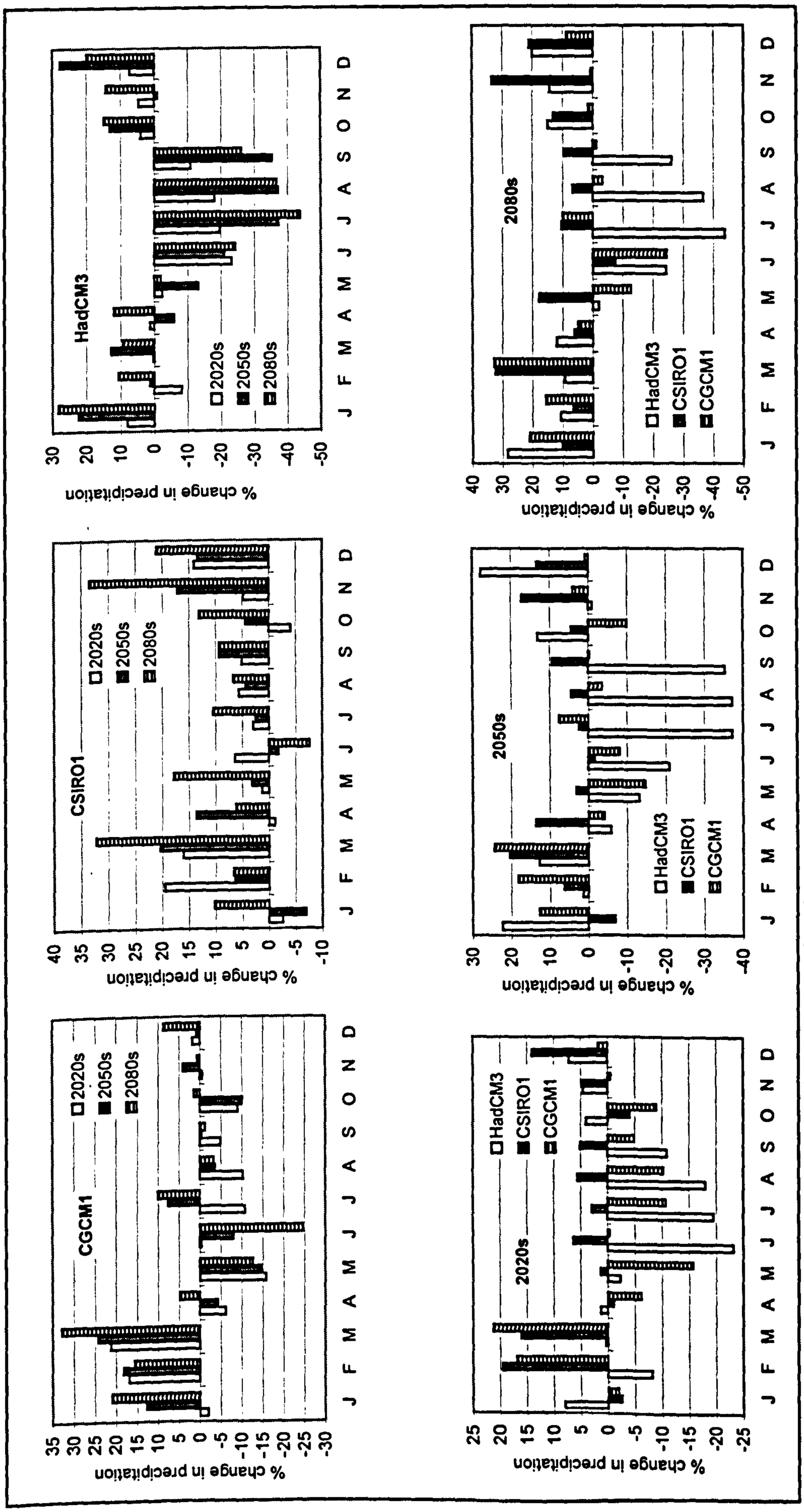

Figure 4.18: Change in future precipitation at Yorkshire sites.

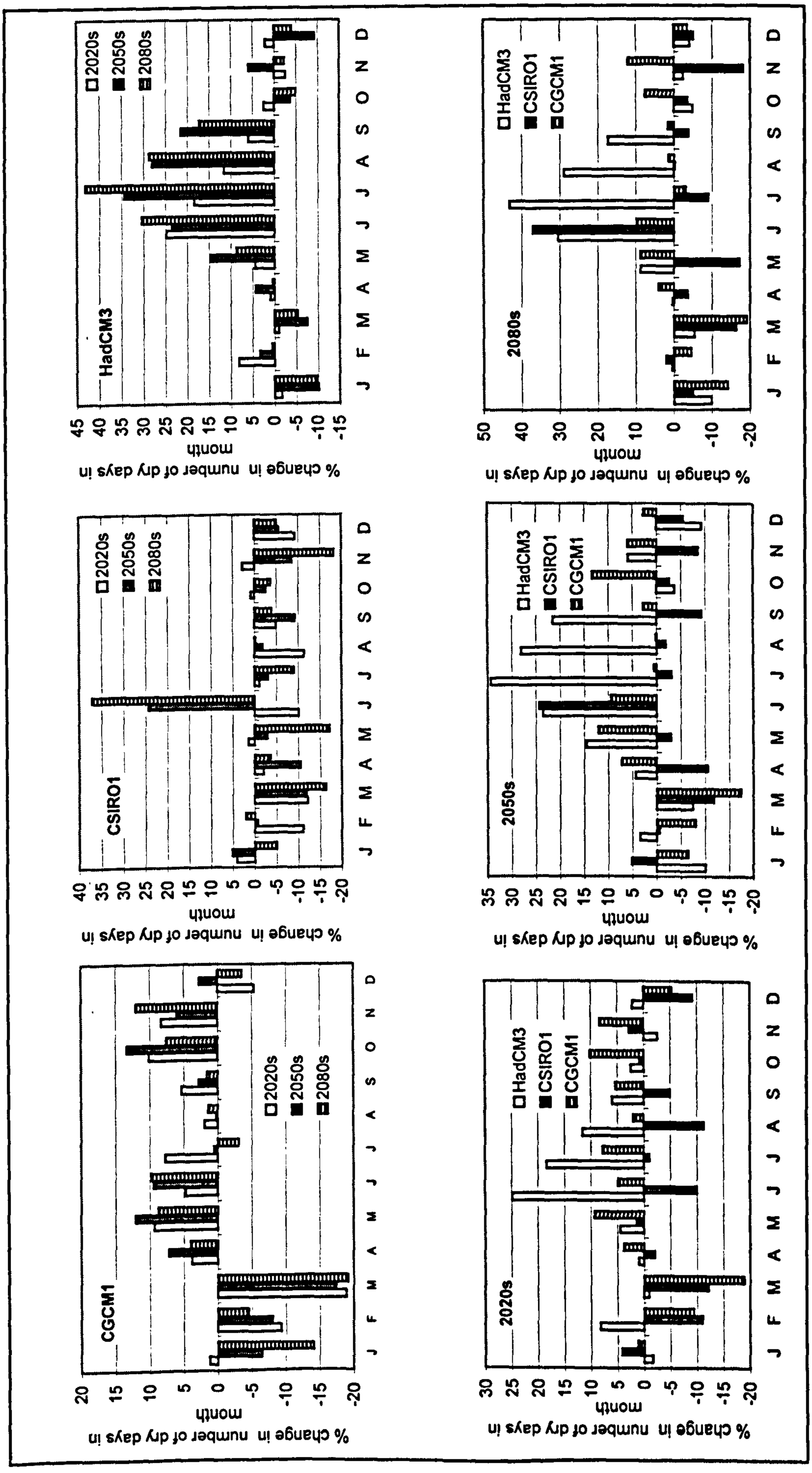

Figure 4.19: Change in number of dry days in month at Yorkshire sites.

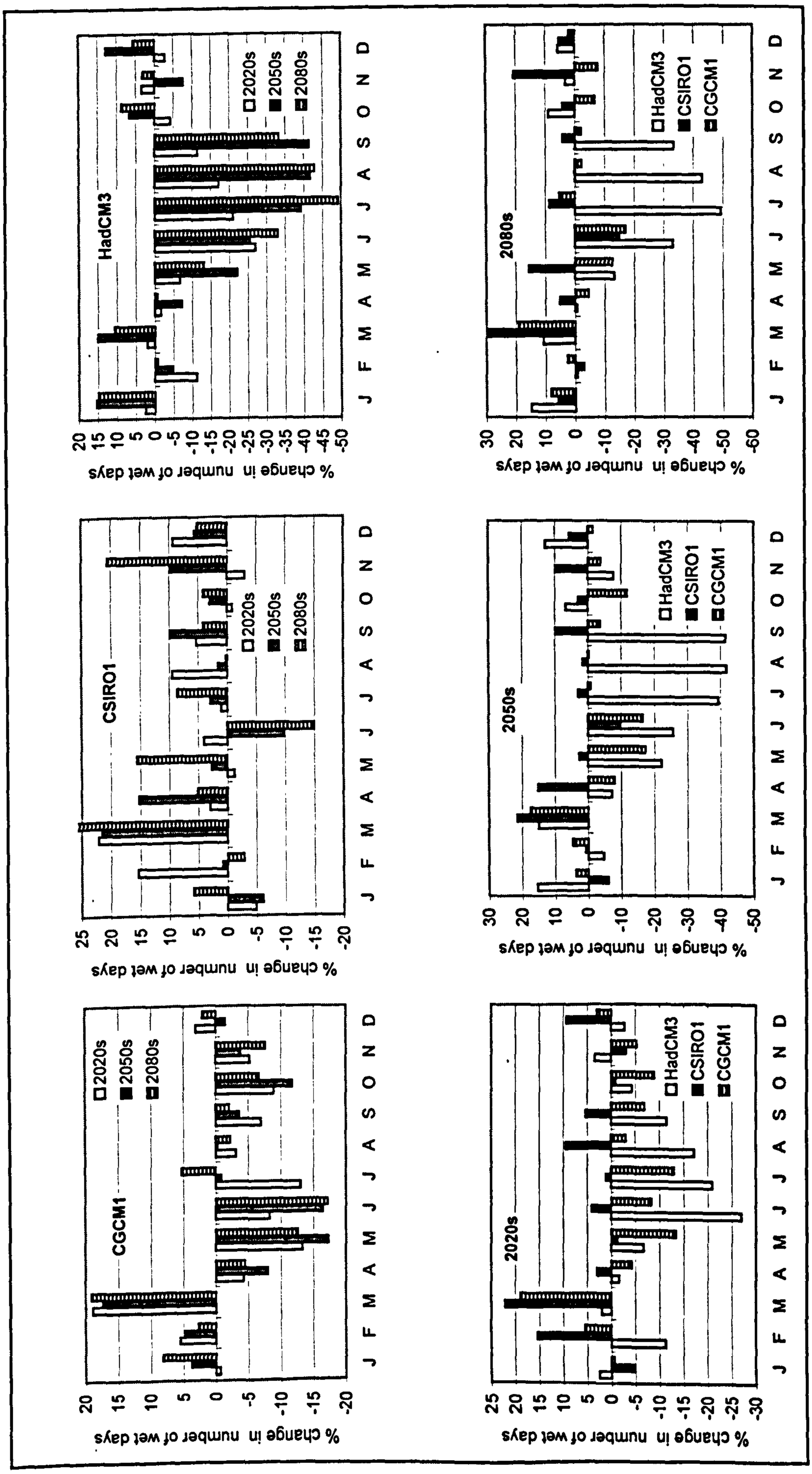

Figure 4.20: Change in number of wet days in month at Yorkshire sites.

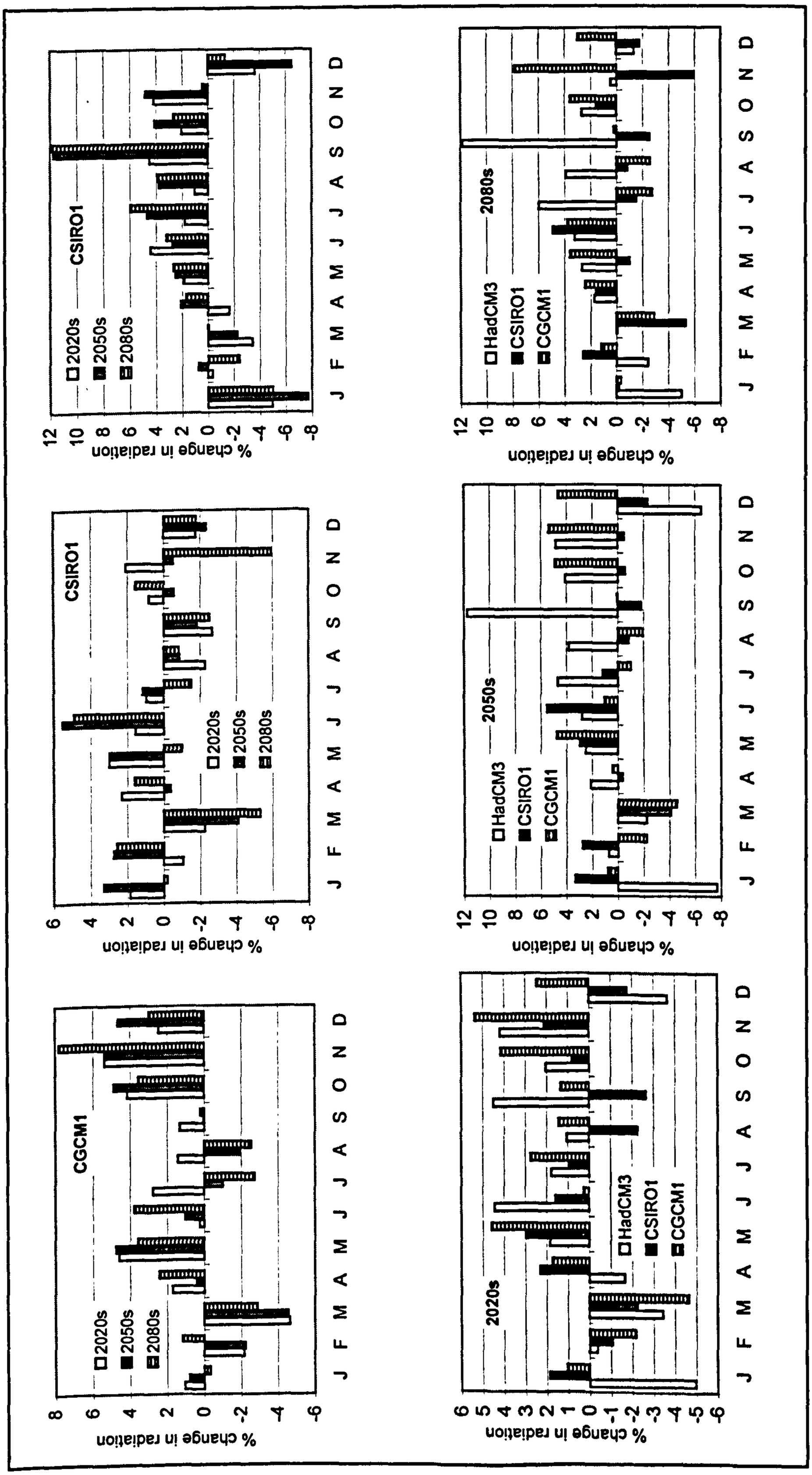

Figure 4.21: Change in future net solar radiation at Yorkshire sites.

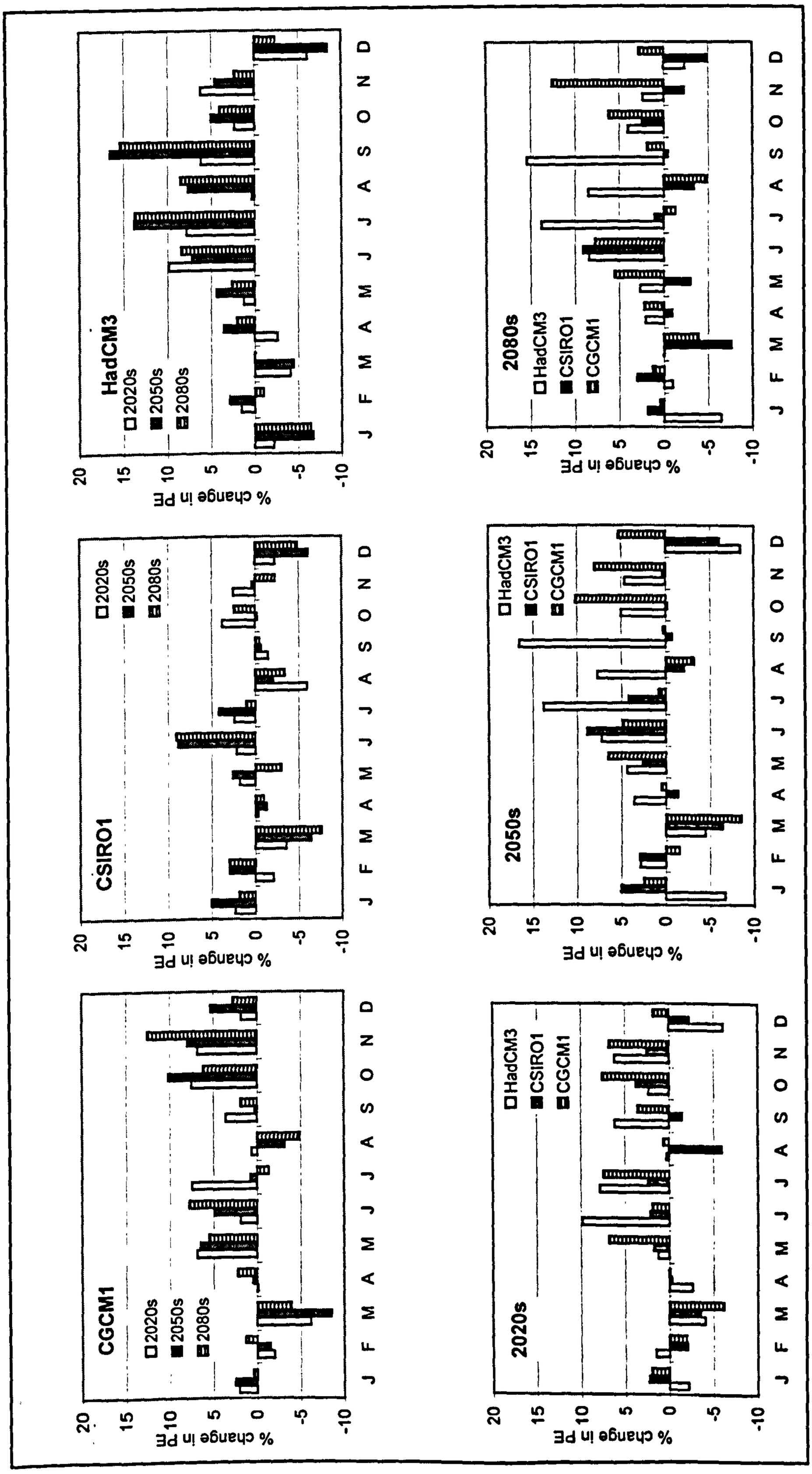

Figure 4.22: Change in potential evapotranspiration at Yorkshire sites.

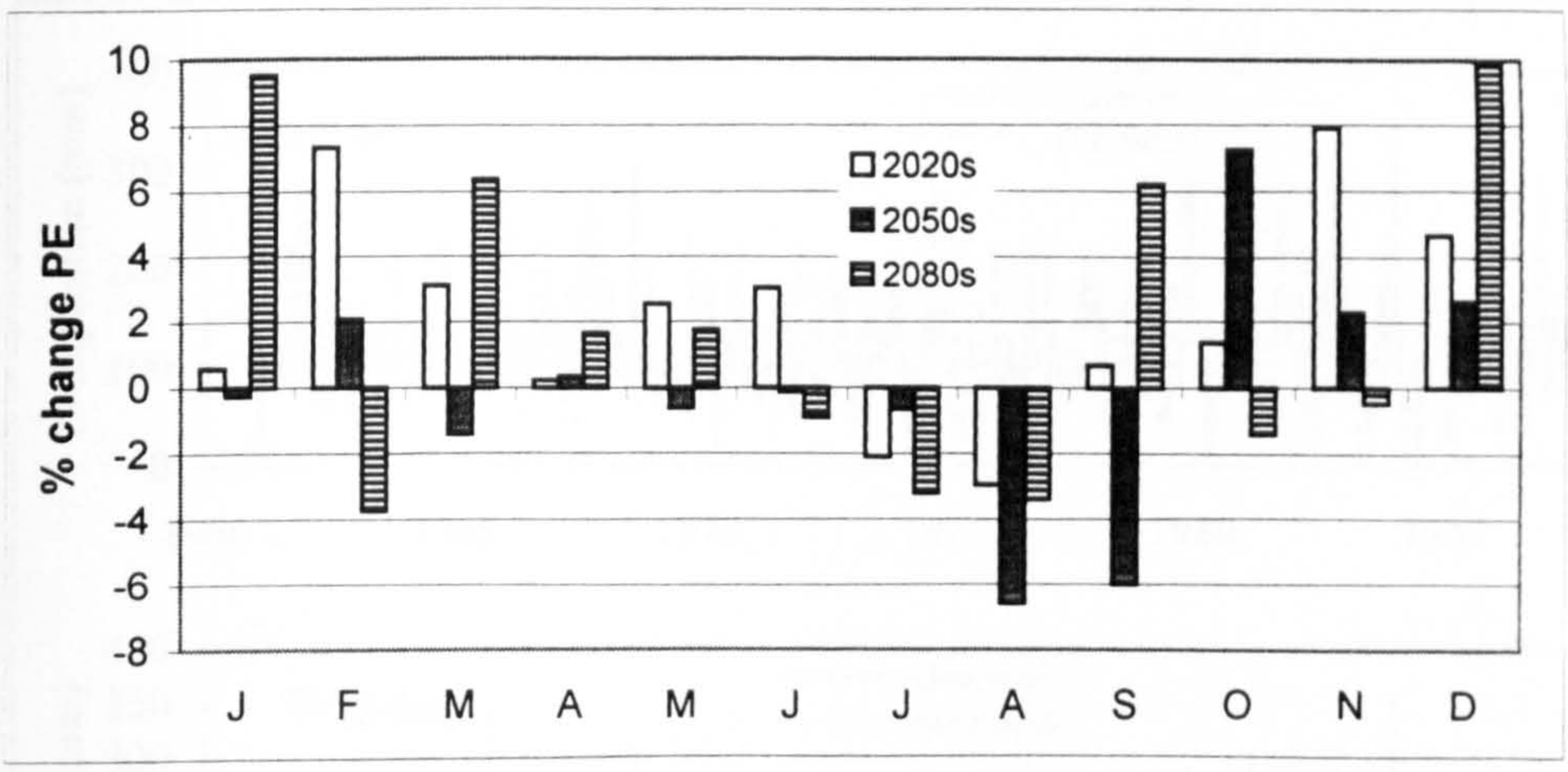

Figure 4.23: HadCM3 simulated change in potential evapotranspiration at Yorkshire sites.

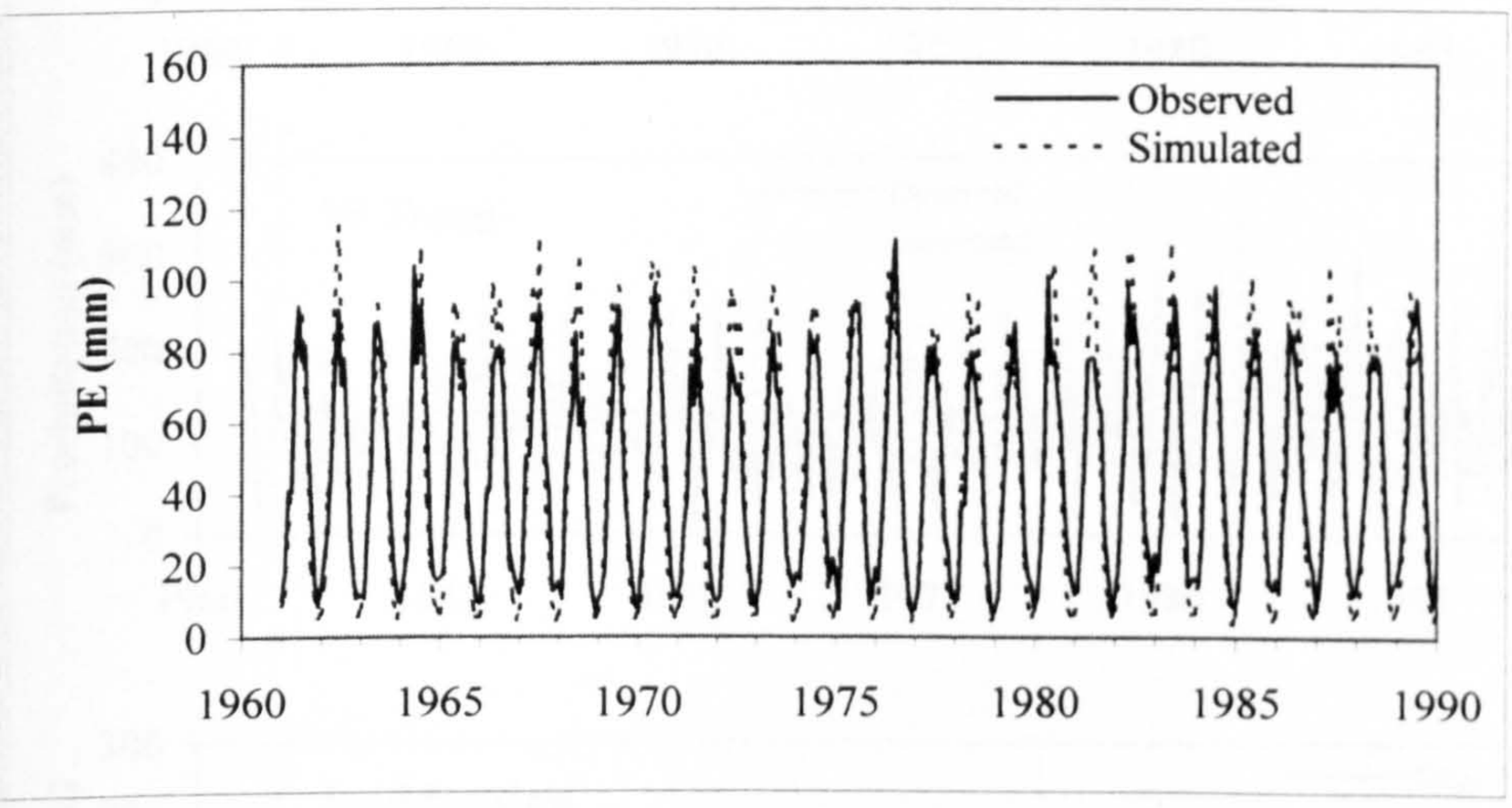

Figure 4.24: LARS-WG simulated and observed time-series of PE for Gorple in Yorkshire (1961-1990).

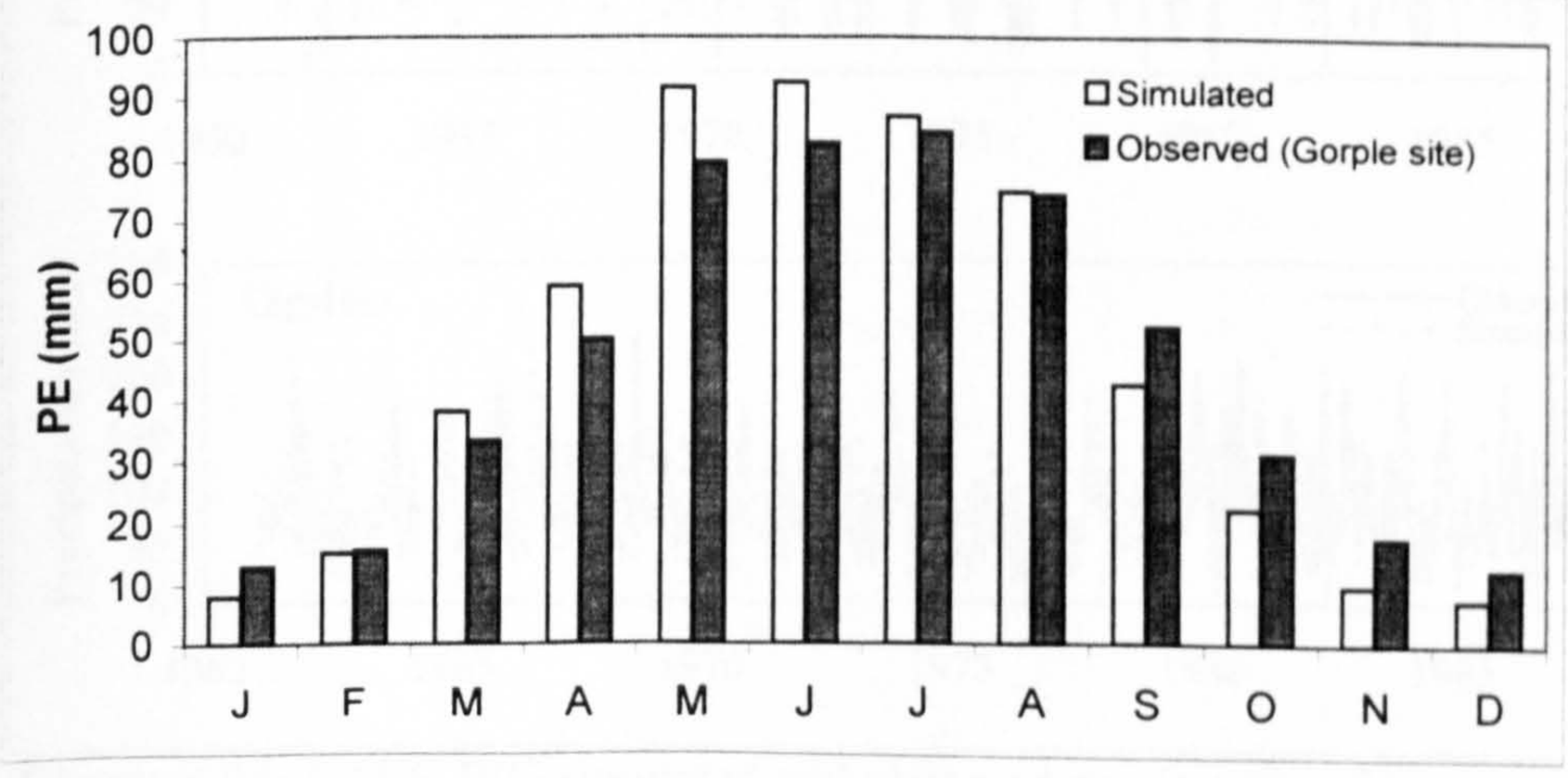

Figure 4.25: LARS-WG based mean monthly PE and observed mean monthly PE over baseline period (Yorkshire catchments).

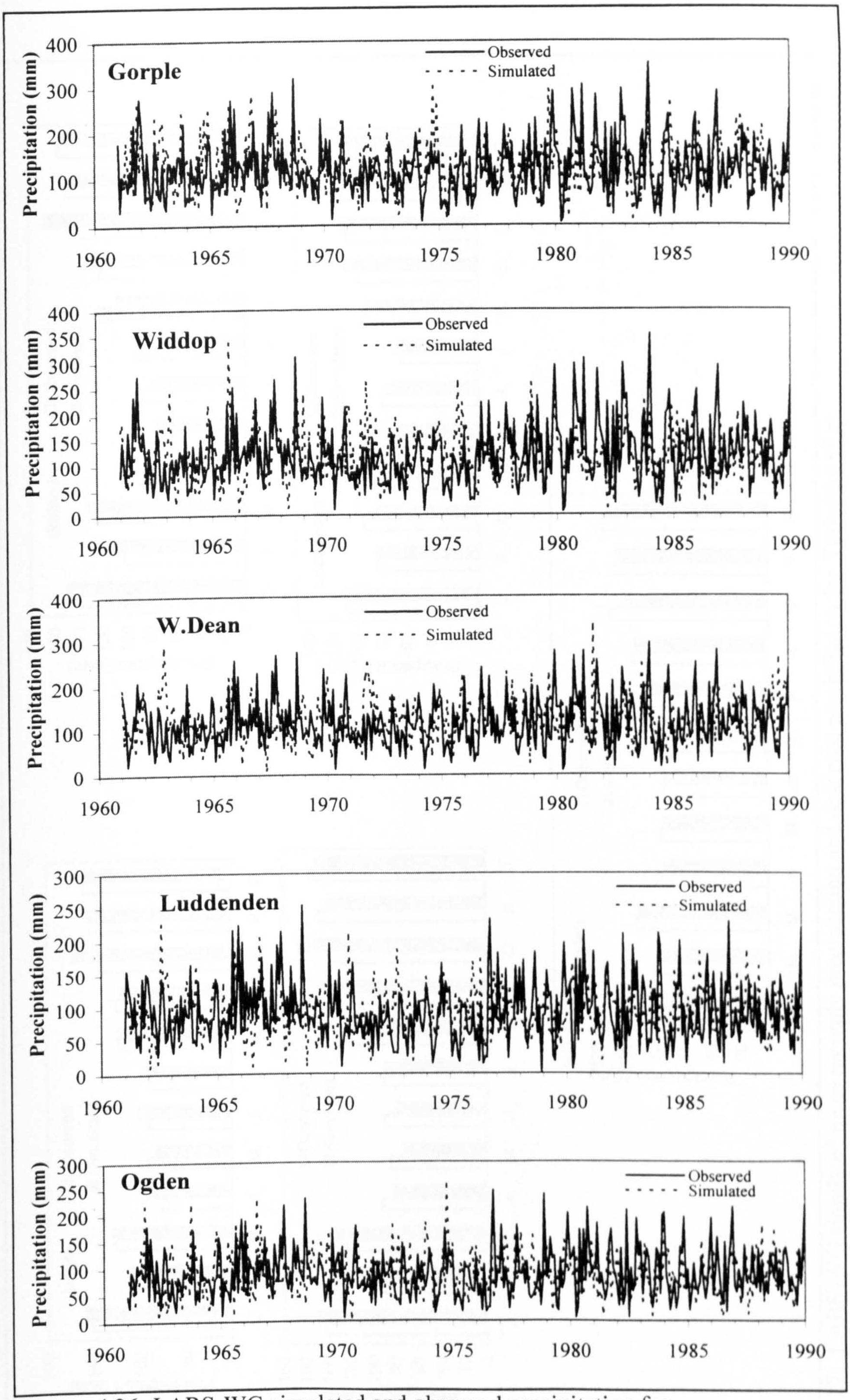

Figure 4.26: LARS-WG simulated and observed precipitation for Yorkshire sites over baseline (1961-1990) period.

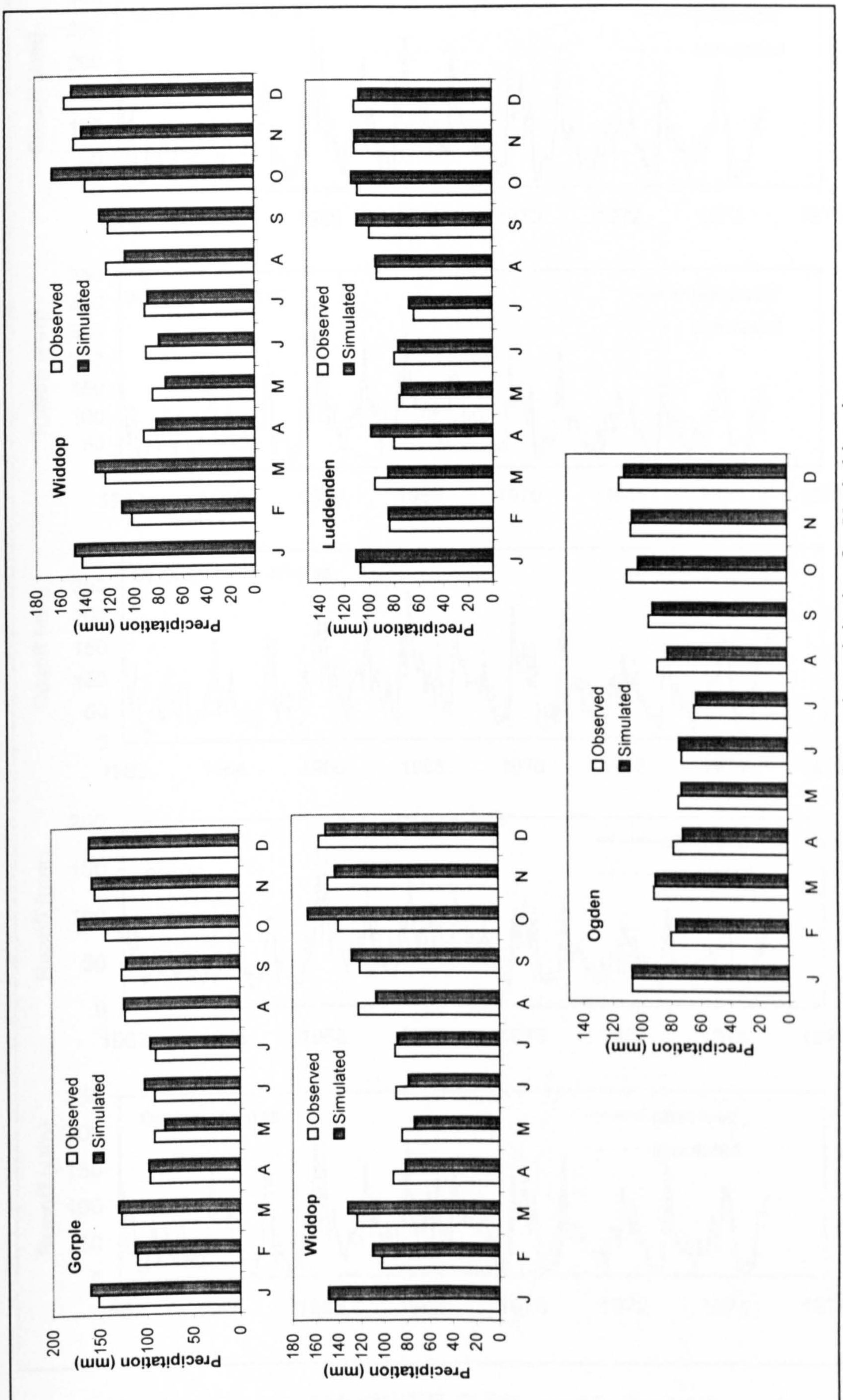

Figure 4.27: LARS-WG simulated mean monthly precipitation and observed precipitation for Yorkshire sites.

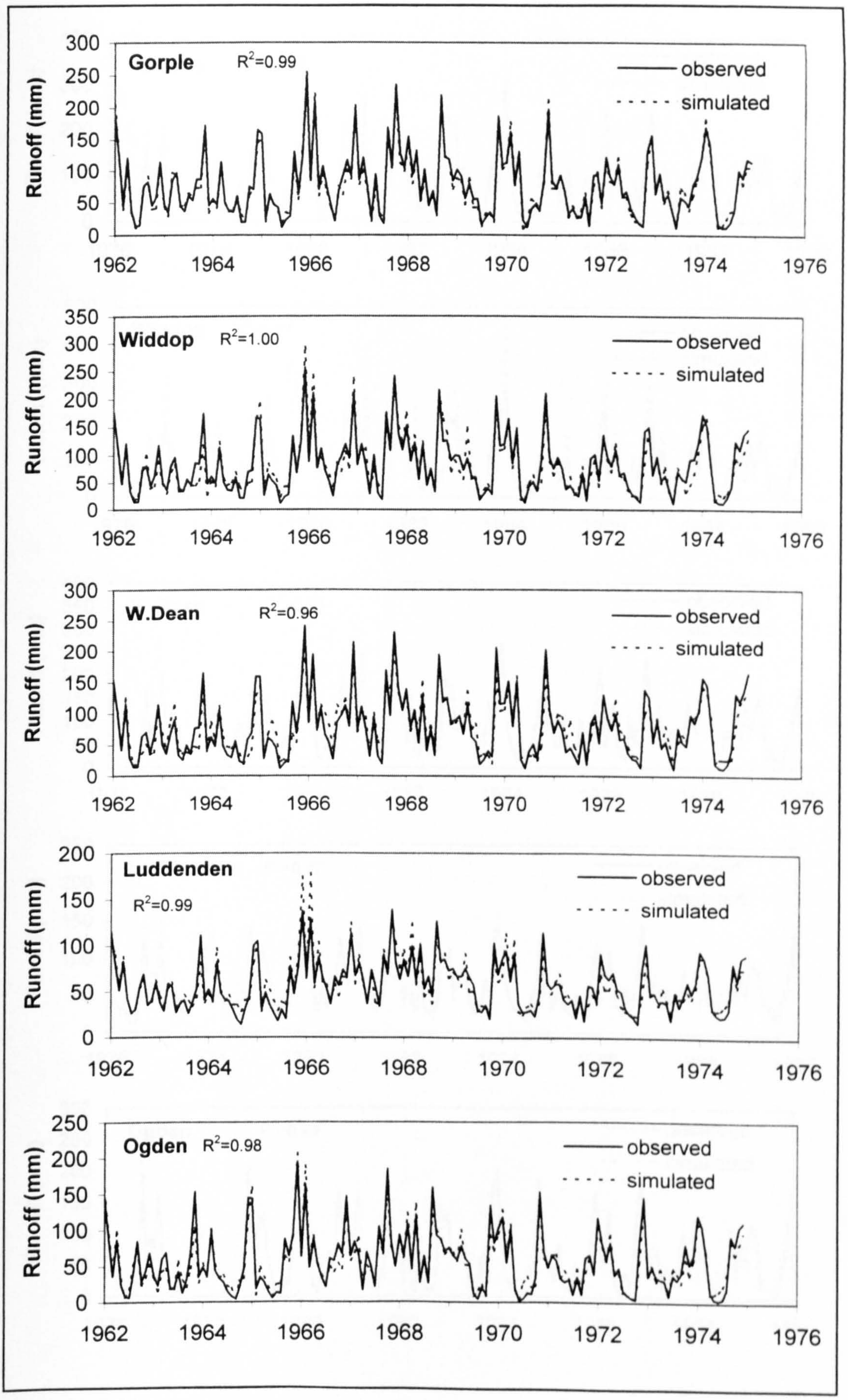

Figure 4.28: Hydrographs of MODHYDROLOG monthly simulated and observed flows in Yorkshire over calibration period.

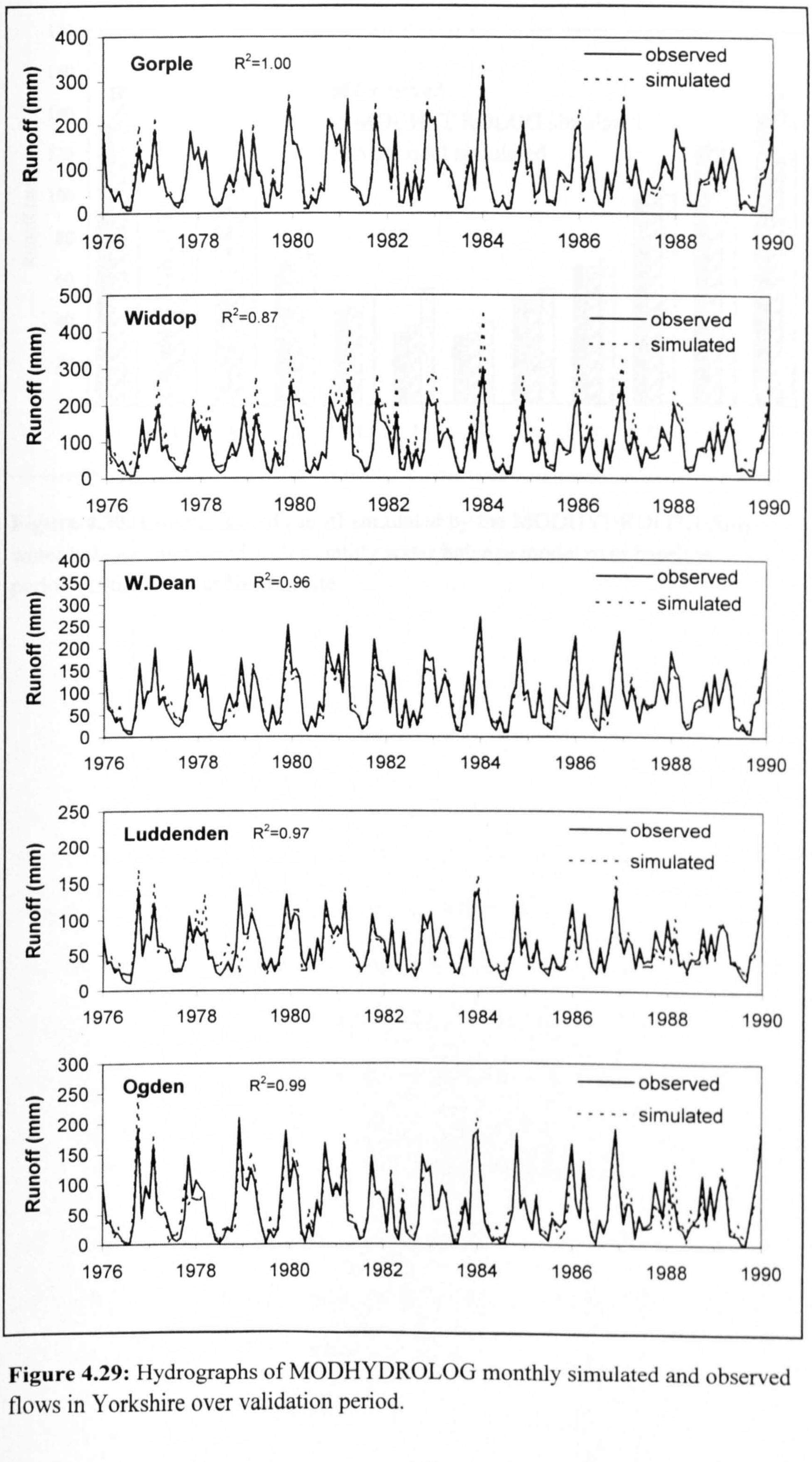

Figure 4.29: Hydrographs of MODHYDROLOG monthly simulated and observed flows in Yorkshire over validation period.

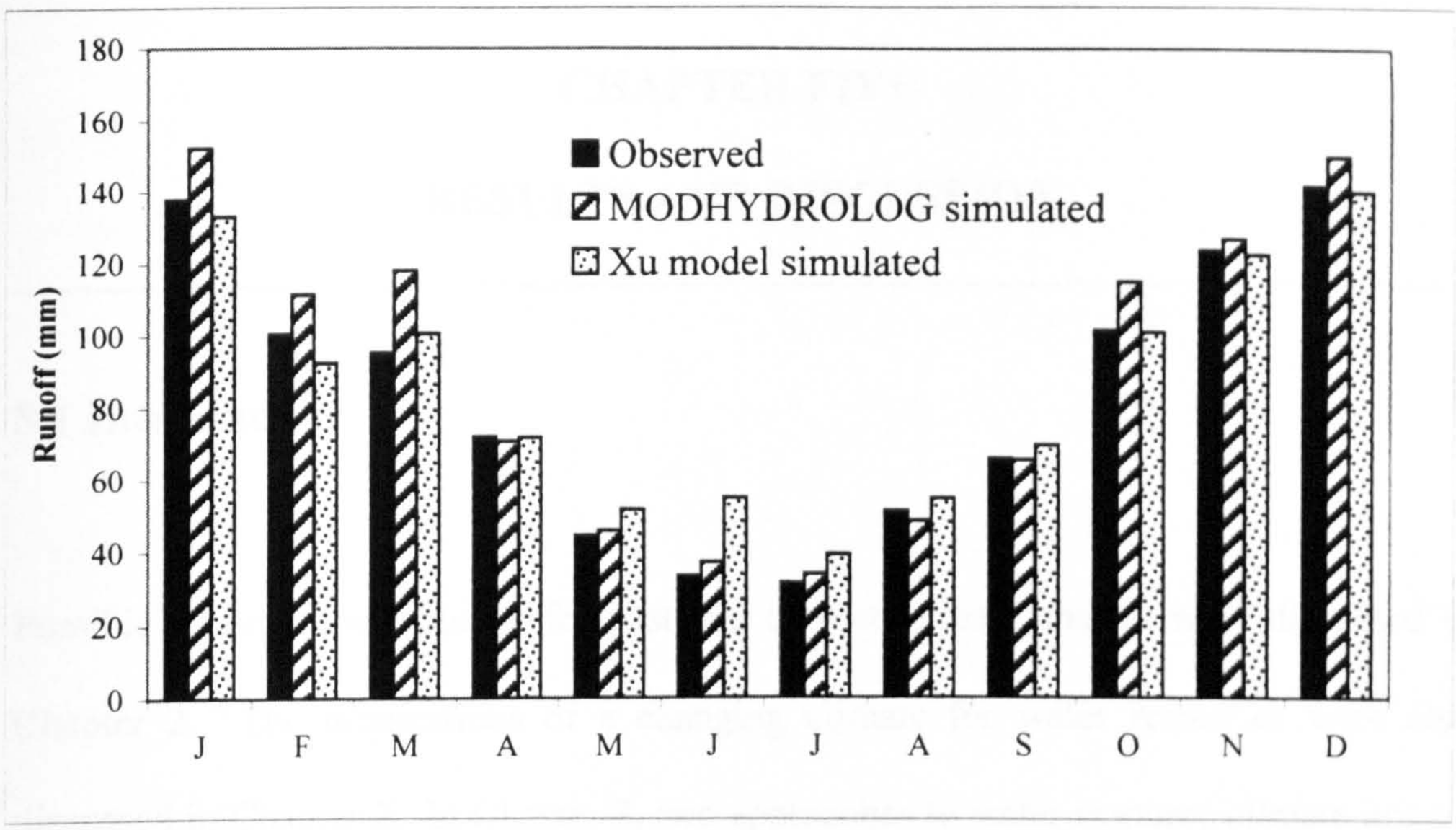

Figure 4.30: Comparison of runoff simulated by the MODHYDROLOG daily water balance model and Xu's monthly water balance model over baseline period (1962-1990) at Hebden site.

CHAPTER FIVE

RESULTS AND DISCUSSION

5.1 Introduction

Possible processes responsible for past and current climate change were discussed in Chapter 2. The implications of a changing climate for water resources were also discussed in Chapter 2. In Chapter 3, two approaches to water resource climate impact assessment were described. These methods are the 'traditional' single record approach and a Monte Carlo simulation approach. The traditional approach is based on single data records whilst the Monte Carlo approach utilises a large sample of data records. By employing numerous, e.g. 1000, equally likely, data records, the Monte Carlo approach allows the statistical distribution of climate change impacts to be characterised.

Chapter 4 contained details of the application of the two methodologies to two water resource systems; one located in England (a temperate climate) and the other in Iran (a semi-arid climate). The investigation was conducted in three phases; preliminary, intermediate and final detailed studies. Information on the adopted models, climate scenarios, and reservoir system parameters considered in each of the sub-studies was also discussed in Chapter 4.

The present chapter presents and discusses results of the study. A similar format of presentation to Chapter 4 has been adopted. Thus the results are presented separately for the preliminary, intermediate and the final detailed investigation.

Section 5.2 contains the results of the preliminary study that are based on the traditional approach. The first part deals with the effects of reservoir surface-fluxes on reservoir storage-yield relationships and is restricted to baseline conditions. The second and third parts report respectively on the sensitivity of runoff and reservoir storage-yield to climatic change.

Intermediate study results are presented in section 5.3. The bulk of the present chapter is occupied by the discussion of results from the final detailed investigation in section 5.4. In this investigation, the Yorkshire system is re-analysed using some of the latest available GCM climate scenarios (e.g. HadCM3). The effects of both the traditional approach and the Monte Carlo approach are considered. In common with the preliminary and intermediate studies, the effects of climate change on runoff and reservoir storage-yield are investigated. Additionally, impacts on (i) low flows, (ii) groundwater recharge, and (iii) reservoir control curves are briefly discussed. In section 5.5, possible adaptation strategies designed to cope with the potential climate change impacts are summarised.

5.2 Preliminary Study Results

5.2.1 Introduction

The storage-yield-reliability curve provides the most complete information about a reservoir system. During planning, it is used to determine the storage required for given yield and reliability. For an existing system with known storage capacity, the curve can be used to determine the yield. Furthermore when, as is usual, the axes are scaled by the mean annual runoff, the curve provides a means for 'regionalising' the storage-yield

function and hence for estimating storage or yield at ungauged sites. As a consequence, the results herein will be presented within the framework of the storage-yield curves. Other issues such as resilience and vulnerability are not explicitly considered in the study although, inferences will be made about how these two performance metrics are likely to be affected.

5.2.2 Effect of Surface Fluxes on Baseline Storage-Yield Relationships

The first stage of the study investigated the effects of surface fluxes, i.e. net evaporation on reservoirs from Yorkshire and Urmia. It did not involve climate impacts assessment and was therefore restricted to baseline conditions. This investigation was necessary to establish whether the effects of reservoir surface fluxes on storage-yield are significant enough to warrant inclusion in subsequent climate impact assessments. Figure 5.1 shows the impact of incorporating reservoir surface water fluxes due to net evaporation on the storage-yield function for the baseline records. For the Yorkshire system (see Figures 5.1 (a) and (b)), the inclusion of reservoir surface net evaporation flux resulted in reductions in the required storage capacity for a given yield. These reductions averaged about 7% for the 70% of mean annual runoff (MAF) yield but lower (2%) for the 30% yield. This is to say that if the capacity were fixed, then more water could be supplied from the fixed storage if net evaporation was considered in the analysis than if it was not. This behaviour can be attributed to the fact that, for the Yorkshire catchments, precipitation generally exceeds the open water evaporation (see Tables 4.3 and 4.4) and so the effect of including the net evaporation flux is an additional inflow into the reservoir.

On the other hand, for the Urmia catchments where open water evaporation exceeds precipitation (see Tables 4.7 and 4.8), the inclusion of net evaporation flux means that there is a net outflow flux from any reservoir surface. Such a net outflow constitutes an additional demand on top of the design yield, thus requiring increased storage to meet such a design yield (Figures 5.1(c) and (d)). Failure to provide such an additional storage will mean that either a reduction in the yield from the reservoir has to occur or a reduction in the reliability of supply has to be contended with if supply at the design yield were to occur. Similarly, any insistence on supplying the design yield in such a situation will inevitably increase the size of the shortfall during failure (i.e. vulnerability) and compromise the ability of the system to recover following failure (i.e. resilience). The fact that both the reductions in required storage (Yorkshire) and increases in required storage (Urmia) magnify with increasing yield is due to the increasing exposed surface area of the reservoirs with yield; hence the loss/gain of water through the surface will magnify as the yield changes. The changes in storage also increase as the system reliability increases for the same reason.

Table 5.1 contains the impact on the yield for a fixed capacity of 30% of mean annual runoff and 100% reliability for the baseline records. The incorporation of net evaporation flux for the Yorkshire system increases the yield from 68.91 Mld (million litres per day) to 71.86 Mld for the baseline record, an increase of 4%, whereas for the Urmia system, there was a 2% reduction in yield from 1126 to 1103 Ml/d.

The above results have practical implications for reservoir water management in temperate climates such as the Yorkshire catchments where for most part surface flux is often ignored on the excuse that it is unimportant. However, as demonstrated in this study, while it is unimportant from the point of view that it may not lead to water

shortage, it does have some practical significance because facilities planned ignoring such fluxes currently represent an over-design, and the buffer of such over-design would go some way in meeting any shortfall in future storage requirements. As a result such reservoirs may be able to accommodate the likely requirement placed by future climate change for example. Results from this investigation therefore indicate that it is important to include reservoir surface-fluxes in climate change water resource impacts assessments. Their inclusion is warranted whether evaporation exceeds precipitation (as in arid and semi-arid climes) or vice-versa (as in humid and temperate climes).

5.2.3 Climate Change Impacts on Runoff

The percentage change in runoff (from the baseline) for the aggregated systems of all the climate change scenarios (see Table 5.2 for scenario description) considered are presented in Figure 5.2 for the Yorkshire catchments. The absolute changes from the baseline are provided in Table 5.3. The changes in Urmia are also given in Table 5.3. For the Yorkshire catchments, most of the scenarios are predicting increased flow in winter months and reduced flows during some of the summer months. This trend broadly agrees with that presented in Arnell et al. (1997) for the region of Yorkshire where these catchments are located, although the inflow perturbations in their study were obtained using a more sophisticated monthly water balance rainfall-runoff modelling approach.

For example, Arnell et al. (1997) presented climate change impacts on runoff averaged over 11 catchments located in northern England. They found the biggest changes in runoff occurred during November (+20%) and April (-9%) according to the H120 scenario and November (+20%) and July (-7%) according to the GG1m scenario. The

respective changes in runoff resulting from the H120 and GG1m scenarios in this study are (see Figure 5.2) +20% (November) and -10% (April), and +18% (November) and -10% (July). The broad agreement of findings from this study and those from Arnell's (1997) investigation is a particularly pertinent result. This is because it is evidence of the adequacy of the simple runoff coefficient Equation 3.21, presented in section 3.4.4.1. It may be recalled that the runoff coefficient approach does not require calibration and is much more straightforward to apply than a rainfall-runoff model. This preliminary result will be further tested by comparing results in this study with those obtained in the intermediate study. As mentioned previously, the intermediate study will adopt a more formal water balance approach in assessing catchment rainfall-runoff response to climate change.

The GS1t scenario, with its most severe reductions in summer rainfall, produced the biggest change (reduction) in the summer runoff. This further confirms observations by previous workers (e.g. Nemec and Schaake, 1982; Arnell, 1996; Chiew et al., 1996; Boorman and Sefton, 1997; DeWalle and Swistock, 2000) that changes in the rainfall have a greater impact on the runoff than changes in the PE (driven largely by temperature), particularly when the baseline rainfall is higher than the baseline evapotranspiration. For example, in Figure 5.2, the GS1t scenario predicts a 49% reduction in the mean June runoff for a mere 15% reduction in mean rainfall (see Table 4.11) and a 5% rise in PE (Table 4.12). However, if the baseline rainfall is very low (relative to the baseline evapotranspiration), then the influence of a rise in evapotranspiration will become more pronounced since the low rainfall is likely to go entirely into satisfying such a rise, leaving little or nothing for runoff. This was the case for August and September when the GS1t scenario was applied to the Urmia catchments. The predicted high increases in evapotranspiration (15% and 12%

respectively for the two months), took up nearly all the rainfall, giving predicted runoff reductions of 88% and 97% respectively. In accordance with findings from numerous other investigations (e.g. Chiew et al., 1996; Dvorak et al., 1997; Mehrotra, 1999) these results suggest that drier catchments are more susceptible to climate change.

•

Chiew et al. (1995) and Nemec and Schaake (1982) also reported similar results. For example, Chiew et al. (1995) noted more than a 100% change in runoff in an arid catchment in North Australia (annual rainfall = 450mm). Similarly, Nemec and Schaake (1982) found that a 15% reduction in precipitation and a 4% rise in PE in a humid catchment in Mississippi, USA reduced runoff by 40%. On the other hand, they noted the same scenario resulted in a 70% reduction in runoff in a drier catchment in Texas, USA.

5.2.4 Climate Change Impacts on Storage-Yield-Reliability Relationships

The impacts of climate change on the storage capacity are illustrated for the Yorkshire system in Figure 5.3 using results for the 30% and 70% yields. It is apparent from the figure that most of the scenarios are predicting lower storages for both yields when compared to the baseline, the only exceptions being the HadCM1-2050 and GS1t scenarios which are predicting larger storages for the 30% yield. Put differently, any existing reservoir of a given capacity which receives the predicted future inflows will generally be able to supply a higher yield than it presently does. However, the per cent reductions in storage are higher at the 30% yield because of its low associated storage, this being dominated by within-year requirements. As the yield increases and over-year requirements become significant, the capacity will increase and any associated difference, in relative terms, will decrease. The importance of within-year requirements

at low yields is also probably responsible for the increase in storage requirements predicted by both HadCM1-2050 and GS1t for the 30% yield. For this yield, these two scenarios are predicting increases in required storage of between 3-5% (HadCM1-2050) or 13-16% (GS1t), the top end of both ranges relating to when surface fluxes are considered. As shown in Figure 5.2, these two scenarios actually resulted in the highest reduction in summer inflows, the effect of which will be to increase the within-year imbalance between inflow and release, which is why larger storages are being required.

The results for the Urmia catchments are shown in Figure 5.4 for the GS1t scenario which, as remarked in section 4.4.1, was applied as a spatial analogue. The results in Figure 5.4, like those for the Yorkshire system with the GS1t scenario, also show an increased storage requirement at low yields and a lower storage at high yields in the future for 100% reliability. This behaviour is further amplified in Figures 5.4(a) and (b) where the complete storage-yield-reliability curves for the Urmia system are shown. In these two Figures, the 100% reliability storage-yield curves for baseline condition occurs to the right of the GS1t curve from the 60% yield onwards (an over-design of storage); before this yield, the storage curve for the GS1t occurs to the right of the baseline curve (an under-design of storage). As the reliability reduces, however, the change from storage under-design to over-design occurs at beyond the 60% yield which is why, for 98% reliability, larger storages (by 2-4%) are being predicted for the 70% yield by GS1t for the Urmia system, in contrast to the 11% reduction in storage at 100% reliability for the same yield. Unlike the Yorkshire system, the incorporation of surface fluxes did increase storage requirement for all yields with the GS1t scenario, when compared to when the fluxes were ignored (see Figure 5.1(d)).

The impact of climate change on yield is illustrated in Table 5.1 for a fixed storage capacity of 30% mean annual flow and 100% reliability. For these conditions, all except the HadCM1 (2050s) scenarios are predicting that higher yields will be possible from this capacity for the Yorkshire system, whether or not surface fluxes are considered in the analysis. The reduction in yield in Yorkshire resulting from the HadCM1 (2050s) scenario suggests that a particular climate change scenario has a significant influence on the change in reservoir yield. In this case the impact resulting from this scenario is the opposite (albeit small) of those based on all other scenarios. For the Urmia system, reductions in the yields are needed if the reliability of the system is to be maintained at 100% as expected.

5.2.5 Comparisons with other Studies

To compare results from this study with other investigations, findings from investigations applying the HadCM1 and HadCM2 scenarios will be summarised. It should however be noted that there are no published studies that have investigated the effects of HadCM1 and HadCM2 scenarios on reservoir storage-yield relationships for systems in Yorkshire or Urmia. Consequently, results from studies investigating reservoir systems in various localities are summarised.

In the UK, Holt and Jones (1996) used HadCM1 scenarios to investigate the effects on three different single reservoirs in Wales, i.e. Craig y Pistyll, Preseli and Crai reservoirs, and noted yield reductions of 24%, 30% and 1%, respectively. The largest yield reduction was experienced by the smallest reservoir, i.e. Craig y Pistyll (capacity 342 x 10^3 m^3). The reservoir experiencing a minimal yield reduction was the largest Crai reservoir (with storage capacity of 4204 x 10^3 m^3).

In another British study, Crookall and Bradford (2000) applied the UKCIP98 scenarios (derived from the HadCM2 GCM experiment) to assess the effects of climate change on reservoir yield in the Severn Trent region. They noted reductions in yield at a small reservoir (Elan reservoir) supplying the city of Birmingham of 2-8Ml/day by 2020s and 8-12 Ml/day by 2050s.

In another, North American study, Lettenmaier et al. (1999) used several climate change scenarios including the HadCM1 to assess climate change impacts on six reservoir systems located across North America. The reservoirs are located in catchments ranging from mountainous to low-lying and classified as temperate to semi-arid. One objective of the study was to investigate the effects of climate change on reservoir water supply reliability. Lettenmaier et al. (1999) noted a reduction in reservoir water supply reliability of about 7% by the 2020s and 15% by the 2050s. Although they did not assess the climate change impacts on reservoir storage-yield, the obtained reductions in reliability can be used to make inferences on the likely implications for reservoir storage-yield. The reliability reductions suggest that to maintain current levels of performance, either reservoir storage would need to be increased or a reduction in yield would be necessary.

A study investigating a reservoir in Greece (Mimikou and Baltas, 1997) - with perhaps similar climatic conditions to Urmia region - used the HadCM1 scenario. They reported that reservoir storage would have to be increased by 25%-50% in order to maintain current levels of reservoir performance. Reservoir performance in this case related to hydropower generation.

Results from various studies summarised above clearly suggest that reservoirs will come under increasing pressure in the future. This slightly contradicts the results of the present study in which increased storage is only predicted for low yields (i.e. increased stress on the system) whereas at higher yields, less storage will be required for meeting the yield. However, this is not surprising given that most of the climate change scenarios used have predicted wetter winters and drier summers. The drier summers have a pronounced effect on within-year storage requirements which dominate total storage at low yields, which is why higher storages are being predicted by the scenarios for such yields. The 25% increase in storage requirement in Urmia at the 30% mean flow demand, level agrees with results from the Greek study of Mimikou and Baltas (1997).

Regarding the impact of surface fluxes on storage-yield curves, the present results broadly agree with what previous investigators have found. For example, Gan et al. (1991) used data from Australia and found that the storage requirement increases slightly with incorporation of surface fluxes, similar to the results obtained for the Urmia catchment. Fennessey (1995) was concerned with testing the sensitivity of model time step of evaporation in yield analysis; nonetheless, he also observed that for any storage, the yield of the Massachusetts systems analysed decreased by about 6% with surface fluxes, which is slightly higher than the 2% recorded for the Urmia system. Fennessey only considered 100% reliability; hence there is no information on the sensitivity of his results to systems' reliability. There has been no previously published work looking specifically at the sensitivity of storage-yield to surface flux for the English conditions with which to compare the present results.

The Preliminary study was published in *Nordic Hydrology* Journal and a copy of the paper is included in Appendix A for completeness.

5.3 Intermediate Study Results

5.3.1 Introduction

As discussed at length in previous chapters (see section 3.6) most investigations on the water resources impacts of climate change are conducted on the basis of single records. No attempt is made at investigating the large range of both baseline and future runoff alternatives that are equally likely. In other words, the traditional single records approach does not investigate the effects of sampling uncertainties. In this study, the effects of sampling uncertainties on reservoirs in both baseline and future streamflow records in Urmia and Yorkshire are investigated. These results are then compared with results from the traditional approach to demonstrate the limitation of the latter approach.

5.3.2 Climate Change Impacts on Runoff

Figure 5.5 summarises the percentage change in runoff for the 2020s. The corresponding absolute changes (mm) are provided in Table 5.4. A definition of the scenarios is provided in Table 5.2.

As in the preliminary study, the scenarios are predicting increased runoff during winter with reductions expected over the summer. Of the three scenarios for Yorkshire, i.e. GS1m, GS1t and UKCIP98, it is the GS1t that results in more extreme changes in

runoff. For example, runoff during May is predicted to rise by about 23% and reduce by 17% in August. On the other hand, the GS1m is leading to relatively moderate changes in runoff that do not exceed 6%. The most severe reduction in summer runoff is predicted by IRHAD scenario for the Urmia catchments where a runoff reduction of 21% during July is expected in the 2020s. The changes in runoff (see Figure 5.5) are generally consistent with the percentage changes in precipitation (Table 4.11) and PE (Table 4.12). For instance, the 21% reduction in July runoff in Urmia corresponds to the largest (absolute) reduction in precipitation that also occurs in July, further confirming the dominance of precipitation on runoff.

It may be recalled that the GS1m and GS1t scenarios also formed the basis for baseline runoff perturbation in the preliminary study. Consequently, it will be appropriate to examine how the impacts of the two scenarios differ between the preliminary and intermediate studies. Annual changes in runoff arising from the GS1m and GS1t scenarios have been extracted from Figures 5.2 and 5.5 and provided in Table 5.5 which are more or less similar. A similar conclusion was also reached by Vogel et al. (1997) who compared runoff simulated by a monthly water balance model used by Tung and Haith (1995) and a relatively simple annual streamflow regression model.

Although mean monthly runoff changes noted in both the preliminary and intermediate studies are similar, there are some differences during summer, particularly for the GS1t scenario. For example, runoff in June in Yorkshire is expected to reduce by 10% based on the water balance approach and the GS1t scenario. For the same scenario, the runoff coefficient approach results in a much larger (49%) reduction in June runoff (see Figures 5.5 and 5.2). Consequently, it is therefore entirely possible that the large

differences in GS1t runoff during the June may lead to large differences in regard to reservoir storage-yield impacts.

It may be recalled from sections 4.4.2.1 and 4.5.3 that the monthly water balance was showing relatively poor performance during the summer. It could therefore be argued that summer runoff changes based on the water balance approach may not be as accurate as those based on the simple runoff coefficient approach thus leading to the discrepancies in monthly runoff changes. Indeed the possibility of a much simpler rainfall-runoff model performing better than a more complex monthly water balance model is not entirely surprising.

For example, Vogel et al. (1997) noted that yield changes resulting from climate change for the same reservoir system based on an annual streamflow regression model and a more complex monthly water balance model compared favourably. However, for one particular climate change scenario (based on a uncoupled UK Hadley Centre GCM), Vogel et al. (1997) noted a significant difference in yield changes based on the two models. The monthly water balance model was predicting unrealistically large reductions in PE by using the unrealistically large increases in relative humidity from the climate scenario. Vogel et al. (1997) noted that their own annual model was not sensitive to spurious changes in relative humidity thus more confidence could be placed in their own results.

Similarly, it is possible that the large June precipitation reduction of 15% (see Table 4.11) for GS1t scenario is translated into runoff change more adequately by the simple runoff coefficient equation than the monthly water balance model.

It is interesting to compare the runoff changes in Urmia (see Figure 5.5) with those obtained by Mimikou et al. (2000) for a catchment in central Greece. Mimikou et al. (2000) used one scenario from the HadCM2 transient experiment and another from the UKHI equilibrium experiment - both representative of the 2050s - within a Monte Carlo framework to assess the mean of climate change impacts. They found that the future mean monthly runoff resulting from the HadCM2 scenario was less than baseline runoff in all months of the year. The pattern of change was for largest runoff reductions during the summer (especially in June and August when up to a 46% reduction was expected), with the expected winter reductions being only 13%. The mean reduction in annual runoff was 18.4%. Both the magnitudes and seasonal patterns of runoff reduction obtained by Mimikou et al. (2000) are broadly similar to those obtained in this study for the Urmia catchments.

The HadCM2 based climate change impacts on summer runoff for Urmia (see Figure 5.5) are in general agreement with Mimikou et al. (2000). For example, the largest reductions in runoff in Urmia are expected during June-August.

5.3.3 Climate Change Impacts on Reservoir Storage-Yield Relationships

Before presenting results from the Monte Carlo simulation exercise, results based on the single records approach will be briefly presented in order to make comparisons with the results from the preliminary investigation.

The impact of climate change on reservoir storage-yield relationships for 100% reliability for the Yorkshire and Urmia aggregated reservoir systems are presented in Figure 5.6. It can be seen that yields for fixed storages of about less than 20% MAF

(within-year system) in Yorkshire are expected to reduce slightly in future whilst increased yields are expected from larger (over-year) systems with storages exceeding about 30% MAF. This result suggests that relatively small, within-year reservoir systems will be more likely to suffer under any climate change. This is consistent with the findings of Gleick (1990). This pattern is broadly similar for the Urmia system although there is hardly any change in yield at storages of less than 20% MAF.

Yields for a fixed storage of 30% MAF have been extracted from the storage-yield curves in Figure 5.6 and are given in Tables 5.6. The table shows that yields are generally expected to increase in Yorkshire whilst reductions are expected in Urmia. A comparison of Tables 5.6 and 5.1 reveals that although yields of the reservoir systems obtained in this study are different to those in the preliminary study, the magnitude of changes are similar. The reason for the higher yields in this study is because a 1961-1990 baseline simulated runoff record was employed. In contrast, the historical runoff record was the basis for yield estimation in the preliminary study. The yield changes in both studies are generally less than 5%.

The results also indicate that there is no significant change in yield for the GS1m and GS1t scenarios applied in the current study and the preliminary study. Table 5.6 shows that a 2.3% yield rise is expected for a storage of 30% MAF based on the preliminary study for both the GS1m and GS1t scenarios. It may be recalled that yield changes for the same scenarios in the preliminary study were increases of 2.0% and 1.7%, respectively. These results reinforce the adequacy of the runoff coefficient approach insofar as yield assessment is concerned.

The 3.5% reduction in yield resulting from the IRHAD scenario in the preliminary study is broadly similar to the 4.1% reduction observed in the preliminary study. This result indicates that the use of GS1t scenario as a spatial analogue was justified.

5.3.4 Sampling Uncertainty of Reservoir Yield Impacts

Since the extended Sequent Peak Algorithm (SPA) is essentially a reservoir-sizing tool, yield for a given storage has to be determined using storage-yield curves such as the one in Figure 5.6. Where single records are used to derive such curves, yield for a given storage capacity can be determined manually by reading off the yield for the fixed capacity from the curve. This has been the procedure adopted in the preliminary study and so far in this study.

However, the current stage of the assessment involved determining 500 yields for fixed storages of 11.69×10^6 m^3 for Yorkshire and 232.6×10^6 m^3 for Urmia. The storage of 11.69×10^6 m^3 at Yorkshire is the existing capacity of the four-reservoir system and corresponds to 30% of the simulated baseline mean annual runoff (MAF). The storage capacity for Urmia was arbitrarily selected so as to give a broadly similar level of development as in Yorkshire. Thus, the 232.6×10^6 m^3 capacity represents about 30% of the MAF for the Urmia system.

The yield determination procedure was automated by fitting a suitable curve to 17 storage-yield data points. The final choice of curve was based on an initial evaluation of four curves, (i) 4-parameter Gompertz, (ii) 4-parameter Logistic, (iii) 3-parameter exponential (EXP3), and the (iv) 2-parameter exponential curve (EXP2).

The EXP2 was found to be the more robust curve and the fitting of 500 reservoir storage-yield relationships consistently gave coefficient of determination (R^2) values in excess of 0.95. EXP2 can be defined as $S = p_1 e^{p_2 D}$, where S is storage capacity (% MAF), D is reservoir yield (% MAF), and p_1 and p_2 are model parameters. This expression can be re-arranged to give the yield for a given capacity as: $D=(\ln[S]-\ln[p_1])/p_2$)

Table 5.7 contains the yield estimates from the single records and the summaries obtained from the Monte Carlo simulations. Based on the single records, all of the scenarios for Yorkshire are predicting an increase in systems yield both at the 100% and 98% reliability levels. The largest predicted increase in yield results from the GS1t scenario which is not surprising given that this same scenario predicted the largest increase in runoff. However, an important observation here is that none of the predicted increases in yield is as high (in relative terms) as the increase in runoff, implying that impacts studies which stop at runoff without looking at yields may be misleading about the water resources impacts of climate change. As the reliability reduces and hence more failures are acceptable, the yield of the system increases as expected. The situation in Urmia is opposite to that observed in Yorkshire in that the IRHAD scenario has predicted reductions in yields in the future. Because IRHAD had predicted consistently lower rainfall which in turn has translated to consistently lower runoff, this observed behaviour of the yield is also expected.

While the predicted changes in yields shown in Table 5.7 are moderate on the basis of the single records, this is untrue when the sampling variability of the input records is taken into account. For example in Table 5.7, although the baseline annual yield for 100% reliability for the Yorkshire system was 80.0% MAF, this yield can be anything

between 16.1% and 90.1% MAF when sampling uncertainties are considered. Similar information for the other scenarios, reliability and the Urmia system is also shown in Table 5.7. In all cases, the variability of the yield impacts is very large which would have been impossible to detect without the Monte Carlo experiments described here. It should be noted that the method used for determining the yield changes may be slightly misleading. This is because the baseline and future yields resulting from each of the 500 runoff sequences were not determined using a multivariate technique. The approach adopted was to first determine the 500 baseline yields which was then followed by estimating the 500 future yields. It is likely that this limitation will lead to the range of yield changes that are unrealistically large. However, results from the final detailed investigation of the Yorkshire system (discussed later in section 5.4) take account of the multivariate aspect of baseline and future yield estimation.

The empirical distributions of the yield are summarised in the box plots shown in Figure 5.7 for Yorkshire and Urmia. Compared to the baseline, the median (i.e. 50 percentile) yield estimates are higher for all three scenarios in Yorkshire, further reinforcing the results in Table 5.7. Similarly, the lower variability in the yield estimates for Urmia compared with Yorkshire revealed in Table 5.7. is also evident in the box plots. Superimposed on the box plots are the yield estimates for the single records from where their probability of exceedance can be estimated. Conversely, the empirical distributions can be used to determine the yield with a given probability of exceedance instead of relying solely on the single yield estimates for decision making. Empirical confidence limits for the yield estimates can also be constructed from the distribution functions. Table 5.7 for example contains the upper and lower 90% confidence limits for the single records yield estimates; these are generally wide.

The results based on the Monte Carlo simulation experiments are quite significant in that they indicate that whilst a single records approach may suggest that yield will increase in the future, when sampling uncertainties are incorporated in the analysis, the results can indicate large reductions. Such reductions will no doubt have implications for water resources planners. In light of this, some adaptation measures designed to cope with adverse climate change water resources impacts will be summarised near the end of the chapter.

5.3.5 Climate Change Impacts on Reservoir Resilience

The resilience was defined in equation (3.50). As was the case with the yield, there was a large variability in the resilience when sampling variability in the inflow records were considered. The average of 500 replicates have been used to construct resilience values shown in Figure 5.8. For given yield and storage, the probability of recovery is, on average, enhanced for Yorkshire but diminished for Urmia. This should be expected given that climate change is predicted to increase future yield in Yorkshire but decrease it for Urmia; consequently any attempt to maintain the pre-change yield and reliability can only be achieved through a modification of the resilience.

Information from Figure 5.8 has been extracted for fixed demands of 80% MAF and 60% MAF for Yorkshire and Urmia, respectively, and different scenarios, and presented in Table 5.8. The table shows that in Yorkshire, resilience is expected to increase in the future by around 3-12% for different reliabilities and scenarios. In contrast, resilience is expected to decrease in Urmia by 1.4 % - 4.5%. The increases in resilience for the Yorkshire system can be traced back to the increase in runoff. A similar conclusion regarding changes in resilience was also reached by Vogel et al. (1997) who investigated

multiple reservoir systems in north east USA. It can also be seen in Table 5.8 that in Yorkshire, the resilience changes generally increase as system reliability reduces (and baseline system resilience reduces). This accords with the finding of Vogel et al. (1997) who noted that it is difficult to increase the resilience of already resilient reservoir systems. This is due the non-linear relationship between reservoir storage (which is related to yield) and resilience, which tends to 'flatten' at both the high and low storage regions.

The Intermediate study was presented at the 2nd Inter-Regional Conference on Environment-Water 99, and a copy of the paper is included in Appendix B.

5.4 Results of Detailed Investigation of the Yorkshire System

5.4.1 Introduction

The nine climate change scenarios presented in section 4.5.1 defining future changes in precipitation and potential evapotranspiration (PE) formed the basis for the impacts assessment. As described in section 4.5.1, each scenario was abbreviated by a letter followed by a number. The letters C, A and H represent the Canadian GCM (CGCM1), Australian GCM (CSIRO1) and UK Hadley Centre GCM (HadCM3), respectively. The numbers 2, 5 and 8 are used to represent the 2020s, 2050s and 2080s, respectively. For example, H8 is an abbreviation for the HadCM3 2080s scenario.

In addition to the nine scenarios, the H5 scenario formed the basis for three additional scenarios. The letters T and M, suffixed on to H5, denote two PE scenarios incorporating the catchment vegetation response (feedback) to CO_2 concentrations. T

represents the effects of a 32% reduction in PE due to plant stomatal closure and M represents GCM simulated changes in PE. The letter P is used to represent the H5 scenario applied by simple perturbation rather than using a stochastic weather generator. A description of each of the scenarios is provided in Table 5.9.

The climate scenarios were applied, together with relevant models, to determine their effect on water resources in Yorkshire. In this detailed investigation, it was thought appropriate to adopt a more complete daily water balance model, MODHYDROLOG. The water resource systems model was the same as the one used previously, i.e. extended Sequent Peak Algorithm.

The HadCM3 scenarios, in particular, were used to obtain results on five aspects of water resources. They are: (i) mean runoff, (ii) low flows, (iii) groundwater recharge, (iv) reservoir storage-yield-performance and (v) reservoir control curves.

5.4.2 Sensitivity of Runoff to Climate Change

Figure 5.9 shows percentage changes in mean monthly runoff for the Yorkshire systems resulting from all the climate scenarios. The corresponding absolute changes from the historical baseline record are provided in Table 5.10. The results indicate that changes in annual runoff follow a similar pattern to precipitation changes discussed in section 4.5.1 (see Figure 4.19). For instance, the CSIRO1 scenario predicted increases in precipitation throughout most of the year with the maximum increases expected in March and November. Similarly, the CSIRO1 scenario results in an increase in runoff during most of the year with maximum increases expected in March and November (see Figure 5.9).

The scenarios based on the CGCM1 and HadCM3 GCMs are showing a tendency for reduced runoff during the summer. The largest reduction in runoff results from HadCM3 in September during the 2050s (66% = 38mm) whilst the largest increase of 54% (59mm) is expected under the CSIRO1 in November during the 2080s. Indeed, the reductions in summer runoff resulting from the HadCM3 2050s (H5) scenario are generally significantly larger than those changes observed in both the preliminary and intermediate studies. Such large reductions will no doubt lead to huge increases in future reservoir storage requirements.

Comparing the result here with those in section 4.5.1, on precipitation, it will be observed that the magnitude of change of runoff is more pronounced than changes in precipitation. This is as a result of the combined effects of changes in precipitation and PE, particularly when changes in these primary climatic factors are opposite in sign. For example, the maximum increase in runoff of 54% resulting from CSIRO1 arises as a result of a 34% rise in precipitation combined with a 3% reduction in PE (see Figures 4.9 and 4.23).

An inter-model comparison suggests the largest increases in runoff result from CSIRO1 and the largest reductions from HadCM3. This pattern can be traced back to the precipitation changes (see Figure 4.18). For example, HadCM3 predicted precipitation reductions from June to September whilst CSIRO1 predicted a general rise through most of the year. In common with findings by various other investigators (e.g. Wigley and Jones, 1985; Chiew et al., 1995; Arnell, 1996; Boorman and Sefton, 1997; DeWalle and Swistock, 2000; Gleick, 2000) these results confirm the significance of precipitation as the major variable driving the hydrological cycle. Wigley and Jones (1985) in

particular, noted that runoff is highly sensitive to precipitation changes in catchments with low runoff ratios.

A summary of mean annual changes in runoff is provided in Table 5.11. The change in mean annual runoff is the highest (30%) for the A8 scenario. In absolute terms, this change translates to a 269 mm increase in annual runoff from the baseline. It was previously noted earlier in this subsection that the largest monthly reduction in runoff results from H5. However, when the annual runoff is considered the H2 scenario resulted in the greatest percentage reduction. This annual reduction of 4.1 % could be attributed to the fact that winter runoff increases for H2, which should compensate for the summer dryness, are significantly less than for H5.

Since changes in runoff at the individual sites were used to obtain changes for the aggregated systems, it was decided to use these annual runoff changes along with annual changes in precipitation and PE to develop a simple annual rainfall-runoff expression using regression. The annual runoff changes at the individual Yorkshire sites resulting from the nine precipitation and PE scenarios (C2, C5, C8, A2, A5, A8, H2, H5 and H8) are provided in Table 5.12. The three sets of 45 data points in the table were then used to relate % changes in annual precipitation (ΔP) and potential evapotranspiration (ΔE) to annual runoff (ΔR) changes using non-linear regression. This resulted in the following expression:

$$\Delta R = \Delta P(0.0148\Delta P + 1.316) + \Delta E(0.0772\Delta E + 0.621) \qquad (5.1)$$

The performance of the expression in simulating runoff changes is shown in Figure 5.10. A coefficient of determination of 0.93 reinforces some of the arguments presented

earlier (see section 5.3.2) on the adequacy of simple rainfall-runoff expressions. Consequently, Equation (5.1) could be used to make estimates on the sensitivity of annual runoff to annual precipitation and PE changes in the surrounding Yorkshire catchments using any number of climate change scenarios. For example, using hypothetical annual precipitations changes (from baseline) of -20%, -10%, +10% and +20% (and no change in PE) in Equation 5.1 results in values of the precipitation elasticity of runoff (ε_p), i.e. runoff change/precipitation change, of 1.0, 1.2, 1.5 and 1.6, respectively. These values of ε_p are within the 1.0-2.5 range of elasticity for the USA reported by Sankarasubramanian et al. (2001).

Values of ε_p based on other studies are also in broad agreement to those noted in this study. The study of Xu and Halldin (1997) investigated eleven catchments in the NOPEX (NOrthern hemisphere climate Processes land-surface EXperiment) catchments near Stockholm in Sweden and noted ε_p values ranging from 1.5 to 2.5. In another study, Mehrotra (1999) noted ε_p values ranging from 1.45-2.05 for three catchments in central India. They noted that the largest ε_p values were observed in an arid catchment. Similarly, Nemec and Schaake, (1982) showed that ε_p could be as high as 5.0 in an arid catchment in the USA.

Figure 5.11 provides a comparison between mean monthly runoff changes resulting from the H5 scenario in addition to the H5P, H5T and H5M scenarios (refer to Table 5.9 for scenario definition). It can be seen that the H5 scenario applied to baseline climate using the simple perturbation method (H5P) results in more moderate changes in runoff than the perturbation using the more complex weather generation approach (H5). However, the monthly runoff changes resulting from the application of climate

scenarios to baseline climate using the two different approaches (i.e. simple perturbation and weather generation approaches) are not significantly different. Information from Figure 5.11 has been used to construct Table 5.13 which shows the differences between the changes in monthly and annual runoff based on the two approaches. Except in October, these differences in absolute terms are not greater than 10%.

This is quite a major finding and one that has not been reported in the published literature. This result has significant implications for climate change water resources impacts assessors who might be considering using a weather generator for climate perturbation. Investigators may adopt this rather laborious, albeit more complete, approach (see section 3.3.6) in the hope of producing more 'accurate' results. However, it is entirely possible that the end result will be no different from one obtained on the basis of the much simpler perturbation approach.

In Figure 5.11, it can be seen that the change in runoff resulting from H5T indicates that as expected, a 32% PE reduction during all months will have the effect of producing larger rises in winter runoff and smaller reductions in summer runoff. As mentioned previously in section 4.5.1, the 32% figure corresponds to the expected reduction in PE due to CO_2 doubling which is based on well documented evidence (e.g. see Kimball and Idso, 1983). The annual change in runoff due to the H5T scenario is 3.3 % (see Table 5.11). Comparing this with the -2.6% change in annual runoff resulting from the H5 scenario suggests that the 32% reduction in PE is having quite a significant impact on runoff. Although this result is in agreement with findings reported in other studies (e.g. Wigley and Jones, 1985; Rosenberg et al., 1990; Kimball et al., 1993), a limitation is that the PE scenarios ignore increased vegetation growth (thus leading to increased PE).

However, as mentioned before, the H5M scenario does take this into account. A comparison of H5M-based runoff changes with runoff resulting from H5 is also provided in Figure 5.11. It may be recalled that the H5M is a variant of H5 in that the basis for the PE scenario is the baseline and future evapotranspiration simulated by the HadCM3 GCM land-surface scheme and includes the effects of the plant sensitivity to CO_2. This is in contrast to the PE scenario for H5 that was derived in this study using the Bowen ratio method (Equation 3.2) along with the baseline and future HadCM3 simulated radiation and temperature. The GCM simulated changes in PE should in fact be more realistic since they include the effects of CO_2 on plant growth (leading to PE increases) and stomatal closure (leading to PE reductions).

The H5M results indicate that the combined effects of changes in PE due to plant stomatal closure and vegetation growth cancel each other out. Consequently there is hardly any difference between changes in H5M based runoff and H5 based runoff. This result suggests that the current assumption of ignoring the effects of CO_2 induced changes in PE in impacts assessments may be valid. However, this preliminary conclusion would need to be rigorously tested using a number of GCM scenarios. Since CGCM1 and CSIRO1 GCMs are not able to simulate changes in PE as a result of atmospheric CO_2 changes, further testing on the preliminary conclusion was not possible in this work.

Changes to the CV of annual runoff resulting from the different scenarios are also presented in Table 5.11. Changes in CV range from -35% (H5) to +16% (A5). The changes in runoff CV can be traced back to the changes in annual CV of precipitation that were presented in Table 4.29. However, some of the scenarios have resulted in little change to CV (e.g. C8, A8 and H5P). The results for C8 and A8 are to be expected

given that the precipitation CV also showed little change (see Table 4.29). As for the H5P scenario, a change of less than 1% is confirmation that, as expected, no variability is being introduced in the future runoff record derived using the simple perturbation approach.

With the exception of three scenarios (C5, H8 and H5T), a trend - with implications for reservoir storage - is noticeable in Table 5.11. The pattern emerging is that the increase in mean annual runoff results in an increase in annual flow variability whilst reductions in CV are expected as runoff decreases. Since storage requirement is directly proportional to the square of streamflow CV (McMahon and Mein, 1986), significant increase in required capacity will be necessary as a result of the increased CV.

The LARS weather generator quoted future streamflow records can be used to obtain monthly runoff perturbation coefficients which automatically incorporate the variability often absent when the same factor is used repeatedly. These factors, provided in Tables 5.14-5.16, are based on HadCM3 for the 2020s, 2050s and 2080s. In addition to being based on the latest HadCM3 GCM, these factors vary from one month to another, thus allowing the incorporation of variability in future streamflow records.

5.4.2.1 Comparisons with other Studies

The climate change impacts on runoff obtained in the final detailed study will firstly be compared with other independent investigations, and secondly, with the preliminary and intermediate study results presented in sections 5.2 and 5.3.

Arnell (1999) applied HadCM3 to some European rivers (Volga, Rhine and Danube) and found annual precipitation changes for the 2050s to range from -12% to +1%, annual PE changes to range from 30%-37% and annual runoff varied from -20% to -35%. Although the annual runoff changes are severer than those found in this study, the reductions in future runoff are in agreement with this study.

Chiew et al. (1995) used five GCMs including previous versions of CGCM1 and CSIRO1 (i.e. uncoupled versions) GCMs to investigate the sensitivity of runoff to climate change by the 2030s. The study considered 28 unregulated catchments across Australia ranging in size from just 3 km^2 to 2500 km^2. They noted that all GCMs resulted in increased annual runoff of up to 25% by 2030 in the humid tropical catchments of north-east coast of Australia. In contrast, there was little agreement amongst the GCMs as regards to runoff impacts in other parts of Australia. For example, runoff changes of ±20% were expected in south-east Australia. Unfortunately, Chiew et al. (1995) made no distinction as to which GCM gave which changes. The results for the south east of Australia confirm that, as found in the present study, different GCMs can lead to opposite effects on runoff.

Wolock and McCabe (1999) also noted the opposite effects on runoff of climate change scenarios from two different GCMs. They used two climate scenarios, CGCM1 and HadCM2 in an assessment of the sensitivity of US water resources to climate change. They found that the HadCM2 scenario generally resulted in increased runoff over much of USA by the 2030s with a maximum increase of 245% expected in the lower Colorado. In contrast, the CGCM1 resulted in reductions in runoff by the 2030s with an expected maximum reduction of 87% in Texas and the Gulf of Mexico.

A scenario based on CGCM1 was also adopted by Dvorak et al. (1997). However, their assessment considered the rainfall-runoff response of four temperate European catchments (in the Czech Republic) with catchment sizes ranging from 94 km^2 to 50,762 km^2. The impacts assessment revealed that the CGCM1 projected 7% increase in precipitation (plus a 3.1°C rise in temperature) resulted in changes in runoff over the four catchments ranging from -10% to +2%. The opposite changes in runoff are probably due to different changes in PE resulting from the same temperature rise in the different catchments.

Studies by other investigators summarised so far did not consider the effects of catchment vegetation feedback (i.e. CO_2-induced changes in PE) on runoff. Examples of some studies that considered the implications of PE changes due to vegetation feedback on runoff include Idso and Brazel (1984); Aston (1984) and Kirshen and Fennessey (1995). For example, Idso and Brazel (1984) assessed the effect of vegetation feedback on streamflow by (i) using hypothetical PE and precipitation scenarios to obtain the resulting runoff impact, and (ii) using the same precipitation scenario but different PE scenarios derived from Equation (3.4) to determine the resulting runoff impact. The PE scenarios were evaluated for five catchments in Arizona, USA, each with differing proportion of vegetative cover - that resulted in PE reductions of 16%-20%. The resulting runoff impact was found to be a -41% change from baseline without the inclusion of vegetation feedback. However, the average change in runoff was estimated as +42% with the inclusion of vegetation feedback effects.

Aston (1984) used a distributed deterministic process model to investigate a catchment in New South Wales, Australia, and concluded that the effects of vegetation feedback

(which would cause PE reductions to vary from 20-40%) would lead to streamflow to increase from 40% to 90%.

Kirshen and Fennesy (1995) used an equilibrium climate change scenario (CO_2 doubling) based on the US Goddard Institute for Space Studies (GISS) GCM for the catchment area surrounding Boston, USA. They input the scenarios to the Penman-Monteith Equation (3.1) and obtained a 20% increase in PE. They then repeated the calculation of PE except this time they used the 22% increase in plant stomatal resistance reported by Rosenberg et al. (1990). The resulting increase in PE for the same GISS scenarios was much lower at 5%. The impact of the PE scenario incorporating the effects of stomatal resistance was to cause annual runoff to increase from -16% (vegetation feedback not included) to -10% (vegetation feedback included).

The results on the effects of vegetation feedback on runoff reported in this research earlier are consistent with those from the studies summarised above. However, some of these studies do report a much larger range in runoff change (e.g. -41% to +42% in the case of Idso and Brazel, 1984), compared with the -2.6% to +3.3% noted in the present work (see Table 5.11). The large runoff changes in the latter studies can be largely put down to very low runoff ratios of the catchments. For instance, the catchments investigated by Idso and Brazel (1984) were located in the arid south-western USA, some with runoff ratios of 0.13. In contrast, the runoff ratio of for example Gorple catchment in Yorkshire is 0.67.

The studies discussed so far were all based on the traditional single record impacts assessment methodology. It is also interesting to briefly discuss some other studies that have adopted a limited Monte Carlo sampling methodology. One relevant study of

Mimikou et al. (2000) has already been discussed in section 5.3.2. It may be recalled that Mimikou et al. (2000) used Hadley Centre GCM scenarios within a Monte Carlo framework to assess the mean of climate change impacts. They showed that the future mean monthly runoff was less than baseline runoff in all months of the year.

In another investigation, Nikolaidas et al. (1994) showed annual runoff changes varied by ±24% based on a Monte Carlo approach. On the other hand, results from deterministic modelling using two climate change scenarios resulted in reductions in annual runoff of 37.5% and 17.9%, respectively.

Results from the present study along with results of some investigations summarised clearly confirm the wider variations in impacts result from different GCM experiments and impact assessment protocols. It is therefore significant that any results should only be viewed as sensitivity studies However, an important point to note is that despite inconsistencies in future runoff impacts, a clear pattern is emerging from the current study and other studies. Results indicate that the impacts of climate change might potentially be very severe thus the need for appropriate planning/adaptation measures - these will be summarised towards the end of the chapter.

5.4.3 Effect of HadCM3 scenario on Low Flow Estimates

It is important to investigate the effect of climate change on low flows because reservoir storage-yield-performance relationships are especially affected by low flows (Nawaz and Adeloye, 1999). Indeed, in the UK, the 1-day Q_{95} low flow measure (i.e. one-day low flow exceeded 95% of the time) has been widely adopted by the water industry as a basis for setting abstraction and discharge licences (Arnell, 1996). Cumulative low

flows over various durations have also been used in the planning analysis of impounding reservoirs (see McMahon and Mein, 1986).

One-month flow frequency curves were constructed using the monthly baseline (1962-1990) simulated streamflow data and future streamflow records resulting from HadCM3 2020s, 2050s and 2080s (i.e. H2, H5 and H8) scenarios. Figure 5.12 compares the baseline and future one-month flow frequency curves for the aggregated Yorkshire catchments plotted on the normal probability paper.

All future curves lie below the baseline curve, i.e. the future will become drier, indicating that a given flow would be exceeded less frequently in the future. For example, the monthly flow currently exceeded 95% of the time - Q_{95} (778×10^3 m^3) would only be exceeded 38% of the time under the H2 scenario. With the H5 and H8 scenarios, the respective exceedance probabilities are even smaller at around 5% and less than 2%, respectively. This suggests that low flow occurrence will increase in the future. The Q_{95} values have been extracted from Figure 5.12 and are shown in Table 5.17. Also shown in the table are the differences in future Q_{95} from the baseline. The respective reductions in Q_{95} resulting from H2, H5 and H8 scenarios are 25%, 35% and 37%. Such large changes in low flows (i.e. increased episodes of droughts in future) indicate that reservoir yield will be severely affected and large reductions are most likely. Indeed, as noted by Foster et al. (1997), an increase in the number of droughts also has implications for water quality. This is because reduced flows will result in less dilution of industrial and other discharges to rivers.

Comparisons with other studies investigating the effects of climate change on low flows will now be provided. However, since the relatively new HadCM3 scenarios have not

yet seen widespread use, studies carried out using earlier GCM experiments will be discussed. One study that adopted a previous version of HadCM3 was that of Arnell (1996), although 1-day Q_{95} was the subject of investigation rather than 1-month Q_{95}.

Arnell (1996) applied HadCM1 scenarios (CCIRG, 1996) and noted a reduction in Q_{95} of 13% for the 2050s. The changes apply to River Greta at Rutherford Bridge, located in Durham County, which is north of the Yorkshire catchments considered in the present work. The smaller differences reported by Arnell (1996) are a reflection of the more moderate HadCM1 scenarios (see CCIRG, 1996 for scenario details). However, it should also be noted that unlike in the current work (which adopted a weather generation approach), Arnell's (1996) future flow series were derived using the simple perturbation approach and hence did not incorporate variability.

In another study, Dvorak et al. (1997) assessed the implications of climate change on 1-month Q_{90} after having determined the effects on mean runoff. They used scenarios from the GISS, GFDL and CGCM1 GCM experiments (see Table 3.1) and noted that the most severe reductions in Q_{90} over three catchments were 14%, 30% and 20%, respectively.

They also showed that the effects of climate change on low flows appear to be more critical than effects on mean flows. For example, they noted that mean annual runoff was expected to reduce by 10% under the most critical scenario (CGCM1) whilst the largest reduction in 1-month Q95 was 30% according to the GFDL experiment. These results are consistent with the current finding. For example, Table 5.11, shows that the largest reduction in mean annual runoff for the H2, H5 and H8 scenarios is 4.1% (H2).

However, the largest reduction in 1-month Q95 is 37% (H8) which is quite the opposite change to the annual runoff impact (+3%).

5.4.4 Climate Change Impacts on Groundwater

Groundwater is an important source of water, especially in southern Britain. Although groundwater does not currently constitute a major supply source in Yorkshire, it was thought appropriate to carry out a brief groundwater assessment. This is because it is likely that groundwater sources in Yorkshire will be expanded in future (Ian Stevens - Yorkshire Water Services Ltd. - Personal Communication). Consequently, results from a brief groundwater assessment will offer insight into the possible effects of climate change.

Use of the MODHYDROLOG water balance model in this study allowed groundwater recharge and baseflow to be simulated in addition to runoff simulation. Mean monthly and annual values of groundwater recharge and baseflow over the 1962-1990 baseline period and the HadCM3 2050s are provided in Table 5.18. The baseline period is different to the standard 1961-1990 period since MODHYDROLOG discards the first year of data. The baseline simulated recharge could not be verified because estimates of historical recharge were unavailable for Yorkshire.

The baseline recharge is at its highest during the winter when summer soil moisture deficits have been filled during the autumn, and before deficits begin to replenish again in spring. The magnitude of recharge is therefore dependent on the amount of winter precipitation and the duration of the recharge season - which depends on autumn and spring precipitation and evapotranspiration.

Also provided in Table 5.18 are the corresponding percentage future changes from the baseline. A common feature is a reduction in groundwater recharge and baseflow during the spring, summer and early autumn. The largest reduction in groundwater recharge is expected to reach around 82% during September. This is consistent with the largest reduction in precipitation in September of 36% for HadCM3 2050s scenario (see Figure 4.18). On the other hand, groundwater recharge is expected to increase during the winter, although these changes are more moderate than the summer/autumn reductions. For example, the largest increase occurs in December (47%). The winter increase in recharge would be driven mainly by the increased winter precipitation (see Figure 4.19) thus allowing more water for recharge. It is worth noting though that high precipitation alone does not necessarily lead to high recharge. This is because episodes of intense rainfall may contribute rapidly to surface runoff rather than infiltrating to groundwater (Price, 1998)

By referring to Figure 4.19, a comparison of changes in groundwater recharge can be made with precipitation changes. The figure indicates that changes in groundwater recharge are larger than precipitation changes. For instance, the HadCM3 2050s change in September precipitation of -36% results in an -82% change in groundwater recharge during the same month. In December, the respective changes in precipitation and recharge are +28% and +47%.

These findings are consistent with results from the study of Arnell et al. (1997) who assessed the impact of climate change on groundwater recharge in ten catchments - mainly in southern England. For example, Arnell et al. (1997) noted that for a chalk aquifer in southern England (with annual recharge of 222mm), the largest reduction in recharge was expected in September. The reductions resulting from four scenarios (i.e.

HadCM1 and 3 variants of HadCM2) for the 2020s ranged from 46% to 88%. As was the case in the current study, the precipitation change, largely responsible for the change in recharge, for the same month was more moderate with a range of -9% to + 6% for the four scenarios. In contrast, December changes in recharge resulting from the four scenarios varied between +13% to -19% whilst the corresponding precipitation changes ranged from -1% to +5%.

The annual change in groundwater recharge of 0.3% (for a -5.7% precipitation change) is much smaller than monthly changes and tends to mask the extreme seasonal changes mentioned above. This change is much smaller than reported changes in recharge of between -15% to +8.4% (precipitation changes from -4% to +3%) for the four climate scenarios in the study of Arnell et al. (1997). This is because the annual PE change is only +0.4% (see Table 4.29) in the current study compared to PE changes ranging from 1%-11% in the study by Arnell et al. (1997).

Indeed, Cooper et al. (1995) have shown that groundwater recharge is particularly sensitive to evaporation changes. In an investigation of a sandstone catchment in the British Midlands, Cooper et. al. (1995) showed that a 4% increase in annual rainfall and a 9% increase in annual PE resulted in a 2% increase in annual recharge. However, if the PE was increased to 30%, the resulting recharge impact was a 13% reduction.

More recently, Crookall and Bradford (2000) reported changes in annual average recharge ranging from +0% to +9% in the Severn Trent region. These changes resulted from four UKCIP98 - based on HadCM2 (UKCIP, 1998) scenarios for the 2050s. The relatively small change in annual recharge found in the current study is consistent with

the insignificant change in recharge resulting from some of the scenarios in Crookall and Bradford's (2000) study.

Mean monthly changes in baseflow, also provided in Table 5.18, follow a similar pattern to recharge changes. However, the changes are smaller than changes in groundwater recharge. A change in recharge will have an effect on groundwater levels with a consequent effect on baseflow. Accordingly, the maximum changes in baseflow coincide with maximum changes in recharge observed during September and December. The extreme monthly changes in groundwater recharge noted in this study are an important result from a practical viewpoint. The brief investigation suggests that the planning of groundwater resources in Yorkshire should perhaps take account of the serious threats posed by climate change.

5.4.5 Climate Change Impacts on Reservoir Yield and its Sampling Uncertainty

In order to assess the effects of climate change on reservoir yield, reservoir analysis was performed using two different levels of reliability, i.e. 100% (no-failure over historical record) and 98% (1 in 50 year failure). Yields were evaluated for a fixed storage capacity of 11.13×10^6 m^3 which is the existing capacity of the five-reservoir system and corresponds to 31% MAF.

In the intermediate study, data replication at the individual sites was carried out independently of one another. However, in the detailed study, a multivariate stochastic data generation procedure (see section 3.5.3) was employed which enabled a simultaneous replication of data at all the sites. This multivariate approach not only ensured that any inter-site correlation between the flows is preserved but also that paired

baseline-perturbed streamflow records are generated which when analysed give the change in yield for that realisation pair. The way in which this has been achieved is to consider the future at each site as an additional fictitious site. For example, assume that there are 5 stations for which baseline data are available. The future data at these sites are therefore assumed to constitute another 5 sites, thus making a total of 10 sites. The multivariate analysis is then used to generate the required length of data at 10 sites, with five of these being the baseline records and the remaining 5 being the future records. This scheme is illustrated schematically below.

					1^F	2^F	3^F	4^F	5^F
1^B	2^B	3^B	4^B	5^B	6	7	8	9	10

Yield analysis is then made for each of the 10 data sets and inter comparisons are then carried out between 1^B and (6) 1^F; 2^B and (7) 2^F..., 5^B and (10) 5^F to determine the impact of the climate change scenario on yield, where B denotes baseline and F denotes future streamflow data record respectively. Once analysis is complete for the first realisation, other realisations of data records at the sites are generated and the process is repeated until 1000 realisations have been considered.

The box plots of the empirical distribution of yield changes for the aggregated systems are shown in Figure 5.13, where the maximum, minimum, 25%, 50% (median) and 75% percentiles of 1000 differences in yield are indicated. Also indicated in Figure 5.13 are the percentage difference in yield estimates obtained using the traditional, single records approach.

The box plots clearly show the range of variability in yield estimate changes obtained using the Monte Carlo approach. In contrast, values above each box plot indicate the

'one off' expected yield change obtained using the traditional approach. The box plots also indicate that the yield changes are positively skewed. Such positive skewness will preclude the use of the normal distribution for modelling the distribution of reservoir yield changes. The positive skewness may also exclude those two-parameter distributions with fixed relations between the CV of yield changes and the skewness (Montaseri, 1999). Montaseri (1999) showed that the three-parameter log-normal distribution (LN3) provides a good fit to data (reservoir storage in their case) exhibiting positive skewness. Indeed, numerous other analysts have also found the LN3 to be the most appropriate probability distribution for fitting positively skewed (storage capacity) data (e.g. Vogel and Stedinger (1987); Bayazit and Bulu, 1991; Bayazit and Onuz, 2000). Consequently, the positively skewed yield changes obtained in the present study will be fitted with the LN3 probability distribution using the approach described by Stedinger et al. (1993).

Relevant information from the box plots for the aggregated systems is summarised in Table 5.19. The table shows that at the 100% reliability level, and based on the traditional approach, yield changes vary from -1.8% to +2.8% for the CGCM1 scenarios. However, use of the extended Monte Carlo approach leads to variations in yield changes from about -15% to +19%. The change in the median is from -2.7% to +0.7%. The results indicate a reduction in yield by the 2020s and a subsequent increase by the 2050s and 2080s. This pattern of change is consistent with the runoff scenarios presented in Figure 5.9. It may be recalled (see section 5.4.2) that the CGCM1 scenarios resulted in summer runoff reduction by the 2020s whilst small increases in runoff were expected throughout most of the year by the 2050s and 2080s.

The changes in yield resulting from the CSIRO1 scenarios are more extreme than the CGCM1 based changes. For these, results based on the traditional approach indicate that the reservoirs will be able to provide more water in the future. The increased reservoir yield is expected to amount to 10.5%, 9.5% and 10.9% by the 2020s, 2050s and 2080s, respectively. Based on the Monte Carlo approach, the yield changes range from -3% (2020s) to a massive +28% (2080s). As with yield changes resulting from CGCM1, the CSIRO1 yield changes can be traced back to runoff changes that were summarised in Figure 5.9. It might be recalled that the CSIRO1 scenarios resulted in increased runoff throughout the year in the future.

In contrast, results for the HadCM3 scenarios indicate reductions in yield. Based on the traditional approach, the reductions range from -1.2% (2020s), -8.2% (2050s) and -3.7% (2080s). The Monte Carlo approach leads to more variability, and the changes range from a minimum of -19% (2050s) to a maximum of 8.5% (2080s).

Highlighted in Table 5.19 (in bold font) are the most severe changes in yield that can be expected to occur based on the traditional and Monte Carlo approach. At the 100% reliability level, and based on the traditional approach, the largest rise in yield results from the A8 scenario (10.9%). On the other hand, the largest reduction results from H5 (8.2%). Based on the Monte Carlo results, these changes are +28.3% (A8) and -19.2% (H5). The current yield in Yorkshire of the aggregated systems is 60.9 Mld. Based on the traditional approach and according to all scenarios, the future yield will vary between 55.9 Mld and 67.5 Mld. However, based on the Monte Carlo approach, future yield is likely to show much greater variations - between 49.2 Mld and 78.1 Mld. The mean yield changes (of 1000 yield estimates) vary from -10.9% to -3.7% for the HadCM3 scenarios.

As remarked earlier, the LN3 distribution was fitted to the yield changes using the approach described by Stedinger et al. (1993) for the estimation of the mean (μ_{ln}), variance (σ^2_{ln}), and lower limit ($\tilde{\tau}$) of the distribution. Estimates of the parameters are provided in Table 5.20.

Based on the fitted distribution, it can be shown in Figure 5.14 that there is 2% chance that a 4% (or lower) reduction in yield will occur in the 2050s with HadCM3 scenario whereas the probability of the yield increasing by 4% (or lower) is much lower at 0.5%. This broadly agrees with the impact of the climate change scenario on runoff discussed earlier where it was shown that runoff will generally decrease in future as a result of HadCM3 climate change scenario. With reduced runoff, the possibility of yield reduction will be much higher than the possibility of yield enhancement.

The 8.2% yield reduction predicted by the traditional single record approach translates to a probability of exceedance of approximately 20%. In other words, there is a probability of 80% that water shortage higher that 8.2% will occur in future. This is a significant risk which any water undertake must take very seriously.

Also provided in Table 5.19, are yield change estimates resulting from the HadCM3 2050s scenario applied using the simple perturbation method (monthly mean factored approach) denoted by H5P. The results from the traditional approach indicate a 8.2% reduction in yield by the 2050s which is an important result. This is because this yield reduction is the same as that obtained from the more complex approach utilising the stochastic weather generator. However, there are some differences in yield changes (albeit relatively small) resulting from the use of these two methods within a Monte Carlo framework. For example, the mean and median reduction in yields are about -9%

and -11% based on the simple perturbation method and the extended method incorporating variability, respectively. Nonetheless, on the basis of these relatively small changes in yield, an important conclusion can be drawn on the validity of yield changes resulting from the same scenario applied in different ways.

As with the results from annual runoff sensitivity to climate change (see section 5.4.2), it can be argued that the extra effort involved in adopting a more complex method of perturbation may be impractical. It may be recalled that the relatively complex method of perturbation employed here was to perturb baseline climate using a stochastic weather generator. This required access to huge amounts of GCM daily data. The data were often supplied for the whole globe, without being processed. Consequently, the file sizes amounted to hundreds of megabytes and the task of post processing was immensely time-consuming. On the contrary, for the simple perturbation approach, mean monthly changes in climate were readily available for grid-points close to the Yorkshire catchments. The small file sizes enabled downscaled scenarios to be produced with relative ease and in a very short space of time.

Comparisons are also provided on yield changes resulting from the HadCM3 2050s scenario, assuming a constant PE reduction of 32% during all the months (H5T). The H5T scenario is rather extreme, reflecting quite a severe response of vegetation stomata to CO_2 doubling. Furthermore, the scenario ignores the increase in plant growth due to CO_2 doubling (which could counteract the expected reductions in PE). The H5T scenario is different to the standard H5 scenario that was derived using the GCM-based radiation and temperature data and the Bowen ratio method. Another variant of the H5 scenario, based on a direct simulation of PE changes by the HadCM3 land-surface model is given the suffix M. The results in Table 5.19 show that there are small

differences in reservoir yield changes resulting from the H5T and H5 scenarios. For example, at the 100% reliability level, the difference in yield changes based on H5T and H5 (single record approach) is about 6%. The mean difference for the same scenarios based on the Monte Carlo approach also approximates to about 6%. As was observed in the case of runoff sensitivity to PE changes, yield changes are to some extent 'diluted' in response to changes in PE.

A similar conclusion to the above was also reached by Kirshen and Fennessey (1995) who investigated the Quabbin and Wachusett reservoirs supplying Boston metropolitan area, USA. It may be recalled from section 5.4.2.1 that Kirshen and Fennessey (1995) found that a 15% reduction in annual PE (due to stomatal closure) resulted in a 6% increase in annual runoff. The subsequent impact of the runoff increase was to increase yield from 9.4 m^3/s (baseline) to 10.5 m^3/s (CO_2 doubling); a percentage difference of 12%.

Differences in yield resulting from the H5M and H5 scenarios are very little. This is due to the insignificant differences in runoff changes resulting from the two scenarios. For instance, at the 100% reliability, the difference in yield resulting from H5M and H5 is less than 1%. This finding proves that ignoring changes in PE due to CO_2 changes will not significantly affect yield estimates. This is because CO_2 has a two-fold effect on vegetation. Firstly, plant growth is accelerated thus leading to an overall increase in PE, and secondly, plant stomata tend to close under increased CO_2 concentrations thus reducing PE. What the HadCM3 GCM simulated changes in PE show is that the combined effects of CO_2 on PE tend to cancel each other out. Consequently, the net change in PE is insignificant. The results therefore suggest that the current practice of ignoring CO_2-induced changes in PE, in climate change yield impacts investigations

may be entirely valid. Results for 98% reliability are also presented in Table 5.19 and show similar pattern of changes to the results for 100% reliability. However the results generally point to less variability in the differences in yield estimates (see also Figure 5.13).

In summary, there is a further significant conclusion that may be drawn from these results. The results highlight the inadequacy of the traditional approach to water resource climate change impact assessment. This is because the traditional approach provides only a single estimate of yield changes for a given scenario rather than the large range of impacts that are likely to occur in the future.

5.4.6 Climate Change Impacts on Reservoir Storage and its Sampling Uncertainty

Reservoir storages were determined for a constant 60% MAF demand - which is the current level of demand in Yorkshire. In reality, demand is unlikely to remain constant due to economic and demographic changes, as well as changes in climate (Herrington, 1996; OCWR, 2001). Consequently, for the HadCM3 2050s (H5) scenario, storages were also determined by raising the level of demand to 70% MAF. This demand rise from 60% MAF to 70% MAF corresponds to a relative change of 17%. This rise is approximately between the high (23%) and medium (8%) demand scenarios expected in Yorkshire by 2021 (Herrington, 1996). The 2020s change in demand was assumed to occur in the 2050s since no such data were available for the latter period. In common with the assessment of climate change on yield, two reliability levels were selected, i.e. 100% and 98%.

Empirical box plots presented in Figure 5.15 summarise the changes in reservoir storage as a result of all the scenarios. Comparing Figure 5.13 with 5.15 shows that, as expected, if a particular scenario resulted in increased yield from the reservoirs, then the same scenario will result in less storage being required.

To illustrate this point, storage changes are provided in Table 5.21. The changes are only presented for the two scenarios that resulted in the most extreme changes in yield. These scenarios are the CSIRO1 and HadCM3. The table shows that at the 100% reliability level, the changes range from -61% (A8) to +167% (H5). At the 98% reliability level, and based on the traditional approach, the largest reduction in storage results from the A8 scenario (30%). The largest increase (123%) results from the H5 scenario. Based on the Monte Carlo approach, the largest reduction and the biggest increase in storage requirements are 61% and 198%, respectively. In common with the conclusion reached earlier in section 5.4.5, these results show just how wide the range of variability in storage changes obtained using the extended Monte Carlo approach can be. In contrast, the traditional single records approach enables only a single storage change impact to be determined which is only one of many possibilities.

It may also be noticed that some of the storage changes obtained in this study are considerably larger than those obtained in both the preliminary and intermediate studies. The reason for this is the severity of some of the scenarios adopted in the final detailed investigation. For example, during June, July & August, the H5 scenario resulted in an average 48% runoff reduction, and an average 27% reduction during September, October and November, respectively. In contrast, the respective seasonal runoff changes resulting from scenarios in the preliminary and intermediate studies were generally considerably less. The large reductions in summer runoff expected under the

H5 scenario are causing the reservoirs to run dry more frequently thus requiring massive storages to maintain the current level of performance in the future. The large changes in storage noted here are in agreement with the findings reported by Nemec and Schaake (1982). The study of Nemec and Schaake (1982) reported up to an 800% increase in storage, however, their investigation was a purely hypothetical study.

The percentage changes in storage can be applied to the existing storage of the five reservoirs under investigation to ascertain the extent of storage changes in absolute terms. At the 100% reliability level, and based on the traditional approach, the current total storage capacity of the five reservoirs (11.13×10^6 m^3) could be reduced by 3.01×10^6 m^3 according to the A8 scenario. This reduction would allow current yield to be met in the future without compromising reservoir reliability. On the other hand, reservoir storage would need to be increased by 8.24×10^6 m^3 to maintain current yield according to the H5 scenario. Absolute changes based on the extended Monte Carlo approach are understandably more severe. Storage could be reduced by 6.79×10^6 m^3 under the wettest (A8) scenario but would need to be increased by 13.70×10^6 m^3 under the driest (H5) scenario. The latter result is rather striking since it suggests that current storage would need to be more than doubled to maintain the current level of yield.

For the H5 scenario (100% reliability), it was thought appropriate to determine the probability of a particular change in storage capacity being exceeded, in much the same way as done previously for yield changes. This required the selection of a suitable probability distribution for fitting the 1000 changes in storage estimates. To test this for a suitable distribution, a simple statistical test was employed.

The statistical test firstly required the estimation of the skewness of the 1000 storage changes which was found to have a value of -0.11. Next, the confidence limits of skewness were derived to compare against the value of skewness. The standard error of estimate (SE) of skewness can be evaluated as (McMahon and Mein, 1986) $SE=\sqrt{\frac{6y(y-1)}{(y-2)(y+1)(y+3)}}$, where y = sample size, which in this case is 1000. Therefore on the assumption of a normal distribution, i.e. that the skewness is zero, the confidence limits of skewness, CL, can be approximated by: CL = 0±k x SE, where k is a standard normal variate for a given level of significance. For example, at the 95% level, k = 1.96. It should be noted that the above expression for calculating SE assumes that skewness has a normal distribution. For a sample size of 1000, the 95% confidence limits about zero for the sample skewness are ±4.80. The sample skewness of -0.11 lies within this range indicating that the skewness is not statistically different from zero. Thus the assumption of normality is valid.

Storage changes (fitted with the normal distribution) resulting from the H5 scenario are shown in Figure 5.16. It can be seen that there is a 2% chance that a 135% (or larger) increase in storage capacity will be required by the 2050s with HadCM3 in order to maintain current level of reservoir performance. The 74% storage increase predicted by the traditional single record approach translates to a probability of exceedance of approximately 80%. These results are significant and indicate that to maintain current levels of reservoir performance, capacity of existing facilities will need to be expanded considerably, or alternatively, new resources will need to be developed.

The storage changes presented thus far are based on the assumption that demand remains unchanged in the future. However, assuming a rise in future demand will obviously lead to requirements for more storage.

The sensitivity of storage to a 17% rise in demand is presented in Table 5.21. The suffix D is used to denote the results of the H5 scenario and the demand rise. As shown in the table, for 100% reliability and based on the traditional approach, reservoir storage would have to be increased by a massive 194% to maintain the current level of yield. Assuming no change in demand, the rise in storage is 123%. The difference of 71% in storage is the increase in storage requirement due to a 17% demand rise alone. Based on the Monte Carlo approach, and 100% reliability, storage would need to be increased by 250% (maximum rise) and 49% (minimum rise). These results are quite significant and reveal that a rise in the demand for water due to climate change will place increasing pressure on already stressed water resources. Indeed, it is increasingly being realised that the effects of climate induced demand changes on water resources may be extremely severe. Consequently, a project is currently underway in the UK that seeks to provide a link between climate variables such as daily sunshine hours and temperature, and demand for water (see OCWR, 2001).

Comparisons between change in storages resulting from the use of the variants of the HadCM3 2050s scenario (i.e. H5P, H5T and H5M) are also presented in Table 5.21. The results indicate that at the 100% reliability level, storage requirements based on the simple perturbation approach (i.e. H5P) increase by 63%. This change is 11% less than the change based on the approach utilising a stochastic weather generator. Based on the Monte Carlo approach, the changes in mean, minimum and maximum, are 72%, 5% and 182% for H5P. It may be recalled that the respective changes resulting from H5

scenario were 93%, 16% and 167%. The differences in storage change at the 98% reliability level are somewhat more extreme. Based on these results, it could be concluded that use of the simple perturbation approach leads to more moderate changes in reservoir storage capacity than using the more complex (weather generation) approach. Results of the H5T scenario (i.e. 32% reduction in PE) indicate more moderate changes in storage. This is expected given that a large PE reduction would dampen the effects of reduced runoff. This would lead to a smaller rise in future storage requirement than if PE rise were relatively small.

The change in storage resulting from the H5M scenario (i.e.0.4% rise in annual PE) is, naturally, having a negligible effect on storage changes. For example, at the 100% reliability level, based on the traditional approach, storage differences are 74% and 71% resulting from the H5 and H5M scenarios respectively. With the Monte Carlo approach, the changes in mean storage respectively are 92.2% and 89.3% resulting from H5 and H5M. This result confirms the earlier result from the yield assessment study (section 5.4.5) that the common practice of ignoring CO_2 induced changes in PE (for the purpose of reservoir storage-yield impacts assessments) are valid.

Another conclusion that may be drawn from these results is that storage changes are more sensitive to precipitation changes than are changes in yield. However, this finding should be viewed with caution since the degree to which the change in yield is different from the storage depends on the particular point of interest on the storage-yield space. In other words, whether the reservoir is exhibiting within-year or over-year behaviour. A reservoir that goes from empty to full several times a year on average is classed as within-year. In contrast, a relatively large reservoir that might take several years to go from empty to full is known as an over-year reservoir.

In the flatter over-year part of the space, large changes in storage merely produce modest changes in yield. However, this is not the case in the steep, low-yield within-year region where small changes in storage produces large increases in yield. This means that the large changes in yield observed in the present study are arising largely because changes are being determined for a within-year system (see Table 4.2).

An example of storage-yield analysis in the flatter over-year space is the study of Mehrotra (1999). He used hypothetical scenarios to investigate the sensitivity of reservoir storage-yield for sites in central India. He showed that at a low level of demand (such that the reservoir was behaving as a within-year system), a precipitation reduction of 10% and a 3°C rise in temperature resulted in 35% increase in storage requirement. The storage change at a capacity of 127% of the mean flow (over-year system) resulted in no change in yield.

5.4.7 Climate Change Impacts on Reservoir Performance

Figure 5.17 presents empirical box plots of the change in resilience resulting from the HadCM3 2050s scenario. The resilience changes based on the single records approach are also provided in Figure 5.17. Resilience, as defined in Equation (3.51), represents the probability that a reservoir system will recover following a failure.

A summary of the changes in the box plots is presented in Table 5.22. The results indicate that at the 30% vulnerability level, and a given reliability of say, 98%, the Yorkshire aggregated reservoir systems resilience changes range from a minimum reduction of 43% to a maximum increase of 60%. The average of the 1000 resilience changes suggest a reduction at all reliability levels and these range from 22% to 7%. In

contrast, the 'one-off' resilience change based on single records approach for 98% reliability is a 23.5% increase. Indeed, the result of the single records approach is quite misleading since it only indicates a rise in resilience. On the contrary, the Monte Carlo approach indicates that resilience could reduce as well as increase in future. A probability of exeedance could then be attached to a particular resilience change in a similar way to the likelihood of a particular yield or storage change being exceeded, reported earlier in sections 5.4.5 and 5.4.6.

The results from this exercise have highlighted the usefulness of a Monte Carlo approach in providing a range of plausible resilience changes rather than the 'one off' change based on the single records approach which might be misleading.

It may also be noticed from Table 5.22 that larger changes in resilience occur at the lower reliability levels. This suggests that already resilient systems (high reliability) are not as sensitive to climate change as systems that currently have a relatively low system resilience. This is consistent with the results in the intermediate study presented in section 5.3.5, and also accords with the findings of Vogel et al. (1997). However, whereas in the intermediate study, resilience was expected to increase in future, reductions are expected in the detailed study. This can be put down to the H5 scenario which predicted very large reductions in summer runoff.

Changes in sustainability index (see Equation 3.53) can be readily estimated based on changes in time-based reliability, resilience and vulnerability. For the H5 scenario these have been estimated as 14.8%, 12.9%, 9.5% and 4.9% reductions for reliability levels of 95%, 96%, 97% and 98%, respectively (and are based on the average of 1000 replicates). Owing to its formulation (see Equation 3.53), the pattern of change in the

sustainability index is similar to the change in resilience, i.e. smaller changes at the higher reliability.

5.4.8 Climate Change Impacts on Reservoir Control Curves

In the preceding sections, some of the results have highlighted the threats facing water supplies by some of the extreme climate change scenarios (e.g. HadCM3 2050s). However, in regard to reservoirs, there is a way of tempering the climate change impacts. One available option is to revise current reservoir control curves on the basis of a more extreme future climate. Reservoir Control curves are widely used by the UK water industry (Thorne et al., 1998) as a guideline on target reservoir contents on a daily or monthly basis.

In the study, reservoir control curves were derived for time-based reliability levels of 100% and 98% and were based on the single records methodology in addition to the Monte Carlo approach. The curves, shown in Figure 5.18, are based on the current and H5 scenario projected future climatic conditions. The curves based on the single records approach were derived by taking the average value of reservoir storage contents simulated by the extended Sequent Peak Algorithm (SPA) for the same month throughout the duration of the single (baseline and future) data records. The methodology adopted for the curves based on the Monte Carlo approach was similar except that the average of 1000 reservoir contents (determined using 1000 baseline or future streamflow sequences) averaged over the same month in each year were used.

To allow a comparison between the control curves, the storage levels are standardised by dividing by the baseline mean annual runoff. In the Monte Carlo approach an average of 1000 control curves (derived on the basis of 1000 runoff sequences) is used. Figure 5.18 provides a comparison between baseline and future control curves for the traditional and extended Monte Carlo methodologies. Both sets of curves indicate that in general, minimum allowable storage levels would have to be raised under the H5 scenario from February-August in order to maintain current levels of system performance.

Information from the curves based on baseline and simulated future reservoir contents is extracted and presented in Table 5.23. The table shows the relative change in minimum allowable storage levels. The results indicate that the largest amount by which the minimum allowable storage level would have to be raised in the future for 100% time-based reliability, and based on the traditional approach, is 30% in April and May. The change in the largest level that storage could be allowed to fall to is 65% in November.

The existing Yorkshire Water (YW) operational control curve (Yorkshire Water RRDY, 1991) has been superimposed in Figure 5.18 to enable comparisons with those derived in the present study. Whilst the shape of the YW existing curve is similar to those curves derived in this work, it is generally above the future curves. However, such a straightforward comparison may be misleading given that neither the basis of the Yorkshire control curve derivation nor its reliability is known. As shown in the curves derived in this study, the time-based reliability has a significant influence on the control curve. Additionally, the control curves derived in this study incorporate an extra vulnerability norm, which may not be present in the existing control curve at Yorkshire.

Barring such differences, it can safely be concluded that the current Yorkshire Water control curve may go some way in tempering the most severe impacts of climate change.

The beneficial impacts of modifying control curves to reflect a changing climate were well documented in the study of Salewicz (1996). He analysed Kariba reservoir designed to provide energy and water to Zambia and Zimbabwe. One of the objectives of the study was to investigate whether currently applied reservoir operating policies remain relevant to a new hydrological regime. Although, the study focussed on energy production, the results are relevant. They used equilibrium scenarios based on the GFDL and GISS GCMs to derive reservoir inflow records. 300 years of monthly reservoir inflows based on historic data and the 2 x CO_2 climate scenarios were stochastically generated using a simple Markov-type generator - CLIRUN (Kaczmarek and Krasuski, 1991). The inflows were then fed into a reservoir optimisation model to assess the effects on reservoir operation and hence energy production. The results showed that due to a change in seasonal reservoir storages (i.e. control curve), energy potential would increase by up to 20% under the GISS based scenarios. However, the effects of the GFDL scenario were opposite, with approximately a 5% reduction.

5.4.9 Comparisons of Detailed Studies and other Studies: A tentative recommendation

The impact of climate change on annual runoff and reservoir yield at the Yorkshire sites based on three studies, namely preliminary, intermediate and final detailed, are summarised in Table 5.24. Results are only presented for Yorkshire to allow comparisons with the final detailed study. Moreover, only results from the HadCM3 scenarios in the final detailed study are given. This makes it possible to compare results

of the detailed study with those of the previous investigations utilising older versions of HadCM GCM.

Two important conclusions may be drawn from Table 5.24 as follows:

(i) Use of different climate change scenarios could result in opposite impacts on the same water resources system.

(ii) assessed climate change impacts on annual runoff and reservoir yield changes are not particularly sensitive to either the baseline climate perturbation scheme or the catchment runoff response model used.

These findings suggest that climate impacts assessors may find it more appropriate to gear their efforts towards obtaining reliable, consistent climate change scenarios rather than worrying too much about using complex methods for baseline climate perturbation or catchment runoff response modelling. Ideally, these conclusions would need to be tested more thoroughly perhaps using a large range of hypothetical scenarios.

5.5 Water Resources Adaptation Planning

After having highlighted the possibility of severe impacts of climate change on water resources, in this chapter, it would be appropriate to end by touching upon some possible adaptation strategies designed to cope with these potential changes. Climate change adaptation was defined by Carter et al. (1994) as being '*concerned with responses to both the adverse and positive effects of climate change.*'

Water resources management is concerned with mitigating the effects of hydrologic extremes and providing a higher degree of reliability in the delivery of water to consumers (Kaczmarek et al., 1996). However, no activity is risk free and, as the reliability approaches 100%, i.e. no risk, then so do the accompanying costs - rising rapidly close to the risk-free zone. Consequently, in water resource studies, reliability levels of 99%, 95% or 90%, representing useful levels of performance are often adopted. There are numerous possibilities for individual adaptation measures. For example, Salewicz (1996) (see section 5.4.8) demonstrated the 'optimal' adaptation strategy in dealing with climate change uncertainty. They recommended that the rigid reservoir operating policy in current use be modified to increase its flexibility and ensure efficient operation of the reservoir in the face of future hydrologic conditions.

Some adaptation measures will be more adequate in dealing with climate change uncertainties. Other strategies may emphasise reliability of supply whilst others might focus on sustainability. There is general agreement that future water resources management strategies should include various cost-efficient combinations of the following responses (Kaczmarek et al., 1996):

(i) regulatory (e.g. metering) or technological (e.g. agricultural water use efficiency) measures to control water use;

(ii) indirect measures designed to affect human attitude to water use (e.g. incentives, tax);

(iii) improvement in the operation of water resource systems (e.g. modification of control curves under a changed climate);

(iv) direct measures designed to increase availability of water supply (e.g. reservoir capacity expansion, pipe leakage reduction).

5.6 Summary

Results from three sub-studies were discussed in this chapter. In the preliminary study, the sensitivity of the storage-yield relationships of two multiple reservoir systems to the incorporation of reservoir surface net evaporation flux and climate change was investigated using the traditional single records approach. One of the systems is located in the temperate England (Yorkshire) and the other in the semi-arid climate of Iran (Urmia). It was observed that for the Yorkshire system, the incorporation of the net evaporation flux in the yield analysis caused the storage required for meeting a given yield to decrease. The behaviour of the Urmia system was opposite to that of the Yorkshire system.

The climate change impacts on runoff and storage-yield were examined using five climate change scenarios. The runoff scenarios were developed using a simple runoff coefficient approach while the storage-yield functions were based on an extended SPA. For the Yorkshire catchments, most of the scenarios predicted wetter conditions in future except for a brief summer period when a reduction in average rainfall was predicted. It was also observed that the reductions in summer runoff coincided with reduction in rainfall, thus confirming the view that the runoff reacts more to rainfall than to evaporation.

The generally higher inflows predicted by the scenarios for the Yorkshire system suggested that lower storages will be required for meeting a given demand or, where the storage is fixed, more water could be supplied from the fixed capacity. Reductions in the required storage was almost universal except at low yields. The behaviour at the low yields was attributed to the within-year storage requirements which dominate total

storage at such low yields. In other words, small reservoirs which are essentially aimed at meeting seasonal discrepancy between runoff and demand will be more prone to climate change impacts because existing facilities will be unable to meet the demand if predicted climate change materialises. For high yield, over-year systems, however, such seasonal requirements are masked by the much larger year-on-year requirements and climate change is not likely to result in severe water shortage.

A similar pattern of change was observed for the Urmia system; however, due to the larger reduction in the Urmia summer runoff, the influence of within-year storage was more pronounced and hence the increased storage requirements predicted at low yields were much higher than those recorded for the Yorkshire system.

In the intermediate study, both the Yorkshire and Urmia systems were re-analysed using two further climate scenarios (in addition to two scenarios adopted in the preliminary study) and a monthly water balance model. It was shown that the change in annual runoff and yield resulting from the two scenarios used in both the preliminary and intermediate studies was similar. This observation confirmed the adequacy of the simple runoff-coefficient approach in assessing climate change impacts and suggests that extra effort expended in calibrating relatively more complex catchment runoff response models may not be productive.

Another important aspect of the intermediate study involved evaluating the effects of sampling uncertainties in both baseline and future streamflow data records. In particular, it was demonstrated that the current approach of basing impacts study on single traces of both the baseline and future data records is limited since it ignores other numerous possible impacts.

The final detailed investigation focused on the Yorkshire system and used climate change scenarios based on three different GCMs. The study also adopted the more complex method of perturbing baseline climate using a stochastic weather generator. Additionally, a daily water balance model of catchment runoff response was used.

Three main conclusions were drawn from the detailed study. Firstly, use of scenarios based on different GCMs could lead to opposite impacts on the same water resources system. This result therefore exposed inconsistencies in climate model projections. Secondly, in common with findings from the intermediate study, the detailed study also demonstrated the inadequacy of the traditional single records approach to climate impacts assessment. It was shown that the impacts of climate change on reservoir storage-yield-performance functions are highly variable and could be very different from the mean impact assessed using single realisations of baseline and future climate data. Thirdly, assessed climate change impacts on mean monthly and annual runoff and reservoir characteristics are not particularly sensitive to the baseline climate perturbation scheme. This finding is rather significant and suggests that climate impacts assessors may find it more appropriate to gear their efforts towards obtaining reliable, consistent climate change scenarios rather than using complex methods for baseline climate perturbation.

Additionally, the HadCM3 climate change scenarios were used to investigate some other water resources issues. These were to assess (i) the effects of vegetation feedback on runoff and reservoir characteristics, (ii) climate change impacts on flow frequency curves, (iii) effects of climate change on groundwater recharge, (iv) climate change-induced increase in water demand on reservoir storage and (v) climate change impacts on reservoir control curves.

The results are summarised as follows:

(i) The dual response of vegetation to increasing CO_2 concentrations makes practically no difference to the net change in potential evapotranspiration. Consequently, the assumption of ignoring vegetation feedback in impacts studies may be a valid one to make.

(ii) As a consequence of the reduced future runoff, the flow quantiles were much lower in the future when compared with the baseline. Since low flow quantiles have a direct impact on rivers and reservoir yields, these obtained reductions in the low flow quantiles resulted in reductions in future yields for the Yorkshire systems.

(iii) Reductions in future groundwater resources were larger than reductions in runoff. This is due to the relatively high sensitivity of groundwater recharge to changes in both precipitation and PE, which was found in the study. Water resources planners wishing to exploit groundwater resources in Yorkshire should therefore be aware of the severity of the possible threats of climate change to groundwater recharge.

(iv) Climate change-induced reductions in future inflows to reservoirs combined with increases in future water demand could put even greater pressure on reservoirs.

(v) Reservoir monthly target storage levels would need to be raised in the future between February and August in order to maintain current levels of system performance. Reservoir control curves for baseline conditions derived in the detailed study were also compared to the existing Yorkshire Water (YW) operational control curve. Although the shape of the YW existing curve is similar to those curves derived in this work, it was found to be generally above the future curves. It was therefore concluded that the current Yorkshire Water

control curve may go some way in tempering the most severe impacts of climate change.

Although (iii) and (iv) suggest serious threats to future water resources, it should be noted they are based on only a single (rather extreme) climate change scenario.

A point evident in all three studies was that runoff changes are more sensitive to precipitation changes than changes in evapotranspiration. This would indicate that reliable precipitation scenarios are essential for impacts studies.

The results in this chapter have highlighted the uncertainty in predicting the impacts of climate change on water resources. Indeed, given that there is no agreement between the GCMs regarding the future climate (e.g. opposite changes in rainfall are being simulated by the GCMs for the same catchment), it could be argued that impact assessments should be delayed until there is more consistency amongst the scenarios.

However, the usefulness of carrying out impacts assessments despite the uncertainties is that they will at least provide some sort of indication of whether or not *possible* impacts are significant. If they are potentially significant, as has been shown in this research, then this should send out a warning signal for more research to be conducted.

Table 5.1: Impact of reservoir surface fluxes and climate change on reservoir yield for storage capacity of 30% MAF (11.69 Mld) - Preliminary study.

Reservoir system	Climate scenario	Yield (Mld)		
		Ignoring surface fluxes	Including surface fluxes	% change from baseline*
Yorkshire	baseline	68.91	71.86	
	HadCM1(2050)	69.52	71.05	-1.1
	HadCM1(2020)	70.44	73.08	1.7
	GG1m	71.45	74.81	4.1
	GS1m	70.03	73.28	2.0
	GS1t	70.03	73.08	1.7
Urmia	baseline	1126.05	1103.25	
	GS1t	1085.02	1057.66	-4.1

* change for yield derived by including surface fluxes in analysis.
Mld: 10^6 litres/day
GG1m, GS1m & GS1t based on HadCM2-2020s and based on different emissions scenarios and ensembles.

Table 5.2: Description of scenarios used in preliminary and intermediate studies.

Scenario abbreviation	GCM	Time period	Emissions scenario	Region	GCM grid-scale or downscaled
H120	HadCM1	2020s	GHG	Yorkshire	Grid-scale
H150	HadCM1	2050s	GHG	Yorkshire	Grid-scale
GG1m	HadCM2	2020s	GHG	Yorkshire	Grid-scale
GS1m	HadCM2	2020s	GHG+SA (ensemble)	Yorkshire	Grid-scale
GS1t	HadCM2	2020s	GHG+SA (ensemble)	Yorkshire	Grid-scale
UKCIP98	HadCM2	2020s	GHG	Yorkshire	downscaled
IRHAD	HadCM2	2020s	GHG	Urmia	downscaled

GHG: greenhouse gases
SA: sulphate aerosols

Table 5.3: Change in mean monthly and annual runoff in Yorkshire and Urmia - Preliminary study.

Scenario	Jan	Feb	Mar	Apr	May	Jun	Jul	Aug	Sep	Oct	Nov	Dec	Ann
Yorks.													
H120	12.3	3.8	10.8	-6.5	-2.2	2.7	5.8	-2.4	2.1	13.7	22.8	4.9	68.3
H150	23.8	7.7	15.6	-16.0	-5.7	-9.3	9.5	-7.5	-6.1	20.1	41.3	6.7	82.7
GG1m	3.7	9.0	5.8	6.6	5.0	-1.0	-3.2	4.1	5.5	14.0	19.9	11.8	80.3
GS1m	6.2	2.8	4.2	5.6	3.6	1.6	-2.1	-0.1	-2.5	7.5	5.5	4.1	34.8
GS1t	5.7	4.7	6.5	16.0	16.0	-18.4	-8.5	-9.1	0.9	26.1	-1.5	0.4	32.7
Urmia													
GS1t	1.8	2.6	3.4	14.0	18.4	-9.8	-5.5	-8.9	-5.4	2.1	0.0	0.8	12.1
	16.8	*23.8*	*19.2*	*29.5*	*22.2*	*-14.6*	*-18.9*	*-87.8*	*-96.7*	*29.4*	*-0.4*	*6.6*	*3.9*

H120: HadCM1-2020s; H150: HadCM1-2050s; GG1m, GS1m & GS1t HadCM2-2020s based on different emissions scenarios & ensembles.
Changes are expressed as absolute change from baseline in mm except values in italics for Urmia are % changes

Table 5.4: Change in mean monthly and annual runoff in Yorkshire and Urmia - Intermediate study.

Scenario	Jan	Feb	Mar	Apr	May	Jun	Jul	Aug	Sep	Oct	Nov	Dec	Ann
GS1m	6.0	2.9	3.5	4.2	2.9	1.1	-0.3	-0.1	-1.6	4.6	5.2	4.2	32.2
GS1t	5.0	4.4	5.1	11.0	10.3	-3.6	-4.2	-8.3	-4.5	16.5	4.0	1.2	33.1
UKCIP98	5.3	9.0	3.7	3.1	2.6	-1.2	-2.5	-2.4	-3.9	1.2	8.4	7.5	28.2
IRHAD	0.12	0.03	1.08	2.59	-5.38	-10.21	-5.59	-1.20	-0.43	-0.45	-0.06	-0.03	-18.92
	1.1	*0.3*	*6.1*	*5.4*	*-6.5*	*-15.2*	*-20.2*	*-11.7*	*-7.7*	*-6.2*	*-0.5*	*-0.2*	*-6.1*

all scenarios based on HadCM2-2020s
Changes are expressed as absolute change from baseline in mm except values in italics for Urmia are % changes

Table 5.5: Annual runoff changes resulting from the GS1m and GS1t scenarios - Preliminary and Intermediate studies.

Scenario	Annual runoff change (%) from baseline obtained using simple runoff coefficient equation (3.21) (Preliminary study)	Annual runoff change (%) from baseline obtained using monthly water balance model (Intermediate study)
GS1m	3.4	3.7
GS1t	3.5	3.4

Both GS1m & GS1t based on HadCM2 (2020s) forced with greenhouse gases plus sulphate aerosols - scenarios differ in that the emissions forcing is introduced at different time periods (i.e. these are ensemble scenarios).

Table 5.6: Climate change impacts on reservoir yield based on single records approach - Intermediate study.

Reservoir system	Climate scenario	Yield (Mld)	% change from baseline
Yorkshire	baseline	82.92	
	GS1m	91.97	2.3
	GS1t	92.00	2.3
	UKCIP98	91.01	1.2
Urmia	baseline	671.0	
	IRHAD	611.9	-3.5

Mld: 10^6 litres/day
Yorkshire scenarios based on HadCM2-2020s forced with different emissions scenarios.
IRHAD: HadCM2-2020s scenario for Urmia region
storage capacity = 30% MAF (11.69 Mld)

Table 5.7: Yield estimates based on single records and Monte Carlo approach - Intermediate study.

Approach	Yorkshire								Urmia			
	100% reliability				98% reliability				100% reliability		98% reliability	
	Bas.	GS1m	GS1t	UKCIP98	Bas.	GS1m	GS1t	UKCIP98	Bas.	IRHAD	Baseline	IRHAD
Single	79.55	81.36	81.39	80.51	82.36	84.34	83.88	83.31	72.51	70.04	76.99	74.30
Monte Carlo												
Mean	70.92	72.88	74.08	72.33	76.83	79.19	80.66	78.68	70.76	68.12	75.55	72.57
Minimum	16.07	15.54	18.45	15.83	17.62	16.97	20.51	17.33	49.77	48.20	54.16	52.24
Maximum	90.11	92.92	93.28	91.22	95.04	96.79	99.25	96.09	81.21	79.40	83.89	81.75
Median	72.58	74.26	75.22	73.64	78.56	81.04	81.82	80.66	71.38	69.08	75.75	73.05
UC90[a]	85.03	87.61	87.82	86.62	91.43	94.39	96.36	93.44	77.94	75.08	82.69	79.54
LC90[b]	51.29	53.01	55.64	53.14	57.45	59.32	61.94	59.36	62.02	58.52	67.33	63.97
Variance	108.78	112.37	98.81	105.40	107.43	115.12	106.08	108.43	23.32	25.28	21.48	21.50
CV	0.147	0.145	0.134	0.142	0.135	0.135	0.128	0.132	0.068	0.074	0.061	0.064

[a, b] denote respectively the upper and lower 90% confidence limits
storage capacity = 30% MAF for both systems

Table 5.8: Climate change impacts on reservoir resilience - Intermediate study.

Rel.	Yorkshire system*							Urmia system$		
	Resiliency (%)				% change from baseline			Resiliency (%)		% change
	Bas.	GS1m	GS1t	UKCIP98	GS1m	GS1t	UKCIP98	Bas.	IRHAD	
99	42.2	43.6	45.0	43.5	3.3	6.6	3.1	61.7	60.3	-2.3
98	34.2	35.1	37.4	35.4	2.6	9.4	3.5	51.6	49.3	-4.5
90	25.9	26.9	29.0	27.1	3.9	12.0	4.6	35.5	35.0	-1.4

average of 500 replicates
*Storage = 30% MAF; yield = 80% MAF
$ Storage = 30% MAF; yield = 60% MAF
rel: time-based reliability
Yorkshire scenarios based on HadCM2-2020s forced with different emissions scenarios.
IRHAD: HadCM2-2020s scenario for Urmia region

Table 5.9: Description of climate change scenarios adopted for the final detailed study of the Yorkshire system.

Scenario abbreviation	Definition
C2	Canadian Climate Centre CGCM1 2020s
C5	Canadian Climate Centre CGCM1 2050s
C8	Canadian Climate Centre CGCM1 2080s
A2	Australian CSIRO1 2020s
A5	Australian CSIRO1 2050s
A8	Australian CSIRO1 2080s
H2	UK Hadley Centre HadCM3 2020s
H5	UK Hadley Centre HadCM3 2050s
H8	UK Hadley Centre HadCM3 2080s
H5T	HadCM3 2050s with catchment feedback mechanisms incorporated by allowing a uniform 32% arbitrary reduction in PE throughout the year
H5M	HadCM3 2050s with catchment feedback mechanisms incorporated by including GCM simulated change in PE.
H5P	HadCM3 2050s scenario applied to baseline climate using mean monthly changes
H5D	HadCM3 2050s assuming a 17% climate change-induced rise in water demand

Table 5.10: Absolute change in mean monthly runoff (mm) in Yorkshire - Detailed study.

Scenario	Jan	Feb	Mar	Apr	May	Jun	Jul	Aug	Sep	Oct	Nov	Dec
C2	-5.1	13.7	26.2	7.1	-8.7	-3.4	-5.0	-7.6	-9.5	-22.8	-8.3	1.3
C5	13.7	19.1	31.9	6.3	-6.7	-5.5	1.7	3.5	2.6	-23.4	0.1	9.6
C8	30.5	16.2	36.2	16.3	-2.4	-8.9	2.1	3.8	1.5	-7.1	-1.4	6.9
A2	0.0	22.4	22.9	8.7	5.2	4.8	4.8	9.0	15.7	-8.6	10.7	30.3
A5	-8.3	4.5	25.5	21.2	7.2	0.6	1.5	8.5	15.0	2.8	20.3	34.8
A8	22.3	9.9	41.7	21.5	19.8	-1.3	3.5	12.7	13.9	13.9	59.3	53.3
H2	11.8	-13.3	-2.7	6.1	1.1	-9.3	-9.7	-15.5	-13.2	-14.7	5.0	17.7
H5	42.2	5.3	16.5	-2.4	-10.3	-11.5	-13.8	-27.1	-38.3	-27.1	-4.8	42.0
H8	47.5	16.5	8.5	9.6	-4.3	-11.0	-15.8	-26.5	-34.4	-14.8	14.8	34.3
H5P	31.7	4.2	12.5	-1.9	-6.3	-8.5	-11.6	-22.5	-32.3	-8.2	-5.3	32.8
H5T	44.0	6.8	20.7	4.8	-2.3	-6.9	-11.6	-24.9	-35.1	-18.4	2.1	45.5
H5M	41.9	5.1	16.0	-2.4	-9.9	-11.3	-13.7	-26.9	-37.7	-25.9	-4.3	41.8

C: CGCM1, A:CSIRO1, H: HadCM3, 2:2020s, 5: 2050s, 8:2080s, P: simple perturbation approach, T: stomatal resistance effects on PE, M: GCM simulated PE.

Table 5.11: Change in annual runoff parameters from baseline (1962-1990) - Detailed study.

Scenario	% change in mean runoff	Absolute change in mean runoff (mm)	% change in CV
C2	-1.9	-17.5	-3.1
C5	6.3	57.2	-12.1
C8	10.9	98.7	0.3
A2	13.9	126.2	7.6
A5	14.6	132.4	15.5
A8	29.6	269.3	1.5
H2	-4.1	-37.7	-25.1
H5	-2.6	-23.7	-35.4
H8	3.0	27.4	-21.3
H5P	-1.2	-10.8	-0.7
H5T	3.3	29.7	-33
H5M	-2.4	-21.8	-32.8

C: CGCM1, A:CSIRO1, H: HadCM3, 2:2020s, 5: 2050s, 8:2080s, P: simple perturbation approach, T: stomatal resistance effects on PE, M: GCM simulated PE..

Table 5.12: Annual runoff changes at Yorkshire individual sites for annual changes in precipitation and PE based on nine climate change scenarios - Detailed study.

Site	Scenario	Precipitation change (%)	PE change (%)	Runoff change (%)
Gorple	C2	-3.4	2.6	-2.8
	C5	0.2	0.9	1.4
	C8	5.2	1.6	8.5
	A2	10.0	-0.9	12.5
	A5	7.9	0.7	9.3
	A8	14.6	0.4	19.1
	H2	-5.8	3.4	-4.9
	H5	-8.4	6.9	-5.1
	H8	-6.5	5.8	-2.5
Widdop	C2	-1.7	4.4	-0.3
	C5	5.4	2.1	9.8
	C8	8.2	2.4	13.4
	A2	10.3	0.6	15.0
	A5	11.7	4.1	19.3
	A8	20.2	1.6	35.3
	H2	-6.4	3.7	-5.3
	H5	-6.1	6.4	1.6
	H8	-2.4	5.8	6.2
W.S. Dean	C2	-1.5	3.0	-2.9
	C5	4.7	2.3	4.9
	C8	5.7	1.7	8.5
	A2	10.4	0.7	13.0
	A5	5.7	2.0	7.7
	A8	18.9	-0.3	26.9
	H2	-2.8	2.5	-3.4
	H5	-9.3	7.1	-11.3
	H8	-2.0	7.2	-1.7
Luddenden	C2	-4.6	3.0	-3.5
	C5	0.6	1.8	3.7
	C8	2.4	1.1	8.3
	A2	7.9	-0.4	9.7
	A5	8.6	0.5	12.8
	A8	19.6	-1.4	28.5
	H2	-6.7	4.6	-2.3
	H5	-10.3	7.7	0.2
	H8	-3.9	8.8	7.6
Ogden	C2	-1.8	2.0	-0.3
	C5	7.0	1.7	14.7
	C8	7.3	3.6	17.5
	A2	12.6	-0.4	20.8
	A5	17.7	0.8	31.1
	A8	23.8	0.7	43.9
	H2	-5.3	2.6	-3.2
	H5	-5.3	6.6	7.9
	H8	-2.7	7.5	11.2

C: CGCM1; A: CSIRO1; H: HadCM3; 2: 2020s; 5: 2050s; 8: 2080s.

Table 5.13: Mean monthly and annual runoff changes based on the simple perturbation approach and an extended approach employing a stochastic weather generator for baseline climate perturbation.

Month	% change in runoff based on simple perturbation approach	% change in runoff based on a stochastic weather generator for baseline climate perturbation	Absolute difference (%)
Jan	25.5	34.0	-9
Feb	4.5	5.7	-1
Mar	14.4	18.9	-5
Apr	-2.8	-3.5	1
May	-14.5	-23.6	9
Jun	-25.7	-34.8	9
Jul	-39.6	-47.2	8
Aug	-49.6	-59.5	10
Sep	-55.5	-65.8	10
Oct	-9.1	-29.9	21
Nov	-4.8	-4.3	0
Dec	25.8	33.0	-7
Ann.	-1.2	-2.6	1

Runoff changes based on the HadCM3 (2050s) scenario for Yorkshire

Table 5.14: Derived Streamflow perturbation factors for the Yorkshire sites for the 2020s based on HadCM3 and LARS weather generator - Detailed study.

Year	Jan	Feb	Mar	Apr	May	Jun	Jul	Aug	Sep	Oct	Nov	Dec
2011	0.94	0.92	1.47	1.19	1.08	1.18	0.54	0.38	0.55	0.72	0.83	0.93
2012	1.29	0.68	0.51	0.89	0.90	0.79	0.66	0.79	1.11	0.90	1.47	1.40
2013	1.37	0.98	1.51	1.67	0.89	0.78	1.64	0.64	1.13	0.97	0.81	0.96
2014	0.98	0.92	0.94	1.29	0.51	0.53	0.46	0.58	0.48	0.49	0.70	1.27
2015	0.78	0.69	1.47	1.83	1.25	0.91	0.65	0.51	0.57	0.64	0.67	0.75
2016	1.17	0.69	1.22	0.95	1.74	0.84	0.62	0.94	0.77	0.97	1.28	1.13
2017	1.01	1.34	0.83	1.04	1.78	0.78	0.69	0.37	0.72	0.71	1.13	1.25
2018	1.16	1.09	1.28	1.78	1.07	0.91	0.87	0.87	0.64	0.75	1.14	1.09
2019	1.19	1.19	1.04	0.79	0.99	0.55	0.71	1.19	0.77	0.80	1.31	1.19
2020	1.03	0.95	1.30	0.94	0.95	0.72	0.82	0.41	0.62	0.94	0.95	0.95
2021	1.22	0.81	0.73	0.58	1.19	0.69	0.70	1.02	0.61	0.74	1.34	1.35
2022	1.18	0.65	1.16	1.16	0.72	0.62	1.13	0.84	1.05	0.92	0.61	0.83
2023	1.21	0.69	1.16	1.21	1.27	0.52	0.35	0.48	0.44	0.32	0.84	0.85
2024	1.02	1.05	0.90	0.94	0.86	0.71	0.58	1.02	1.29	0.67	1.18	1.04
2025	1.08	0.77	0.64	1.06	0.95	0.77	1.19	1.13	0.65	0.66	1.03	1.14
2026	0.83	0.99	1.07	1.06	0.82	0.74	0.36	0.41	0.57	1.29	1.11	1.37
2027	1.05	0.96	0.93	1.09	0.98	0.76	0.52	0.73	0.62	0.93	1.06	1.15
2028	1.27	0.69	0.91	1.58	1.01	0.53	0.92	0.77	0.88	0.82	1.09	0.87
2029	1.02	0.49	0.96	0.71	1.15	0.74	0.55	0.93	0.80	1.14	1.18	1.05
2030	1.32	1.03	1.09	1.30	0.90	0.64	0.56	0.47	0.71	1.12	1.14	1.33
2031	1.19	1.30	2.06	1.02	1.17	0.70	0.54	0.37	0.90	0.91	0.98	1.11
2032	0.81	0.74	0.66	1.12	1.74	1.36	0.81	1.22	1.12	0.98	1.12	1.56
2033	0.72	0.77	1.05	1.48	0.86	0.93	0.79	0.44	0.92	1.65	1.18	1.56
2034	1.41	1.02	0.87	0.82	0.83	0.42	0.70	0.70	0.56	0.61	1.15	0.99
2035	1.15	0.68	0.86	2.02	1.65	1.01	0.76	0.97	1.79	0.72	1.10	1.31
2036	1.09	0.85	0.87	0.68	1.00	0.42	0.35	0.82	0.89	1.02	1.22	0.96
2037	1.21	0.83	0.54	0.89	0.84	0.46	0.67	0.71	0.55	1.20	1.33	1.43
2038	1.17	0.84	1.35	1.02	1.08	1.13	0.68	0.40	0.62	0.96	1.12	1.08
2039	1.20	0.77	0.70	0.91	0.86	0.78	0.55	0.84	1.10	0.87	1.00	1.61

Note: Using these factors will ensure the needed variability in future streamflow

Table 5.15: Derived Streamflow perturbation factors for the Yorkshire sites for the 2050s based on HadCM3 and LARS weather generator - Detailed study.

Year	Jan	Feb	Mar	Apr	May	Jun	Jul	Aug	Sep	Oct	Nov	Dec
2041	1.28	1.28	1.85	0.99	0.93	1.48	0.56	0.21	0.24	0.83	1.03	0.96
2042	1.70	0.79	0.85	0.96	0.69	0.77	0.48	0.41	0.62	0.81	1.41	1.49
2043	1.92	1.25	1.54	0.95	0.60	0.51	0.77	0.52	0.65	1.10	0.81	1.26
2044	1.58	1.01	0.77	0.90	0.77	0.67	0.54	0.43	0.33	0.65	0.72	1.36
2045	1.33	0.86	1.41	1.93	1.47	1.15	0.61	0.31	0.23	0.45	0.50	1.19
2046	1.33	0.83	1.53	1.51	1.72	0.59	0.51	0.43	0.41	0.49	0.86	1.53
2047	1.33	1.25	1.10	0.83	0.92	0.85	0.51	0.30	0.28	0.58	1.31	1.41
2048	1.11	1.61	1.21	1.00	0.57	0.45	0.64	0.44	0.35	0.60	1.14	1.29
2049	1.71	1.41	1.30	0.78	0.68	0.47	0.53	0.54	0.35	0.79	1.15	1.09
2050	1.55	1.20	1.55	1.09	0.82	0.84	0.61	0.35	0.29	0.44	0.85	1.35
2051	1.26	0.98	1.02	1.01	1.50	0.59	0.55	0.47	0.29	0.40	0.59	1.69
2052	1.43	1.36	1.35	0.95	0.37	0.57	0.51	0.68	0.54	1.33	0.82	0.92
2053	1.34	0.65	1.28	1.30	0.60	0.59	0.29	0.53	0.35	0.41	1.04	1.14
2054	1.36	1.65	1.41	0.73	0.54	0.48	0.57	0.43	0.33	0.47	1.12	0.89
2055	1.10	0.75	0.77	0.89	0.57	0.86	0.76	0.54	0.30	0.50	1.02	1.40
2056	1.39	1.21	1.33	0.68	0.56	0.92	0.33	0.40	0.34	1.16	0.94	1.35
2057	1.32	1.03	1.15	0.53	0.50	0.63	0.59	0.47	0.23	0.84	1.34	1.13
2058	1.07	0.91	0.99	1.09	0.74	0.47	0.45	0.40	0.27	0.76	0.88	1.62
2059	1.20	0.93	1.26	0.54	0.95	0.91	0.48	0.74	0.61	0.80	1.02	1.24
2060	1.69	1.32	1.09	1.14	0.89	0.93	0.64	0.24	0.32	0.80	0.91	1.51
2061	1.57	1.25	3.10	1.07	1.02	0.51	0.63	0.32	0.20	0.68	1.10	1.44
2062	1.23	0.92	0.94	1.19	1.01	1.33	0.54	0.51	0.39	0.68	1.19	1.40
2063	0.98	1.07	1.15	1.19	1.00	0.72	0.76	0.34	0.41	0.98	0.97	1.13
2064	1.44	0.97	1.03	0.84	0.62	0.30	0.48	0.50	0.45	0.79	0.98	1.30
2065	1.29	0.72	1.23	1.93	1.11	0.73	0.48	0.50	0.50	1.02	1.48	1.41
2066	1.12	1.47	1.67	1.01	0.97	0.40	0.37	0.39	0.17	0.79	0.89	1.62
2067	1.11	0.92	0.67	0.86	0.74	0.38	0.61	0.36	0.31	0.73	1.02	1.32
2068	1.44	0.82	1.11	0.94	0.44	0.65	0.50	0.29	0.31	0.98	0.90	2.13
2069	1.28	0.99	1.18	0.66	0.63	0.68	0.54	0.58	0.38	0.75	0.68	1.62

Note: Using these factors will ensure the needed variability in future streamflow

Table 5.16: Derived Streamflow perturbation factors for the Yorkshire sites for the 2080s based on HadCM3 and LARS weather generator - Detailed study.

Year	Jan	Feb	Mar	Apr	May	Jun	Jul	Aug	Sep	Oct	Nov	Dec
2071	1.37	1.44	1.70	1.42	1.32	1.37	0.62	0.25	0.33	0.93	0.80	0.85
2072	1.55	0.81	0.87	1.11	0.70	0.91	0.61	0.37	0.62	0.92	1.54	1.54
2073	1.80	1.44	1.40	1.41	0.85	0.65	0.83	0.48	0.61	0.81	1.22	1.33
2074	1.57	1.05	0.69	1.43	0.86	0.44	0.40	0.35	0.33	0.44	0.80	0.92
2075	1.42	0.95	1.69	2.83	1.68	0.96	0.51	0.25	0.26	0.33	0.80	1.04
2076	1.44	1.11	1.03	1.22	1.48	0.53	0.45	0.43	0.66	0.82	1.32	1.09
2077	1.43	1.68	1.24	1.23	0.98	0.69	0.37	0.31	0.37	0.85	1.39	1.53
2078	1.07	1.93	1.19	1.29	1.02	0.78	0.52	0.68	0.70	1.09	1.32	0.96
2079	1.84	1.49	1.34	1.01	0.82	0.45	0.55	0.77	0.35	0.68	1.83	1.26
2080	1.41	1.02	1.65	0.72	0.73	0.84	0.45	0.36	0.36	0.47	0.96	1.02
2081	1.36	1.18	0.91	0.74	0.95	0.80	0.38	0.59	0.42	0.89	1.38	1.49
2082	1.19	1.17	1.31	0.95	0.36	0.63	0.54	0.53	0.50	1.48	1.00	1.19
2083	1.27	0.89	0.71	1.04	0.73	0.67	0.29	0.39	0.32	0.83	1.34	1.26
2084	1.39	2.01	1.46	0.89	0.82	0.46	0.43	0.44	0.38	0.64	1.05	0.98
2085	1.34	1.02	0.86	1.11	0.56	0.48	0.49	0.52	0.48	1.12	1.47	1.70
2086	1.20	1.38	0.72	1.01	0.74	1.07	0.34	0.31	0.44	1.48	0.92	1.17
2087	1.23	1.09	1.21	1.28	0.90	0.67	0.38	0.42	0.28	0.59	1.06	1.05
2088	1.34	1.23	0.91	1.26	0.68	0.40	0.30	0.44	0.39	0.83	0.89	1.40
2089	1.46	1.00	1.34	0.89	0.89	0.67	0.42	0.62	0.34	1.83	1.87	1.15
2090	1.76	1.49	1.02	1.15	1.06	0.93	0.50	0.22	0.30	1.10	1.71	1.73
2091	1.74	1.14	2.86	1.46	1.32	0.60	0.50	0.43	0.35	0.84	0.90	1.30
2092	1.22	1.09	0.81	1.46	1.48	1.10	0.72	0.58	0.44	0.55	0.75	1.77
2093	1.06	1.09	1.04	1.11	1.46	0.82	0.72	0.40	0.56	1.24	1.30	1.31
2094	1.27	1.42	0.66	1.06	0.76	0.36	0.43	0.36	0.35	1.07	1.05	1.13
2095	1.46	1.01	0.93	1.29	1.28	1.05	0.62	0.53	0.52	1.37	1.91	1.52
2096	1.25	1.22	1.36	1.10	1.02	0.42	0.32	0.46	0.28	0.68	0.86	1.23
2097	1.46	0.73	0.72	0.90	1.12	0.57	0.48	0.32	0.29	0.58	0.98	1.55
2098	1.53	1.15	1.40	1.33	0.49	0.65	0.50	0.46	0.74	1.01	0.99	1.38
2099	1.21	0.88	1.07	0.93	0.87	0.74	0.43	0.67	0.35	0.50	0.81	1.70

Note: Using these factors will ensure the needed variability in future streamflow

Table 5.17: 1-month low flow exceeded 95% of the time (Q_{95}) in Yorkshire - based on HadCM3 - Detailed study.

Time -period	Flow ($x\ 10^3\ m^3$)	% change from baseline
Baseline	778.83	
2020s	583.47	-25
2050s	509.84	-35
2080s	487.50	-37

Table 5.18: Baseline (1962-1990) and HadCM3 2050s simulated groundwater recharge (GWR) and baseflow (BF) for Yorkshire aggregated system - Detailed study.

Month	Baseline (1962-1990)		HadCM3 2050s		% change from baseline	
	GWR (mm)	BF (mm)	GWR (mm)	BF (mm)	GWR	BF
Jan	80.0	5.1	111.4	6.2	39.3	21.8
Feb	53.1	4.2	56.4	4.6	6.1	9.0
Mar	53.5	4.4	69.1	4.9	29.2	9.7
Apr	29.0	3.4	25.9	3.5	-10.4	2.7
May	12.9	2.8	8.0	2.4	-37.9	-15.2
Jun	10.8	2.4	5.0	1.9	-53.7	-20.6
Jul	9.8	2.3	2.4	1.7	-75.7	-23.3
Aug	17.3	2.5	3.3	1.8	-80.9	-30.1
Sep	24.9	2.8	4.6	1.8	-81.7	-37.0
Oct	52.2	3.5	32.1	3.2	-38.6	-10.1
Nov	65.7	4.0	55.4	4.2	-15.7	4.1
Dec	79.1	4.9	116.0	6.1	46.7	23.4
Ann	488.3	42.3	489.6	42.0	0.3	-0.7

GWR: groundwater recharge
BF: baseflow

Table 5.19: Percentage change in yield (from baseline) for the Yorkshire grouped reservoir system resulting from different scenarios - Detailed study.

Reliability (%)	Scenario	Single Record Method	Monte Carlo Method			
			Mean	Minimum	Maximum	Median
100	C2	-1.8	-2.6	-14.9	8.7	-2.7
	C5	2.0	0.9	-7.8	18.7	0.7
	C8	2.8	0.6	-9.1	13.2	0.5
	A2	10.5	5.9	-3.0	21.1	5.8
	A5	9.5	5.5	-4.7	19.9	5.3
	A8	**10.9**	9.7	-0.3	**28.3**	9.4
	H2	-1.2	-3.7	-12.5	7.4	-4.0
	H5	**-8.2**	-10.9	**-19.2**	5.7	-11.1
	H8	-3.7	-6.9	-17.8	8.5	-7.1
	H5P	-8.2	-8.8	-17.2	-0.3	-8.7
	H5T	-2.3	-5.3	-16.5	8.4	-5.5
	H5M	-7.5	-10.3	-18.9	5.5	-10.5
98	C2	-3.0	-3.4	-7.5	2.1	-3.5
	C5	-0.5	0.3	-4.3	11.3	0.1
	C8	0.5	0.7	-6.1	8.5	0.6
	A2	5.5	5.0	1.2	12.7	4.9
	A5	6.4	5.4	-0.1	15.3	5.2
	A8	**11.1**	9.1	2.5	**18.5**	8.9
	H2	-4.2	-4.6	-8.6	4.0	-4.8
	H5	**-10.5**	-10.7	**-14.1**	-0.6	-10.9
	H8	-6.1	-6.7	-11.2	5.1	-6.8
	H5P	-8.0	-8.0	-13.5	-0.8	-8.0
	H5T	-7.5	-7.1	-11.2	1.7	-7.4
	H5M	-10.2	-10.1	-13.6	0.0	-10.3

Bold font indicates extreme changes in yield
C: CGCM1, A: CSIRO1, H: HadCM3, 2: 2020s, 5: 2050s, 8: 2080s, P: simple perturbation approach, T: stomatal resistance effects, M: GCM simulated PE.

Table 5.20: Parameter estimates of the three-parameter log-normal distribution used for fitting 1000 yield changes - Detailed study.

Parameter	Abbreviation	Estimate
Estimate of lower bound quantile	$\tilde{\tau}$	-26.76
Moment estimate of mean	μ_{ln}	2.75
Moment estimate of variance	σ^2_{ln}	0.0329

Table 5.21: Percentage change in storage (from baseline) for the Yorkshire system resulting from different scenarios - Detailed study.

Reliability (%)	Scenario	Single Record Method	Monte Carlo Method			
			Mean	Minimum	Maximum	Median
100	A2	-20.5	-12.6	-54.1	60.9	-14.4
	A5	-19.4	-10.9	-53.3	59.0	-12.8
	A8	**-26.6**	-16.1	**-61.2**	43.9	-16.9
	H2	31.6	41.4	-17.9	105.2	40.9
	H5	**73.7**	92.2	16.1	**167.2**	92.7
	H8	63.0	80.6	2.2	147.4	81.2
	H5P	63.3	72.4	4.5	181.6	71.6
	H5T	55.5	70.7	8.9	132.5	71.1
	H5M	71.0	89.3	14.6	164.2	89.6
	H5D	126.0	148.2	49.1	250.1	148.4
98	A2	-25.0	-25.9	-50.7	12.3	-26.1
	A5	-16.7	-18.0	-43.1	20.3	-18.9
	A8	**-29.7**	-29.9	**-61.4**	1.2	-30.4
	H2	56.6	55.2	7.0	118.2	54.4
	H5	**122.5**	131.2	68.3	**198.0**	130.3
	H8	109.2	115.5	60.9	193.1	115.2
	H5P	96.1	100.2	61.1	154.3	99.2
	H5T	91.6	97.6	44.6	160.7	97.1
	H5M	121.1	127.4	64.2	194.4	126.5
	H5D	193.5	201.8	119.7	290.8	200.5

Bold fonts indicate extreme changes in storage
A: CSIRO1, H: HadCM3, 2: 2020s, 5: 2050s, 8: 2080s, P: simple perturbation approach, T: stomatal resistance effects, M: GCM simulated PE, D: 17% demand rise.

Table 5.22: Percentage difference (from baseline) in reservoir resilience for different reliabilities based on the HadCM3 2050s climate change scenario - Detailed study.

Approach	Time-based reliability (%)			
	95	96	97	98
Single record	28.6	30.0	28.6	23.5
Monte Carlo				
Mean	-22.2	-19.3	-13.9	-7.1
Minimum	-53.0	-50.0	-40.0	-43.0
Maximum	38.0	39.0	50.0	60.0
Median	-24.0	-21.0	-20.0	-14.0

Demand = 30% MAF

Table 5.23: Climate change impact on reservoir control curves for the Yorkshire grouped reservoir system - Detailed study.

Month	Traditional (single record) approach		Extended (Monte Carlo) approach*	
	δ=100%	δ=98%	δ=100%	δ=98%
Jan	-9	11	-4	19
Feb	24	49	28	60
Mar	28	53	31	64
Apr	30	56	33	66
May	30	57	33	68
Jun	28	59	33	71
Jul	25	65	33	77
Aug	18	73	30	87
Sep	-5	48	9	61
Oct	-52	-40	-40	-36
Nov	-65	-63	-57	-60
Dec	-51	-43	-44	-37

Values are the % difference from (1961-1990) baseline in minimum allowable storage levels as a result of the HadCM3 2050s scenario
δ = time-based reliability
* average of 1000 replicates

Table 5.24: Summary of assessed climate change impacts in Yorkshire obtained in the Preliminary, Intermediate and Detailed studies.

Study	Perturbation approach	Catchment rainfall-runoff response model	GCM	Scenario	ΔP	ΔE	ΔR	ΔD
Preliminary	Mean monthly factors	Runoff coefficient Equation (3.21)	HadCM1	H120	6.8	42.5	7.2	1.7
				H150	4.1	5.8	8.7	-1.1
			HadCM2	GG1m	4.4	-15.5	8.4	4.1
				GS1m	2.7	5.6	3.7	2.0
				GS1t	2.0	-7.0	3.4	1.7
Intermediate	Mean monthly factors	Monthly water balance model	HadCM2	GS1m	2.7	5.6	3.4	2.3
				GS1t	2.0	-7.0	3.5	2.3
				UKCIP98	3.4	22.6	3.0	1.2
Final	Stochastic weather generation	Daily water balance model	HadCM3	H2	-4.7	1.3	-4.1	-1.2
				H5	-5.7	0.4	-2.6	-8.2
				H8	-1.7	1.3	3.0	-3.7
	Mean monthly factors			H5	-5.7	0.4	-1.2	-8.2

Results based on single records approach
ΔP, ΔE, and ΔR are respectively the annual changes (%) from baseline in precipitation , PE and runoff; and ΔD is % change from baseline in reservoir yield
time-based reliability = 100%
Values in bold font are provided to allow clear comparisons between results of studies adopting different rainfall-runoff modelling and climate perturbation schemes.

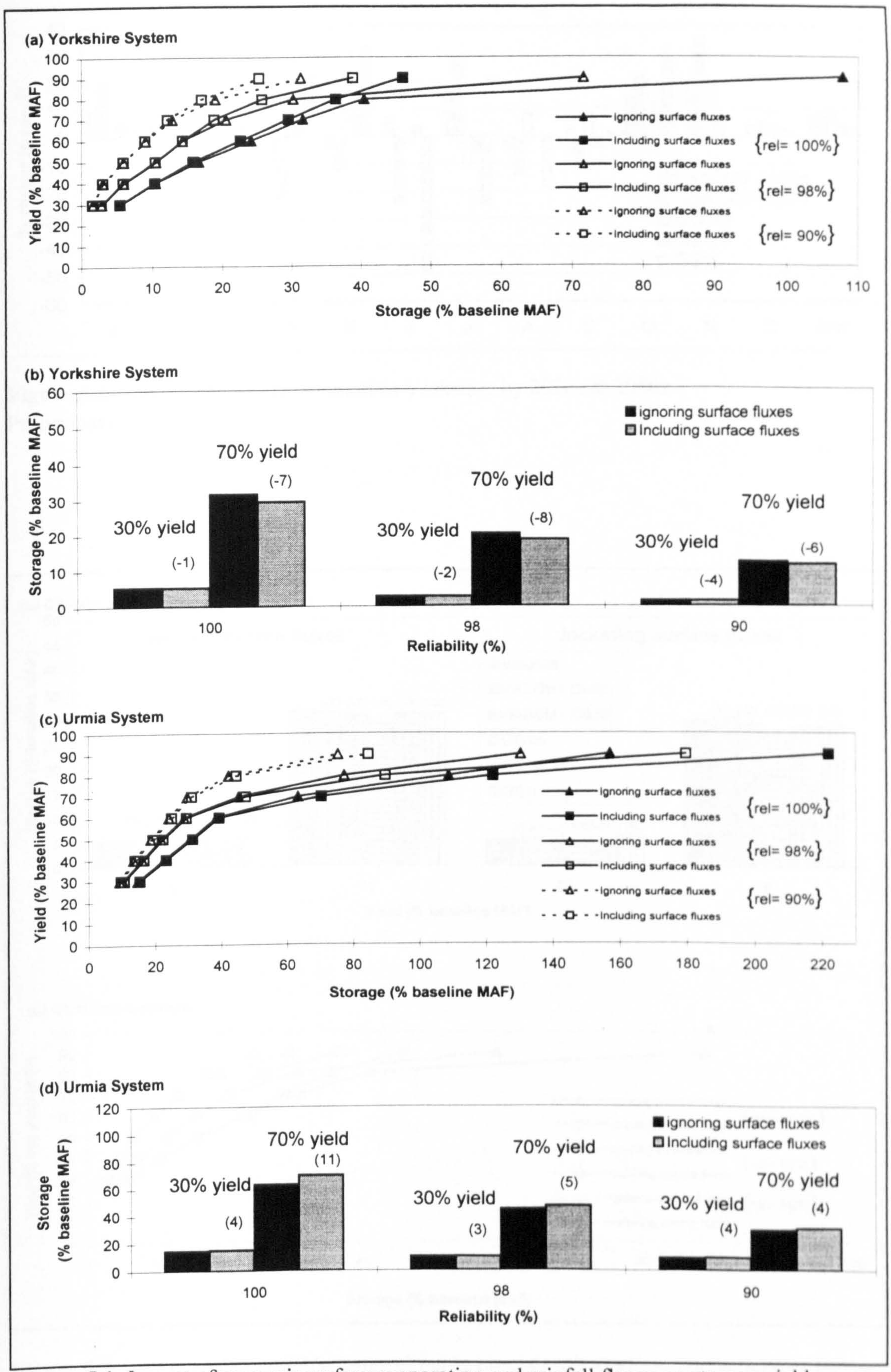

Figure 5.1: Impact of reservoir surface evaporation and rainfall fluxes on storage-yield-reliability relationship (baseline records). Values in parenthesis in (b) and (d) are % difference in storage due to incorporation of surface fluxes - Preliminary study.

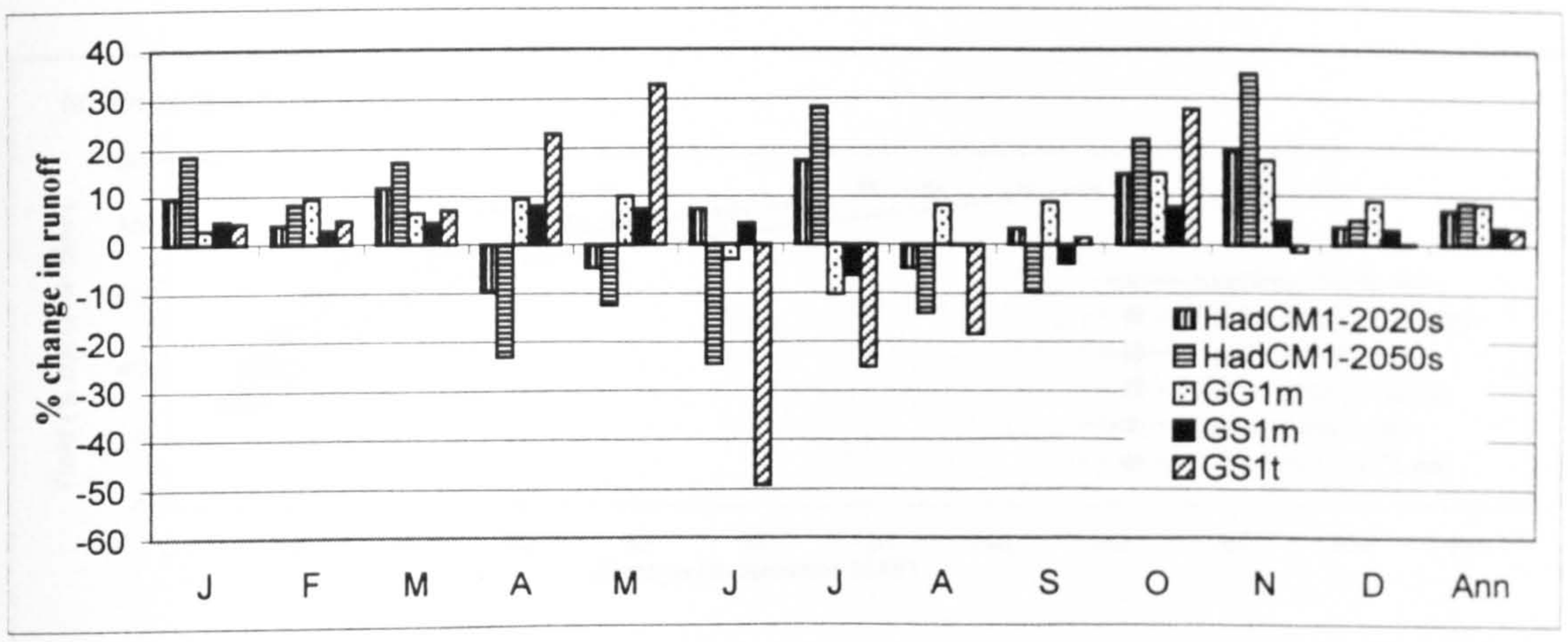

Figure 5.2: Percentage change in runoff in Yorkshire by 2020s & 2050s - Preliminary study.

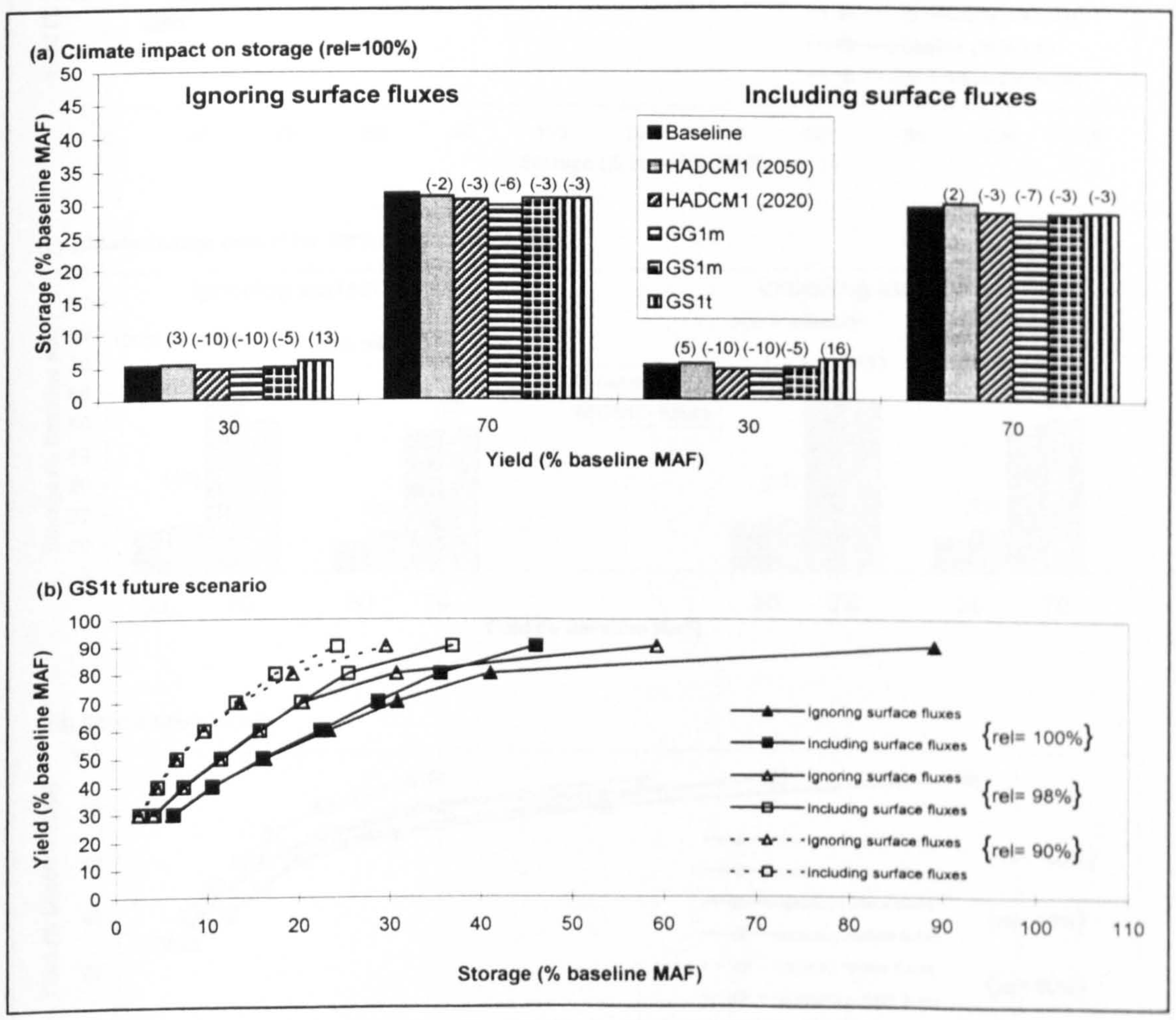

Figure 5.3: Impact of five possible future climates on reservoir storage-yield-reliability for the Yorkshire system. Values in parenthesis in (c) are % difference in storage from - Preliminary study.

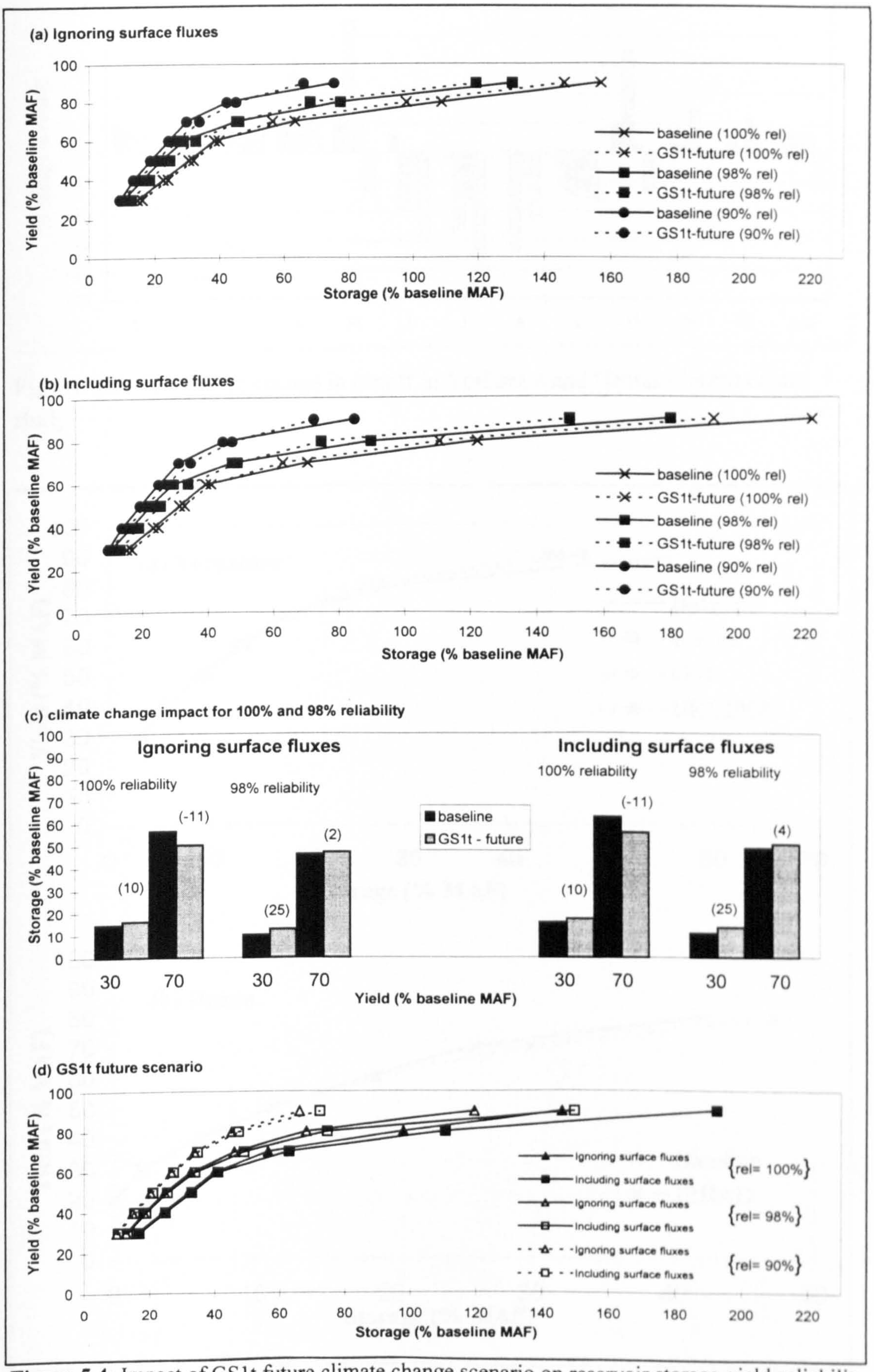

Figure 5.4: Impact of GS1t future climate change scenario on reservoir storage-yield-reliability for Urmia system. Values in parenthesis in (c) are the % difference in storage from baseline - Preliminary study.

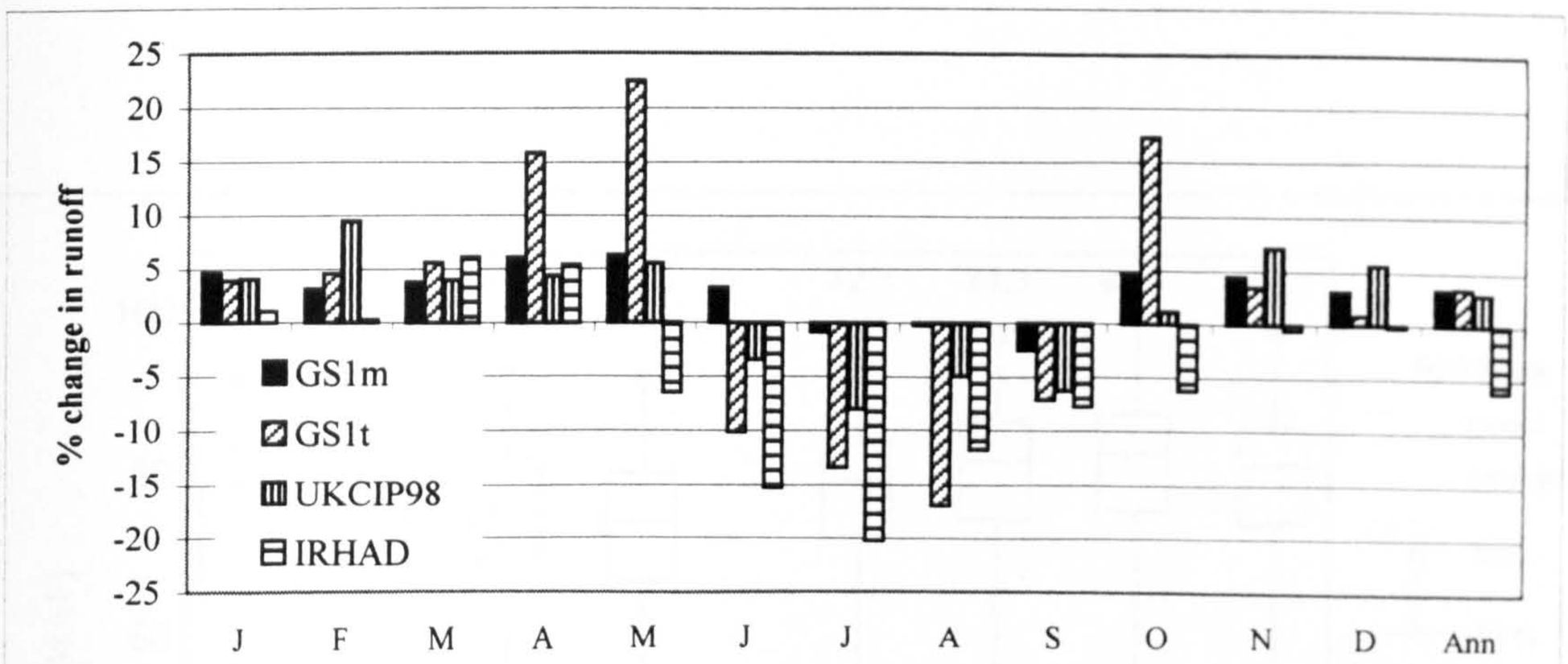

Figure 5.5: Percentage change in runoff in Yorkshire and Urmia - Intermediate study.

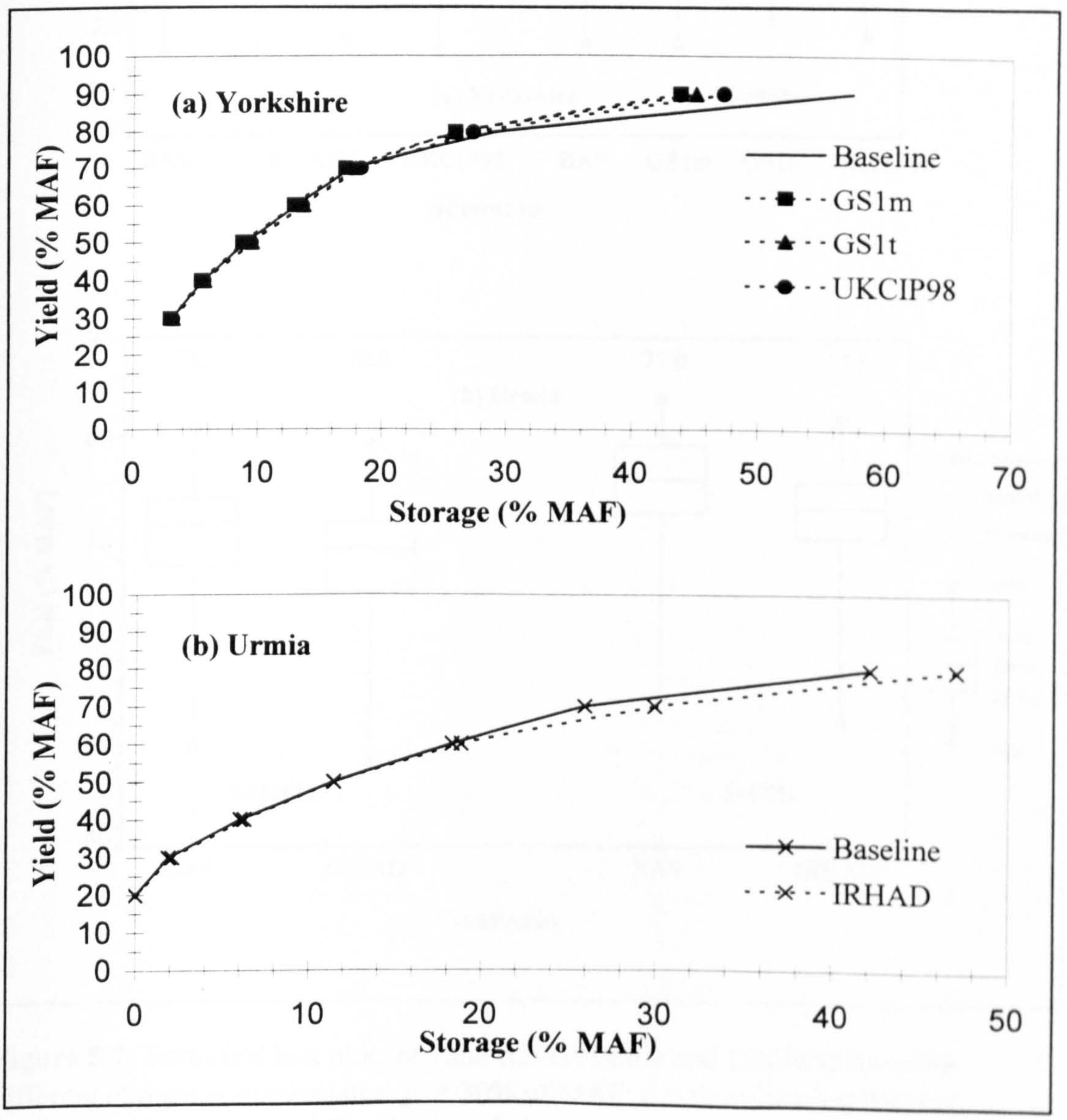

Figure 5.6: Climate change impact on storage-yield curves in Yorkshire and Urmia by the 2020s - Intermediate study.

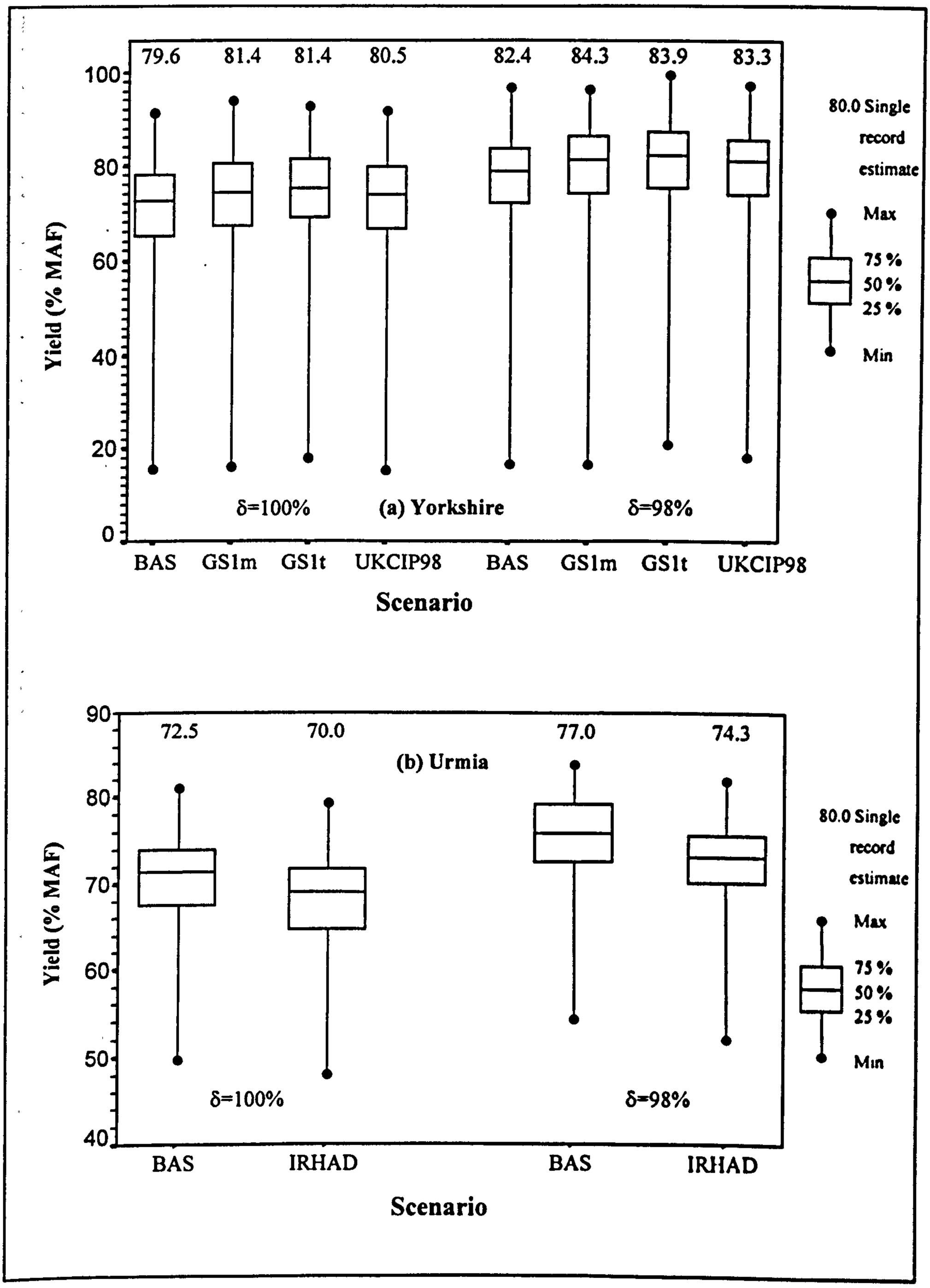

Figure 5.7: Empirical box plots of yield for Yorkshire and Urmia systems for different climate scenarios (storage = 30% of MAF; δ = time-based reliability; BAS = baseline (1961-1990)) – Intermediate study.

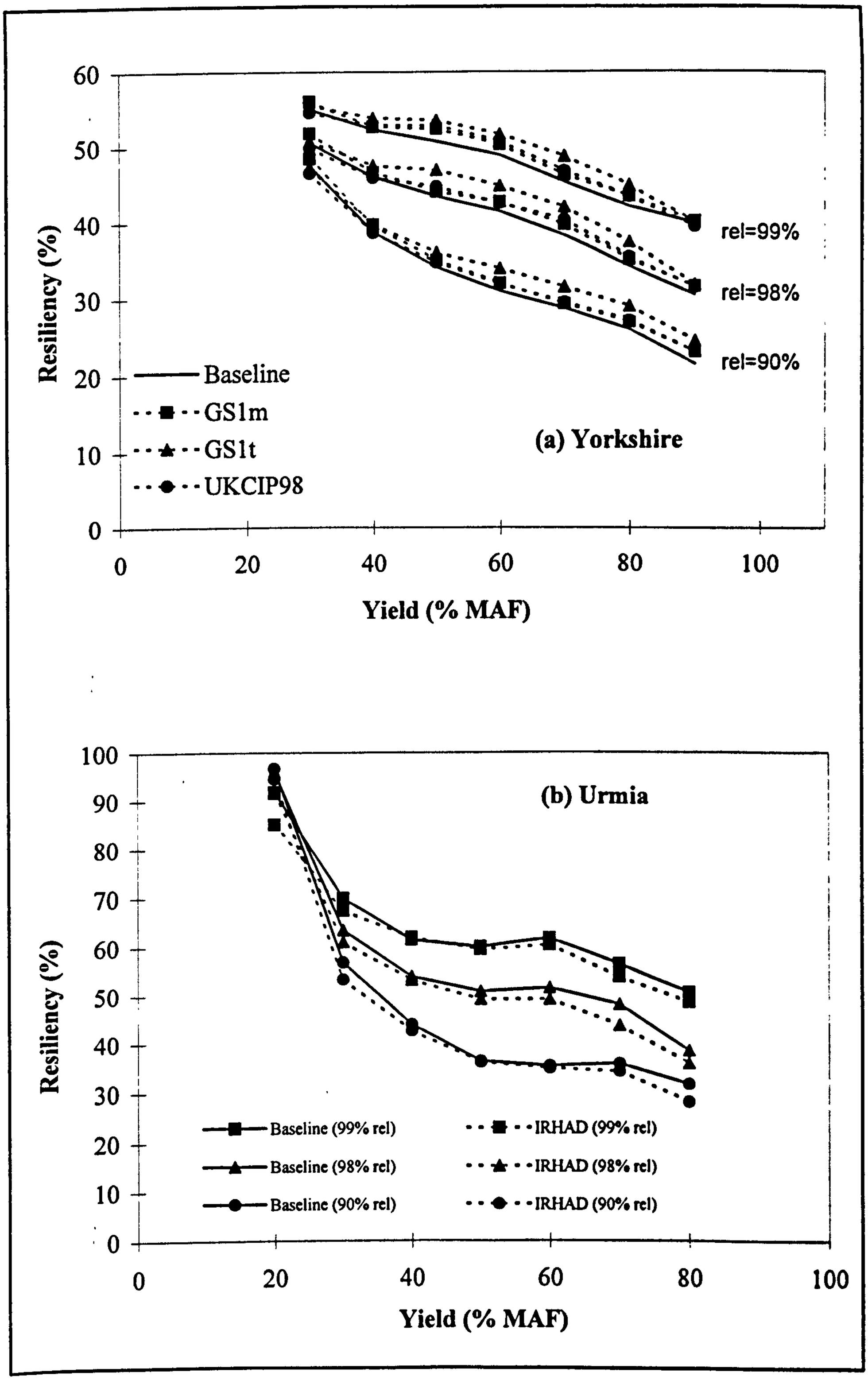

Figure 5.8: Climate change impact on reservoir resilience for Yorkshire and Urmia reservoir systems - Intermediate study.

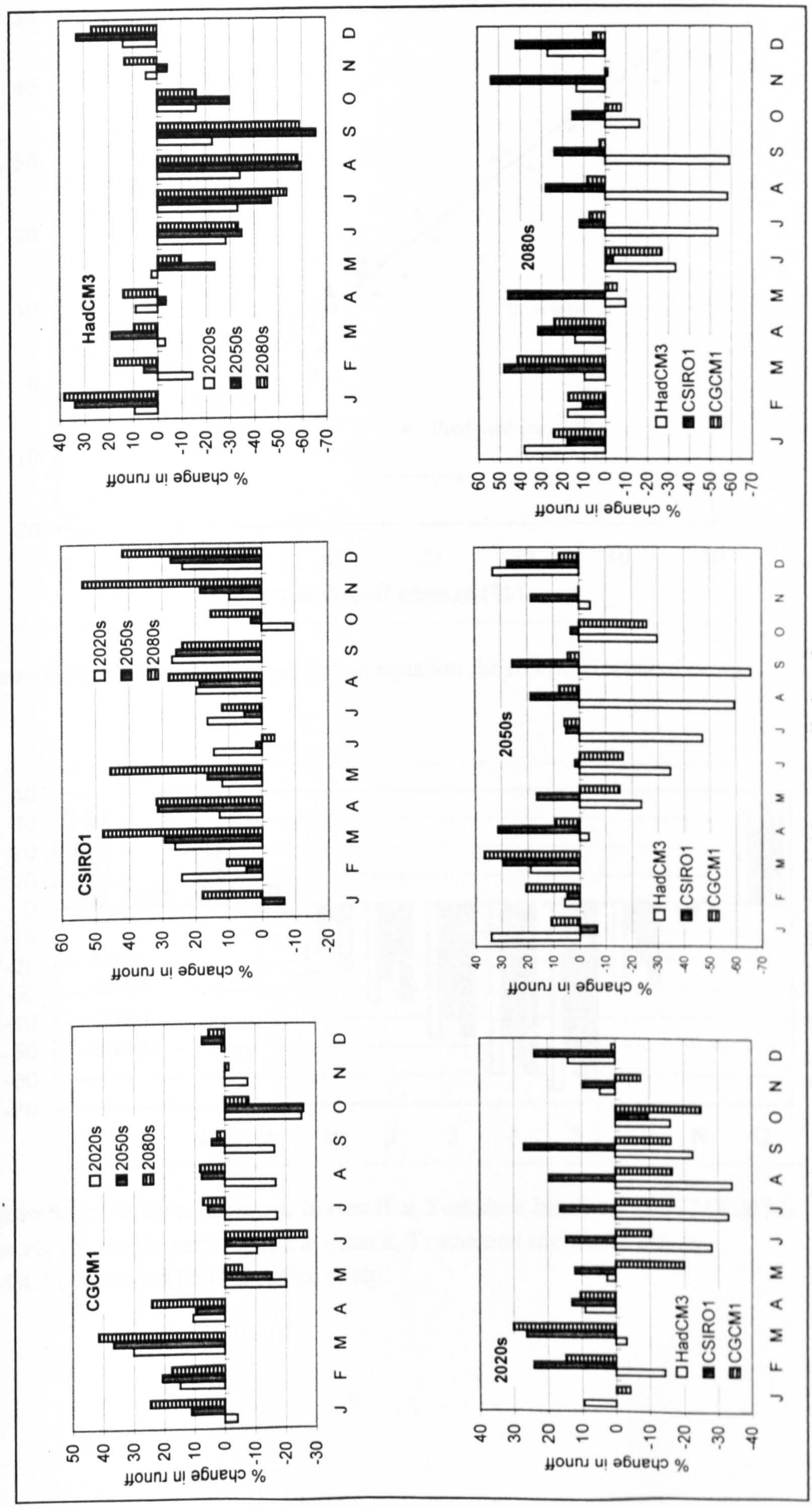

Figure 5.9: Percentage change in mean monthly runoff in Yorkshire - Detailed study.

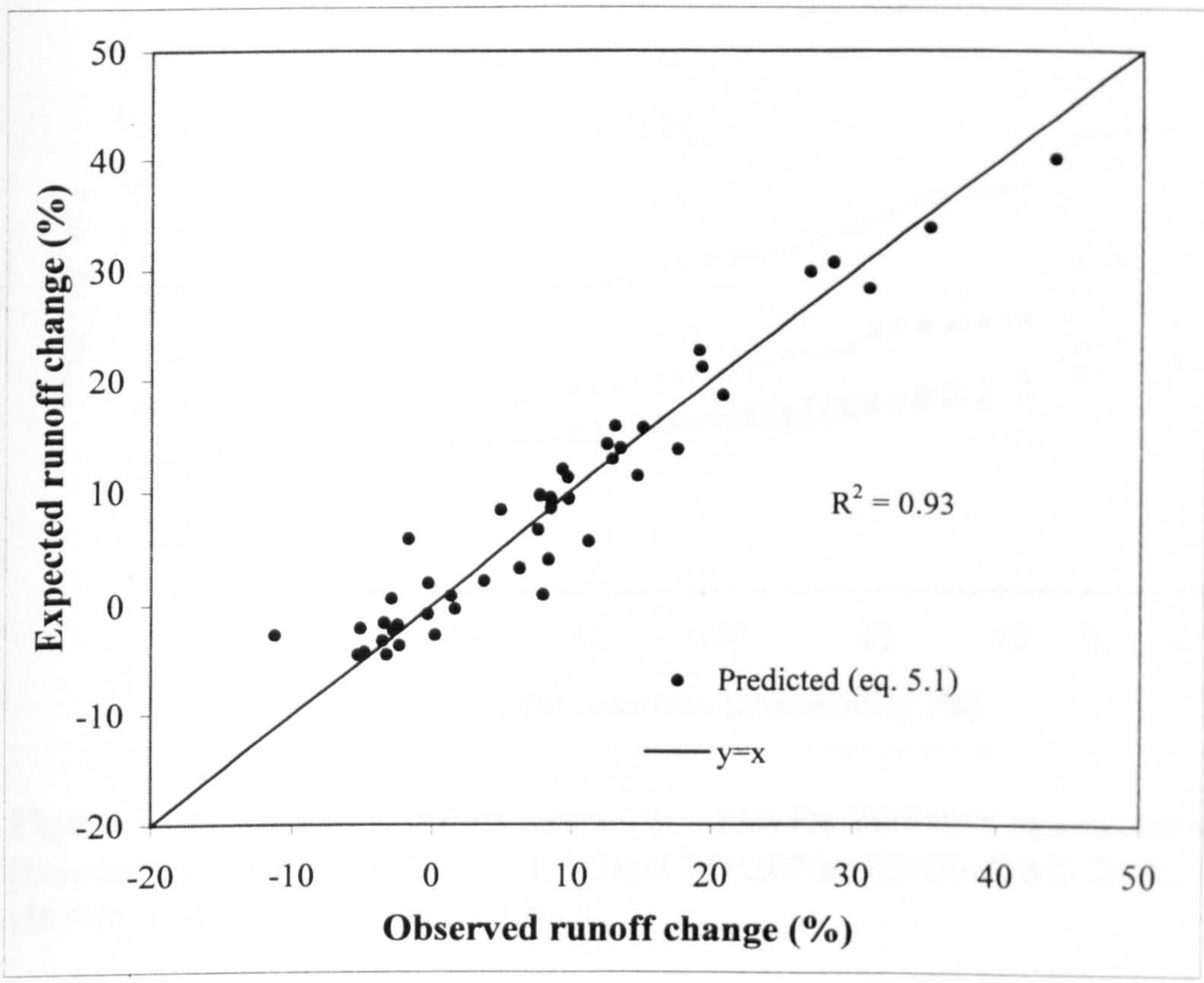

Figure 5.10: Performance of prediction equation for runoff - Detailed study.

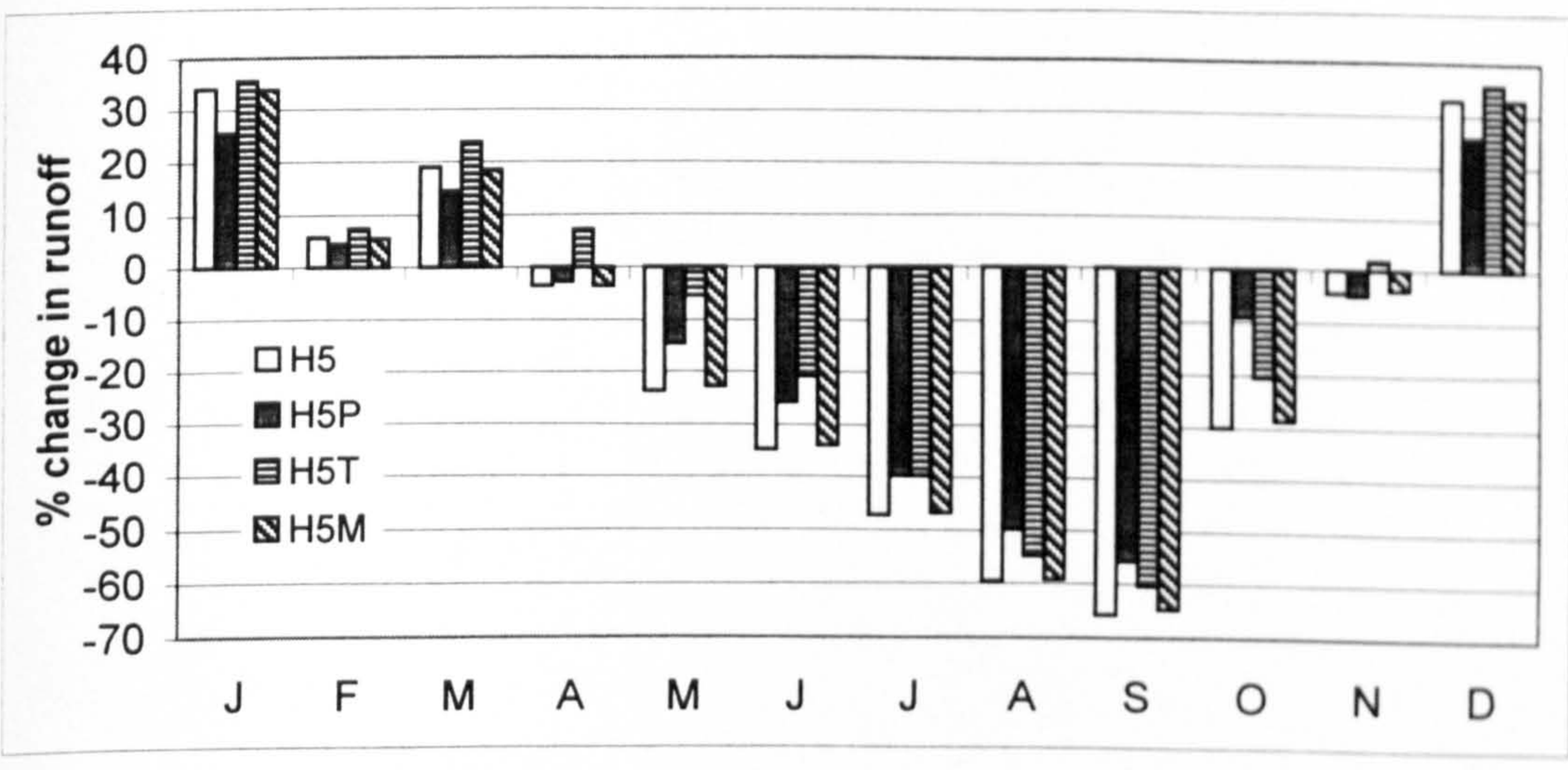

Figure 5.11: Percentage change in runoff in Yorkshire based on HadCM3 2050s scenario (P: simple perturbation approach, T: stomatal resistance effects, M: GCM simulated PE) - Detailed study.

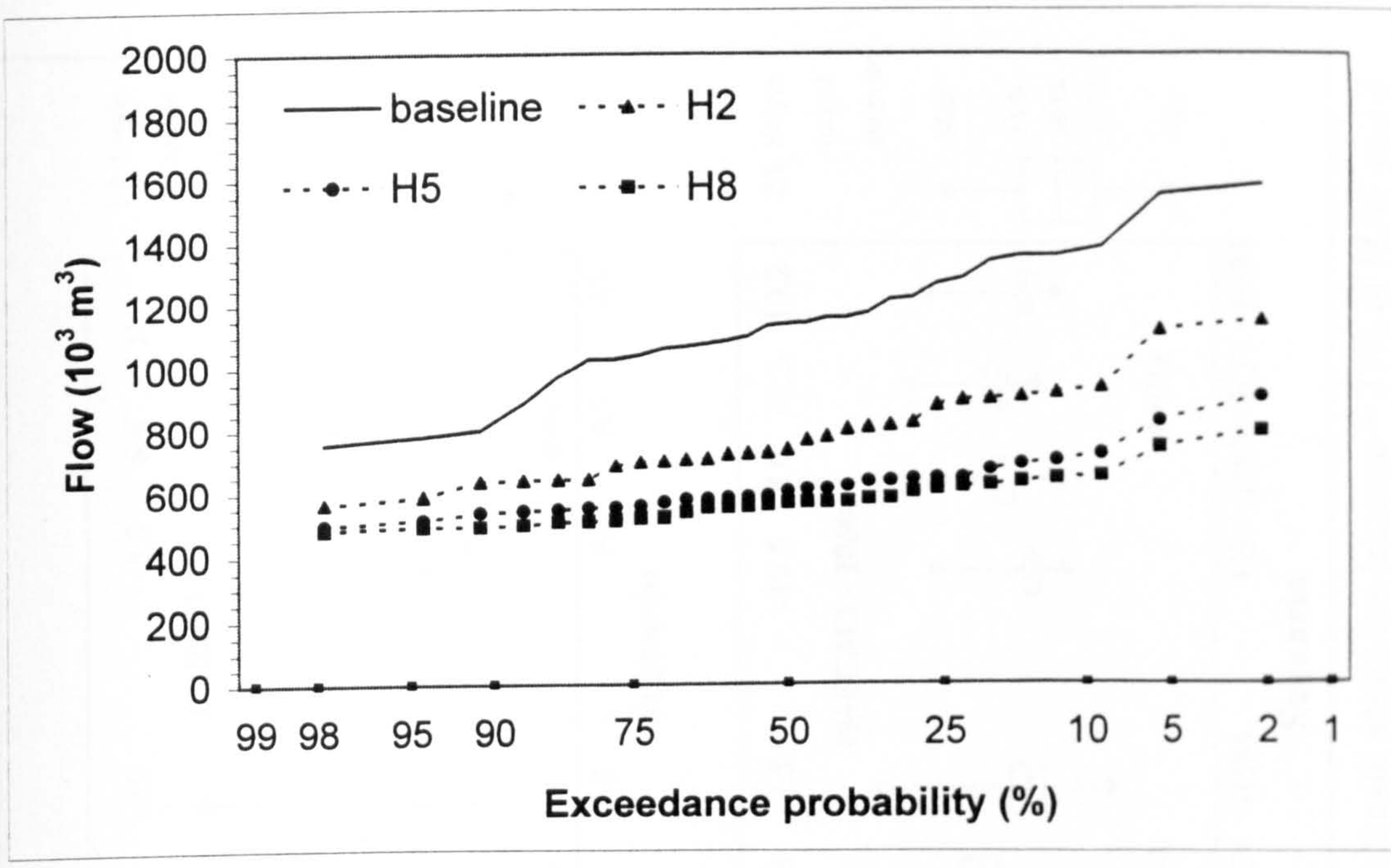

Figure 5.12: 1-month low flow frequency curves for Yorkshire aggregated system (Normal probability distribution; H2=HadCM3 2020s; H5=HadCM3 2050s; H8=HadCM3 2080s.) - Detailed study.

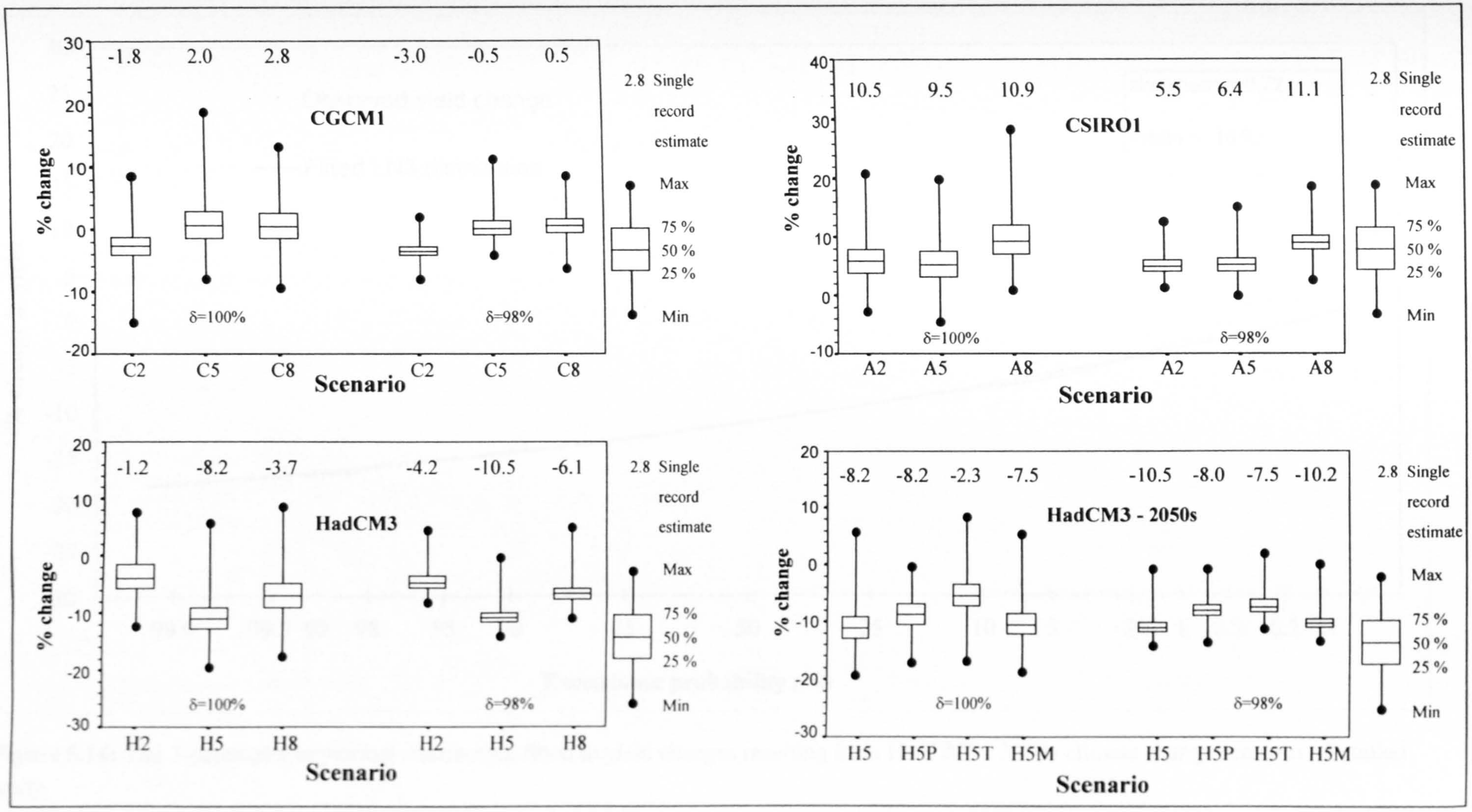

Figure 5.13: Empirical box plots of yield changes for Yorkshire aggregated system for different climate scenarios (storage = 31% of MAF and δ = time-based reliability; C = CGCM1; A = CSIRO1; H = HadCM3; 2 = 2020s; 5 = 2050s, 8 = 2080s; P = simple perturbation; T = stomatal resistance feedback; M = GCM simulated feedback) – Detailed study.

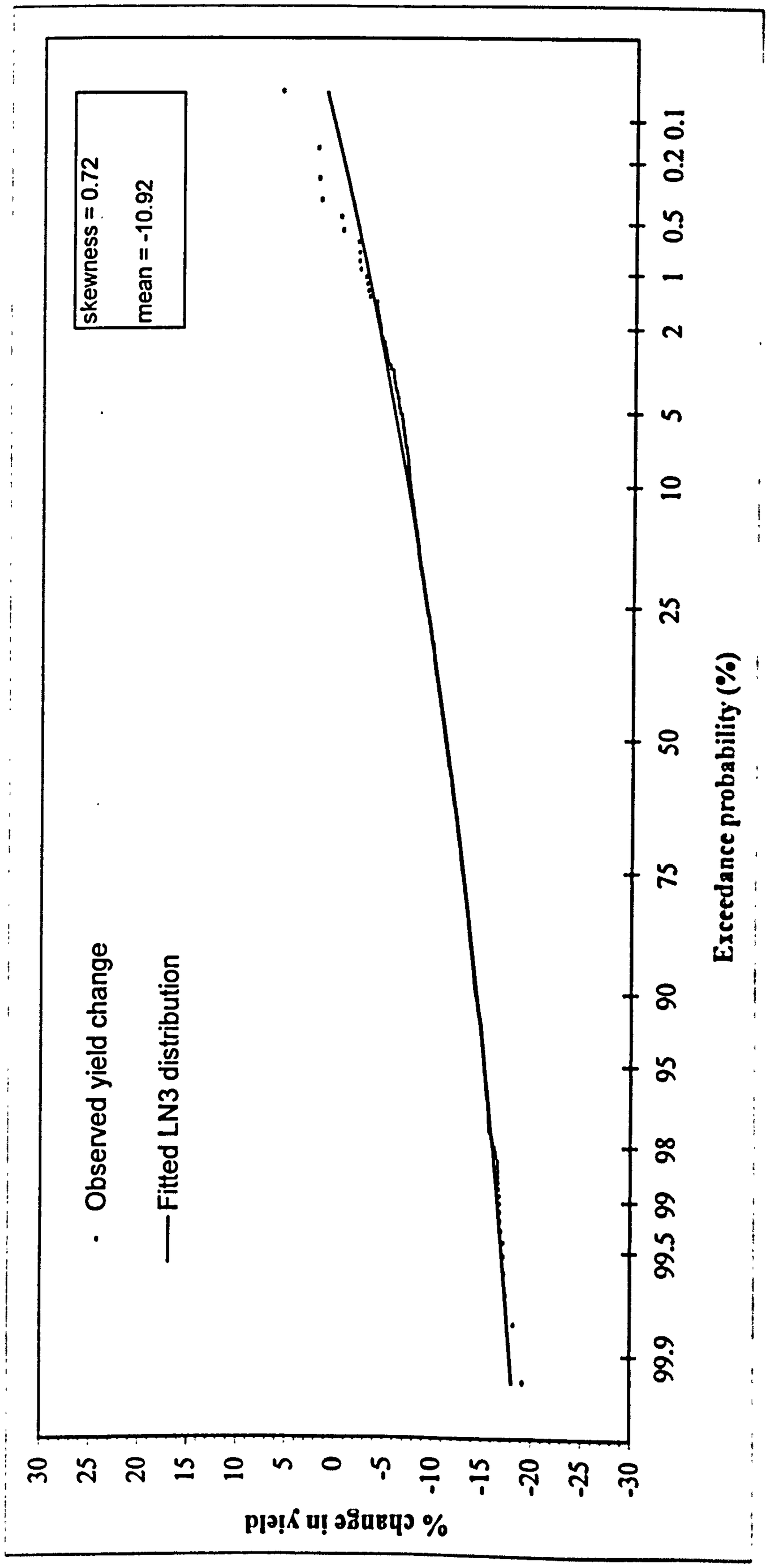

Figure 5.14: The 3-parameter lognomal distribution fitted to yield changes resulting from HadCM3 - 2050s climate change scenario - Detailed study.

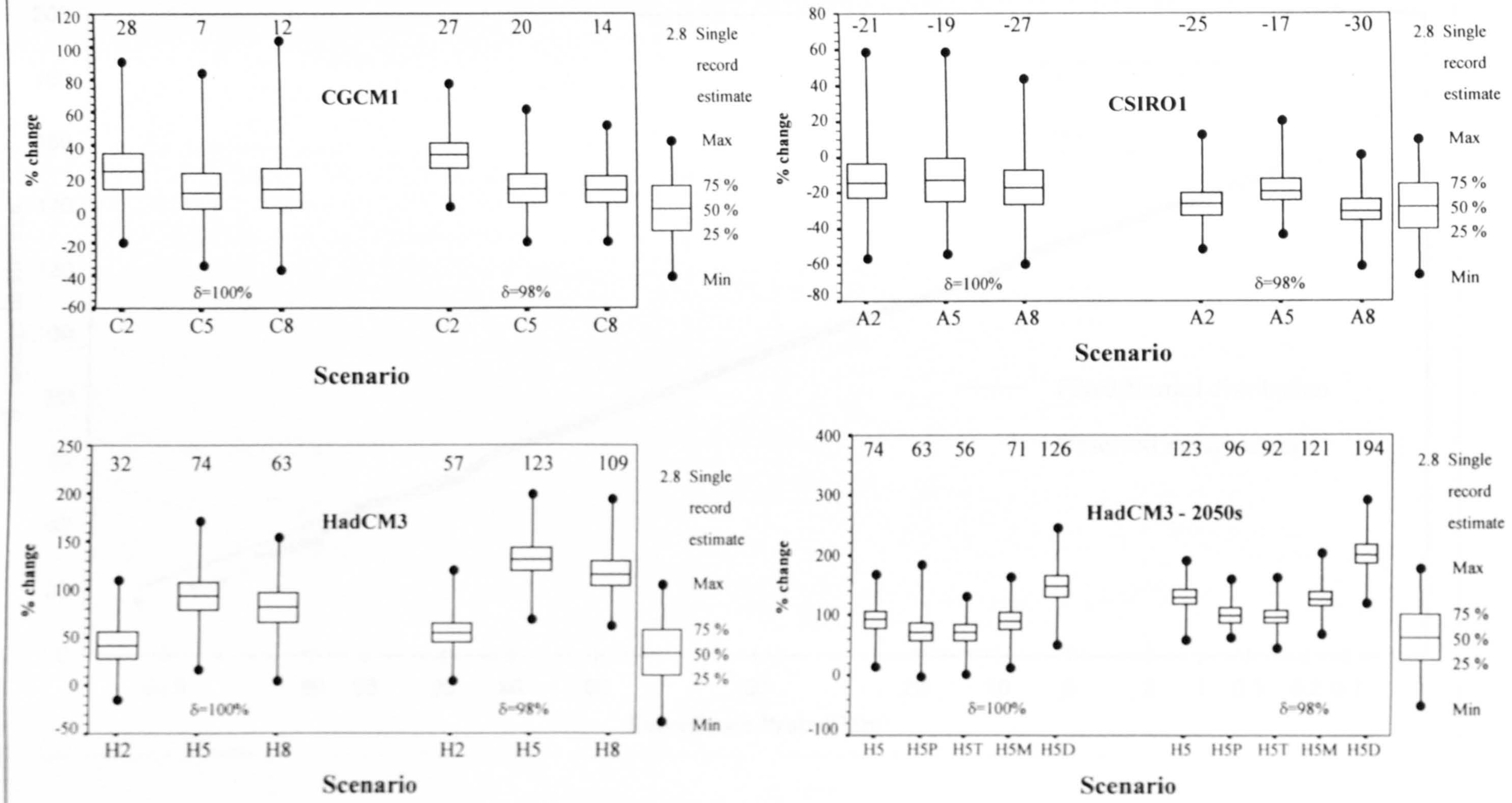

Figure 5.15: Empirical box plots of storage changes for Yorkshire aggregated system for different climate scenarios (demand = 60% of MAF and δ = time-based reliability; C = CGCM1; A = CSIRO1; H = HadCM3; 2 = 2020s; 5 = 2050s, 8 = 2080s; P = simple perturbation; T = stomatal resistance feedback; M = GCM simulated feedback; D = 17% demand rise) – Detailed study.

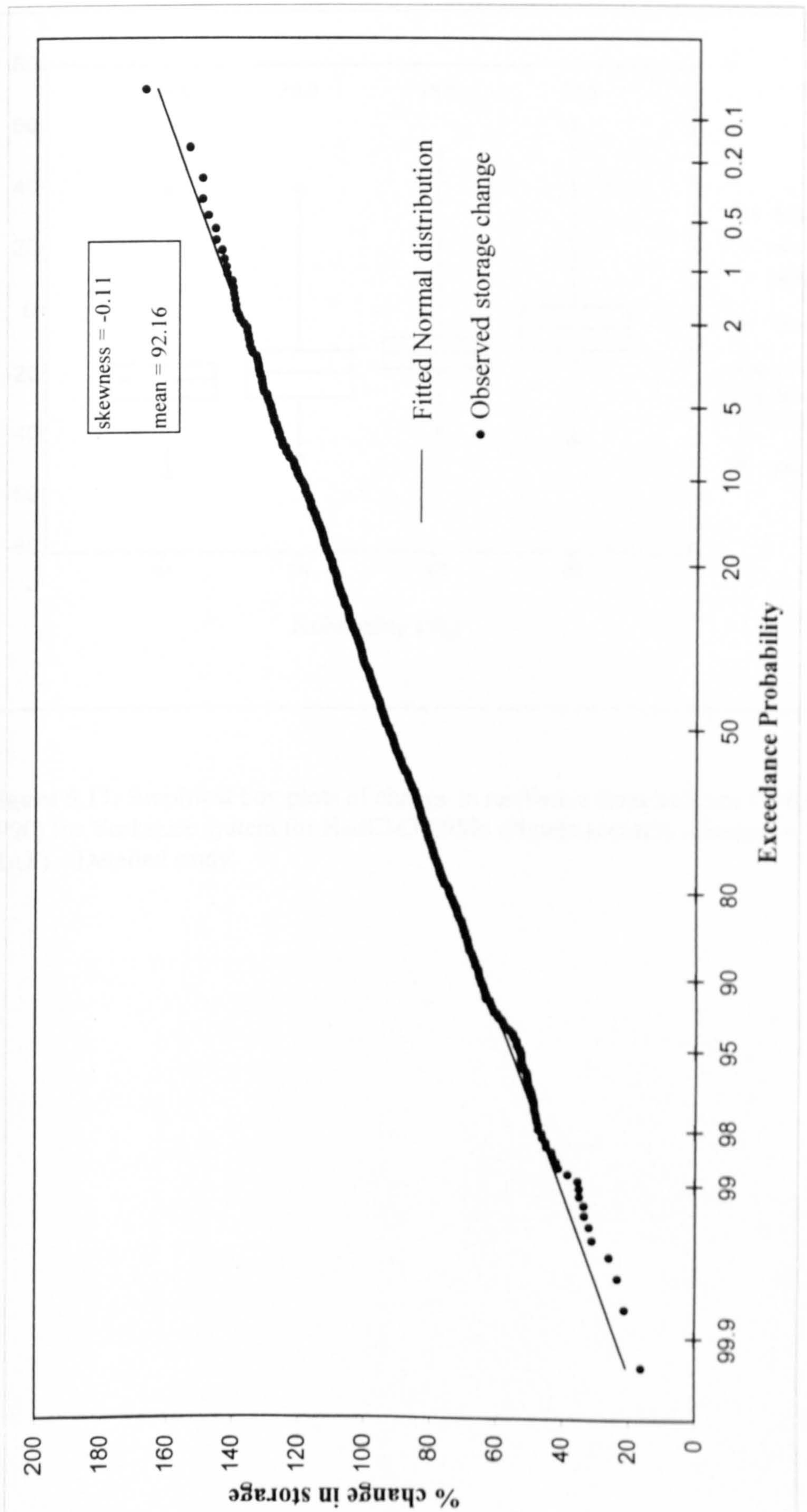

Figure 5.16: The Normal distribution fitted to storage changes caused by HadCM3 - 2050s climate change scenario - Detailed study.

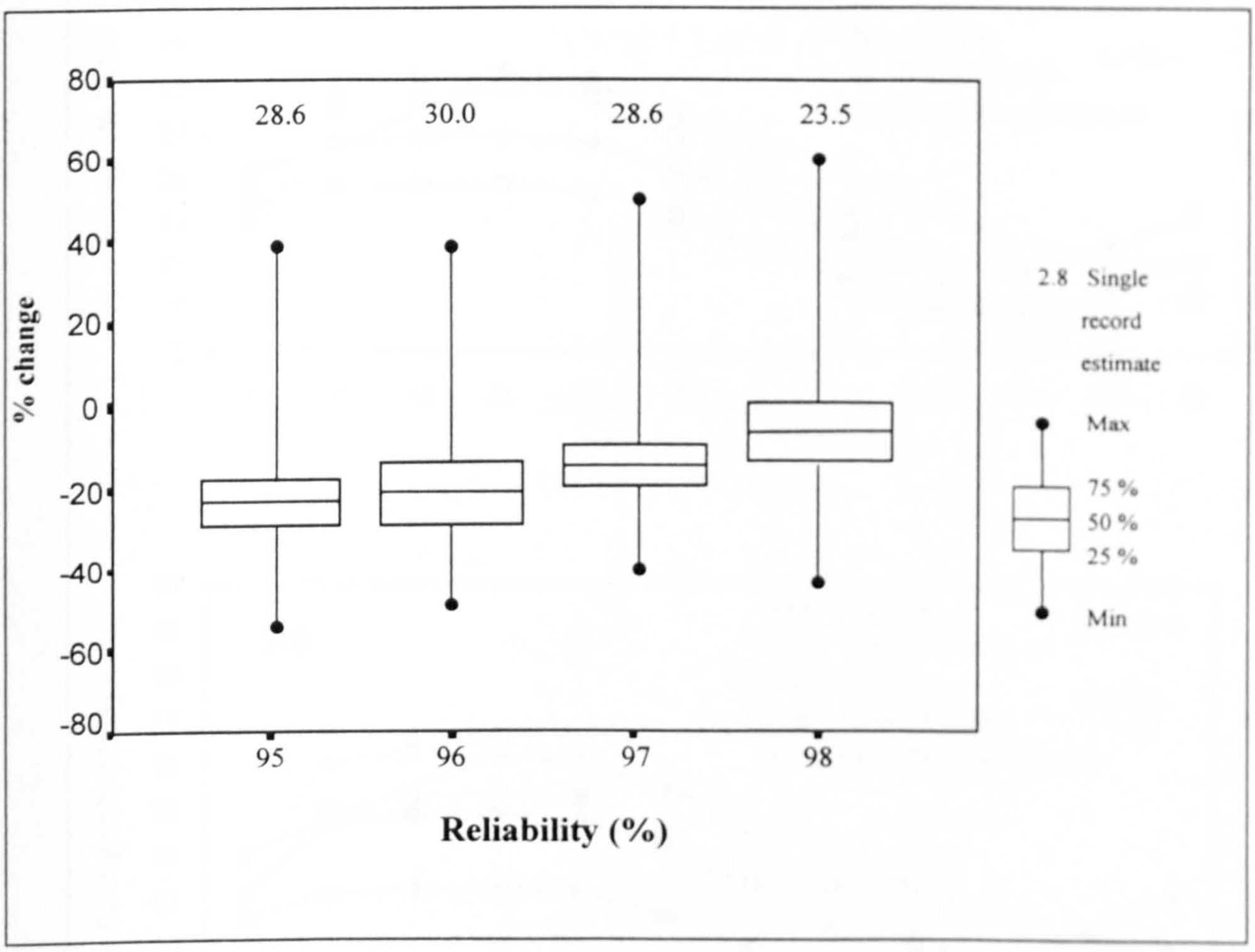

Figure 5.17: Empirical box plots of change in resilience from baseline (1961-1990) for Yorkshire system for HadCM3 2050s climate scenario (demand = 30% MAF) – Detailed study.

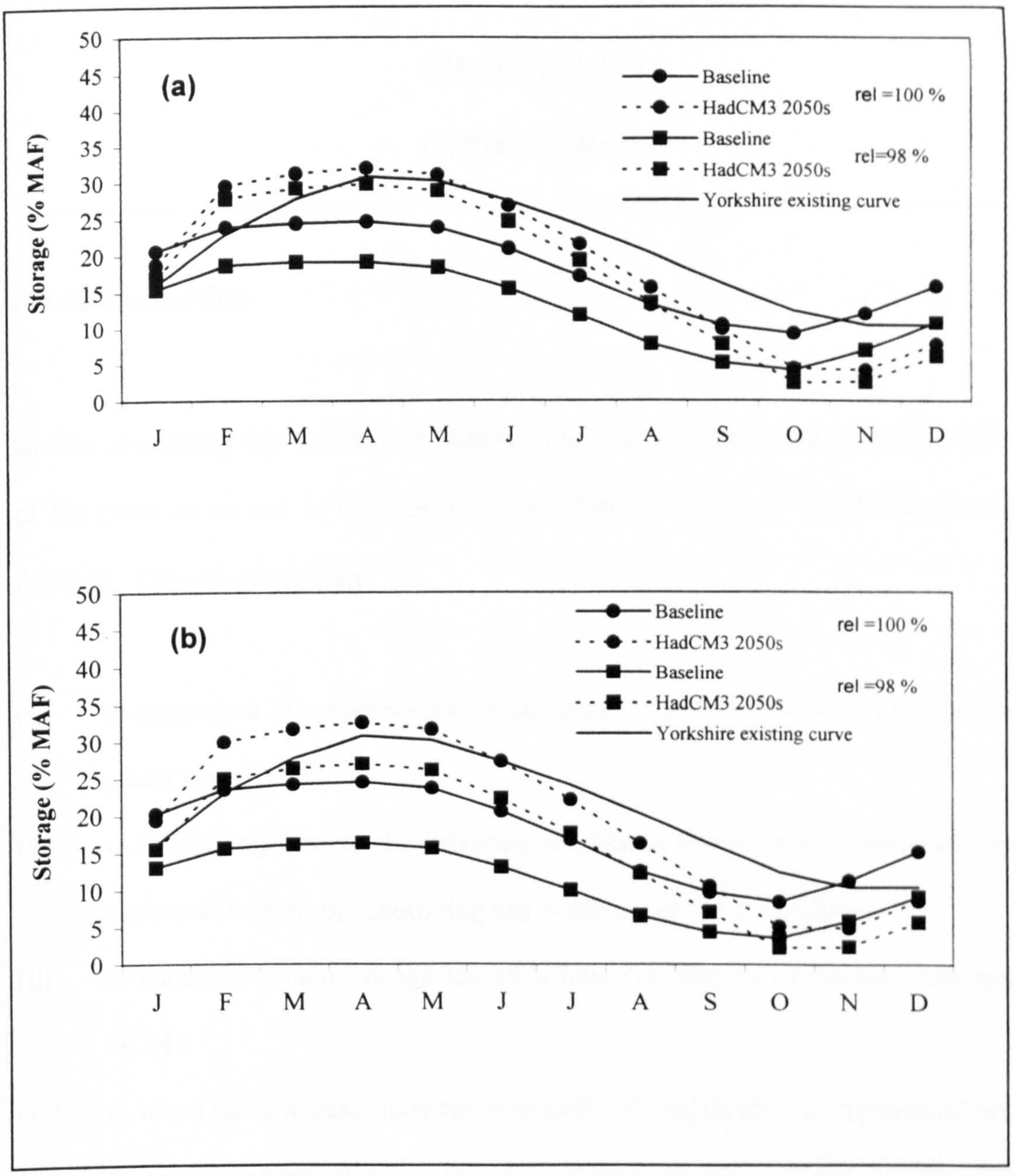

Figure 5.18: Yorkshire reservoir control curves under present and future conditions ((a) traditional approach, (b) extended approach with control curve ordinates being averaged over 1000 replicates; rel = time-based reliability.) Detailed study.

CHAPTER SIX

CONCLUSION

6.1 Introduction

Before concluding this thesis, it is important to first summarise the aim and objectives of the study as set out in Chapter 1, to establish the extent to which they have been fulfilled. The objectives were:

(i) to carry out a literature review on the origin of rapid global warming observed in recent years;

(ii) to extensively review the literature on climate change water resources impacts assessments, thereby identifying any voids in current knowledge;

(iii) to construct climate change scenarios based on outputs of several recommended GCMs;

(iv) to select suitable case study catchments for the application of the methodology;

(v) to apply climate change scenarios to baseline climate data of the selected catchments (to obtain future climate) using both a simple mean monthly factored approach and a statistically more robust stochastic weather generation model;

(vi) to calibrate catchment rainfall-runoff response models of varying complexity for the selected catchments for use in the climate change water resource impacts assessment;

(vii) to calibrate stochastic models of streamflow for replicating streamflow data;

(viii) to investigate the effects of climate change on water resources using both the traditional and a Monte Carlo simulation approach;

(ix) to compare the obtained climate change water resource impacts based on the simple and more detailed methodologies and make appropriate recommendations.

Both objectives (i) and (ii) concerning the literature review of current knowledge about possible causes of climate change and its effects on water resources respectively formed the subject of Chapters 2 and 3 of this thesis. The review in Chapter 2 revealed that the global mean temperature has been at its highest during the last decade since records began. Moreover, evidence based on proxy records indicates that mean temperature in the northern Hemisphere observed during the end of the 20th century was the highest in a 600-year reconstructed record dating back to 1400AD. There is ample evidence to suggest that anthropogenic greenhouse gases are responsible for rapid global warming which is bringing about climatic shifts across the world (e.g. IPCC, 1996; 2001a). Indeed, according to the IPCC (2001a), it is likely that anthropogenic activities will continue to influence the world's climate for many centuries to come.

The review in Chapter 3 highlighted the tremendous volume of published literature dealing with climate change water resources impacts assessment (e.g. Lemmelä and Helenius, 1998). Indeed, even studies categorising the large volume of climate change impacts investigations have been published (e.g. Chalecki and Gleick, 1999). From the review in Chapter 3, it became apparent that the traditional 'single records' approach to climate change water resource impacts assessment often involves three distinct stages. The first stage is to construct catchment-scale GCM-based climate change scenarios and use these to perturb baseline (current) climate to obtain future climate. This is then followed by forcing a catchment response model with both the current and future

climate to obtain the corresponding runoff records. Finally, the hydrological data series are then input into a water resource simulation model to obtain possible impacts.

Because of uncertainties introduced at successive stages of the assessment, it is important that the assessed impacts are viewed with caution (Hulme et al., 1999a). An underlying source of uncertainty stems from an inability to accurately forecast levels of greenhouse gases and hence the degree of global warming. Additionally, there are other uncertainty errors in global climate modelling and in 'downscaling' climate to the catchment scale, the imprecision in hydrological and water resource systems modelling, and the limitation caused by using only single records for the impacts assessment (sampling uncertainty) (see Figure 3.6). It also became apparent from the literature review that few studies have addressed these uncertainties using a formal quantitative approach.

Objectives (iii) - (vii) were achieved in Chapter 4 and much of the work carried out in Chapter 4 centred on testing the performance of various models to be used in the research. Objectives (viii) and (ix) constituted the subject of Chapter 5.

Thus it can be seen that all the objectives set out in Chapter 1 for the PhD research have been achieved. From the entire study, specific conclusions may be drawn as set out below.

6.1.1 A Monte Carlo simulation approach to climate change water resources impacts assessments is more comprehensive than the traditional 'single' records approach. This is because Monte Carlo simulation experiments enable the 'population of impacts' to be obtained as opposed to the single realisation of impact possible with traditional methods

of assessment. These impacts can then be subject to standard statistical analysis to determine the probability attached to a specific 'impact' for instance.

6.1.2 Assessed climate change impacts on runoff are more sensitive to precipitation changes than to changes in potential evapotranspiration. Therefore, water resources availability has been mostly affected by precipitation change. This result would suggest that reliable precipitation scenarios are crucial in any climate change water resources impacts studies.

6.1.3 Climate change water resources impacts are highly uncertain because of differences in GCM projections. While all the three GCMs agree on the likely change and direction of future temperature in the Yorkshire catchments, projections of precipitation changes often vary from one GCM to another. This is a major problem for water resources impacts assessment since precipitation often has a much bigger impact on runoff than evaporation. Of the climate change scenarios used in the detailed study, those based on the UK HadCM3 GCM indicate drier future conditions whilst wetter conditions are predicted by the Australian CSIRO1 GCM for the same catchments in Yorkshire. Consequently, use of scenarios based on different GCMs had led to opposite impacts on the same water resources system. The impacts reported in this research should therefore be viewed as a likely range of projections rather than predictions.

6.1.4 Assessed climate change impacts on annual runoff and reservoir characteristics are not particularly sensitive to either the baseline climate perturbation scheme or the catchment runoff response model used (see Tables 5.13 and 5.24). This is quite significant for climate change water resources impacts assessors who might be considering using a weather generator for climate perturbation. Investigators often

adopt this rather laborious, albeit more complete, approach in the hope of producing more 'accurate results'. However, it is entirely possible that the end result (regarding reservoir yield assessment) will be no different from one that could be obtained on the basis of the much simpler perturbation approach.

6.1.5 Based on the detailed study carried out on the Yorkshire catchments, it was found that HadCM3 GCM simulated vegetation feedback had little effect on changes in runoff and reservoir yield. This is because of the dual response of vegetation to increasing CO_2 concentrations. Increased CO_2 will have a twofold effect on PE; firstly, a reduction is likely as a result of increased plant stomatal resistance, and secondly, increased vegetative cover will lead to an increase. What this study has revealed is that these two opposing effects are probably equal thus resulting in a nil residual effect. Consequently, the assumption of ignoring vegetation feedback in impacts studies may be a valid one to make.

6.1.6 As a consequence of the reduced future runoff (resulting from the HadCM3 scenarios) obtained for the Yorkshire catchments in the detailed study, the flow quantiles were much lower in the future when compared with the baseline (see Figure 5.12). Since low flow quantiles have a direct impact on rivers and reservoir yields, these obtained reductions in the low flow quantiles are expected to produce reductions in future yields for the Yorkshire systems. This would put considerable stress on existing water resources facilities in future which would require appropriate measures such as leakage reduction and other demand management strategies to be taken in order to maintain current levels of performance.

6.1.7 Based on the preliminary study it was found that under baseline conditions, the inclusion of net reservoir surface evaporation fluxes in reservoir yield analysis resulted in increased yield from reservoir systems in the Yorkshire catchments, where precipitation exceeds open water evaporation. In contrast, yield reductions were observed for the Urmia reservoirs that are located in catchments where open water evaporation exceeds precipitation. This result has practical implications for reservoir water management in temperate climates such as the Yorkshire catchments where for most part surface flux is often ignored on the excuse that it is unimportant. However, while it is unimportant from the point of view that it may not lead to water shortage, it does have some practical significance because facilities planned ignoring such fluxes currently represent an over-design, and the buffer of such over-design would go some way in meeting any shortfall in future storage requirements. As a result such reservoirs may be able to accommodate the likely requirement placed by future climate change for example.

6.1.8 Climate change-induced reductions in future inflows to reservoirs combined with increases in future water demand could put even greater pressure on reservoirs. For example, it was shown that according to the HadCM3 (2050s) scenario, reservoir storage capacity of the Yorkshire reservoirs must be increased by 74% under climate change (at current demand level) to maintain current levels of performance in future. If the effects on storage requirement of a 17% demand rise are also included, then storage capacity must be increased by a further 52% (total increase of 126%).

6.1.9 Results from the detailed study of the climate change impacts on reservoir control curves in Yorkshire revealed that reservoir monthly target storage levels would need to be raised in the future (as a result of the HadCM3 2050s scenario) between February

and August in order to maintain current levels of system performance. Reservoir control curves for baseline conditions derived in the detailed study were also compared to the existing Yorkshire Water (YW) operational control curve (see Figure 5.18). Whilst the shape of the YW existing curve is similar to those curves derived in this work, it was found to be generally above the future curves. On the basis of Figure 5.18, it was concluded that the current Yorkshire Water control curve may go some way in tempering the most severe impacts of climate change.

6.1.10 The detailed Yorkshire studies also indicated that reductions in future groundwater resources resulting from the HadCM3 2050s climate change scenario were larger than reductions in runoff. For example, runoff reductions during May, July and September were 23%, 47% and 65%, respectively (see Figure 5.9), while the respective reductions in groundwater recharge were 38%, 76% and 82% (see Table 5.18). This is due to the relatively high sensitivity of groundwater recharge to changes in both precipitation and PE, which was found in the study. Water resources planners wishing to exploit groundwater resources in Yorkshire should therefore be attentive to the severity of the possible threats of climate change to non-renewable groundwater resources.

6.1.11 Due to the range of uncertainties in climate change impact assessments (as summarised in Figure 3.6), little confidence can be placed on a particular climate change impact assessment. In both the intermediate and detailed studies, the sampling uncertainties were quantified and it was shown that the range of changes in reservoir characteristics (e.g. yield, resilience) could be very large if sampling uncertainties are taken into account. For instance, it was shown that yield changes ranged from -8% to +11% for different scenarios and 100% reliability (see Table 5.19) without a consideration of sampling uncertainties. In contrast, the changes were far larger (for the

same reliability level), varying between -19% and +28, when sampling uncertainties were incorporated. These results indicate the importance of taking account of sampling uncertainties in climate change water resources impacts studies since this will allow the larger range of possible impacts to be exposed.

6.2 Areas of Further Research

The following are recommended as areas for further research:

6.2.1 The Monte Carlo approach used single baseline and future streamflow records as the basis of forcing the stochastic streamflow models. To remove any uncertainty due to catchment models; both these single baseline and future flows were simulated by the catchment hydrological model using baseline and future climate variables respectively. However, an alternative approach, particularly when the stochastic weather generator is being used, would be to generate replicates of the baseline and future weather variables and feed each of these replicates to the catchment model to simulate corresponding replicates of the flow. This will remove the need for a stochastic flow model and, although is likely to be more complex, would be better at characterising the stochasticity of the inputs (e.g. precipitation and PE) which drive the catchment hydrological response.

6.2.2 The stochastic replication of the flow data in the study assumed that the data series are individually stationary (i.e. the baseline is stationary and the future is stationary). However, the prospect of climate change, which can introduce trend, makes justifying this assumption rather difficult. There are available long-memory stochastic streamflow generation models (see e.g. Mandelbroit and Wallis, 1968; Landwehr and Matalas,

1986; Strupczewski and Mitosek, 1996) which could be used to model non-stationary time series. Such models are often much more difficult to implement than those assuming stationarity; nonetheless they represent the only realistic way of accommodating the trend associated with climate change when stochastically replicating flow data.

6.2.3 This research ignored the progressive responses to climate change. These may be in the form of adaptation measures taken to guard against water supply failure (e.g. through modification of reservoir operation rules, or through demand management initiatives such as leakage reduction), or they may be attributable directly to global warming (e.g. the rise in water demand). In the final detailed study, the effect of a (sudden) demand rise on reservoir storage requirement was briefly investigated. As seasonal water demand forecasting techniques improve (see e.g. OCWR, 2001), a gradual demand rise (which is more realistic) would need to be incorporated in climate impacts assessments.

6.2.4 Although the results reported in this thesis reveal the large range of possible climate change-induced impacts on water resources, the precise cause of the impacts is not clearly defined. It would be useful to policy makers and adaptation planners to know whether the impacts result largely from human activities or are merely due to natural climate variability. If the extent of natural climate variations was found to be greater than anthropogenic climate change, then the emphasis would shift more towards the planning of adaptation measures. Output from GCM control experiments (i.e. models forced only with a constant pre-industrial greenhouse gas concentrations) and GCM simulation experiments (i.e. models forced with observed and projected greenhouse gas concentrations) could be used to establish the sensitivity of water

resources to natural climate variability and anthropogenic climate change. It would be particularly useful to assess the sensitivity of water resources in Yorkshire to changes in climate as a result of the natural phenomenon known as the North Atlantic Oscillation (NOA) which is known to affect the climate of Britain. Efforts are currently underway at the Climate Research Unit at the University of East Anglia (see http://www.cru.uea.ac.uk/link) to try and predict the evolution of the NAO within HadCM3 GCM control experiments. Once completed, output from such control experiments could form the basis for a valuable and original impacts assessment exercise.

REFERENCES

Abott, M. B., Bathurst, J.C., Cunge, J. A., O' Connell, P. E. and Rasmussen, J. (1986) An introduction to the European Hydrological System - Système Hydrologique Européen, SHE. 1. History and philosophy of a physically-based, distributed modelling system, *J. Hydrology,* 87, 45-59.

Abramowitz, M. and Stegun, A. (1972) *Handbook of mathematical functions*, Dover, New York.

Adeloye, A. J. (1994) A Simulation Approach for Assessing the Reliability of Single Historic Capacity Estimates, *Advances in Water Resour. Tech. and Managt.*, 85-92.

Adeloye, A. J. (1996) An opportunity loss model for estimating the value of streamflow data for reservoir planning, *Water Resour. Managt.*, 10(1), 45-79.

Adeloye, A. J. and Montaseri, M. (1998) Adaptation of a single reservoir technique for multiple reservoir storage-yield-reliability analysis, in *Water: a looming crisis? Proc. Int. Conf. on world water resources at the beginning of the 21st Century, UNESCO*, edited by Zebidi, H., Paris, 349-355.

Adeloye, A. J. and Montaseri, M. (1999) Development of a simple rule for evaporation losses adjustment in reservoir capacity-yield-performance assessment, in *Proc. 4th Biennial Congress of the African Division of the International Association of Hydraulic Research, Windhoek, Namibia.*

Adeloye, A. J. and Nawaz, N. R. (1997) *The inherent time-based reliability of storage-yield estimates for some reservoir sites in Yorkshire*, Dept. Civil & Offshore Eng., Heriot-Watt University.

Adeloye, A. J. and Nawaz, N. R. (1998) Assessing the adequacy of Wright's model reconstructed stream-flow data for reservoir storage-yield-reliability analysis, *J. Chartered. Inst. Water Envir. Managt.*, 12(2), 130-138.

Adeloye, A. J., Montaseri, M. and Garmann, C. (2001) Curing the misbehaviour of reservoir capacity statistics by controlling shortfall during failures using the modified sequent algorithm, *Water Resour. Res.* 37(1), 73-82.

Alcamo, J., Bouwan, A., Edmonds, J., Grubler, A., Morita, T. and Sugandhy, A. (1995) An evaluation of the IPCC IS92 emission scenarios, in *Climate change 1994: radiative forcing of climate change and an evaluation of the IPCC IS92 emission scenarios.*, edited by Houghton, J. T., Meiro Filho, L.G., Callander, B.A., Harris, N., Kattenberg, A. and Maskell, K., Cambridge University Press.

Arnell, N. W. (1992) Factors controlling the effects of climate change on river flow regimes in a humid temperate environment, *J. Hydrology*, 132, 321-342.

Arnell, N. W. (1996) *Global warming, river flows and water resource*, Wiley, Chichester.

Arnell, N. W. (1999) The effect of climate change on hydrological regimes in Europe: a continental perspective, *Glob. Environ. Change*, 9, 5-23.

Arnell, N. W. (2000) Thresholds and response to climate change forcing: the water sector, *Climatic Change*, 46, 305-316.

Arnell, N. and Reynard, N. (1989) *Estimating the impacts of climatic change on river flows: some examples from Britain*, Conference on Climate and Water, September 11-15, Helsinki, Finland, 1, 426-436.

Arnell, N. W. and Reynard, N. S. (1993) *On impacts of climate change on river flow regimes in the UK*, Institute of Hydrology Report (to department of the environment water directorate).

Arnell, N. W., Bates, B., Lang, H., Magnuson, J. J. and Mulholland, P. (1996) Hydrology and freshwater ecology, in *Climate change 1995: impacts, adaptations and mitigation, 1996 contribution of Working Group II to the second assessment report of the Intergovernmental Panel on Climate Change,* edited by Watson, R. T., Zinyowera, M. C. and Moss, R. H., Cambridge University Press, Cambridge.

Arnell, N. W., Reynard, N., King, R., Prudhomme, C. and Branson, J. (1997*) Effects of climate change on river flows and ground-water recharge: Guideline for resource assessment*, UKWIR/Environment Agency Report: Ref: 97/CL/04/1.

Aston, A. R. (1984) The effect of doubling atmospheric CO_2 on streamflow: A simulation, *J. Hydrology*, 67, 273-280.

Bardossy, A and Platte, E. J. (1992) Space-time model for daily rainfall using atmospheric circulation patterns, *Water Resour. Res.*, 28(5), 1247-1259.

Bathurst, J. C. and O' Connell, P. E. (1992) Future of parameter modelling: the Système Hydrologique Européen, SHE, *Hydrol. Process.*, 6, 265-277.

Bayazit, M. and Bulu, A. (1991) Generalised probability distribution of reservoir capacity, *J. Hydrology*, 125, 195-206.

Bayazit, M. and Onuz, B. (2000) Conditional distributions of ideal reservoir storage variables, *J. Hydrologic Engrg., ASCE,* 5(1), 52-58.

Bergström, S., Carlsson, B., Gardelin, M., Lindström, G., Pettersson, A and Rummukainen, M. (2001) Climate change impacts on runoff in Sweden - assessments by global climate models, dynamical downscaling and hydrological modelling, *Climate Research,* 16, 101-112.

Beven, K. J. (1979) A sensitivity analysis of the Penman-Monteith actual evapotranspiration estimates, *J. Hydrology*, 44, 169-190.

Beven, K. J. (1989) Changing ideas in hydrology - the case of physically-based models, *J. Hydrology,* 105, 157-172.

Beven, K. J. (1993) Prophecy, reality and uncertainty in distributed hydrological modelling, *Adv. in Water Resour.*, 16, 41-51.

Beven, K. J. (2001) On an acceptable criterion for model rejection, *Circulation plus, the newsletter of the British Hydrological Society*, 68, 9-10.

Beven, K. J. and Binley, A. (1992) The future of distributed models: model calibration and uncertainty prediction, *Hydrol. Process.*, 6, 279-298.

Blake, R., Khanbilvardi, R. and Rosenzweig, C. (2000) Climate change impacts on New York City's water supply system, *J. Amer. Water Resour. Assoc.*, 36(2), 279-292.

Boer, G. J., Flato, G. M., Reader, M. C. and Ramsden, D. (2000) A transient climate change simulation with greenhouse gas and aerosol forcing: experimental design and comparison with the instrumental record for the 20th century, *Climate Dynamics*, 16, 405-425.

Boorman, D. B. and Sefton, C. E. M. (1997) Recognising the uncertainty in the quantification of the effects of climate change in hydrological response, *Climate Change*, 35, 415-434.

Braga, B. P. F. and Molion, L. C. B. (1999) Assessment of the impacts of climate variability and change on the hydrology of South America, in *Impacts of climate change and climate variability on hydrological environments, Int. Hydrology Series,* edited by van Dam, Jan C., Cambridge University Press, chapter 3, 21-34.

Bras, R. L. and Rodrigues-Iturbe, I. (1985) *Random functions and hydrology*, Addison-Wesley, Reading, Mass.

Buishand, T. A. and Beckmann, B. R. (2000) Development of daily precipitation scenarios at KNMI, paper presented at the ECLAT-2 Blue Workshop (EW-3): Climate scenarios for water related and coastal impact, a concerted action towards the improved understanding and application of results from climate model experiments in European climate change impact research, May 10-12, 2000.

Bultot, F., Coppens, A., Dupriez, G. L., Gellens, D. and Meulenberghs, F. (1988) Repercussions of a CO_2 doubling on the water cycle and on the water balance - a case study for Belgium, *J. Hydrology,* 99(3/4), 319-347.

Burges, S. J. and Linsley, R. K. (1971) Some factors influencing reservoir storage, *J. Hydraul. Div., ASCE*, 97, 977-991.

Cameron, D. S., Beven, K. J., Tawn, J., Blazkova, S. and Naden, P. (2000) Flood frequency estimation for a gauged upland catchment (with uncertainty), *J. Hydrology,* 219, 169-187.

Carter, T. R., Parry, M. L., Nishioka, S. and Harasawa, H. (1994) Technical guidelines for assessing climate change impacts and adaptations, Intergovernmental Panel on Climate Change, University College London, Centre for Global Environmental Research, Tsukuba.

Carter, T.R., Hulme, M. and Lal, M. (1999) Guidelines on the use of scenario data for climate impact and adaptation assessment, version 1, Intergovernmental Panel on Climate Change, Task Group on Scenarios for Climate Impact Assessment.

CCIRG (Climate Change Impacts Review Group) (1996) *Review of the potential effects of climate change in the United Kingdom*, Second Report, Department of Environment, London. HMSO.

Chalecki, E.L. and Gleick, P.H. (1999) A comprehensive bibliography of the impacts of climatic change and variability on water resources of the United States, *J. Amer. Water Resour. Assoc.*, 35, 1657-1665.

Charles, S. P., Bates, B. C., Whetton, P. H. and Hughes, J. P. (1999) Validation of downscaling models for changed climate conditions: case study of south-western Australia, *Climate Research*, 12(1), 1-14.

Chiew, F. H. S. and McMahon, T. A. (1993) Assessing the adequacy of catchment streamflow yield estimates, *Aust. J. Soil. Res.*, 31, 665-680.

Chiew, F. H. S. and McMahon, T. A. (1994) Application of the daily rainfall-runoff model MODHYDROLOG to 28 Australian catchments, *J. Hydrology*, 153(1-4), 383-416.

Chiew, F. H. S., Whetton, P. H., McMahon, T. A. and Pittock, A. B. (1995) Simulation of the impacts of climate change on runoff and soil moisture in Australian catchments, *J. Hydrology*, 167(1-4), 121-147.

Chiew, F. H. S., Wang, T. A., McMahon, T. A., Bates, B. C. and Whetton, P. H. (1996) Potential hydrological responses to climate change in Australia, in *Regional hydrological response to climate change*, edited by Jones, J. A. A., Liu, C., Woo, M-K. and Kung, H-T, Kluwer Academic Press, London.

Chow, V. T., Maidment, D. R. and Mays L. W. (1988) *Applied hydrology*, McGraw-Hill Book Co, New York.

Coe, R. and Stern, R. D. (1982) Fitting models to daily rainfall data, *J. Appl. Meteorol.*, 21, 1024-1031.

Cohen, S.J. (1991) Possible impacts of climatic warming scenarios on water resources in the Saskatchewan River sub-basin, Canada, *Climatic Change*, 19, 291-317.

Cole, J. A., Slade, S., Jones, P. D. and Gregory, J. M. (1991) Reliable yield of reservoirs and possible effects of climatic change, *Hydrological Sci. J.*, 36(6), 579-598.

Cooper, D. M., Wilkinson, W. B. and Arnell, N. W. (1995) The effects of climate changes on aquifer storage and river baseflow, *Hydrological Sci. J.*, 40(5), 615-632.

Cox, P., Betts, R., Bunton, C., Essery, R., Rowntree, P. R. and Smith, J. (1998) The impact of new land surface physics on the GCM simulation of climate and climate sensitivity, *Climate Dynamics*, 15, 183-203.

Crane, R. G. and Hewitson, B. C. (1998) Doubled CO_2 precipitation changes for the Susquehanna Basin: down-scaling from the GENESIS General Circulation Model, *Int. J. Climatology*, 18, 65-76.

Crookall, D. and Bradford, W. (2000) Impact of climate change on water resources planning, Proceedings of the Institute of Civil Engineers, *Civil Engineering*, 138, 44-48.

Crowley, T. J. and Kim, K-Y. (1993) Towards development of strategy for determining the origin of decadal-centennial scale climate variability, *Quat. Sci. Rev.*, 12, 375-385.

Cure, J. D. (1985) Carbon dioxide doubling responses: a crop survey, in *Direct effects of increasing carbon dioxide on vegetation*, edited by Strain, B. R. and Cure, J. D., U.S. Department of Energy, Washington, D.C.

Cure, J. D. and Acock, B. (1986) Crop responses to carbon dioxide doubling: a literature survey, *Agricul. and Forest Met.*, 38, 127-145.

Dansgaard, W., White, J. W. C. and Johnsen, S. J. (1989) The abrupt termination of the Younger Dryas, *Nature*, 339, 532-534.

Dandy, G. C., Connarty, M. C. and Loucks, D. P. (1997) Comparisons of methods of yield assessment of multiple reservoir systems. *J. Water Resour. Plan. Managt., ASCE*, 123(6), 350-357.

DeWalle, D. R. and Swistock, B. R. (2000) Potential effects of climate change and urbanization on mean annual streamflow in the United States, *Water Resour. Res.* 36(9), 2655-2664.

Dooge, J. C. I. (1977) Problems and methods of rainfall-runoff modelling, in *Mathematical models for surface water hydrology*, edited by Ciriani, T. A., Maione, U. and Wallis, J. R., Wiley, New York.

Dooge, J. C. I. (1992) Hydrologic models and climate change, *J. Geophys. Res.*, 97(D3), 2677-2686.

Doorenbos, J. and Pruitt, W. O. (1975) Crop water requirements, irrigation and drainage paper 24., F.A.O., United Nations, Rome.

Duan, Q., Soorshian, S. and Gupta, V. K. (1994) Optimal use of the SCE-UA global optimisation method for calibrating watershed models, *J. Hydrology*, 158, 265-284.

Duell Jr, L. F. W. (1992) Use of regression models to estimate effects of climate change on seasonal streamflow in the American and Carson River basins, California-Nevada, in *Managing water resources during global change, Proceedings of the 28th American Water Resources Association Annual Conference*, Bethesda, MD.

Dvorak, V., Hladny, J. and Kasparek, L. (1997) Climate change, hydrology and water resources impact and adaptation for selected river basins in the Czech Republic, *Climatic Change*, 36, 93-106.

Eeles, C. W. O. (1994) *Parameter optimization of conceptual hydrological models*, PhD Thesis, Open University, Milton Keynes, U.K.

Emori, S, (1999) Coupled ocean-atmosphere model experiments of future climate change with an explicit representation of sulfate aerosol scattering, *J. Meteor. Soc. Japan*, 77(6), 1299-1307.

Faulkner, D. S., Arnell, N. W. and Reynard, N. S. (1997) Everyday aspects of climate change in Europe, in *Proceedings of the British Hydrological Society Hydrology Symposium*, Salford, UK.

Fennessey, N. M. (1995) Sensitivity of reservoir-yield estimates to model time step surface-moisture fluxes, *J. Water Resour. Plan. Managt., ASCE*, 121(4), 310-317.

Fiering, M. B. (1982), Alternative indices of resilience, *Water Resour. Res.*, 18(1), 33-39.

Firor, S. E., Finney, B. A., Willis, R. and Dracup, J. A. (1996) Disaggregation modelling process for climatic time series, *J. Water Resour. Plan. Managt., ASCE*, 122(3), 205-212.

Flato, G. M., Boer, G. J., Lee, W. G., McFarlane, N. A., Ramsden, D., Reader, M. C. and Weaver, A. J. (2000) The Canadian Centre for Climate Modelling and Analysis Global Coupled Model and its climate, *Climate Dynamics*, 16, 451-467.

Foster, M., Werritty, A. and Smith, K. (1997) The nature, causes and impacts of recent hydroclimatic variability in *Scotland and Northern Ireland,* in *Proceedings of the British Hydrological Society Hydrology Symposium*, 8.9-8.17, Salford, UK.

Franchini, M., Galeati, G., and Berra, S. (1998) Global optimisation techniques for the calibration of conceptual rainfall-runoff models, *Hydrological Sci. J.*, 43(3), 443-458.

Frick, D. M. and Salas, J. D. (1991) Evaluating modelling strategies for a complex water resource system, in *Hydrology for the Water Management of Large River Basins (Proceedings of the Vienna Symposium)*, IAHS Publ., 201.

Gan, K. C., McMahon, T. A. and O'Neil, I. C. (1991) Sensitivity of reservoir sizing to evaporation estimates, *J. Irrig. Drain. Engrg.*, ASCE, 177 (3), 324-335.

Gates, W. L., Henderson-Sellers, A., Boer, G. J., Folland, C. K., Kitoh, A., McAvaney, B. J., Semazzi, F., Smith, N., Weaver, A. J. and Zeng, Q-C. (1996) Climate models-evaluation, in *Climate change 1995: impacts, adaptations and mitigation, 1996 contribution of Working Group II to the second assessment report of the Intergovernmental Panel on Climate Change,* edited by Watson, R. T., Zinyowera, M. C. and Moss, R. H., Cambridge University Press, Cambridge.

Glantz, M. H. and Wigley, T. M. L. (1987) Climatic variations and their effects on water resources, in *Resources and World Development*, edited by McLaren, D. J. and Skinner, B. J., Wiley, 625-641.

Gleick, P. H. (1987) The development and testing of a water-balance model for climate impact assessment: modelling the Sacramento Basin, *Water Resour. Res.* 23(6), 1049-1061.

Gleick, P. H. (1990) Vulnerability of water systems, in *Climate change and U.S. water resources,* edited by Waggoner, P. E., chapter 10, 223-240.

Gleick, P. H. (2000) *The World's Water 2000-2001*, Island Press, Washington D.C.

Gordon, H. B. and O' Farrel, S. P. (1997) Transient climate change in the CSIRO coupled model with dynamic sea ice, *Monthly Weather Review*, 125, 875-907.

Gordon, C., Cooper, C., Senior, C. A., Banks, H., Gregory, J. M., Johns, T. C., Mitchell, J. F. B. and Wood, R. A. (2000) The simulation of SST, sea ice extents and ocean heat transports in a version of the Hadley Centre coupled model without flux adjustments, *Climate Dynamics*, 16, 147-168.

Goulden, M. L., Wofsy, S. C., Harden, J. W., Trumbore, S. E., Crill, P. M., Gower, S. T., Fries, T., Daube, B. C., Fan S. M., Sutton, D. J., Bazzaz, A. and Munger, J. W. (1998) Sensitivity of boreal forest carbon balance to soil thaw, *SCIENCE*, 279(5348), 214-217.

Grootes, P. M., Stuiver, M., White, J. W. C., Johnsen, S., and Jouzel, J. (1993) Comparison of oxygen isotope records from the GISP2 and GRIP Greenland ice cores, *Nature*, 366, 552-554.

Grygier, J. C. and Stedinger, J. R. (1988) Condensed disaggregation procedures and conservation corrections for stochastic hydrology, *Water Resour. Res.*, 24(10), 1574-1584.

Hashimoto, T., Stedinger, J. R. and Loucks, D. P. (1982) Reliability, resiliency and vulnerability criteria for water resource system performance evaluation, *Water Resour. Res.*, 18(1), 14-20.

Hasselmann, K., Bengtsson, L., Cubasch, U., Hegerl, G. C., Rodhe, H., Roeckner, E., von Storch, H. and Voss, R. (1995) Detection of anthropogenic climate change using a fingerprint method, Max-Planck Institut fur Meteorological Report, 168.

Hedger, M., Gawith, M., Brown, I., Connell, R. and Downing, T. E. (Eds) (2000) Climate change: assessing the impacts - identifying responses, the first three years of the UK Climate Impacts Programme, UKCIP Technical Report. UKCIP and DETR, Oxford.

Hegerl, G., von Storch, H., Hasselmann, K., Santer, B. D., Cubasch, U. and Jones, P. D. (1996) Detecting anthropogenic climate change with a fingerprint method, *J.Climate*, 9, 2281-2306.

Herrington, P. (1996) *Climate change and the demand for water*, Department of the Environment, HMSO.

Hirst, A. C., O' Farrell, S. P. and Gordon, H. B. (2000) Comparison of a coupled ocean-atmosphere model with and without oceanic eddy-induced advection, 1: Ocean spin-up and control integrations, *J. Climate*, 13 (1): 139-163.

Hoestetler, S. W. and Giorgi, F. (1993) Use of output from high-resolution atmospheric models in landscape-scale hydrologic models: an assessment, *Water Resour. Res*, 29(6), 1685-1696.

Holt, C. P. and Jones, J. A. A (1996) Equilibrium and transient global warming scenario implications for water resources in Wales, *Water Resour. Bull.*, 32(4), 711-721.

Hooke, R. and Jeeves, T. A. (1961) Direct search solutions of numerical and statistical problems, J. *Assoc. Comput. Mach.*, 8(2), 212-229.

Houghton, J. (1997) *Global warming - the complete briefing*, Cambridge University Press.

Hulme, M. (1996) *The 1996 CCIRG scenario of changing climate and sea level for the United Kingdom*, Climate Impacts LINK technical note 7, Climatic Research Unit, University of East Anglia, Norwich.

Hulme, M. and Jenkins, G. J. (1998) *Climate change scenarios for the UK: Scientific Report*, UKCIP Technical Report No. 1, Climatic Research Unit, Norwich.

Hulme, M., Raper, S. C. B. and Wigley, T. M. L. (1995) An integrated framework to address climate change (ESCAPE) and further developments of the global and regional climate modules (MAGICC), *Energy Policy*, 23(4/5), 347-355.

Hulme, M., Mitchell, J., Ingram, W., Lowe, J., Johns, T. C., New, M. and Viner, D. (1999a) Climate change scenarios for global impacts studies, *Glob. Environ. Change*, 9, S3-S19.

Hulme, M., Barrow, E. M., Arnell, N. W., Harrison, P. A., Johns, T. C., Downing, T. E. (1999b) Relative impacts of human-induced climate change and natural climate variability, *Nature*, 397(6721), 688-691.

Hurst, H. E. (1951) Long-term storage capacities of reservoirs, *Trans. Amer. Soc. Civ. Eng.* , *ASCE*, 116, 770-799.

Huth, R. (1997) Potential of continental-scale circulation for the determination of local daily surface variables, *Theor. Appl. Climatol*, 56, 165-186.

Idso, S. B. and Brazel, A. J. (1984) Rising atmospheric carbon dioxide concentration may increase streamflow, *Nature*, 312, 51-53.

Idso, S. B., Kimball, B. A., Anderson, M. G. and Mauney, J. R. (1987) Effects of atmospheric CO_2 enrichment on plant growth: the interactive role of air temperature, *Agric. Ecosys. Environ.*, 20, 1-10.

IPCC (1990) *Climate change: The IPCC Scientific Assessment*, edited by Houghton, J., Jenkins, G. and Ephraums, J., Cambridge University Press, Cambridge.

IPCC (1992) *Climate change 1992: The Supplementary Report to the IPCC Scientific Assessment,* edited by Houghton, J. T., Callander, B. A. and Varney, S. K., Cambridge University Press.

IPCC (1996) *Climate change 1995: The Science of Climate Change: Contribution of Working Group I to the second Assessment Report of the Intergovernmental Panel on Climate Change,* edited by Houghton, J. T., Meiro Filho, L.G., Callander, B. A., Harris, N., Kattenberg, A. and Maskell, K., Cambridge University Press.

IPCC (2000) *Special report on emission scenarios, summary for policymakers*: a special report of Working Group III of the Intergovernmental Panel on Climate Change.

IPCC (2001a) *Climate change 2001: The scientific basis, contribution of working group I to the Third Assessment Report of the Intergovernmental Panel on Climate Change (IPCC),* edited by Houghton, J. T., Ding, Y., Griggs, D. J., Noguer, M., van der Linden, P. J. and Xiaosu, D., Cambridge University Press.

IPCC (2001b) *Climate change 2001: Impacts, adaptation and vulnerability, contribution of Working Group II to the Third Assessment Report of the Intergovernmental Panel on Climate Change (IPCC),* edited by McCarthy, J. J., Canziani, O. F., Leary, N. A., Dokken, D. J. and White, K. S., Cambridge University Press.

Jones, J. A. A. (1999) Climate change and sustainable water resources: placing the threat of global warming in perspective, *Hydrological Sci. J.*, 44(4), 541-557.

Jones, R. N. (2000) Analysing the risk of climate change using an irrigation demand model, *Climate Research*, 14(2), 89-100.

Jones, P. D. and Lister, D. (1995) Extended flow records at key locations in England & Wales (Phase 1), Environment Agency Publication.

Jones, P. D. and Hulme, M. (1996) Calculating Regional climatic time series, *Int. J. Climatology,* 16(4), 361-377.

Kaczmarek, Z. and Krasuski, D. (1991) Sensitivity of water balance to climate change and variability, Working Paper WP-91-047, IIASA, Laxenburg, Austria.

Kaczmarek, Z., Arnell, N. W. and Starkel, L. (1996) Climate, hydrology and water resources, in *Water resources management in the face of climatic/hydrologic uncertainties,* edited by Kaczmarek, Z., Strzepek, M., Somlyody, L. and Priazhinskaya, V., chapter 1, 3-27.

Kates, R. W. (1985) The interaction of climate and society, in *Climate impact assessment: studies of the interaction of climate and society*, edited by Kates, R. W., Ausubel, J. H. and Berberian, J. H., SCOPE 27, John Wiley, Chichester.

Kelly, P. M. and Wigley, T. M. L. (1992) Solar cycle lengths, greenhouse forcing and global climate, *Nature*, 360, 328-330.

Kimball, B. A. (1986) Influence of elevated CO_2 on crop yield, in *Carbon dioxide enrichment of greenhouse crops, II: Physiology, yield and economics*, CRC Press, Boca Raton, FL, 105-115.

Kimball, B. A. and Idso, S. B. (1983) Increasing atmospheric CO_2: effects on crop yield, water use and climate, *Agric. Water Managt.*, 7, 55-72.

Kimball, B. A., Mauney, J. R., Nakayama, F. S. and Idso, S. B. (1993) Effects of increasing atmospheric CO_2 on vegetation, *Vegetation*, 104/105, 65-75.

Kirshen, P. H and Fennessey, N. M. (1995) Possible climate change impacts on water supply of Metropolitan Boston, *J. Water Resour. Plan. Managt.*, 121(1), 61-70.

Klemes, V. (1980) Aspirations and realities, *in Proc. Canadian climate program water workshop*, Edmonton, Alberta.

Klemes, V. (1985) Sensitivity of water resource systems to climate variations, WCP, 98, WMO, Geneva.

Klemes, V. (1986) Operational testing of hydrological simulation models, *Hydrological Sci. J.*, 31, 13-24.

Klemes, V., Srikanthan, R. and McMahon, T. A. (1981) Long-memory flow models in reservoir analysis: what is their practical value?, *Water Resour. Res.*, 17(3), 737-751.

Knox, J. C. (1995) Fluvial systems since 20,000 years BP, in *Global continental palaeohydrology*, edited by Gregory, K. J., Starkel, L., and Baker, V. R., John Wiley, Chichester, 87-108.

Knuth, D. E. (1988) *The Art of computer programming*, Vol. 2, third edition, Addison-Wesley.

Kuczera, G. (1997) Efficient subspace probabilistic parameter optimisation for catchment models, *Water Resour. Res.*, 33(1), 177-185.

Lamb, H. H. (1965) The medieval warm epoch and its sequel., *Palaeogeography, Palaeoclimatology, Palaeoecology*, 1, 13-37.

Lamb, H. H. (1972) British Isles weather types and a register of the daily sequence of circulation patterns, 1861-1971, *Met. Office Geophys. Memoir.*, 116, HMSO, London.

Lamb, H. H. (1988) Climate and life during the middle ages studied especially in the mountains of Europe, in Weather, climate, and human affairs, Routledge, London, 40-74.

Lane, W. L. (1979) *Applied stochastic techniques, user's manual*, Bureau of Reclamation, Engineering and Research Centre, Denver, Colorado.

Lean, J., Skumanich, A. and White, O. (1992) Estimating the sun's radiative output during the Maunder minimum, *Geophys. Res. Lett.* 19, 1591-1594.

Leavesley, G. H. (1994) Modelling the effects of climate change on water resources, a review, *Climate Change*, 28(1-2), 159-177.

Leavesley, G. H. (1999) Overview of models for use in the evaluation of the impacts of climate change on hydrology, in *Impacts of climate change and climate variability on hydrological environments, Int. Hydrology Series,* edited by van Dam, Jan C., Cambridge University Press, chapter 8, 107-122.

Lele, S. M. (1987) Improved algorithms for reservoir capacity calculation incorporating storage-dependent losses and reliability norm, *Water Resour. Res.*, 23(10), 1819-1823.

Lemmelä, R. and Helenius, N. (editors) (1998) *Proc. The Second International Conference on Climate and Water, in 3 volumes*, Espoo, Helsinki, Finland.

Lettenmaier, D. P., Wood, A.W., Palmer, R. N., Wood, E. F. and Stakhiv, E. Z. (1999) Water resources implications of global warming: a U.S. regional perspective, *Climatic Change*, 43, 537-579.

Lins, H. F., Wolock, D. M. and McCabe, G. J. (1997) Scale and modeling issues in water resources planning, *Climatic Change*, 37(1), 63-88.

Loucks, D. P. (1997) Quantifying trends in system sustainability, *Hydrological Sci. J.*, 42(4), 513-530.

Loucks, D. P., Stedinger, J. R. and Haith, D. A. (1981) *Water resource systems planning and analysis*, Prentice-Hall, Englewood Cliffs, N. J.

Loukas, A. and Quick, M. (1996) Effect of climate change on the hydrologic regime of two climatically different watersheds, *J. Hydrologic Eng.*, 1(2), 77-87.

Loveland, P., Audsley, E., Berry, P., Dawson, T., De Baets, A., Harrison, P., Holman, I., Nicholls, R., Rounsevell, M., Sells, J., Shackley, S., Wilson, T. and Wood, R. (2000) REGIS: Regional climate change impact and response studies in East Anglia and North West England, in *Climate change: assessing the impacts-identifying responses, the first three years of the UK Climate Impacts Programme, UKCIP technical report,* edited by Hedger, M., Gawith, M., Brown, I., Connell, R. and Downing, T. E., UKCIP and DETR, Oxford, 81-86.

Maass, A., Hufschmidt, M. M., Dorfman, R., Thomas, H. A., Marglin, S. A. and Fair, G. M. (1962) *Design of water resource systems*, Harvard University Press, Cambridge, Mass.

MAFF (Ministry of Agriculture, Fisheries and Food) (1967) *Potential transpiration,* Tech. Bull. 16., HMSO.

Magnuson, J. J., Robertson, D. M., Benson, B.J., Wynne, R. H., Livingstone, D. M., Arai, T., Assel, R. A., Barry, R. G., Card, V., Kuusisto, E., Granin, N. G., Prowse, T. D., Stewart, K. M. and Vuglinski, V. S. (2000) Historical trends in lake and river ice cover in the northern hemisphere, *Science*, 289, 1743-1746.

Manabe, S. (1969) Climate and the ocean circulation: I, the atmospheric circulation and the hydrology of the Earth's surface, *Monthly Weather Rev.*, 7, 739-774.

Manabe, S. and Stouffer, R. J. (1996) Low frequency variability of surface air temperature in a 1000-year integration of a coupled atmosphere-ocean-land surface model, *J. Climatology*, 9, 376-393.

Mandelbrot, B. B. and Wallis, J. R. (1968) Noah, Joseph and operational hydrology, *Water Resour. Res.*, 4(5), 909-918.

Manley, G. (1974) Central England temperatures: monthly means 1659 to 1973 *Quart. J. Roy. Met. Soc.* 100, 389-405.

Manley R. E. (1975), A hydrologic model with physically realistic parameters, UNESCO symposium, Bratislava, IASH Publication No 115.

Manley, R. E. and Water Resource Associates Ltd, UK (2001*) A guide to using HYSIM*, Water Resource Associates Ltd.

Mann, M. E. and Bradley, R. S. (1999) Northern hemisphere temperatures during the past millennium: inferences, uncertainties, and limitations, *Geophys. Res. Letts.*, 26(6), 759-762.

Mann, M. E., Raymond, A., Bradley, S. and Hughes, M. K. (1998) Global six century temperature patterns, World Data Centre, Data Contribution Series, 16., NOAA/NGDC, Boulder CO, USA.

Marsh T. J. (1996) River flow and groundwater level records-the instrumented era, Palaeohydrology British Hydrological Society occasional paper no. 7, edited by Branson, J.

Mavromatis, T. and Jones, P. D. (1998) Comparison of climate change scenario construction methodologies for impact assessment studies, *Agric. & Forest Met.*, 91(1-2), 51-67.

McCabe, G. J. and Hay, L. E. (1995) Hydrological effects of hypothetical climate change in the East River basin, Colorado, USA., *Hydrological Sci. J.*, 40(3), 303-318

McGregor, J .L. and Walsh, K. (1994) Climate change simulations of Tasmanian precipitation using multiple nesting, *J. Geophys. Res.*, 99, D10, 20899-20905.

McMahon, T. A. and Mein, R. G. (1986) *River and reservoir yield*, Water Resources Publications, Littleton, Colorado.

McMahon, T. A., Finlayson, B. L., Srikanthan, R. and Haines, A. T. (1992) *Global runoff: continental comparisons of annual flows and peak discharges*, Catena Verlag, Gremlingen-Desteedt, Germany.

Meehl, G. A., Washington, W. M., Arblaster, J. M., Bettge, T. W. and Strand Jr, W.G. (2000) Anthropogenic forcing and climate system response in simulations of 20th and 21st century climate, *J. Climate*, 13 (21), 3728-3744.

Mehrotra, R. (1999) Sensitivity of runoff, soil moisture and reservoir design to climate change in central Indian River basins, *Climatic Change*, 42(4), 725-757.

Michaels, P. J. and Knappenberger, P. C. (1996) The United nations intergovernmental panel on climate change and the scientific 'consensus' on global warming, the global warming debate, *Eur. Science and Environment Forum*, 158-178.

Miller, J. R. and Russell, G. L. (1992) The impacts of global warming on river runoff, *J. Geophys. Res.* 97, 2757-64.

Mimikou, M. A. and Baltas, E. A. (1997) Climate change impacts on the reliability of hydroelectric energy production, *Hydrological Sci. J.*, 42(5), 661-678.

Mimikou, M. A., Baltas, E., Varanou, E. and Pantazis, K. (2000) Regional impacts of climate change on water resources quantity and quality indicators, *J. Hydrology*, 234, 95-109.

Mitchell, J. F. B. and Johns, T. C. (1997) On the modification of global warming by sulphate aerosols, *J. Climate*, 10, 245-267.

Montanari, A., Rosso, R. and Taqqu, M. S. (1997) Fractionally differenced ARIMA models applied to hydrologic time series: Identification, estimation, and simulation, *Water Resour. Res.*, 33(5), 1035-1044.

Montaseri, M. (1999) *Stochastic investigation of the planning characteristics of within-year and over-year reservoir systems*, PhD thesis, Dept. Civil and Offshore Engrg., Heriot-Watt Univ., Edinburgh.

Montaseri, M. and Adeloye, A. J. (1999) Critical period of reservoir systems for planning purposes, *J. Hydrology*, 224, 115-136.

Monteith, J. L. (1965) Evaporation and the environment, *Symp. Soc. Expl. Biol.*, 19, 205-234.

Montgomery, D. C. (1984) *Design and analysis of experiments*, second edition, John Wiley & Sons, New York.

Morrison, J. I. L. (1987) Intercellular CO_2 concentration and stomatal response to CO_2, in *Stomatal Function*, edited by Zeiger, E., Farquhar, G. D. and Cowan, I. R., Stanford University Press, Stanford, CA, 229-251.

Mott MacDonald (1995) *Calder area reservoir hydrological records*, report prepared for Yorkshire Water Services Ltd., ref. 28918BA01/1/B.

Moy, W. S., Cohon, J. L. and Revelle, C. S. (1986) A programming model for analysis of reliability, resilience, and vulnerability of a water supply reservoir, *Water Resour. Res.*, 22(4), 489-498.

MWP (Ministry of Water and Power, Iran) (1995) Reservoir systems project at Urmia Region (translated from Persian).

Nalbantis, I. and Koutsoyiannis, D. (1997) A parametric rule for planning and management of multiple-reservoir systems, *Water Resour. Res.*, 33(9), 2165-2177.

Nash, J. E. and Sutcliffe, J. V. (1970) River flow forecasting through conceptual models, 1. a discussion of principles, *J. Hydrology*, 10, 282-290.

Nash, L. L. and Gleick, P. H. (1991) Sensitivity of streamflow in the Colorado basin to climatic change, *J. Hydrology*, 125, 221-241.

Nawaz, N. R. (1996) Assessing the adequacy of Wright Model's reconstructed streamflow data for reservoir storage-yield-reliability analysis, unpublished MSc Thesis, Heriot-Watt University, Edinburgh, UK.

Nawaz, N. R. and Adeloye, A. J. (1999) Evaluation of monthly runoff estimated by a rainfall-runoff regression model reservoir yield assessment, *Hydrological Sci. J.*, 44(1), 113-134.

Nawaz, N. R., Adeloye, A. J. and Montaseri, M. (1999) Impact of climate change on storage-yield curves for multi-reservoir systems, *Nordic Hydrology*, 30(2), 129-146.

Neilsen, R. P. (1998) Simulated changes in vegetation distribution under global warming, in *The regional impacts of climate change - an assessment of vulnerability,* edited by Watson, R. T., Zinyowera, M. C. and Moss, R. H., Cambridge University Press.

Nelder, J. A. and Mead, R. (1965) A simplex method for function minimisation, *Computer J.*, 7, 308-313.

Nemec, J and Schaake, J. (1982) Sensitivity of water resources systems to climate variation, *Hydrological Sci. J.*, 27, 327-345.

Nicholls, N., Gruza, G. V., Jouzel, J., Karl, T. R., Ogallo, L. A. and Parker, D. E. (1996) Observed climate variability and change, in *Climate Change 1995: The Science of Climate Change*, edited by Houghton, J. T., Meira Filho, L. G., Callander, B. A. and Maksell, K., Cambridge University Press.

Nikolaidis, N. P., Hu, H-L., Ecsedy, C. and Lin, J. D. (1993) Hydrologic response of freshwater watersheds to climatic variability: model development, *Water Resour. Res.*, 29(10), 3317-3328.

Nikolaidis, N. P., Hu, H-L. and Ecsedy, C. (1994) Effects of climatic variability on the hydrologic response of a freshwater watershed, *Aquatic Sciences*, 56(2), 161-178.

NRA (1994) *Water: nature's precious resource - an environmentally sustainable water resources development strategy for England and Wales*, Enivronment Agency (formerly the National Rivers Authority).

OCWR (2001) Climate change and demand for water Progress Report, Oxford Centre for Water Research (OCWR).

Oliveira, R. and Loucks, D. P. (1997). Operating rules for multiple reservoir systems. *Water Resour. Res.*, 33(4), 839-852.

Olsen, J. R., Stedinger, N. C., Matalas, N. C. and Stakhiv, E. Z. (1999) Climate variability and flood frequency estimation for Upper Mississippi and lower Missouri rivers, *J. Amer. Water Resour. Assoc*, 35(6), 1509-1524.

Parker, D. E., Legg, T. P. and Folland, C. K. (1992) A new daily central England temperature series, *Int. J. Climatology*, 12, 317-342.

Parry, M. (1992) The potential effect of climate changes on agriculture and land use, *Adv. Ecol. Res.*, 22, 63-91.

Parry, M. L. (editor) (2000) *Assessment of potential effects and adaptations for climate change in Europe: Summary and conclusions*, Jackson Environment Institute, University of East Anglia, Norwich.

Penman, H. L. (1948) Natural evaporation from open water, bare soil and grass, *Proc. Roy. Soc. Lond.*, 193, 120-145.

Pitman, A. J. and Chiew, F. H. S. (1996) Testing a GCM land surface scheme against catchment-scale runoff data, *Climate Dynamics*, 12(10), 685-699.

Prescott, J. A. (1940) Evaporation from a water surface in relation to solar radiation., *Trans. R. Soc. S. Austr.*, 64, 114-118.

Pretto, P. B., Chiew, F. H. S., McMahon, T. A., Vogel, R. M. and Stedinger, J. R. (1997) The (mis)behavior of behaviour analysis storage estimates, *Water Resour. Res.*, 33(4), 703-709.

Price, M. (1998) Water storage and climate change in Great Britain - the role of groundwater, *Proc. Institution of Civil Engineers-Water Maritime and Energy*, 130(1), 42-50.

Racsko, P., Szeidl, L. and Semenov, M. (1991) A serial approach to local stochastic weather models, *Ecol. Modelling*, 57, 27-41.

Rasmussen, E. M. (1985) El Niño and variations in climate, *Am. Sci.* 73, 168-177.

Reungoat, A. (2000) Rainfall-runoff modelling with MODHYDROLOG, unpublished MSc Thesis, Heriot-Watt University, Edinburgh, UK.

ReVelle, C. (1997) *Optimizing reservoir resources*, John Wiley & Sons.

ReVelle, R. R. and Suess, H. E. (1957) Carbon dioxide exchange between atmosphere and ocean and the question of an increase of atmospheric CO_2 during the past decades, *Tellus*, 9, 18-27.

ReVelle, R. R. and Waggoner, P. E. (1983) Effects of a carbon dioxide-induced change on water supply in the western United States, in *Changing Climate*, National Academy of Sciences, Washington DC, 419-432.

Richardson, C. W. (1981) Stochastic simulation of daily precipitation, temperature and solar radiation, *Water Resour. Res.*, 17, 182-190.

Rietveld, M. R. (1978) A new method for estimating the regression coefficients in the formula relating solar radiation to sunshine, *Agric. Meteorology*, 19, 243-252.

Robock, A., Turco, R. P., Harwell, M. A., Ackerman, T. P., Andressen, R., Chang, H. and Sivakumar, M. V. K. (1993) Use of general circulation model output in the creation of climate change scenarios for impact analysis, *Climatic Change*, 23, 293-335.

Rogers, H. H., Thomas, J. F. and Bingham, G. E. (1983) Response of agronomic and forest species to elevated atmospheric carbon-dioxide, *Science*, 220, 428-429.

Rosenberg, N. J., Kimball, B. A., Martin, P. and Cooper, C. F. (1990) From climate and CO_2 enrichment to evapotranspiration, in *Climate change and U.S. water resources*, edited by Waggoner, P. E., chapter 7, 151-175.

Rosenberg, N. J., Crosson, P. R., Frederick, W. E., Easterling, I. I., McKenney, I., Bowes, M. D., Sedjo, R. A., Darmstader, J., Katz, L. A. and Lemon, K. M. (1993) Paper 1, the MINK methodology: background and baseline, *Climatic Change*, 24, 7-22.

Rosenbrock, H. H. (1960) An automatic method for finding the greatest or least value of a function, *Comput. J.*, 3, 175-184.

Rotter, R. and Van de Geijn, S. (1999) Climate change effects on plant growth, crop yield and livestock, *Climatic Change*, 43, 651-681.

Rowntree P. R. and Lean, J. (1994) Validation of hydrological schemes for climate models against catchment data, *J. Hydrology*, 155(3-4), 301-323.

Running, S. W. and Nemani, R. R. (1991) Regional hydrologic carbon balance responses of forecasts resulting from potential climate change, *Climatic Change*, 19, 349-368.

Salas, J. D. (1993) Analysis and modelling of hydrologic time series, in *Handbook of hydrology*, edited by Maidment, D. R., McGrawhill Inc.

Salewicz, K. A. (1996) Impact of climate change on the Lake Kariba hydropower scheme, in *Water resources management in the face of climatic/hydrologic uncertainties*, edited by Kaczmarek, Z., Strzepek, M., Somlyody, L. and Priazhinskaya, V., chapter 11, 300-322.

Sankarasubramanian, A., Vogel, R. M. and Limbrunner, J. F. (2001) Climate elasticity of streamflow in the United States, *Water Resour. Res.*, 37(6), 1771-1781.

Santer, B. D., Wigley, T. M. L., Barnett, T. P. and Anyamba, E. (1996) Detection of climate change and attribution of causes, in *Climate Change 1995: the Science of Climate Change,* edited by Houghton, J. T., Meira Filho, L. G., Callander, B. A. and Maksell, K., Cambridge University Press.

Savic, D. A., Burn, D. H. and Zrinji, Z. (1989) A comparison of streamflow generation models for reservoir capacity-yield analysis, *Water Resour. Bull.*, 25(5), 977-983.

Schimel D., Alves, D., Enting, I. and Heimann, M. (1996) Radiative forcing of climate change, in *Climate Change 1995: the Science of Climate Change,* edited by Houghton, J. T., Meira Filho, L. G., Callander, B. A. and Maksell, K., Cambridge University Press.

Semenov, M. A. and Barrow, E. M. (1997) Use of a stochastic weather generator in the development of climate change scenarios, *Climatic Change*, 35(4), 397-414.

Semenov, M. A. and Porter, J. R. (1994) The implications and importance of non-linear responses in modelling of growth and development of wheat, in *Predictability and non-linear modelling in natural sciences and economics,* edited by Grasman, J. and van Straten, G., Wageningen.

Shackley, S., Young, P., Parkinson, S. and Wynne, B. (1998) Uncertainty, complexity and concepts of good science in climate modelling: are GCM's the best tools?, *Climatic Change*, 38, 159-205.

Shaw, E. M. (1994) *Hydrology in practice,* Chapman and Hall, London.

Shnaydman, V. M. and Niemann, J. D. (1996) Climate change and water resources management strategy: the Terek River basin, in *Water resources management in the face of climatic/hydrologic uncertainties*, edited by Kaczmarek, Z., Strzepek, M., Somlyody, L. and Priazhinskaya, V., 322-339.

Shuttleworth, W.J. (1993) Evaporation, in *Handbook of hydrology,* edited by Maidment, D. R., McGrawhill Inc.

Simonovic, S. P. (1992) Reservoir systems analysis: closing the gap between theory and practice, *J. Water Res. Plan. Managt., ASCE*, 118(3), 262-280.

Smith, J. B. and Hulme, M. (1998) Climate change scenarios, in *Handbook on methods for climate change impact assessment and adaptation strategies,* edited by Feenstra, J. F., Burton, I., Smith, J. B. and Tol, R. S. J., United Nations Environment Programme and Institute for Environmental Studies, version 2.0, chapter 3, 3-1,3-40.

Smith, T. M., Leemans, R. and Shugart, H. H. (1992) Sensitivity of terrestrial carbon storage to CO_2-induced climate change: comparisons of four scenarios based on general circulation models, *Climatic Change*, 21, 367-384.

Srikanthan, R. and McMahon, T. A. (1982) Stochastic generation of monthly streamflows, *J. Hydraul. Div., ASCE*, 108(HY3), 419-441.

Stedinger J. R. and Taylor M. R. (1982) Synthetic streamflow generation, Part 2. Effect of parameter uncertainty, *Water Resour. Res.*, 18(4), 919-924.

Stedinger, J. R., Vogel, R. M. and Foufoula-Georgiou, E. (1993) Frequency analysis of extreme events, in *Handbook of hydrology*, edited by Maidment, D. R., McGraw-Hill Book Co., Inc., New York.

Stone, P. H. (1992) Forecast cloudy - the limits of global warming models, *Tech. Review*, 95(2), 32-40.

Stonefelt, M. D., Fontaine, T. A. and Hotchkiss, R. H. (2000) Impacts of climate change on water yield in the Upper Wind River Basin, *J. Amer. Water Resour. Assoc.*, 36(2), 321-336.

Stouffer, R. J., Manabe, S. and Vinnikov, Y. A. (1994) Model assessment of the role of natural variability in recent global warming, *Nature*, 367, 634-636.

Street-Perrott, F. A. and Roberts, N. (1994) Past climates and future greenhouse warming, in *the changing global environment*, edited by Roberts, N., Blackwell, Oxford.

Strupczewski, W. G. and Mitosek, H. T. (1996) Some aspects of hydrological design under non-stationarity, in *New uncertainty concepts in hydrology and water resources*, edited by Kundzewicz, Z. W., International Hydrology Series.

Strzepek, K. M. (1998) Water resources, in *Handbook on methods for climate change impact assessment and adaptation strategies,* edited by Feenstra, J. F., Burton, I., Smith, J. B. and Tol, R. S. J., United Nations Environment Programme and Institute for Environmental Studies, version 2.0, chapter 6, 6-1, 6-36.

Svanidze, G. G. (1964) Osnovy Rascheta Regulirovaniya Rechnigo Stoka Metodum Monte-Karlo (Elements of river-runoff regulation computation by Monte Carlo method), Izdatel'stru, Metsmiereba.

Takeuchi, K. and Hamlin, M. (1998) *Sustainable reservoir development and management*, IAHS Publication No. 251.

Tanakumara, H. and Burges, S. J. (1996) Application of global optimisation to parameter estimation of the Tank Model, in *Proc. Int. Conf. Water Resour. Environ. Res.*: *towards the 21st century*, Kyoto, Japan, 39-46.

Tett, S., Stott, P., Mitchell, J. F. B., Johns, T. C., Ingram., W., Sexton, P., Rayner, N., Folland, C., Parker, D., Gordon, M., Cullum, D., Horton, B., Lavery, J., O' Donnell, M. and Jenkins, G. (1997) Is humankind already changing global climate?, *Hadley Centre for Climate Prediction and Research*, Meteorological Office.

Thomas, H. A. and Burden R. P. (1963) *Operations research in water quality management*, Harvard University Press, Cambridge, Mass.

Thomas, H. A. and Fiering, M. B. (1962) Mathematical synthesis of streamflow sequences for the analysis of river basins by simulation, in *Design of water resource systems*, edited by Maass, A., Hufschmidt, M. M., Dorfman, R., Thomas, H. A., Marglin, S. A. and Fair, G. M., Harvard University Press, Cambridge, Mass.

Thompson, N., Barrie, I. A. and Ayles, M. (1981) *The Meteorological Office rainfall and evaporation calculation system: MORECS*, Hydrological Memorandum No. 45., Meteorological Office.

Thorne, J. M., Savic, D. A. and Weston, A. (1998) Development of optimised conjunctive control rules for a system of water supply sources, Centre for Water Systems, University of Exeter, presented at the BHS meeting.

Trenberth, K. E., Houghton, J. T. and Meira Filho, L. G. (1996) The climate system: an overview, in *Climate change 1995: the science of climate change,* edited by Houghton, J. T., Meira Filho, L. G., Callander, B. A., and Maksell, K., Cambridge University Press, Chapter 1.

Tung, C-P. and Haith, D. A. (1995) Global warming effects on New York streamflows, *J. Water Resour. Plan. Managt., ASCE*, 121(2), 216-225.

Valencia, D. and Schaake, J. C. (1973) Disaggregation processes in stochastic hydrology, *Water Resour. Res.*, 9(3), 580-585.

Vandeweile, G. L. and C-Y Xu. (1991) Regionalisation of physically-based water balance models in Belgium, application to ungauged catchments, *Water Resour. Managt*, 5, 199-208.

Vandewiele, G. L. and Ni-Lar-Win. (1998) Monthly water balance models for 55 basins in 10 countries, *Hydrological Sci. J.*, 43(5).

Vogel, R. M. and Stedinger, J. R. (1987) Generalised storage-reliability-yield relationships, *J. Hydrology*, 89, 303-327.

Vogel, R. M. and Stedinger, J. R. (1988) The value of stochastic streamflow models in over-year reservoir design applications, *Water Resour. Res.*, 24(9), 1483-90.

Vogel, R. M. and McMahon, T. A. (1996) Approximate reliability and resilience indices for over-year reservoirs fed by AR(1) Gamma and normal flows, *Hydrological Sci. J.*, 41(1), 75-96.

Vogel, R. M., Bell, C. J. and Fennessey, N. M. (1997) Climate, streamflow and water supply in the northeastern United States, *J. Hydrology,* 198, 42-68.

Von Storch, H., Zorita, E. and Cubasch, U. (1993) Downscaling of global climate change estimates to regional scales: an application to Iberian rainfall in wintertime, *J. Climate,* 6,(6), 1161-1171.

Whetton, P. H., Fowler, A. M., Haylock, M. R. and Pittock, B. (1993) Implications of climate change due to the enhanced greenhouse gas on floods and droughts in Australia, *Climatic Change*, 25 289-317.

Wigley, T. M. L. and Jones, P. D. (1985) Influences of precipitation changes and direct CO_2 effects on streamflow, *Nature*, 314(6007), 149-152.

Wigley, T. M. L. and Kelly, P. M. (1990) Holocene climatic change, ^{14}C wiggles and variations in solar irradiance, *Phil. Trans. R. Soc. Lond.*, A 330, 547-560.

Wigley,T. M. L. and Raper, S. C. B. (1992) Implications for climate and sea-level of revised IPCC Emissions Scenarios, *Nature*, 357(6376), 293-300.

Wigley, T. M. L., Lough, J. M. and Jones, P. D. (1984) Spatial patterns of precipitation in England and Wales and a revised homogenous England and Wales precipitation series, *J. Climatol.*, 4, 1-26.

Wigley, T. M. L., Jones, P. D., Briffa, K. R. and Smith, G. (1990) Obtaining sub-grid-scale information from coarse-resolution general circulation model output, *J. Geophys. Res.* 95, D2, 1943-1953.

Wilby, R. L. (1997) Statistical downscaling of general circulation model output for climate change impact assessment, British Hydrological Society Hydrology Symposium, Salford, UK, 8.19-8.30.

Wilby, R L. and Wigley, T. M. L. (1997) Downscaling general circulation model output: a review of methods and limitations, *Progress in Physical Geography*, 21(4), 530-548.

Wilks, D. S. (1992) Adapting stochastic weather generation algorithms for climate change studies, *Climatic Change*, 22, 67-84.

Winkler, J. A., Palutikof, J. P., Andresen, J. A. and Goodess, C. M. (1997) The simulation of daily temperature time series from GCM output, Part II, sensitivity analysis of an empirical transfer function methodology, *J. Climate*, 10, 2514-2532.

Win-Nielsen, A. (1999) The Greenhouse effect. Yes or no? A scientific evaluation, *Water Resour. Managt.*, 13, 59-72.

Wolock, D. M. and McCabe, G. J. (1999) Estimates of runoff using water-balance and atmospheric general circulation models, *J. Amer. Water Resour. Assoc*, 35, 1341-1350.

Wood, A. W., Lettenmaier, D. P. and Palmer, R. N. (1997) Assessing climate change implications for water reservoirs planning, *Climate Change*, 37, 203-228.

Woodward, W. A. and Gray, H. L. (1993) Global warming and the problem of testing for trend in time series data, *J. Climate*, 6, 953-962.

Woodward, W. A. and Gray, H. L. (1995) Selecting a model for detecting the presence of a trend, *J. Climate*, 8, 1929-1937.

Wright, C. E. (1978) Synthesis of river flows from weather data, technical note No.26., UK Central Water Planning Unit Publication.

Xu, C-Y. (1999) From GCMs to river flow: a review of downscaling methods and hydrologic modelling approaches, *Progress in Physical Geography*, 23(2), 229-249.

Xu, C-Y. and Halldin, S. (1997) The effect of climate change on riverflow and snow cover in the Nopex area simulated by a simple water balance model, *Nordic Hydrology*, 28(4/5), 273-282.

Xu, C-Y. and Singh, V. P. (1998) A review on monthly water balance models for water resources investigations, *Water Resour. Managt.*, 12, 31-50.

Xu,C-Y., Seibert, J. and Halldin, S. (1996) Regional water balance modelling in the Nopex area: development and application of monthly water balance models, *J. Hydrology*, 180(1-4), 211-236.

Yapo, P. O., Gupta, H. V. and Sorooshian, S. (1996) Automatic calibration of conceptual rainfall-runoff models: sensitivity to calibration data, *J. Hydrology*, 181(1-4), 23-48.

Yapo, P. O., Gupta, H. V. and Sorooshian, S. (1998) Multi-objective global optimization for hydrologic models, *J. Hydrology*, 204(1-4), 83-97.

Yates, D. N. and Strzepek, K. M. (1994) Potential evapotranspiration methods and their impact on the assessment of river basin runoff under climate change, IIASA working paper, WP-94-46 (Laxenburg, Austria, IIASA).

Yates, D. N. and Strzepek, K. M. (1998) Modelling the Nile Basin under climatic change, *J. Hydrologic Engrg.*, 3, 98-108.

Yorkshire Water RRDY (1991) Re-*assessment of resource design yield (RRDY) project 3: Calder area*, technical report, 1, prepared by W. S. Atkins Ltd, England.

Yoshino, F. (1999) Studies on the characteristics of variation and spatial correlation of the long-term annual runoff in the world rivers, *J. Japan Soc. Hydrology & Water Resour.*, 12, 109-120.

Zhang, X-H., Oberhuber, J. M., Bacher, A. and Roeckner, E. (1998) Interpretation of interbasin exchange in an isopycnal ocean, *Climate Dynamics*, 14(10), 725-740.

Zongxue, X., Jinno, K., Kawamura, A., Takesaki, S. and Ito, K. (1998) Performance risk analysis for Fukuoka water supply system, *Water Resour. Managt.*, 12, 13-30.

Personal Communications

Stevens, I. Water Resources Manager, Yorkshire Water Services Ltd., Bradford, UK.

Xu, C-Y. Lecturer in Hydrology, Department of Earth Sciences, Uppsala University, Uppsala, Sweden.

Appendix A

Impact of Climate Change on Storage-Yield Curves for Multi-Reservoir Systems

Nawaz, N.R., Adeloye, A.J. and Montaseri, M

Nordic Hydrology

Vol. 30 No. 2

Pages 129-146

1999

Nordic Hydrology, 30 (2), 1999, 129-146

The Impact of Climate Change on Storage-Yield Curves for Multi-Reservoir Systems

N. R. Nawaz, A. J. Adeloye, and M. Montaseri

Dept. of Civil & Offshore Eng., Heriot-Watt University,
Edinburgh, EH14 4AS, UK

In this paper, we report on the results of an investigation into the impacts of climate change on the storage-yield relationships for two multiple-reservoir systems, one in England and the other in Iran. The impact study uses established protocol and obtains perturbed monthly inflow series using a simple runoff coefficient approach which accounts for non-evaporative losses in the catchment, and a number of recently published GCM-based scenarios. The multi-reservoir analysis is based on the sequent-peak algorithm which has been modified to analyse multiple reservoirs and to accommodate explicitly performance norms and reservoir surface fluxes, *i.e.* evaporation and rainfall. As a consequence, it was also possible to assess the effect of including reservoir surface fluxes on the storage-yield functions. The results showed that, under baseline conditions, consideration of net evaporation will require lower storages for the English system and higher storages for the Iranian system. However, with perturbed hydroclimatology different impacts were obtained depending on the systems' yield and reliability. Possible explanations are offered for the observed behaviours.

Introduction

A recent report by the Intergovernmental Panel on Climate Change (IPCC 1996) has produced the most compelling evidence yet that global warming is taking place as a result of increased atmospheric concentrations of "greenhouse" gases due to industrial and other anthropogenic activities. The greenhouse effect occurs as a result of

outgoing long-wave radiation emitted by the Earth being unable to escape the earth's atmosphere due to the presence of the greenhouse gases, notably carbon dioxide (CO_2), methane and water vapour.

A warmer climate is sure to put phenomenal pressures on water resources in many parts of the world and so the need then arises for climate change impacts assessment to ascertain the extent of the problem and plan mitigating measures. A considerable number of studies have addressed this problem (see Arnell 1996 for a review), frequently using climate change scenarios developed from simulation experiments of General Circulation Models (GCMs). Another common feature of the previous studies is that only single reservoir systems have been considered. There have been very little in the way of multiple reservoirs or of how considerations of reservoir surface fluxes, such as evaporation and direct rainfall which are also liable to climate change impacts, can affect the storage-yield relationship. These fluxes may be important in arid and semi-arid regions since any accentuation of the net evaporation (due to climate change) can cause a significant reduction in the useable yield of water resources systems.

The main objective of this study is to investigate the likely impacts of climate change on the storage-yield relationships of multiple reservoir systems. Complete storage-yield-reliability curves will be constructed for aggregate multi-reservoir systems, both for baseline and perturbed hydroclimate, and used to assess the impacts. A secondary objective examines how the incorporation of surface fluxes, *i.e.* rainfall onto and evaporation from the reservoir surface, in the analysis will affect the climate change impacts. Both these objectives will use two case studies, one from each of two different climatic regions.

Methodology

Storage-Yield-Reliability Analysis

Given the objectives of the study, the storage-yield-reliability technique adopted must be capable of analysing multiple reservoir systems and including, explicitly, reservoir surface-area-dependent fluxes such as the net evaporation. The modified sequent peak algorithm, SPA (Lele 1987; Adeloye and Montaseri 1998) is capable of these. Preference for the modified SPA stems from the fact that, unlike the behaviour approach (Adeloye and Nawaz 1998; McMahon and Mein 1986), the determination of storage-yield for a desired reliability is no longer a trial and error procedure. Being able to impose a limit on supply shortfall during failure periods with the modified SPA also means that system's vulnerability or volumetric failure risk (Hashimoto *et al.* 1982) can be selected *a priori*. Furthermore, because the SPA by default uses two cycles of the historical record, the usual problems associated with the choice of the starting state of the reservoir is no longer an issue. The initial state of the reservoir has a significant impact on the outcome of a behaviour analysis. The SPA is es-

sentially a single reservoir technique; however, an extension of the technique to multiple reservoirs analysis, using the Space Rule operating policy (Bower *et al.* 1962) is described in Adeloye and Montaseri (1998) and was used for the study.

Climate Change Impact Study

The climate change impact was conducted in accordance with the protocol outlined in Carter *et al.*(1994). The perturbation of the baseline hydrology was achieved using a runoff coefficient technique (Wigley and Jones 1985; Glantz and Wigley 1987). Arnell (1996) and Xu and Singh (1998) review a number of rainfall-runoff models of varying degrees of sophistication which could be used to simulate runoff from rainfall and other climatic variables; however, because sufficient data may not always be available for calibrating such sophisticated models, it is important that simplicity and flexibility is ensured in the choice of the scheme for translating rainfall into runoff.

Starting from the annual water balance equation (and ignoring any non-evaporative losses such as infiltration-percolation for the moment), we have

$$R_b = P_b - E'_b \tag{1}$$

$$R_f = P_f - E'_f \tag{2}$$

where the subscripts b and f denote baseline and future conditions respectively, R is annual runoff (mm), P is the annual precipitation (mm) and E' is the annual actual evapotranspiration, AE, (mm). Now let $P_f = \alpha P_b$ and $E'_f = \beta E'_b$, where α and β are factor changes in the annual precipitation and AE, respectively, as a result of climate change, then from Eqs. (1) and (2),

$$\frac{R_f}{R_b} = \frac{P_f - E'_f}{R_b} = \frac{\alpha P_b - \beta E'_b}{R_b} = \frac{\alpha P_b - \beta(P_b - R_b)}{R_b} = \frac{\alpha - (1 - R_b/P_b)\beta}{R_b/P_b} \tag{3}$$

Replacing R_b/P_b in Eq. (3) by γ_b, the baseline runoff coefficient, the sensitivity of annual runoff becomes

$$\frac{R_f}{R_b} = \frac{\alpha - (1 - \gamma_b)\beta}{\gamma_b} \tag{4}$$

Eq. (4) is a simple way to assess the relative sensitivity of annual runoff to changes in annual precipitation and AE. However, while it is not unreasonable to ignore the non-evaporative losses in the annual model, such losses must be accounted for in monthly models. Glantz and Wigley (1987) extended the above approach to incorporate non-evaporative losses to obtain

$$\frac{\Delta R}{R_b} = \frac{1}{\gamma_b}\frac{\Delta P}{P_b} - \frac{\Delta E'}{E'_b}\left\{\frac{1 - \xi_b}{\gamma_b} - 1\right\} - \frac{\xi_b}{\gamma_b}\frac{\Delta L}{L_b} \tag{5}$$

where Δx refers to the difference between future and baseline values of variable x; L is the sum total of all other losses (*e.g.* infiltration, seepage and deep percolation) and $\xi = L/P$. (Note that E' in Eq. (5) now refers to the monthly AE). Eq. (5) can be re-written in the form of Eq. (4) as

$$\frac{R_f}{R_b} = \frac{1}{\gamma_b}\left\{(\alpha-1)-\left((\beta-1)\,(1-\xi_b-\gamma_b)\right)-\left(\xi_b(\theta-1)\right)\right\}+1 \qquad (6)$$

where $\theta = L_f/L_b$. ξ_b can also be written as

$$\xi_b = 1-\gamma_b-\frac{E_b'}{P_b} \qquad (7)$$

If a further assumption is made that the non-evaporative losses remain unchanged with time, then L_f/L_b becomes unity and hence the monthly changes in runoff become

$$\frac{R_{f_i}}{R_{b_i}} = \frac{1}{\gamma_{b_i}}\left\{(\alpha_i-1)-\left((\beta_i-1)\,(1-\xi_{b_i}-\gamma_{b_i})\right)\right\}+1, \quad i=1, 2, \ldots, 12 \qquad (8)$$

To apply Eq. (8) will require γ_{b_i}, α_i, β_i and ξ_{b_i}. Both α_i and β_i are provided by the climate change scenarios for rainfall and evapotranspiration, respectively for each month i. γ_{b_i}, the baseline runoff coefficient for month i, was obtained by dividing the corresponding mean monthly runoff by the corresponding rainfall for that month. ξ_{b_i} was evaluated according to Eq. (7) using estimates of the mean AE and the mean rainfall for month i. The method used to calculate the AE is described in the next section.

Eq. (8), unlike most other rainfall-runoff schemes used in climate change impact studies to produce perturbed inflow series, is simple and does not require any formal calibration. As noted by Beven (1989), there are large uncertainties associated with calibrating the parameters of catchment models primarily due to lack of model identifiability; such uncertainties tend to magnify as the model becomes complex and the number of parameters grows (Dooge 1977). On the contrary, Eq. (8) does not have any parameters and is directly applicable to any catchment in any region, which is an important consideration given the desire to investigate data from two different climatic regions.

The assumption underpinning Eq. (8), *i.e.* that θ is unity, is necessary to avoid the problem associated with quantifying L_f which is not an output of GCMs and hence for which scenarios are not available. Admittedly, the dominant component in L, *i.e.* infiltration, will be greatly affected by land use changes. However, until climate has actually changed and L is measured under the new climate, there will be no other way of knowing by how much L has been affected. It can therefore be taken that the current assumption about θ remains a reasonable one.

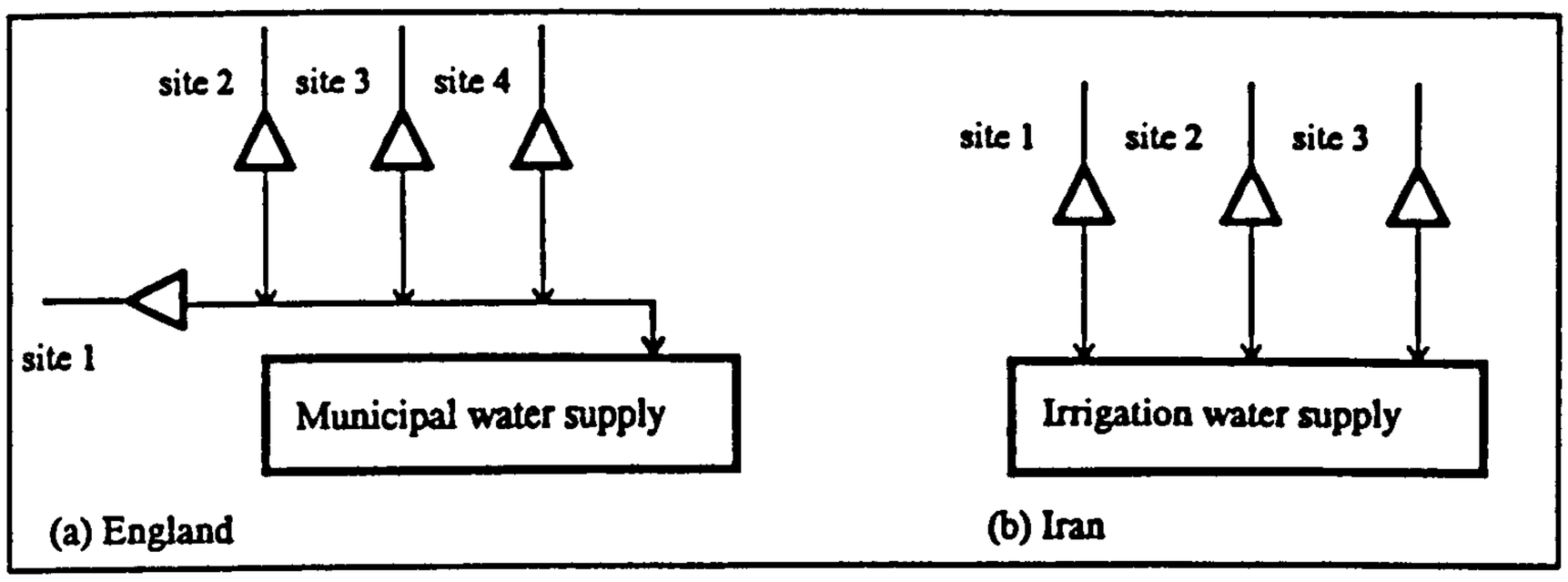

Fig.1. Simplified schematics of the multiple-reservoir systems.

Application

Catchments and Data

Two multiple reservoir systems formed the basis of this investigation. The first system, from north-east England and simplified into the schematic in Fig. 1(a), is an existing complex multi-reservoir system which provides for domestic, industrial and compensation releases. Its operation is aimed at satisfying the full demand, although during extreme droughts, reductions in releases can be made. The second system, typifying a semi-arid climate, is in Iran and comprises three reservoirs in parallel to be used for providing irrigation water (Fig. 1b). Operation of the reservoirs will be aimed at satisfying the demand at all times if possible and at least 75% of the demand during droughts. Relevant characteristics of the two systems are shown in Table 1. Although as shown in Table 1, data are available over different periods, the baseline analyses were for the standard period 1961-1990, the same standard period for the GCMs' predictions (Arnell *et al.* 1997).

Table 1 – Characteristics of the catchments analysed.

System Location	Site	Name	Area (Km^2)	Ann. flow ($x\ 10^6\ m^3$)	Annual flow CV	Availability of records Rainfall	*PE*	Flow
England	1	Gorpley	2.8	2.6	0.22			
	2	Hebden	26.4	25.1	0.20	1961-	1918-	1936-
	3	Luddenden	5.4	5.1	0.18	1990	1995	1995
	4	Ogden	5.4	4.3	0.22			
Iran	1	Baranduz	618	272	0.34	1950-	1950-	1950-
	2	Nazlu	1715	390	0.41	1993	1993	1993
	3	Shahr	418	170	0.38			

Mean monthly rainfall and open-water evaporation, as estimated from the available time series data, were used to obtain reservoir surface net water flux. Fennessey (1995) found this approach to give almost the same results as using time series data of rainfall and evaporation. Open water evaporation data, derived from Class A Pan evaporation measurements, were available for the Iranian catchments. For the English system, open-water evaporation data were obtained by scaling from the available MORECS (Meteorological Office 1981) potential evapotranspiration, PE, estimates, using $E_p = kE_o$ where E_o is the open-water surface evaporation (mm); E_p is the PE (mm) and k has the value of 0.6 for November-February; 0.7 for March, April, September and October and 0.8 for the remaining months, based on European conditions (Shaw 1994). The area-storage relationship for converting evaporation (m) to (10^6 m^3) for use in the SPA was approximated by $A = 0.0815S + 0.0056$ for the English reservoirs and by $A = 0.0317S + 1.688$ for the Iranian reservoirs, where A is the surface area (km^2) and S is the storage (10^6 m^3). The former expression was found by fitting a linear regression equation to area-capacity data for fifty reservoirs in England and Wales ($R^2 = 0.8817$) while the Iranian expression was based on area-storage data for three Iranian reservoirs ($R^2 = 0.9947$). Each of the Iranian reservoirs had ten measurements of area and corresponding storage, giving a total of thirty data points for deriving the average area-storage relationship.

Mean monthly AE data are required for computing ξ_{b_i} in Eq. (7). For the English catchments, long time series data records of AE with which to estimate the monthly means with sufficient accuracy were not available for the reservoir catchments. However, there was a much shorter (1993-1996) monthly data record of MORECS-based AE and PE for a 40 km by 40 km square grid which encompasses all the studied reservoir groups. This latter record was used to derive the AE data for the period 1918-1995, corresponding to the period of the available PE data record (see Table 2), as follows. First, using the four year grid data, the ratio of the mean AE to the mean PE for each month of the year was obtained. These ratios were then used to scale the available PE time series data to obtain the time series data of AE, whence derive the monthly mean estimates. This approach assumes that the ratio of AE to PE at the catchments is equal to that for the grid, which is reasonable given that all the catchments are located within the MORECS grid. Despite this, however, it was decided still not to use the grid's monthly mean actual evapotranspiration directly in

Table 2 – Rainfall ratio ($\alpha_i = P_{fi}/P_{bi}$).

Scenario	Jan	Feb	Mar	Apr	May	Jun	Jul	Aug	Sep	Oct	Nov	Dec
HADCM1(2050)	1.18	1.10	1.15	0.95	0.92	1.07	1.14	0.94	1.02	1.18	1.30	1.03
HADCM1(2020)	1.09	1.05	1.09	0.97	0.96	1.05	1.08	0.98	1.03	1.11	1.16	1.02
GG1m	1.02	1.08	1.04	1.06	1.08	0.99	0.97	1.05	1.06	1.11	1.11	1.06
GS1m	1.04	1.02	1.03	1.05	1.05	1.01	0.98	1.01	0.99	1.06	1.03	1.02
GS1t	1.04	1.04	1.05	1.13	1.16	0.85	0.91	0.95	1.05	1.22	0.99	1.00

Eq. (7) because of the potentially large sampling variability of such small sample (*i.e.* four years) estimates. On the contrary, the sampling variability of the monthly means derived with the 1918-1995 record will be much lower, implying that such estimates will be more reliable and hence more representative of the true mean *AE*.

In the absence of needed data, the same monthly ratios derived for the English catchments were used in scaling the evaporation data at the Iranian sites to obtain their *AE*.

Scenarios

Arnell *et al.* (1997) summarise changes in climate by the 2020's for six regions in the UK as obtained from two UK Hadley Centre's GCMs: HADCM1 and HADCM2. HADCM1 and HADCM2 output is in the form of monthly percentage change (relative to the 1961-1990 baseline period) in rainfall, temperature, radiation, humidity and wind speed for 80,000 km^2 grid squares. Changes in climate by the 2050's produced by HADCM1 for eight regions in the UK are also summarised by Arnell (1996), which also contains further details about the GCMs' experiments and the development of the climate scenarios. The basic 2050's UK-wide scenarios upon which Arnell's more detailed work are based were developed by the UK Climate Change Impacts Review Group (CCIRG 1996).

The rainfall and *PE* scenarios are presented in Table 2 and Table 3, respectively. The *PE* scenarios were obtained by Arnell *et al.* (1997) using both the Penman and Penman-Monteith formulae. Five scenarios from both HADCM1 and HADCM2 GCMs as reported in Arnell *et al.* (1997) for north-east of England and Arnell (1996) for the north of England, where the English system is located. HADCM1-2020 and HADCM1-2050 are from HADCM1 which assumes a gradual compound increase of 1% in CO_2 concentrations each year from 1990 to the end of the next century (Arnell *et al.* 1997). GG1m, GS1m and GS1t, are produced by HADCM2 which is an updated version of HADCM1 (Arnell 1996). Natural climate variability and change need to be separated because the modelling process only accounts for the latter; hence GG1m and GS1m scenarios have both involved "re-scaling" for a *medium* climate sensitivity thus the term "m" (Arnell *et al.* 1997). This problem was avoided in the GS1t scenario by using results from repeated runs of the model with each run made from a slightly different starting condition. Additional differences are that

Table 3 – *PE* ratio ($\beta_i = E_{fi}/E_{bi}$).

Scenario	Jan	Feb	Mar	Apr	May	Jun	Jul	Aug	Sep	Oct	Nov	Dec
HADCM1(2050)	1.00	1.40	1.15	1.25	1.00	1.27	1.00	1.07	1.23	1.10	1.50	0.78
HADCM1(2020)	0.95	1.11	1.02	1.08	0.99	1.04	0.99	1.02	1.03	1.00	1.21	0.80
GG1m	0.86	0.91	0.96	0.99	1.01	1.00	1.03	1.01	1.02	0.99	0.83	0.75
GS1m	0.88	0.93	0.98	0.99	1.00	0.99	1.02	1.03	1.04	1.00	0.95	0.90
GS1t	0.95	0.94	0.99	0.94	0.93	1.05	1.06	1.15	1.12	1.06	0.99	0.95

GG1m is based on greenhouse gases only; GS1m includes the effects of sulphate aerosols as well as greenhouse gases; GS1t is similar to GS1m except that it has a different spatial pattern of change (Arnell *et al.* 1997).

Climate scenarios were not immediately available for the Iranian catchments. However, because the GS1t scenario gave the highest reduction in summer rainfall and the highest rise in summer evapotranspiration (see Tables 2 and 3), it was employed as a spatial analogue for the Iranian catchments.

Results and Discussion

The storage-yield-reliability curve provides the most complete information about a reservoir system. During planning, it is used to determine the storage required for given yield and reliability. For an existing system with known storage capacity, the curve can be used to determine the sustainable yield. Furthermore when, as is usual, the axes are scaled by the mean annual runoff, the curve provides a means for "regionalising" the storage-yield function and hence for estimating storage or yield at ungauged sites. As a consequence, the results herein will be presented within the framework of the storage-yield curves. Other issues such as resiliency and vulnerability are not explicitly considered in the study although, inferences will be made about how these two performance metrics are likely to be affected. It should be noted, however, that the modified SPA can analyse for pre-specified vulnerability and resiliency (Montaseri and Adeloye 1998). For reasons of lack of space, results will only be presented for the aggregated system rather than for each individual reservoir in a multi-reservoir system.

Effect of Surface Fluxes on Baseline Storage-Yield Relationships

Fig. 2 shows the impact of incorporating reservoir surface water fluxes due to net evaporation on the storage-yield function for the baseline records. For the English system (see Figs. 2a and b), the inclusion of reservoir surface net evaporation flux resulted in reductions in the required storage capacity for a given yield. These reductions averaged about 7% for the 70% yield but lower (2%) for the 30% yield. This is to say that if the capacity were fixed, then more water could be supplied from the fixed storage if net evaporation was considered in the analysis than if it was not. This behaviour can be attributed to the fact that, for the English catchments, rainfall generally exceeds the evaporation and so the effect of including the net evaporation flux is an additional inflow into the reservoir.

On the other hand, for the Iranian catchments where evaporation exceeds rainfall, the inclusion of net evaporation flux means that there is a net outflow flux from any reservoir surface. Such a net outflow constitutes an additional demand on top of the design yield, thus requiring increased storage to meet such a design yield (Figs. 2c) and d). Failure to provide such an additional storage will mean that either a reduc-

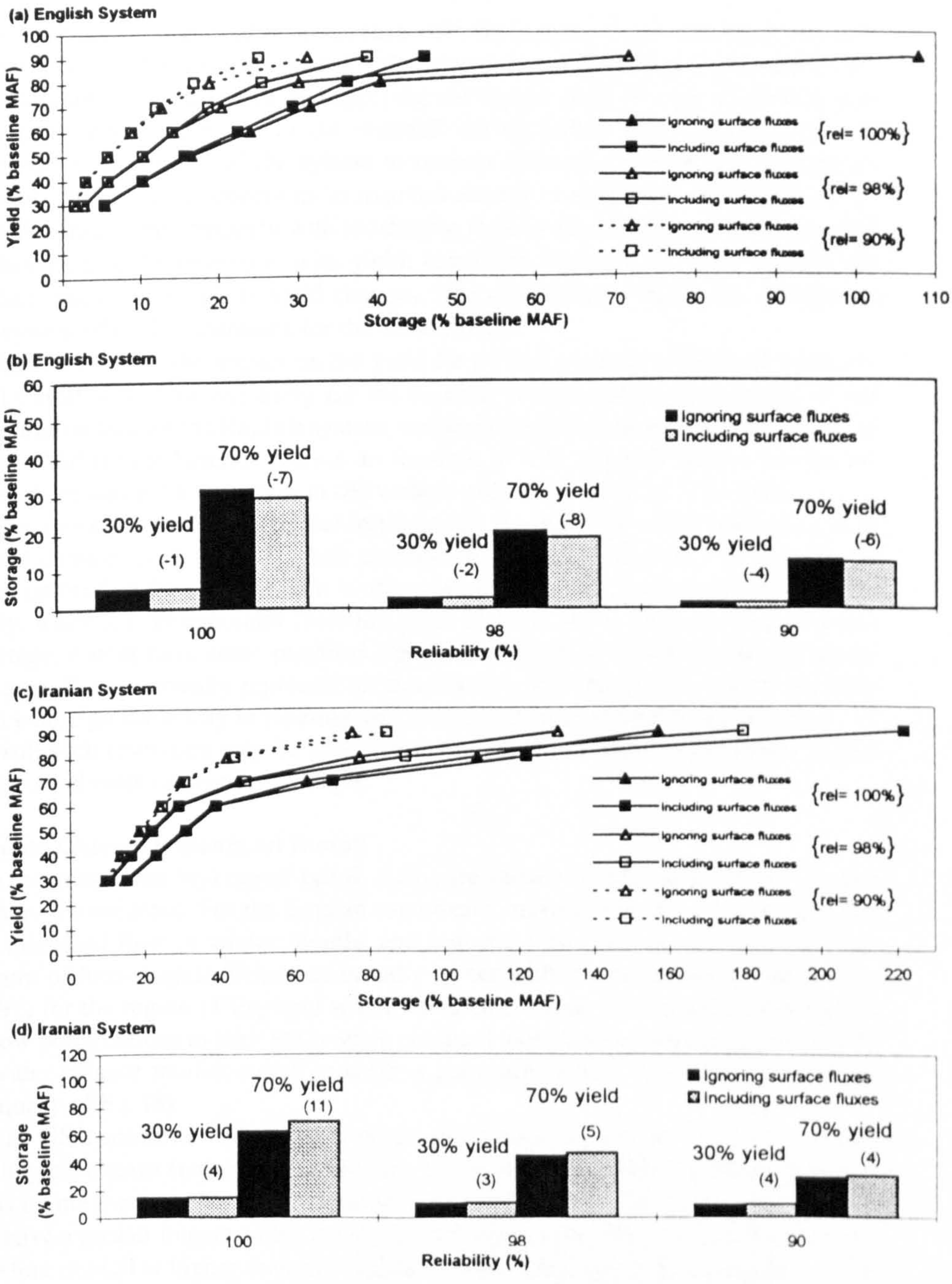

Fig. 2. Impact of reservoir surface evaporation and rainfall fluxes on storage-yield-reliability relationship (baseline records). Values in parenthesis in (b) and (d) are % difference in storage due to incorporation of surface fluxes.

tion in the deliverable yield from the reservoir has to occur or a reduction in the reliability of supply has to be contented with if supplying at the design yield were to occur. Similarly, any insistence on supplying the design yield in such a situation will inevitably increase the size of the shortfall during failure (*i.e.* vulnerability) and compromise the ability of the system to recover following failure (*i.e.* resilience). The fact that both the reductions in required storage (England) and increases in required storage (Iran) magnify with increasing yield is due to the increasing exposed surface area of the reservoirs with yield; hence the loss/gain of water through the surface will magnify as the yield changes. The changes in storage also increase as the system reliability increases for the same reason.

Table 5 contains the impact on the yield for a fixed capacity of 30% of mean annual runoff and 100% reliability for the baseline records. The incorporation of net evaporation flux for the English system increases the deliverable yield from 68.91 to 71.86 Ml/d for the baseline record, an increase of 4%, whereas for the Iranian system, there was a 2% reduction in deliverable yield from 1126 to 1103 Ml/d.

The above results have practical implications for reservoir water management in humid climates such as the English catchments where for most part surface flux is often ignored on the excuse that it is unimportant. However, as demonstrated in this study, while it is unimportant from the point of view that it may not lead to water shortage, it does have some practical significance because facilities planned ignoring such fluxes currently represent an over-design, and the buffer of such over-design would go some way in meeting any shortfall in future storage requirements. As a result such reservoirs may be able to accommodate the likely requirement placed by future climate change for example.

Climate Change Impacts on Runoff

The resulting (monthly) runoff ratios, R_f/R_b, are shown in Table 4 for all the climate scenarios considered. For the English catchments, most of the scenarios are predicting increased flow in winter months and reduced flows during the three summer months of June-August. This trend broadly agrees with that presented in Arnell *et al.* (1997) for the region of England where these catchments are located, although the inflow perturbations in their study were obtained using a more sophisticated monthly water balance rainfall-runoff modelling approach. This is a further proof of the adequacy of Eq. (8).

The GS1t scenario, with its most severe reductions in summer rainfall, produced the biggest change (reduction) in the summer runoff. This further confirms observations by previous workers (*e.g.* Boorman and Sefton 1997) that changes in the rainfall have a greater impact on the runoff than changes in the *PE*, particularly when the baseline rainfall is higher than the baseline evapotranspiration. For example, in Table 4, the GS1t scenario predicts a 49% reduction in the mean June runoff for a mere 15% reduction in mean rainfall and an unchanged *PE*. However, If the baseline rainfall is very low (relative to the baseline evapotranspiration), then the influence of a

Table 4 – Future streamflow factors.

System Location	Scenario	Jan	Feb	Mar	Apr	May	Jun	Jul	Aug	Sep	Oct	Nov	Dec
England	HADCM1 (2050)	1.19	1.08	1.17	0.77	0.88	0.75	1.28	0.86	0.90	1.22	1.35	1.05
	HADCM1 (2020)	1.10	1.04	1.12	0.91	0.95	1.07	1.17	0.95	1.03	1.15	1.19	1.04
	GG1m	1.03	1.09	1.06	1.09	1.10	0.97	0.90	1.08	1.09	1.15	1.17	1.09
	GS1m	1.05	1.03	1.05	1.08	1.07	1.04	0.94	1.00	0.96	1.08	1.05	1.03
	GS1t	1.04	1.05	1.07	1.23	1.33	0.51	0.75	0.82	1.01	1.28	0.99	1.00
Iran	GS1t	1.17	1.24	1.19	1.29	1.22	0.86	0.81	0.12	0.03	1.29	1.00	1.07

rise in evapotranspiration will become more pronounced since the low rainfall is likely to go entirely into satisfying such a rise, leaving little or nothing for runoff. This was the case for August and September when the GS1t scenario was applied to the Iranian catchments. The predicted high increases in evapotranspiration (15% and 12% respectively for the two months), took up nearly all the rainfall, giving predicted runoff ratios of only 12% and 3% respectively.

Climate Change Impacts on Storage-Yield-Reliability Relationships

The impacts of climate change on the storage capacity are illustrated for the English system in Fig. 3 using results for the 30% and 70% yields. In this Figure, it is apparent that most of the scenarios are predicting lower storages for both yields when compared to the baseline, the only exceptions being the HADCM1-2050 and GS1t scenarios which are predicting larger storages for the 30% yield. Put differently, any existing reservoir of a given capacity which receives the predicted future inflows will generally be able to supply a higher yield than it presently does. However, the per cent reductions in storage are higher at the 30% yield due to its low associated storage, this being dominated by within-year requirements. As the yield increases and over-year requirements become significant, the capacity will increase and any associated difference, in relative terms, will decrease. The importance of within-year requirements at low yields is also probably responsible for the increase in storage requirements predicted by both HADCM1-2050 and GS1t for the 30% yield. For this yield, these two scenarios are predicting increases in required storage of between 3-5% (HADCM1-2050) or 13-16% (GS1t), the top end of both ranges relating to when surface fluxes are considered. As shown in Table 4, these two scenarios actually resulted in the highest reduction in summer inflows, the effect of which will be to increase the within-year imbalance between inflow and release, which is why larger storages are being required.

The results for the Iranian catchments are shown in Fig. 4 for the GS1t scenario. As noted previously, only this scenario was considered for the Iranian catchments.

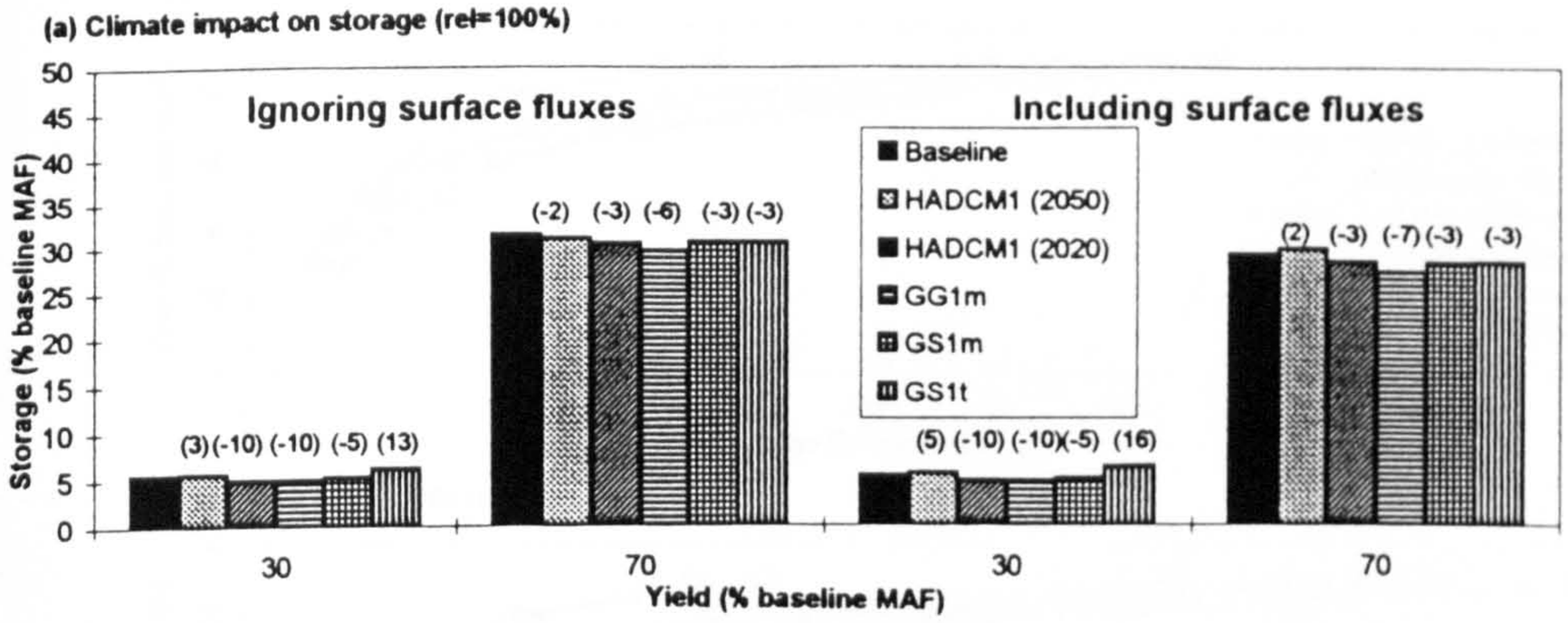

Fig. 3. Impact of five possible future climates on reservoir storage-yield-reliability for the English system. Values in parenthesis in (a) are % difference in storage from the baseline.

The results in Fig. 4, like those for the English system with the GS1t scenario, also show an increased storage requirement at low yields and a lower storage at high yields in the future for 100% reliability. This behaviour is further amplified in Figs. 4(a) and (b) where the complete storage-yield-reliability curves for the Iranian system are shown. In these two Figures, the 100% reliability storage-yield curves for baseline condition occurs to the right of the GS1t curve from the 60% yield onwards (an over-design of storage); before this yield, the storage curve for the GS1t occurs to the right of the baseline curve (an under-design of storage). As the reliability reduces, however, the change from storage under-design to over-design occurs at beyond the 60% yield which is why, for 98% reliability, larger storages (by 2-4%) are being predicted for the 70% yield by GS1t for the Iranian system, in contrast to the 11% reduction in storage at 100% reliability for the same yield. Unlike the English system, the incorporation of surface fluxes did increase storage requirement for all yields with the GS1t scenario, when compared to when the fluxes were ignored (see Fig. 4d).

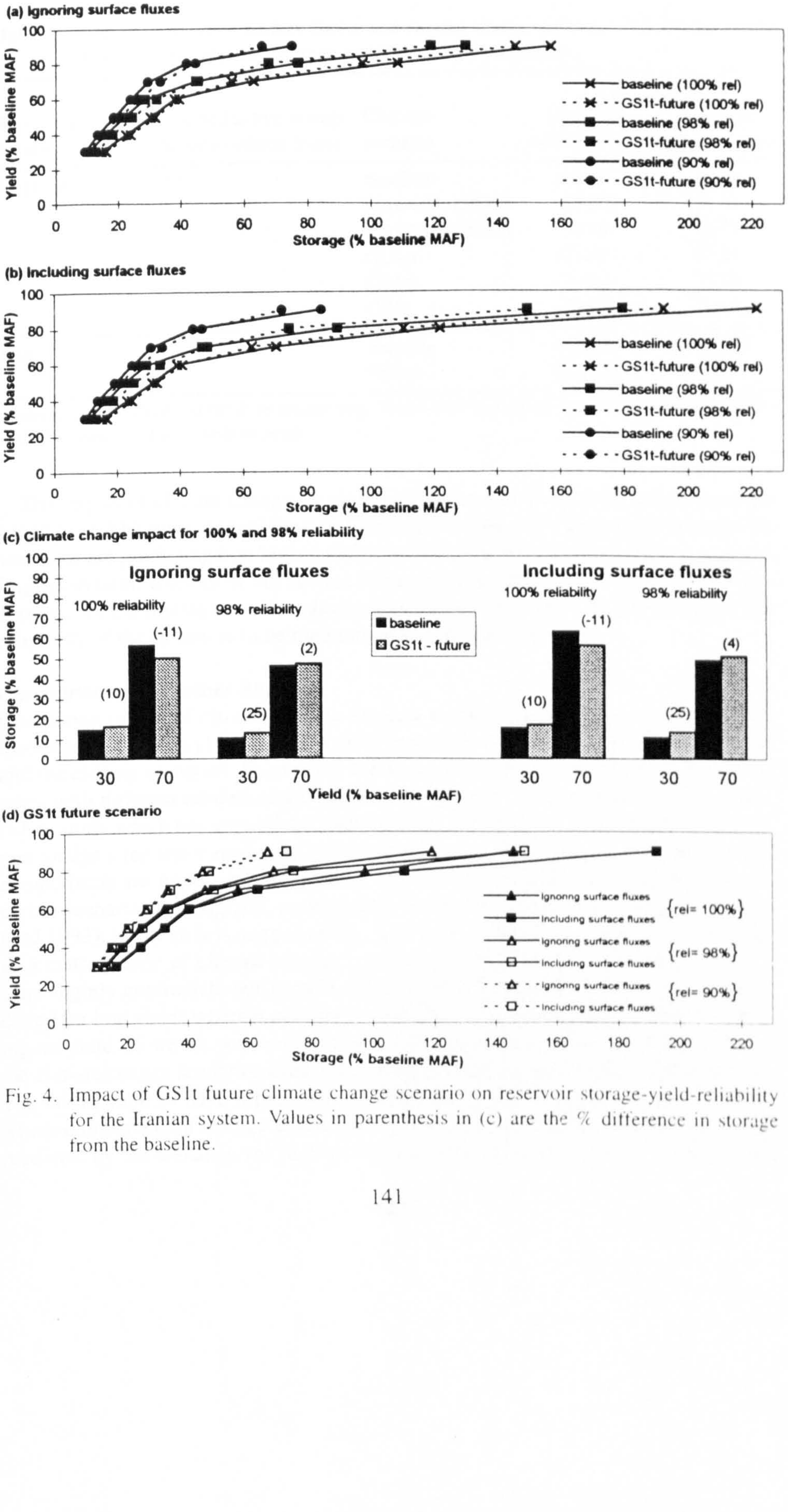

Fig. 4. Impact of GS1t future climate change scenario on reservoir storage-yield-reliability for the Iranian system. Values in parenthesis in (c) are the % difference in storage from the baseline.

Table 5 – Impact of reservoir surface fluxes and climate change on reservoir yield for 100% reliability and assumed storage capacity of 30% mean flow.

Reservoir system location	Assumed active storage capacity (billion litres)	Climate scenario	Yield (Ml/d) Ignoring surface fluxes	Yield (Ml/d) Including surface fluxes
England	11.13	baseline	68.91	71.86
		HADCM1(2050)	69.52	71.05
		HADCM1(2020)	70.44	73.08
		GG1m	71.45	74.81
		GS1m	70.03	73.28
		GS1t	70.03	73.08
Iran	249.60	baseline	1126.05	1103.25
		GS1t	1085.02	1057.66

Address: Dept of Civil and Offshore Engineering, Heriot-Watt University, Riccarton, Edinburgh, EH14 4AS, UK. Email: A.J.Adeloye@hw.ac.uk

The impact of climate change on yield is illustrated in Table 5 for a fixed storage capacity of 30% mean annual flow and 100% reliability. For these conditions, all the scenarios are predicting that higher yields will be possible from this capacity for the English system, whether or not surface fluxes are considered in the analysis. On the contrary for the Iranian system, reductions in the deliverable yields are needed if the reliability of the system is to be maintained at 100% as expected.

Comparisons with other Studies

Comparing results of climate change impacts studies is risky because, as noted by Boorman and Sefton (1997), such results depend on the rainfall-runoff model used and the climate scenarios. Even using the same scenarios will produce different impacts with different rainfall-runoff models. At present, we are unaware of any published study which has applied the 1996 CCIRG and later scenarios used in our current analysis for water resources impact study in England and, on that score, strict comparisons are impossible. However, there have been published results based on earlier scenarios for England, such as the 1991 CCIRG scenarios (Arnell and Reynard 1993), in which it is suggested that reservoir storage requirement will increase as a consequence of climate change (see for example Arnell 1996) for any yield. This slightly contradicts our present result in which increased storage is only predicted for low yields whereas at higher yields, less storage will be required for meeting the yield. However, we are not surprised by our current results given that most of the climate change scenarios used have predicted wetter winters and drier summers. The drier summers have a pronounced effect on within-year storage requirements which dominate total storage at low yields, which is why higher storages are being predicted by the scenarios for such yields. The Iranian study is unique in being first

of its kind as far as we know, although the use of the GS1t scenario as a spatial analogue is a slight limitation.

Regarding the impact of surface fluxes on storage-yield curves, the present results broadly agree with what previous investigators have found. For example, Gan *et al.* (1991) used data from Australia and found that the storage requirement increases slightly with incorporation of surface fluxes, similar to the results obtained for the Iranian catchment. Fennessey (1995) was concerned with testing the sensitivity of model time step of evaporation in yield analysis; nonetheless, he also observed that for any storage, the yield of the Massachusetts systems analysed decreased by about 6% with surface fluxes, which is slightly higher than the 2% recorded for the Iranian system (see Table 5). Fennessey only considered 100% reliability; hence there is no information on the sensitivity of his results to systems' reliability. There have been no previously published work looking specifically at the sensitivity of storage-yield to surface flux for the English conditions with which to compare the present results.

Conclusion

This study has investigated the sensitivity of the storage-yield relationships of two multiple reservoir systems to climate change and to the incorporation of reservoir surface net evaporation flux. One of the systems is located in the humid England and the other in the semi-arid climate of Iran. It was observed that for the English system, the inclusion of the net evaporation flux in the yield analysis caused the storage required for meeting a given yield to decrease. The average reduction was 7% for 70% yield and 2% for 30% yield. Put differently, such an inclusion will allow more water to be available for release from an existing reservoir system with a given capacity. This behaviour was attributed to the additional net inflow caused by the evaporation being generally less than the rainfall in the catchments. The effect of net evaporation is accentuated at high yields and reliability levels, because of the larger exposed reservoir surface under such conditions. The behaviour of the Iranian system was opposite to that of the English system. Because for the Iranian catchments evaporation is higher than rainfall, there is a net additional outflow which leads to an increase in storage requirement for a given yield or a reduction of the useable yield from a reservoir of a given capacity. The average increase in storage requirement for the Iranian system was 7% at the 70% yield and 4% for the 30% yield.

Both of the above results have implications for reservoir management in the two regions. For example, while it will always be important to account for net evaporation in Iranian situation so as not to under-design for yield, its neglect for the English system may actually be beneficial because it would result in over-design of the storage capacity and hence represents a built-in factor of safety as far as systems' yield, resilience, reliability and vulnerability are concerned. Such built-in safety factor could help in mitigating against climate change impacts and other uncertainties such

as those associated with the use of limited data record lengths for reservoir analysis.

Climate change impacts were examined in terms of the effect of five climate change scenarios on the runoff and the reservoir storage-yield-reliability relationships. These scenarios were based on various UK Hadley Centre GCMs. The runoff scenarios were developed using a runoff coefficient approach while the storage-yield functions were based on an extended SPA. For the English catchments, most of the scenarios predict wetter conditions except for the brief (summer) period between June – August when a reduction in average rainfall is predicted. These findings generally agree with the results in Arnell *et al.* (1997), who also constructed runoff scenarios for the region of England in which the catchments are located using a different rainfall-runoff scheme. It was also observed that the reductions in the runoff coincided with reduction in rainfall, thus further confirming the view that the runoff reacts more to rainfall than to evaporation. In fact, the reduction in rainfall is magnified several times in the runoff as shown in one of the scenarios, GS1t, where almost a 50% reduction in runoff resulted from a reduction of only 15% in the rainfall. This same scenario applied as a spatial analogue for the Iranian catchments predicted a 97% reduction in September runoff because much of the baseline rainfall went into satisfying the high evapotranspiration increase predicted by GS1t for the month.

The generally higher inflows predicted by the scenarios for the English system mean that lower storages will be required for meeting a given demand or, where the storage is fixed, more water can be supplied from the fixed capacity. Reductions in the required storage was almost universal except at low yields of 30% or below where some of the scenarios, notably those predicting the largest reduction in summer runoff (*i.e.* HADCM1-2050 and GS1t), predict an increase in storage. The behaviour at the low yields was attributed to the within-year storage requirements which dominate total storage at such low yields. In other words, small reservoirs which are essentially aimed at meeting seasonal discrepancy between runoff and demand will be more prone to climate change impacts because existing facilities will be unable to meet the demand if predicted climate change materialises. Any insistence on meeting the yield under such circumstances can only be at the expense of systems reliability, resilience and vulnerability because they will deteriorate. For high yield, over-year systems, however, such seasonal requirements are masked by the much larger year-on-year requirements and climate change is not likely to result in severe water shortage.

The GS1t applied to the Iranian system produced the same pattern of change as the corresponding one recorded for the English system; however, due to the larger reduction in the Iranian summer runoff, the influence of within-year storage is more pronounced and hence the increased storage requirements predicted at low yields, which can reach 25%, are much higher than those recorded for the English system.

In concluding, it should be stressed that this work has only used climate scenarios from one GCM and given the often wide variability of scenarios among GCMs, it will be important to repeat the study using other GCMs scenarios. Another area

where the study could be improved is to use more appropriate set of scenarios for the Iranian catchments instead of the spatial analogue employed in the study. These together with issues of climate change impacts on systems' resilience and vulnerability, and how adaptation and multi-reservoir operational practices can mitigate such impacts constitute areas for further study.

Acknowledgements

The authors would like to thank two anonymous reviewers whose comments on the initial draft helped to improve upon the clarity and substance of the paper. Thanks also to Ian Stevens and Jason Ball for providing data on the English systems.

References

Adeloye, A. J., and Montaseri, M. (1998) Adaptation of a single reservoir technique for multiple reservoir storage-yield-reliability analysis. In (ed. H. Zebidi) Water: a looming crisis? Proc. Int. conf. on world water resources at the beginning of the 21st Century, UNESCO, Paris, pp. 349-355.

Adeloye, A. J., and Nawaz, N. R. (1998) Assessing the adequacy of Wright's model reconstructed stream-flow data for reservoir storage-yield-reliability analysis, *J. Chartered. Inst. Wat. Envir. Managt., Vol. 12 (2)*, pp. 130-138.

Arnell, N. W. (1996) *Global warming, river flows and water resources* Wiley, Chichester.

Arnell, N. W., and Reynard, N. (1993) Impact of climate change on river flow regimes in the United Kingdom. Institute of Hydrology Report to Department of Environment, Water Directorate, London.

Arnell, N. W., Reynard, N., King, R., Prudhomme, C., and Branson, J. (1997) Effects of climate change on river flows and ground-water recharge: Guideline for resource assessment. UKWIR/Environment Agency Report: Ref: 97/CL/04/1.

Boorman, D. B., and Sefton, C. E. M. (1997) Recognising the uncertainty in the quantification of the effects of climate change in hydrological response, *Climate Change, Vol. 35*, pp. 415-434.

Bower, B. T., Hufschmidt, M. M., and Reedy, W. W. (1962) Operating procedures: Their role in the design and implementation of water resource systems by simulation analysis. In: *(eds. Maass et al.) Design of Water Resource Systems*, chap. 11, pp. 443-456, Harvard Univ. Press, Cambridge, Mass.

Beven, K. J. (1989) Changing ideas in hydrology – the case of physically-based models, *J. Hydrol. Vol. 105*, 157-172.

Carter, T. R., Parry, M. L., Harasawa, H., and Nishioks, S. IPCC (1994) Technical guidelines for assessing climate change impacts and adaptations. Intergovernmental Panel on Climate Change, University College London, and Centre for Global and Environ. Res, Tsukuba.

CCIRG (Climate Change Impacts Review Group) (1996) Review of the Potential Effects of Climate Change in the United Kingdom, Second Report, Department of Environment, London. HMSO

Dooge, J. C. I. (1977) Problems and methods of rainfall-runoff modelling. In (eds. Ciriani, T. A., Maione, U. and Wallis, J. R.) *Mathematical models for surface water hydrology*, Wiley, New York, pp. 71-108.

Fennessey, N. M. (1995) Sensitivity of reservoir-yield estimates to model time step surface-moisture fluxes, *J. Wat. Resour. Plan. Managt., ASCE, Vol. 121 (4)*, pp. 310-317.

Gan, K. C., McMahon, T. A., and O'Neil, I. C. (1991) Sensitivity of reservoir sizing to evaporation estimates, *J. Irr. Drain. Engrg., ASCE, Vol. 177 (3)* , pp. 324-335.

Glantz, M. H., and Wigley, T. M. L. (1987) Climatic variations and their effects on water resources. In (eds. McLaren, D. J. and Skinner, B. J.) *Resources and world development*, Wiley, pp. 625-641.

Hashimoto, T., Stedinger, J. R., and Loucks, D. P. (1982) Reliability, resiliency and vulnerability criteria for water resource system performance evaluation, *Wat. Resour. Res., Vol. 18 (1)*, pp. 14-20.

IPCC (1992) Climate Change 1992. The Supplementary Report to the IPCC Scientific Assessment (eds. Houghton, J. T., Callander, B. A., and Varney, S. K.), Cambridge University Press.

IPCC (1996) Climate Change 1995. The Science of Climate Change: Contribution of Working Group I to the Second Assessment Report of the Intergovernmental Panel on Climate Change (eds. Houghton, J. T., Meiro Filho, L. G., Callander, B. A., Harris, N., Kattenberg, A. and Maskell, K.), Cambridge University Press.

Lele, S. M. (1987) Improved algorithms for reservoir capacity calculation incorporating storage-dependent losses and reliability norm, *Wat. Resour. Res., Vol. 23 (10)*, pp. 1819-1823.

Meteorological Office (1981) The meteorological office rainfall and evaporation calculation system (MORECS). Hydrol. Memo. No. 45.

McMahon, T. A., and Mein, R. G. (1986) *River and reservoir yield*. Wat. Resour. Publications, Littleton, Colorado, USA.

Shaw, E. M. (1994) *Hydrology in practice*. Chapman and Hall, London.

Wigley, T. M. L., and Jones, P. D. (1985) Influences of precipitation changes and direct CO_2 effects on streamflow, *Nature, Vol. 314 (6007)* , pp. 149-152.

Xu, C-Y., and Singh, V. P. (1998) A review on monthly water balance models for water resources investigations, *Wat. Resour. Managt., Vol. 12*, pp. 31-50.

Received: 19 October, 1998
Revised: 6 January, 1999
Accepted: 18 January, 1999

Address:
Dept. of Civil and Offshore Engineering,
Heriot-Watt University,
Riccarton,
Edinburgh EH14 4AS,
U.K.
Email: A.J.Adeloye@hw.ac.uk

Appendix B

Assessing the Uncertainty of Climate Change Water Resources Impacts using a Monte-Carlo Simulation Approach

Adeloye, A.J., **Nawaz, N.R.** and Montaseri, M

In *Emerging Technologies for Sustainable Land Use and Water Management, Proceedings of the 2nd Inter-regional Conference on Environment-Water, edited by Musy, A., Santos, L. and Fritsch, M.,* Presses Polytech. Et Univ. Romandes, Laussane, Switzerland.

Chap. 6.5

Pages 1-11

1999

2nd Inter-Regional Conference on Environment-Water 99

ASSESSING THE UNCERTAINTY OF CLIMATE CHANGE WATER RESOURCES IMPACTS USING A MONTE-CARLO SIMULATION APPROACH

A. J. Adeloye, N. R. Nawaz, M. Montaseri
Department of Civil & Offshore Engineering
Heriot-Watt University, Riccarton, Edinburgh, EH14 4AS, United Kingdom

Most studies on the water resources impacts of climate change have been carried out using climate scenarios obtained from GCM simulation experiments to perturb baseline hydroclimate to give future hydroclimate. Both the baseline and future data series are then input into simulation models of catchment and water resources systems response to obtain possible impacts. Each of these steps gives rise to uncertainties which must be quantified. In this work, we have developed the sampling uncertainties in climate change water resources impacts using a Monte Carlo simulation technique.

1 INTRODUCTION

There have been many recent studies investigating the possible impacts of anthropogenically induced climate change on water resource systems [1]. In such investigations, the impacts assessment is often carried out by comparing systems' behaviour under baseline and perturbed (future) hydroclimatology. The bases of the perturbed hydroclimatology are climate scenarios constructed from General Circulation Models (GCMs) forced with various future scenarios of greenhouse gases, notably carbon dioxide. However, estimates of future climate for a given location vary between GCMs because of different model designs and parameterisations. There are also the uncertainties caused by "downscaling" climate prediction at the global scale to the catchment scale, the imprecision of rainfall-runoff modelling, and the limitation caused by using only single records for the impacts assessment. Wood [2] state that if the problem is posed in a sensitivity analysis context rather than prediction, then GCM errors and possibly downscaling errors are largely removed. Similarly, where both the baseline and perturbed hydrology are based on the hypothesised rainfall-runoff scheme, the uncertainty due to this should also cancel out, leaving the uncertainty due to ignoring the stochasticity of the hydroclimate.

The underlying assumption in most climate impact studies is that both the baseline and future series are stationary in their own right; however, even if this assumption were valid, it does not remove from the fact that both records are a single realisation of the relevant processes. Consequently, any assessed impacts are subject to sampling uncertainties.

In this study, we have developed the sampling uncertainties of climate change water resources impacts using Monte Carlo simulation techniques. The analysis utilised water resources systems in the UK and Iran as case studies. The results are presented and discussed for pertinent water resources systems charactersitics such as the yield and resiliency.

2 METHODOLOGY

2.1 Impact assessment and hydrologic modelling

An overview of the methodology is shown in fig. 1. The water resources impacts assessment was based on recommended protocol [3]. The hydrologic modelling to determine rainfall-runoff response used the monthly conceptual water balance model of Xu and Halldin [4]. This is a single store model which, in its basic form, has three parameters controlling respectively, actual evapotranspiration (AE), slow and fast runoff. The model has been successfully calibrated for many catchments from ten countries with satisfactory results [5]. An extended version of the model can simulate snow accumulation and melting and has six parameters. Together with monthly runoff, the model can accept as inputs different combinations of monthly precipitation, potential evapotranspiration (PE), temperature and humidity. In general, time series data of monthly PE are preferred but where these are unavailable, the PE is estimated internally from temperature and/or humidity using empirical relationships. The snow module is also driven by the temperature. Monthly runoff and other water balance components are the outputs. Table 1 summarises the equations of the model incorporating the snow module.

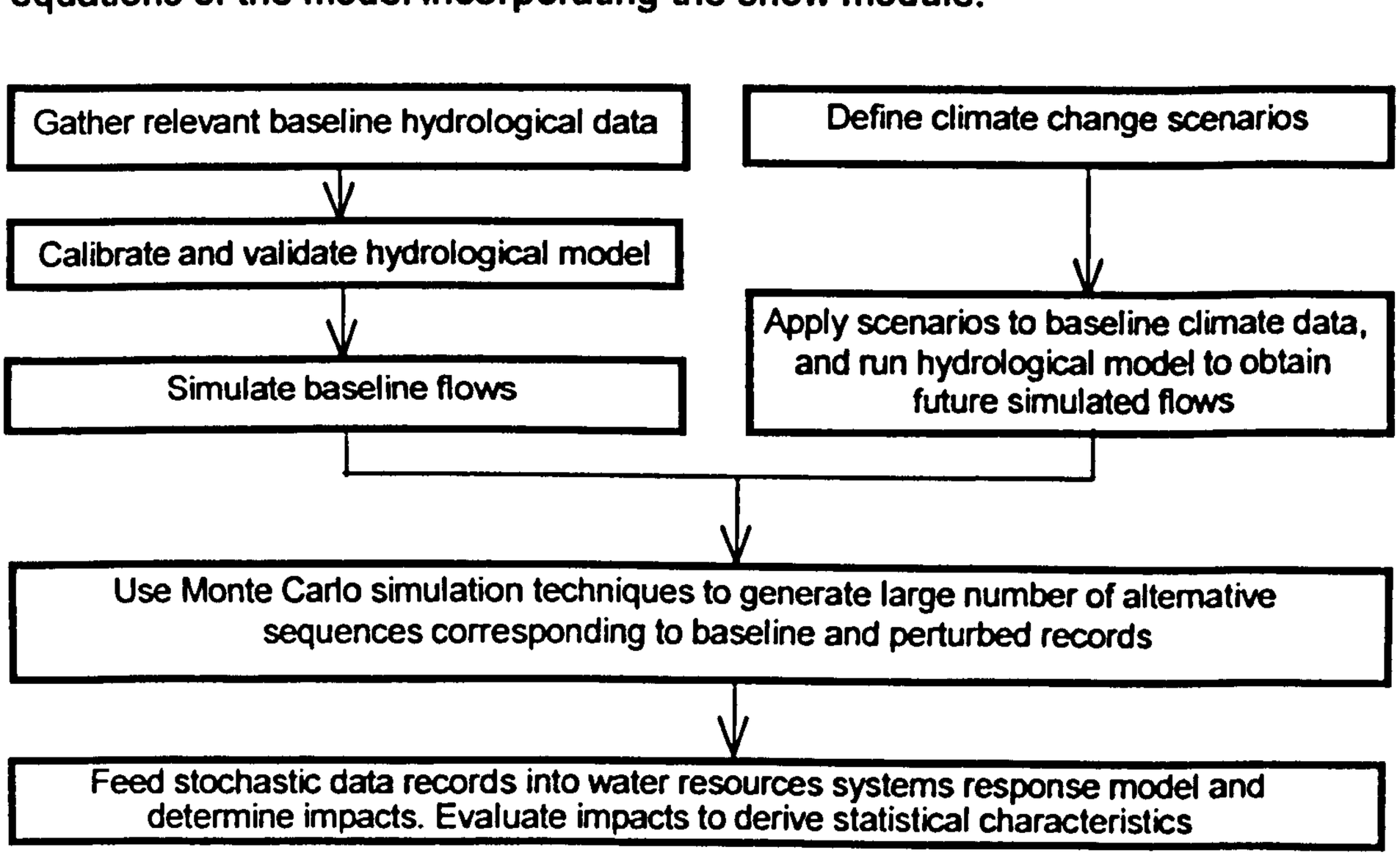

Fig.1 Methodology for climate change impacts assessment

Snowfall:	$s_t=p_t\{1-\exp[-(c_t-a_1)/(a_1-a_2)]^2\}^+$	(1)
Snowpack:	$sp_t = sp_{t-1} + s_t - m_t$	(2)
Snowmelt:	$m_t = sp_{t-1}\{1-\exp[(c_t - a_2)/(a_1 - a_2)]^2\}^+$	(3)
Rainfall:	$m_t = p_t - s_t$	(4)
Potential evapotranspiration:	$e_t = [1+a_3(c_t-c_m)]e_m$	(5)
Actual evapotranspiration:	$r_t = \min [e_t(1-a_4^{w_t/e_t}), w_t]$	(6)
Slow runoff:	$s_t = a_5\left(sm_{t-1}^+\right)^{b_1}$	(7)
Fast runoff:	$f_t = a_6\left(sm_{t-1}^+\right)^{b_2}(m_t + n_t)$	(8)
Total runoff:	$d_t=s_t+f_t$	(9)
Complete water balance equation:	$sm_t = sm_{t-1} + m_t - m_t - r_t - d_t$	(10)

Where: $w_t = r_t + sm_{t-1}^+$ is the available water; $sm_{t-1}^+ = \max(sm_{t-1}, 0)$ is the available storage; $n_t = m_t - e_t(1-\exp(-m_t/e_t))$ is the active rainfall; p_t and c_t are monthly precipitation and air temperature, respectively; e_m and c_m are long-term average potential evapotranspiration and air temperature, respectively; a_j ($j = 1,2,....6$) are model parameters.

Table 1 The main equations of Xu and Halldin [4] conceptual monthly water balance model

2.2 Reservoir analysis

The reservoir analysis was achieved using the modified sequent peak algorithm (SPA) [6]. The SPA is similar to a behaviour simulation analysis and, due to numerous modifications, it can now handle evaporation from and rainfall on reservoir surfaces, and can design for any resiliency and time-based reliability. It is also possible to restrict the amount of water shortages during failure periods, which means that vulnerability [7] can be designed for. Traditionally, the SPA is a single reservoir technique; however, it has been further extended recently to analyse multiple reservoir systems [8].

2.3 Stochastic runoff data generation

The generation of alternative runoff data utilised a parametric, multivariate annual lag-1 auto-regressive AR(1) model followed by disaggregation to monthly flows using a Valencia-Schaake (VS) scheme [9]. The multivariate AR(1) model scheme will ensure that both the spatial correlations between the annual flows at the sites in the multiple reservoir systems, as well as the at-site serial correlations, are preserved. The VS scheme, parameterised independently for the baseline and future runoff, helps to preserve correlations between the monthly and annual flows. The coupled multivariate annual AR(1)-VS model was used to generate 500 replicates of monthly runoff (baseline and perturbed) at each of the sites used in the analysis.

3 CASE STUDY

3.1 Catchments and data

Multiple reservoir systems in two different climatic regions were investigated. The first system is located in the Yorkshire region of north-east England and provides domestic, industrial and compensation water releases. For the purpose of the study, this complex system was simplified into four parallel reservoirs. The second system is located in the semi-arid Urmia region of north-west Iran and consists of three reservoirs in parallel providing water for irrigation. Although the mean annual temperatures for both the Yorkshire and Urmia regions are about the same at 9°C, the average temperature for the winter period (January-March) at Urmia is -2°C compared with 4°C for Yorkshire. The three Urmia catchments are situated in the mountainous areas of the region where the winter is even much colder, with an average number of freezing days of 125 [10]. Consequently, snowmelt plays a major role in the hydrology of the Urmia catchments which must be accommodated. Some relevant catchment characteristics for both systems are shown in table 2. Monthly rainfall, PE and runoff data were available for Yorkshire for the period 1961-1980. For Urmia, the available data comprise monthly rainfall, runoff and temperature for 1968-1990. Both periods are within the 1961-1990 period commonly adopted as the baseline in climate change impact studies [1]. In addition, the monthly mean PE data are also published for the Urmia catchments [10].

System	Name	Area (km^2)	Mean runoff, (BMAF,mm)	Annual flow CV	Ann. rainfall (mm)	Ann. PE (mm)
Yorkshire	Gorpley	2.8	967.91	0.18	1462	412
	Hebden	26.4	996.52	0.18	1414	412
	Luddenden	5.4	985.31	0.18	1414	412
	Ogden	5.4	831.46	0.20	1414	412
	Group total	40.0	1031.45	0.18	1417	412
Urmia	Baranduz	618	411.91	0.20	429	1363
	Nazlu	1715	215.45	0.25	447	1363
	Shahr	418	361.98	0.23	429	1363
	Group total	2751	281.85	0.21	440	1363

Table 2 Characteristics of the catchments analysed

3.2 Climate change scenarios

Published UK climate scenarios for the 2020's based on the UK Hadley centre GCM, HADCM2, were used for Yorkshire. Three of these scenarios - UKCIP98, GS1m, and GS1t [1,11] - were implemented. The UKCIP98 scenario includes the effects of CO_2 only whereas the two GS1 scenarios include, in addition, the cooling effects of sulphate aerosols.

Published scenarios for Urmia were not readily available; consequently we have used a simple climate model called MAGICC (Model for the Assessment of Greenhouse-gas Induced Climate Change) and a regional climate change scenario generator called SCENGEN (SCENario GENerator) to generate the needed rainfall, PE and temperature scenarios. Full details about MAGICC-SCENGEN implementation are available in [12].

Tables 3 and 4 summarise the change in rainfall and PE by the 2020's for Yorkshire and Urmia, respectively. Table 5 shows the rise in 2020's temperature in Urmia where a maximum of 1.3°C rise is expected in the month of September.

Scenario	Jan	Feb	Mar	Apr	May	Jun	Jul	Aug	Sep	Oct	Nov	Dec
GS1m	5.7	2.0	3.5	4.9	4.4	1.1	-1.8	1.2	-1.2	8.3	4.4	3.2
	(4)	(2)	(3)	(5)	(5)	(1)	(-2)	(1)	(-1)	(6)	(3)	(2)
GS1t	5.7	4.0	5.8	12.8	14.0	-16.3	-8.2	-5.9	5.9	30.6	-1.5	0.0
	(4)	(4)	(5)	(13)	(16)	(-15)	(-9)	(-5)	(5)	(22)	(-1)	(0)
UKCIP98	5.7	11.1	3.5	3.9	5.2	-3.3	-3.7	2.4	5.9	11.1	11.7	8.0
	(4)	(11)	(3)	(4)	(6)	(-3)	(-4)	(2)	(5)	(8)	(8)	(5)
IRHAD	-1.1	-1.5	-1.6	-1.0	-1.9	-1.2	-0.5	-0.1	-0.3	0.8	0.6	-0.7
	(-3)	(-4)	(-3)	(-1)	(-3)	(-4)	(-7)	(-3)	(-6)	(3)	(1)	(-2)

Table 3 Change in 2020s rainfall both in mm and % of baseline mean (% in parenthesis)

Scenario	Jan	Feb	Mar	Apr	May	Jun	Jul	Aug	Sep	Oct	Nov	Dec
GS1m	-0.9	-0.7	-0.4	-0.4	0.0	-0.7	1.4	1.8	1.6	0.0	-0.6	-0.8
	(-12)	(-7)	(-2)	(-1)	(0)	(-1)	(2)	(3)	(4)	(0)	(-5)	(-10)
GS1t	0.4	-0.6	-0.2	-2.2	-4.0	3.4	4.2	8.8	4.8	1.3	-0.1	-0.4
	(5)	(-6)	(-1)	(-6)	(-7)	(5)	(6)	(15)	(12)	(6)	(-1)	(-5)
UKCIP98	0.2	0.9	0.0	0.7	2.3	2.7	5.6	3.5	14.5	2.6	0.7	0.3
	(3)	(9)	(0)	(2)	(4)	(4)	(8)	(6)	(36)	(12)	(6)	(3)
IRHAD	2.4	2.7	4.0	3.4	4.3	5.1	5.6	5.3	5.9	3.3	1.6	1.7
	(5)	(5)	(5)	(3)	(3)	(3)	(3)	(3)	(4)	(3)	(2)	(3)

Table 4 Change in 2020s PE both in mm and % of baseline mean (% in parenthesis)

Scenario	Jan	Feb	Mar	Apr	May	Jun	Jul	Aug	Sep	Oct	Nov	Dec
IRHAD	0.7	0.8	1.0	0.8	0.8	1.1	1.2	1.0	1.3	1.0	0.5	0.5

Table 5 Rise in 2020s temperature in Urmia (°C)

4 RESULTS AND DISCUSSION

4.1 Hydrologic modelling

In the hydrologic modelling, the snow process was ignored for Yorkshire and the available PE data were used as input. In Urmia, however, snow was considered and the snow module was driven by the temperature. Also given that time series PE data were unavailable for Urmia, the temperature data were used internally to estimate the PE. The Yorkshire models were calibrated for the period 1980-1986 and validated for the period 1987-1990. In Urmia, the calibrations were over 1970-1980 with validation being over 1981-1985. In general, the performance of the models during calibration was very good with an R^2 range of 0.74-0.95 for Yorkshire and 0.71-0.82 for Urmia. Figs. 2a and 2b compare the observed and simulated runoff for two of the sites over the respective validation periods. The fits are generally good.

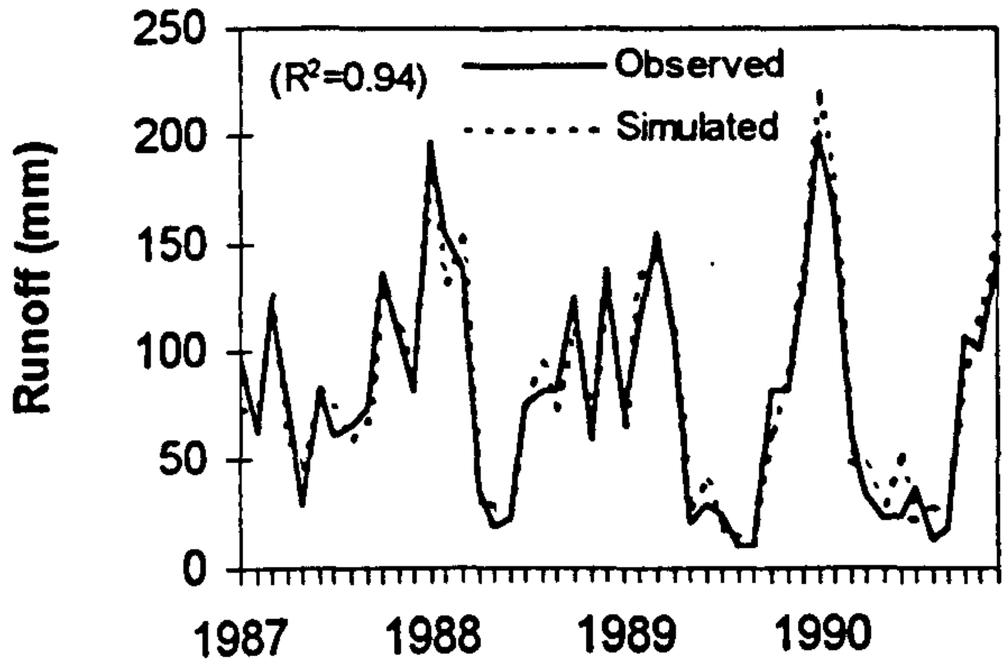

(a) Hebden at Yorkshire

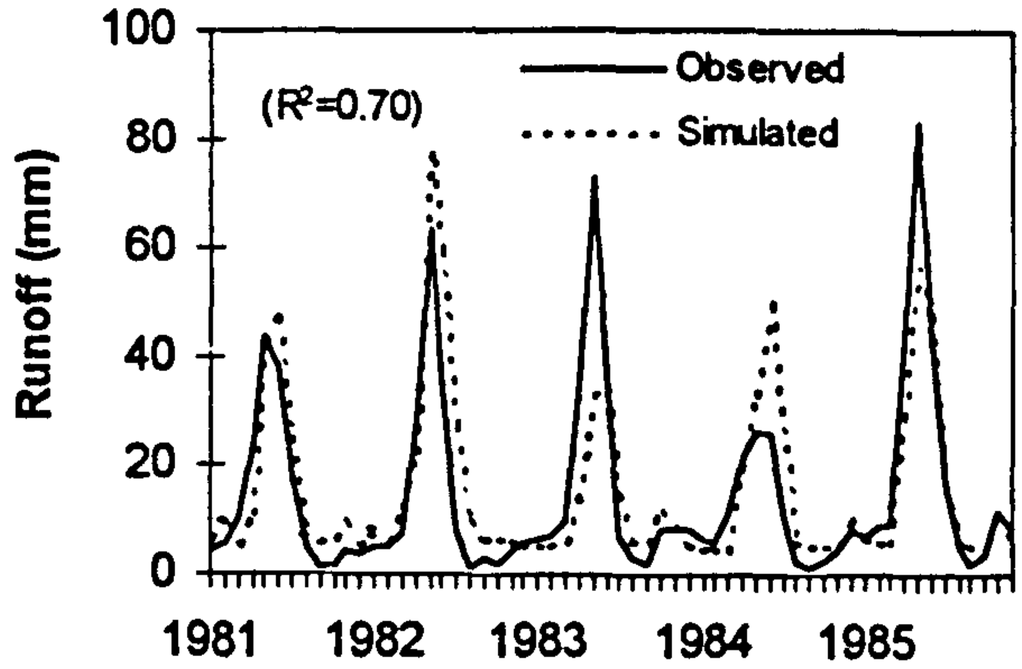

(b) Nazlu at Urmia

Fig. 2 Monthly runoff validation plots

4.2 Climate change impacts on runoff

Fig. 3 summarises the impact of climate change on runoff according to UKCIP98 and IRHAD climate scenarios, for two of the sites. For Hebden in Yorkshire, an increase in future runoff is to be expected all year round except during June-August. The maximum 10% rise in February runoff coincides with the maximum increase in rainfall (see table 3), further confirming the dominance of rainfall on runoff [13]. At Nazlu (Urmia), a reduction in runoff is expected all year round except in March and April. The largest reduction in future runoff (-28%) is anticipated in July because of the largest reduction in July rainfall (see table 3).

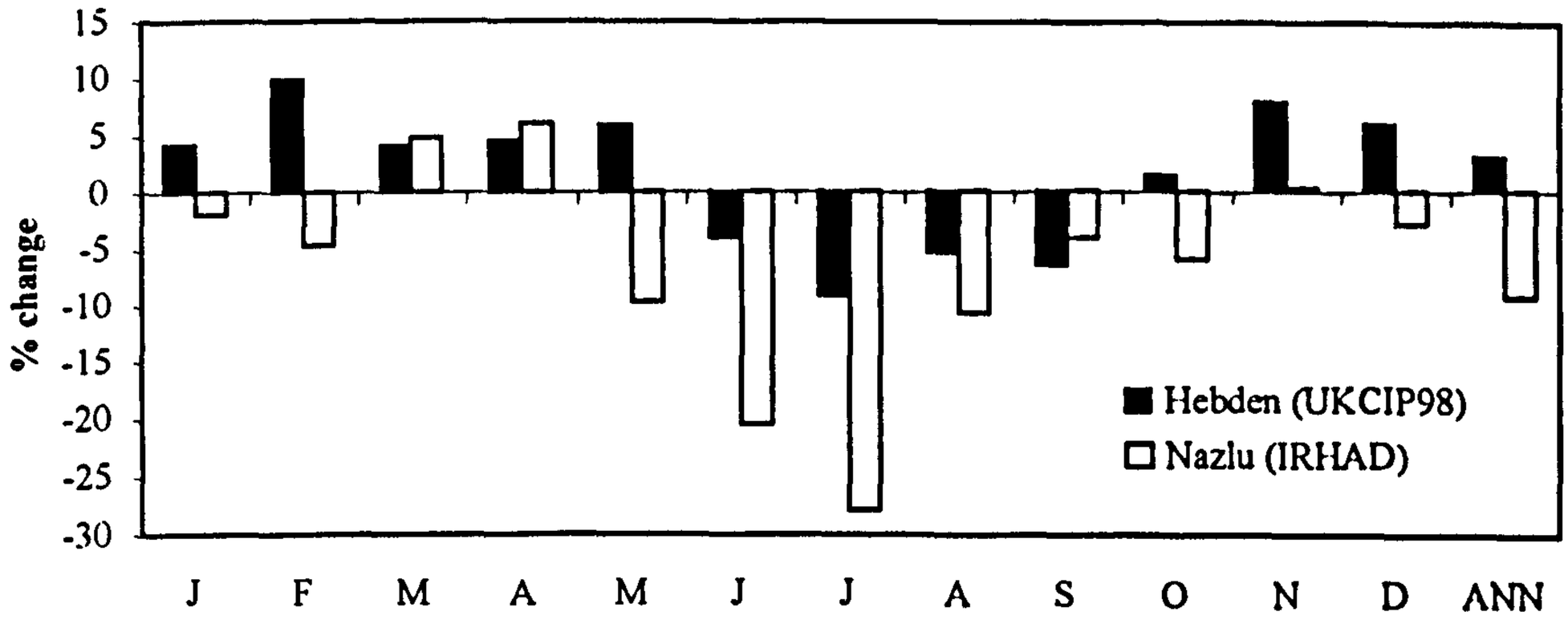

Fig. 3 Climate change impacts on mean monthly and annual runoff for two catchments

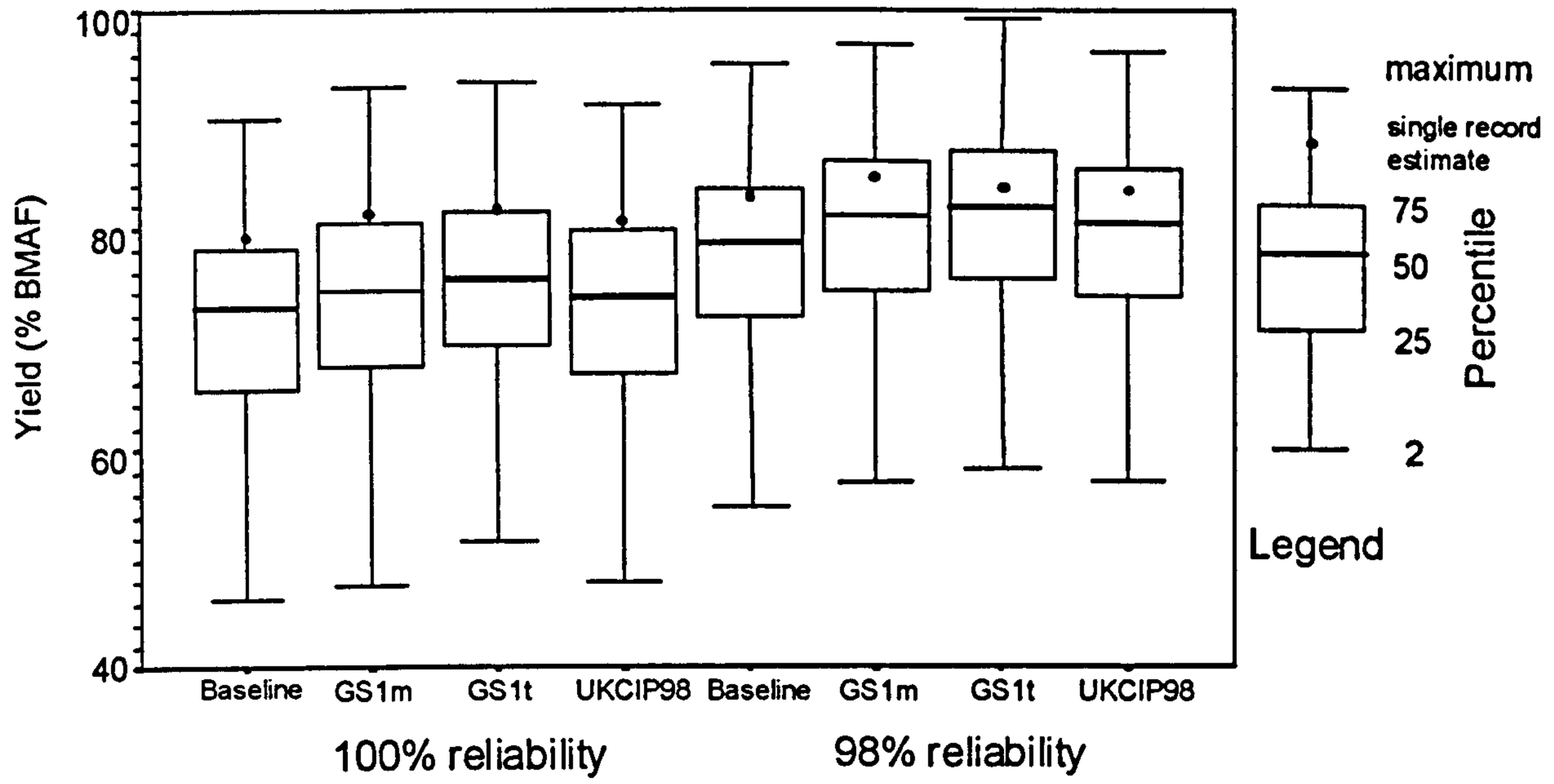

a) Yorkshire system

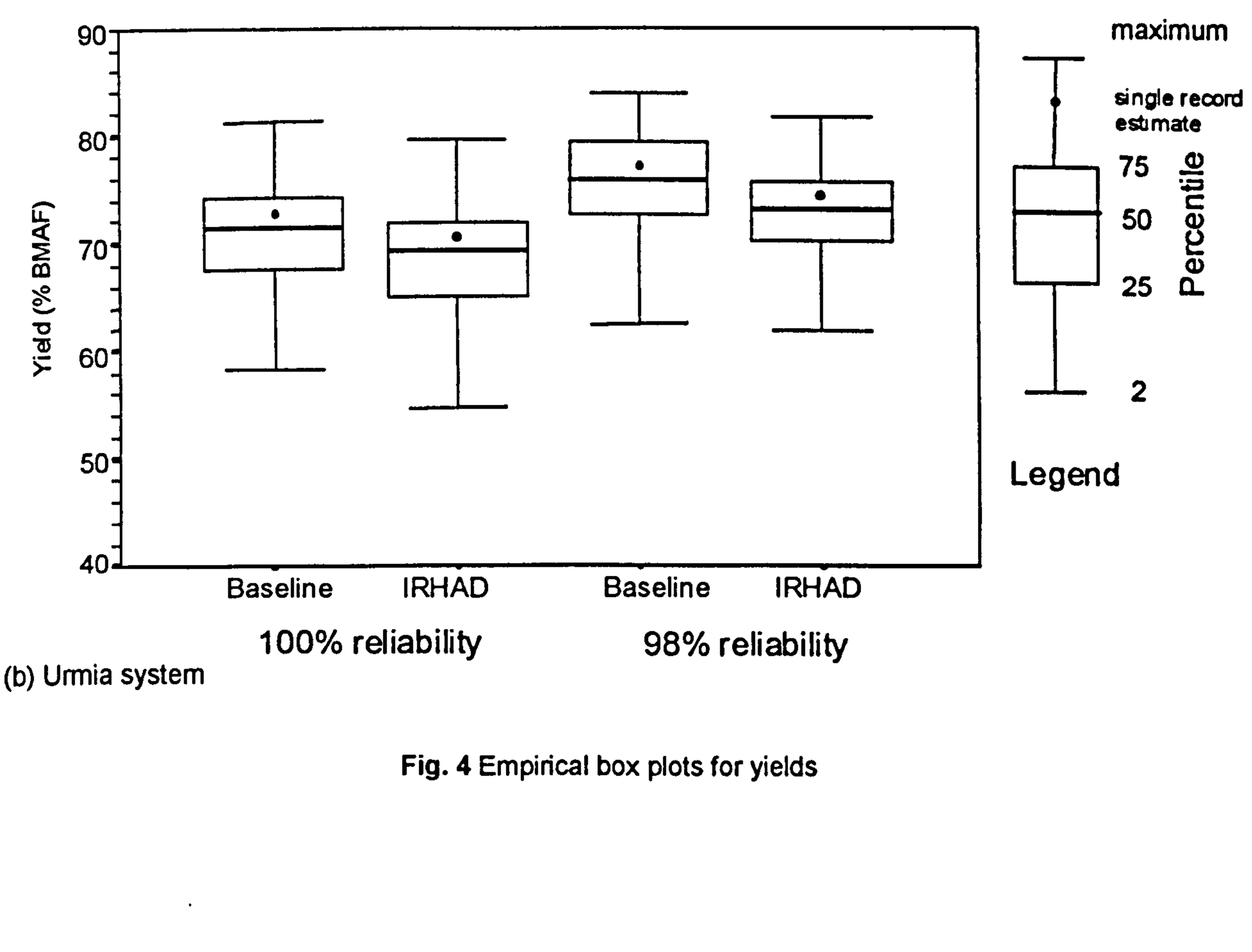

(b) Urmia system

Fig. 4 Empirical box plots for yields

4.3 Climate change impacts on reservoir yield and its sampling uncertainty

Yields were evaluated for fixed storages of 11.67 x 10^6 m^3 for Yorkshire and 232.6 x 10^6 m^3 for Urmia. The storage of 11.67 x 10^6 m^3 at Yorkshire is the existing capacity of the four-reservoir system and corresponds to 28.3% of the simulated baseline mean annual runoff (BMAF- see table 2). The storage capacity for Urmia was arbitrarily selected so as to give a broadly similar level of development as in Yorkshire. Thus, the 232.6 x 10^6 m^3 capacity represents about 30% of the BMAF for the Urmia system (see table 2). Table 6 contains the yield estimates from the single records and the summaries obtained from the Monte Carlo simulations. Based on the single records, all of the scenarios for Yorkshire are predicting an increase in systems yield both at the 100% and 98% reliability levels. The largest predicted increase in yield results from the GS1t scenario which is not surprising given that this same scenario predicted the largest increase in runoff. However, an important observation here is that none of the predicted increases in yield is as high (in relative terms) as the increase in runoff, implying that impacts studies which stop at runoff without looking at yields may be misleading about the water resources impacts of climate change. As the reliability reduces and hence more failures are acceptable, the yield of the system increases as expected. The situation in Urmia is opposite to that observed in Yorkshire in that the IRHAD scenario has predicted reductions in yields in the future. Because IRHAD had predicted consistently lower rainfall which in turn has translated to consistently lower runoff, this observed behaviour of the yield is also expected.

While the predicted changes in yields shown in table 6 are modest on the basis of the single records, this is untrue when the sampling variability of the input records is taken into account. For example in table 6, although the baseline annual yield for 100% reliability for the Yorkshire system was 80.0% BMAF, this yield can be anything between 16.1% and 90.1% BMAF when sampling uncertainties are considered. Based on the corresponding results for the GS1m scenario for example, it means that the actual change in system yield as a consequence of climate change can vary from a surplus of 76.9% BMAF (= 92.9 - 16.1) to a deficit of 74.6% BMAF (= 15.5 - 90.1). Similar information for the other scenarios, reliability and the Urmia system is shown in table 6. In all cases, the variability of the yield impacts is very large which would have been impossible to detect without the Monte Carlo experiments described here.

The empirical distributions of the yield are summarised in the box plots shown in figs. 4a and 4b for Yorkshire and Urmia respectively. Compared to the baseline, the median (i.e. 50 percentile) yield estimates are higher for all three scenarios in Yorkshire, further reinforcing the results in table 6. Similarly, the lower variability in the yield estimates for Urmia compared with Yorkshire revealed in table 6 is also evident in the box plots. Superimposed on the box plots are the yield estimates for the single records from where their probability of exceedance can be estimated. Conversely, the empirical distributions can be used to determine the yield with a given probability of exceedance instead of relying solely on the single yield estimates for decision making. Empirical confidence limits for the yield estimates can also be constructed from the distribution functions. Table 6 for example contains the upper and lower 90% confidence limits for the single records yield estimates; these are generally wide.

	Yorkshire (storage = 28% BMAF)								Urmia (storage = 30% BMAF)			
	100% reliability				98% reliability				100% reliability		98% reliability	
	Baseline	GS1m	GS1t	UKCIP98	Baseline	GS1m	GS1t	UKCIP98	Baseline	IRHAD	Baseline	IRHAD
Single	79.55	81.36	81.39	80.51	82.36	84.34	83.88	83.31	72.51	70.04	76.99	74.30
Monte Carlo												
Mean	70.92	72.88	74.08	72.33	76.83	79.19	80.66	78.68	70.76	68.12	75.55	72.57
Minimum	16.07	15.54	18.45	15.83	17.62	16.97	20.51	17.33	49.77	48.20	54.16	52.24
Maximum	90.11	92.92	93.28	91.22	95.04	96.79	99.25	96.09	81.21	79.40	83.89	81.75
Median	72.58	74.26	75.22	73.64	78.56	81.04	81.82	80.66	71.38	69.08	75.75	73.05
UC90[a]	85.03	87.61	87.82	86.62	91.43	94.39	96.36	93.44	77.94	75.08	82.69	79.54
LC90[b]	51.29	53.01	55.64	53.14	57.45	59.32	61.94	59.36	62.02	58.52	67.33	63.97
Variance	108.78	112.37	98.81	105.40	107.43	115.12	106.08	108.43	23.32	25.28	21.48	21.50
CV	0.147	0.145	0.134	0.142	0.135	0.135	0.128	0.132	0.068	0.074	0.061	0.064
Impact[c]	-	-74.6	-71.7	-74.3	-	-78.1	-74.5	-77.7	-	-33.0	-	-31.7
	-	+76.9	+77.2	+75.2	-	+79.2	+81.6	+78.5	-	+29.6	-	+27.6

Table 6 Yield estimates (% BMAF) for Yorkshire & Urmia systems ([a, b] denote respectively the upper and lower 90% confidence limits; [c] represent the possible range for yield impacts with – denoting deficit and + denoting surplus)

4.4 Climate change impacts on reservoir resiliency

Resiliency is taken here to be the probability of recovery following failure [7]. The estimated impacts on reservoir resiliency are shown in table 7. Only average values are presented in table 7; the complete information on the statistical distribution has not been reproduced for lack of space. For given yield and storage, the probability of recovery is, on average, enhanced for Yorkshire but diminished for Urmia. This should be expected given that climate change is predicted to increase future yield in Yorkshire but decrease it for Urmia; consequently any attempt to maintain the pre-change yield and reliability can only be achieved through a modification of the resiliency. As was the case with the yield, there was a large variability in the resiliency when sampling variability in the inflow records were considered.

	Yorkshire system (Storage = 28% BMAF; yield = 80% BMAF)							Iranian system (Storage = 30% BMAF; yield = 60% BMAF)		
Rel. (%)	Resiliency (%)				Change in resiliency from baseline (%)			Resiliency (%)		% diff.
	Bas.	GS1m	GS1t	UKCIP98	GS1m	GS1t	UKCIP98	Bas.	IRHAD	
99	42.2	43.6	45.0	43.5	3.3	6.6	3.1	61.7	60.3	-2.3
98	34.2	35.1	37.4	35.4	2.6	9.4	3.5	51.6	49.3	-4.5
90	25.9	26.9	29.0	27.1	3.9	12.0	4.6	35.5	35.0	-1.4

Table 7 Climate change impacts on reservoir resiliency *(average of 500 replicates)*

5 CONCLUSION

The study has evaluated the effects of sampling uncertainty in both the baseline and perturbed inflow series on the estimates of climate change water resources impacts. In particular, it has been demonstrated that the current practice of basing impacts study on single traces of both the baseline and perturbed series is flawed because such an approach ignores other numerous possibilities of such traces. Conse-

quently, the estimated impacts based on such single traces may depart widely from what could happen as a result of climate change. Using Monte Carlo techniques, it was possible to produce alternative, equally likely inflow sequences and hence to evaluate the extent of this departure and to also develop statistical characteristics of the estimated impacts on the yield and resiliency of water resources systems. This should aid better decision making when planning mitigating measures for predicted climate change impacts.

ACKNOWLEDGEMENTS

Thanks are due to Chong-Yu Xu of Uppsala University, Sweden, for supplying the monthly water balance model and for his advice. Thanks also to Ian Stevens, Jason Ball and Ian Hampson for supplying relevant data on the Yorkshire system

6 REFERENCES

[1] Arnell, N.W., N.Reynard, R.King, C.Prudhomme, J Branson, Effects of climate change on river flows and ground water recharge: guidelines for resource assessment, *UKWIR/Environment Agency publication*, report ref no. 97/CL/04/1, 1997.

[2] Wood, A.W., D.P. Lettenmaier and R.N. Palmer, Assessing climate change implications for water resources planning, *Climatic change*, vol 37 no 1, 203-228, 1997.

[3] Carter, T.R., M.L.Parry, H.Harasawa and S.Nishioka, IPCC technical guidelines for assessing climate change impacts and adaptations, *IPCC special report to Working Group II*, London, 1994.

[4] Xu, C-Y. and S. Halldin, The effect of climate change on riverflow and snow cover in the NOPEX area simulated by a simple water balance model, *Nordic Hydrology*, vol 28 no 4/5, 273-282, 1997.

[5] Vandewiele, G.L. and Ni-Lar-Win, Monthly water balance models for 55 basins in 10 countries, *Hydrological Sciences Journal*, vol 43 no 5, 1998.

[6] Lele, S.M., Improved algorithms for reservoir capacity calculation incorporating storage-dependent losses and reliability norm, *Water Resources Research*, vol 23, no 10, 1819-1823, 1987.

[7] Hashimoto, T., J.R. Stedinger and D.P. Loucks, Reliability, resiliency and vulnerability criteria for water resource system performance evaluation, *Water Resources Research*, vol 18, no 1, 14-20, 1982.

[8] Adeloye, A.J. and M.Montaseri, Adaptation of a single reservoir technique for multiple reservoir storage-yield-reliability analysis, In (ed. Zibidi) water: a looming crisis? *Proc. Int. conf. World Water Resources,* UNESCO, Paris, 349-355, 1998.

[9] Valencia, R. and J.C. Schaake, Disaggregation processes in stochastic hydrology, *Water Resources Research,* vol 9, 580-585, 1973.

[10] Ministry of Water and Power, Iran, Reservoir systems in Urmia Region (translated from Persian), 1995

[11] Hulme, M. and G.J. Jenkins, Climate change scenarios for the UK: Scientific report, UKCIP Technical Report No. 1, *Climatic Research Unit*, Norwich, 80pp, 1998.

[12] Hulme, M., S.C.B. Raper and T.M.L. Wigley, An integrated framework to address climate change (ESCAPE) and further developments of the global and regional climate modules (MAGICC). *Energy Policy*, vol 23, no 4/5, 347-355, 1995.

[13] Boorman, D.B. and C.E.M. Sefton, Recognising the uncertainty in the quantification of the effects of climate change on hydrological response, *Climatic Change*, vol 35, no 4, 415-434, 1997.